Identification of a C-FABP-PPARγ-VEGF axis promoting tumorigenicity in Prostate cancer cells

THESIS SUBMITTED IN ACCORDANCE WITH THE REQUESTMENTS OF
THE UNIVERSITY OF LIVERPOOL
FOR THE DEGREE OF DOCTOR IN PHILOSOPHY

By:

Farzad Seyed Forootan

July 2014

Department of Molecular and Clinical Cancer Medicine (Pathology)

In the name of Allah

Who all the knowledge and wisdom come from him

To Prophet Mohammad, peace upon him and his family

To the souls of my grandparents

To my parents

To my wife and kids

Last but not least, to my sisters and brother

ABSTRACT

The over-expression of C-FABP plays an important role in promoting tumorigenicity of prostate cancer. It has been hypothesized that the overexpressed C-FABP may transport an excessive amount of intracellular fatty acids into cancer cells to activate their nuclear receptor PPARγ to trigger a chain of molecular events that may lead to a facilitated malignant progression of the cancer cells.

To investigate whether PPARγ involved in activities exerted by C-FABP in prostate cancer, their expression status was assessed in prostate cell lines and tissues. Results showed that their expression levels in malignant cell lines and tissues (cytoplasm and nucleus) were significantly higher than those expressed in benign cells and in BPH and it appeared that their expression levels were increased as the increasing malignancies of the cell lines and tissues. The increased expression of both C-FABP and PPARγ were significantly correlated to a reduced survival time. Suppression of *PPARγ* in highly malignant prostate cancer cells produced a significant reduction in growth rate (up to 53%), invasiveness (up to 89%) and anchorage-independent growth (up to 94%) *in vitro*. Suppression of *PPARγ* in PC3-M cells could significantly reduce the sizes of tumours formed in nude mice by 99%. Tumour incidence was reduced to 10% and the latent period was significantly increased by 3.5 fold.

The results in this study also showed that C-FABP promoted VEGF expression and angiogenesis by PPARγ (through the stimulation of the fatty acids transported by C-FABP). When PPARγ was blocked with its antagonists, cells did not respond to stimulation signal produced by fatty acids, even when high level of fatty acids was available. Further study showed that the activated PPARγ regulated VEGF expression through acting with the *PPRE*s in the promoter region of *VEGF* in prostate cancer. Although androgen can modulate *VEGF* expression through Sp1/Sp3 binding site on VEGF promoter in androgen-dependent prostate cancer cells, this route was disappeared and gradually replcaced by the C-FABP-PPARγ route as the cells gradually lost their androgen dependency.

The results of this study suggested that C-FABP, together with fatty acids, PPARγ and VEGF should be considered as key factors in the fatty acids-initiated signalling pathway that promoted the malignant progression. Therefore, the C-FABP-PPARγ-VEGF axis may be a novel therapeutic target for prostatic cancer.

ACKNOWLEDGMENTS

I would like to express my deepest gratitude to Professor Youqiang Ke and Professor Christopher Foster, my research supervisors, for providing me the invaluable opportunity to undertake the PhD study in this department and for their patient guidance, enthusiastic encouragement and useful critiques of this research work. Also I take this opportunity to express my profound appreciation and deep regards to my sister, Dr Shiva S. Forootan for her exemplary guidance, monitoring and constant encouragement throughout the program of PhD. The blessing, help and guidance given by them time to time shall carry me a long way in the journey of life on which I am about to embark.

I own a big appreciation to my family and friends for their endless love. I thank my parents for giving me the strength to overcome all the difficulties. The hard working spirits and intelligence inherited from them made me coming through all the way here. Special thanks must go to my beloved wife, Helen and my children, Faraz and Hasti for their love, understanding and confidence in me. Appreciation should also give to my sister and her family, for all their supports which made my life in Liverpool enjoyable.

Last but not least, I would like to thank all the technical staffs in Molecular Pathology department, especially Mrs. Carol Beesley, Mr. Gregor Govan, Mr. Timothy Dickinson, Mrs. Patricia Gerald, Mrs. Sharon Forest and Mr. Andrew Dodson. They helped me with their experience and insightful feedbacks on the most experimental aspects of this research.

DECLARATION

No portion of the work referred to in the thesis has been submitted in support of an application for another degree or qualification of this or other university or other institute of learning.

DECLARATION OF ORIGINALITY

This thesis is a product of my own work which has been carried out during my PhD study in the Department of Molecular and Clinical Cancer Medicine (Pathology), University of Liverpool, between September 2011 and January 2014. All the experiments presented in the result chapter were performed by me under the supervision of my supervisor, Professor Youqiang Ke and Dr Shiva S. Forootan, senior research associate in molecular Pathology department. The thesis was written by me with their guidance.

Publications

- **Farzad S. Forootan**, Shiva S. Forootan, Mohamad I. Malki, Danqing Chen, Gandi Li, Ke Lin, Philip S. Rudland, Christopher S. Foster and Youqiang Ke. The expression of C-FABP and PPARγ and their prognostic significance in prostate cancer, *International Journal of Oncology*, 44: 265-275, 2014.

- **Farzad S. Forootan**, Shiva S. Forootan, Syed A Hussain, Youqiang Ke. Inter-action of C-FABP and PPARs in prostate cancer. 23rd Biennial Congress of the European Association for Cancer Research (EACR), Munich, Germany, 5-8 July 2014 and North West Cancer Research (NWCR) annual meeting, March 24st 2014, Liverpool, UK (Poster presentation).

- **Farzad S. Forootan**, Shiva S. Forootan, Ke Lin, Christopher S Foster, Youqiang Ke. Evaluation the expression of C-FABP and PPARs in Prostate cancer, North West Cancer Research (NWCR) annual meeting, May 21st 2013, Liverpool, UK and NCRI conference, 3-6 Nov. 2013, Liverpool, UK (Poster presentation).

- Danqing Chen, Shiva S. Forootan, John R. Gosney, **Farzad S. Forootan** and Youqiang Ke. Increased expression of Id1 and Id3 promotes tumorigenicity by enhancing angiogenesis and suppressing apoptosis in small cell lung cancer, Genes & Cancer, published on July 6, 2014.

- Zhengzheng Bao, Mohammad I. Malki, Shiva S. Forootan, Janet Adamson, **Farzad S. Forootan**, Danqing Chen, Christopher S. Foster, Philip S. Rudland and Youqiang Ke. Binding Protein-Related Signalling Pathway Leading to Malignant -A Novel Cutaneous Fatty Acid Progression in Prostate Cancer Cells, Genes & Cancer, published on September 18, 2013 as doi: 10.1177/1947601913499155.

- S.S. Forootan, Z.Z. Bao, **F. S. Forootan**, L. Kamalian, Y. Zhang, C. Foster, A. Bee, Y. Ke. Atelocollagen-delivered small interference RNA targeting *C-FABP* gene as experimental prostate cancer therapeutics in nude mice, *International Journal of Oncology*, 36:69-76, 2010.

Table of Contents

List of Figures

Chapter 1

Chapter 2

Chapter 3

Chapter 4

List of Tables

Chapter 1

Chapter 2

Chapter 3

List of Abbreviations

Abbreviation	Full name
AICR	American Institute for Cancer Research
APC	Adenomatous Polyposis Coli
AR	Androgen Receptor
BCL gene	B-cell lymphoma–leukemia gene
BPH	Benign Prostatic Hyperplasia
BRCA	BReast Cancer
BSA	Bovine Serum Albumin
cDNA	Complementary DNA
CFU	Colony Forming Unit
CK	Cytokeratin
C-FABP	Cutaneous fatty acid binding protein
CRPC	Castration resistant prostate cancer
DHT	5-alpha-Dihydrotestostron
DLR assay	Dual-Luciferase®Reporter Assay
DMSO	Dimethyl sulfoxide
DR	Direct Repeat
DRE	Digital Rectal Examination
E coli	Escherichia coli
EDTA	Ethylenediaminetetraacetic acid
E-FABP	Epidemic-FABP
EL	Expression Level
ELISA	Enzyme-Linked Immunosorbent Assay
ENOS	Endothelial Nitric Oxide Synthase
EPCA	Early Prostate Cancer Antigen
ER	Esterogen Receptor
ERSPC	European Randomized Study of Screening for Prostate Cancer
FASN	Fatty Acid Synthase
FAT	Fatty Acid Translocase
FATP	Fatty Acid Transport Protein
FGF	Fibroblast Growth Factor

Abbreviation	Full name
GS	Gleason scores
HIF	Hypoxia Inducible Factor
HK	Human glandular Kallikrein
HUVEC	Human Umbilical Vein Endothelial Cells
IGF	Insulin-like Growth Factor
IHC	Immunohistochemistry
IL	Interleukin
IMS	Industrial Methylated Spirits
kDa	kilo Dalton
K-FABP	Keratinocyte-FABP
LAR II	Luciferase Assay Reagent II
LB medium	Lysogeny broth medium
L-FABP	Liver Cytosolic Fatty Acid-Binding Protein
LUTS	Lower Urinary Tract Symptoms
mRNA	Messenger RNA
MTT	3-(4, 5-dimethylthiazl-2-yl)-2, 5-diphenylterazolium bromide
MVD	Micro Vessel Density
NF-KappaB	Nuclear Factor-KappaB
NSCLC	Non-small cell lung cancer
OD	Optical density
PA-FABP	Psoriasis Associated-FABP
PAGE	Poly Acrylamide Gel Electrophoresis
PAP	Prostatic Acid Phosphatase
PCA	Prostate Cancer Antigen
PI-3K	Phosphatidylinositol-3 Kinase
PIN	Prostatic Intraepithelial Neoplasia
PKB	Protein Kinase-B
PlGF	Placental Growth Factor
PPAR	Peroxisome proliferator-activated receptors
PPRE	Peroxisome Proliferator Response Elements
PSA	Prostate-Specific Antigen
PSCA	Prostate Stem Cell Antigen
PVDF	PolyVinylidene DiFluoride

Abbreviation	Full name
PZ	Peripheral Zone
RM	Routine Medium
RNAi	RNA interference
RSM	Routine Selective Medium
RT-PCR	Reverse transcriptional polymerase chain reaction
RXR	Retinoic X Receptor
SDS	Sodium Dodecyl Sulphate
SE	Standard error
shRNA	short hairpin RNA
siRNA	small interfering RNA
SLB	Sample Loading Buffer
SOB medium	Super Optimal Broth
SOC medium	Super Optimal broth with Catabolic repressor
Sp	Specificity protein
SPSS	Statistical Package for Social Sciences
STAT1	Signal Transducer and Activator of Transcription-1
SV	Simian virus
TAE buffer	Tris-Acetate EDTA *buffer*
TBE buffer	Tris-Borate-EDTA buffer
TBS-T	Tris Base Salt-Tween
TCF-4	T-Cell Factor-4
TGF β1	Transforming growth factor β1
tPSA	total PSA
TURP	Trans Urethral Resection of Prostate
TZ	Transitional Zone
UCP	Uncoupling Proteins
VEGF	Vascular endothelial growth factor
VSMC	Vascular Smooth Muscle Cell
WCRF	World Cancer Research Fund
WHO	World Health Organization
χ^2 test	Chi square test

CHAPTER ONE:

INTRODUCTION

1 Introduction

1.1 Epidemiology of prostate cancer

1.1.1 Cancer epidemiology

In the UK, it was estimated that one in three people develop cancer in their lifetime, and it is predicted to rise by more than 3% each year [1]. In 2011, 331,487 new malignant cases (excluding non-melanoma skin cancer) were diagnosed in the UK; 164,000 cases in females and 167,487 cases in males. Breast, lung, colorectal and prostate cancer account more than half (54%) of all new cases [2-5] (**Fig. 1.1**). Cancer is primarily an old people's disease and risk of cancer generally increases with age. About 63% of cancers are diagnosed in people with the age of 65 and over and more than 36% are diagnosed in elderly (aged 75 and over) [2-5] (**Fig. 1.2**). The European Age Standardised Incidence Rates for all cancers in the Great Britain shows an increase by 22% in males from 1975 to 2011 (from 351.8 to 429.8 per 100,000 people) and by 42% in females with an entire rise before the late 1990s (from 263.3 to 375.1 per 100,000) [2-4] (**Fig. 1.3**).

Figure 1.1: Cancer incidence, UK, 2011 [6].

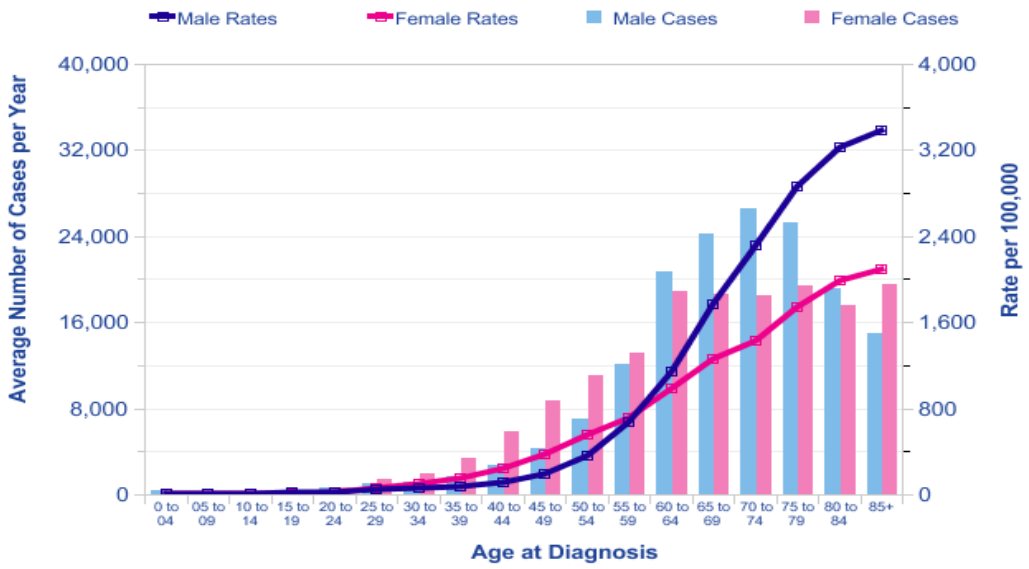

Figure 1.2: Average numbers of new cases for all cancers (excluding non-melanoma skin cancer) per year and age-specific incidence rate, UK, 2009-2011 [7].

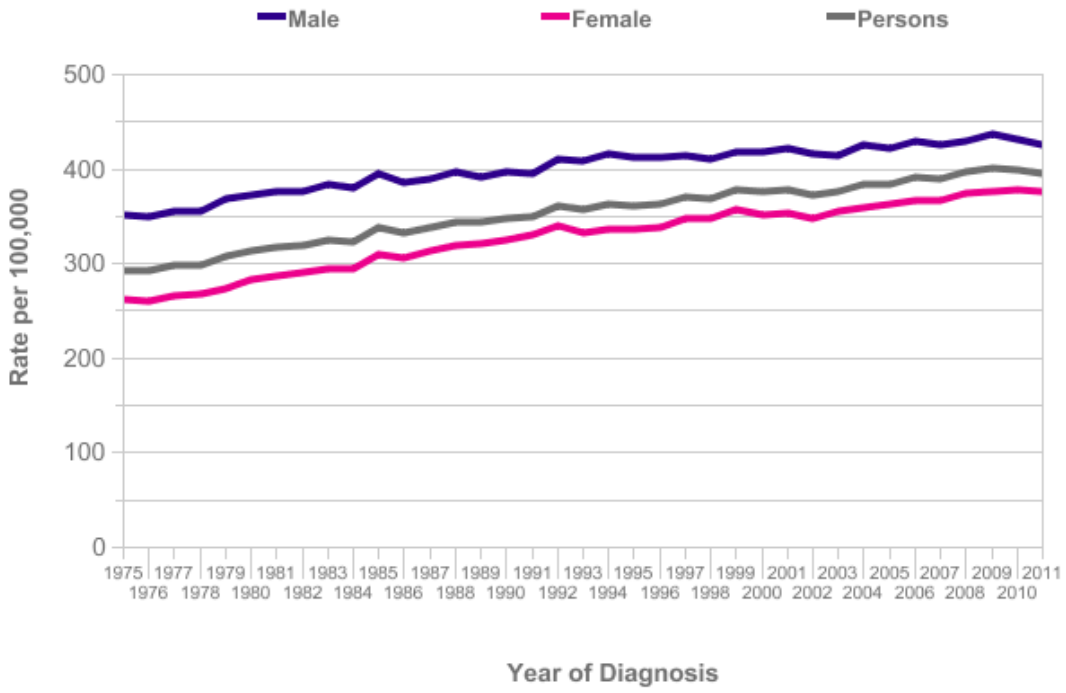

Figure 1.3: All cancers (excluding non-melanoma skin cancer), European Age Standardised Incidence Rates, Great Britain, 1975-2011 [8].

1.1.2 Prostate cancer epidemiology

1.1.2.1 Incidence

Prostate cancer is the most common cancer among men in the UK (2010) which accounting for 25% of all new cases of men cancer [2-5] (**Fig. 1.4**). In 1990, both lung and colorectal cancers were more common in males than prostate cancer but from 1998, prostate cancer became the most common in UK. In 2011, prostate cancer is the 6th most common cancer in whole population and the second common diagnosed cancer among men, worldwide [9]. Also it is the second leading cause of male cancer death (after lung cancer) in the Western countries [10]. In 2011, there were 41,736 new diagnosed cases of prostate cancer in the UK (**Table 1.1**).

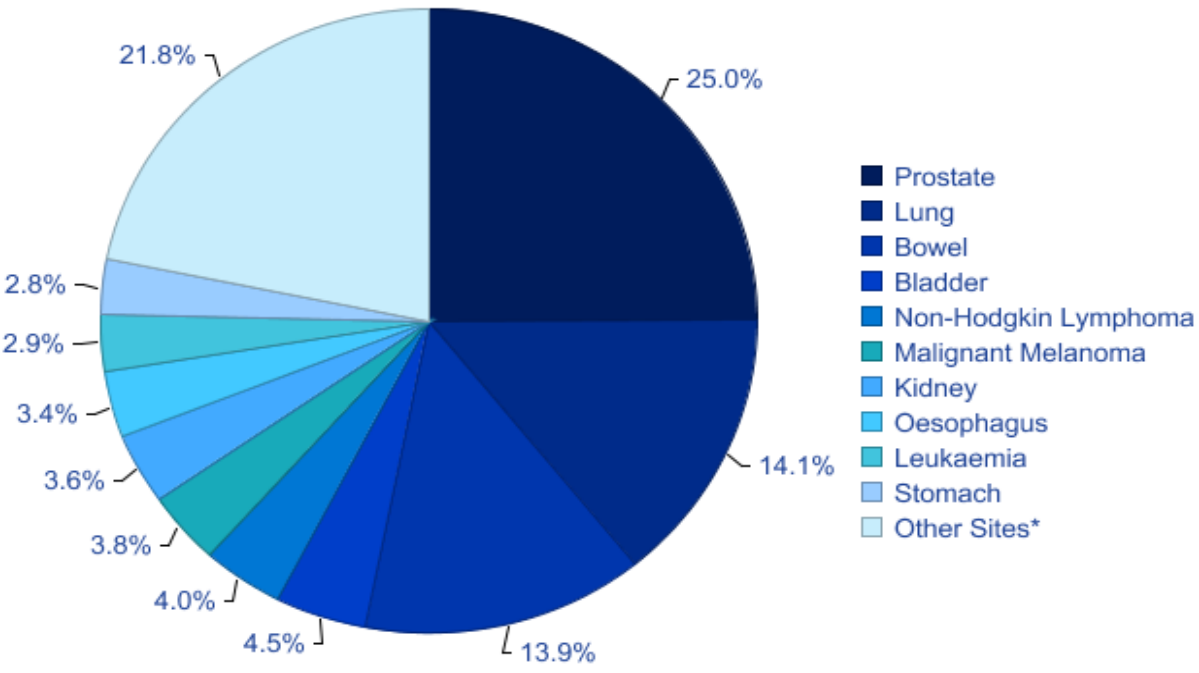

Figure 1.4: Ten most common cancers among men (excluding non-melanoma skin cancer) in the UK, 2010 [11]; Prostate cancer accounted for 25% of cancers following by lung cancer (14.1%), Bowel cancer (13.9%), Bladder cancer (4.5%), Non-HodgkinLymphoma (4%), Malignant Melanoma (3.8%), Kindney cancer (3.6%), Oesophagus cancer (3.4%), Leukemia (2.9%), Stomach cancer (2.8%) and other organ cancer (21.8%).

	England	Wales	Scotland	Northern Ireland	United Kingdom
Cases	**35,567**	**2,346**	**2,817**	**1,006**	**41,736**
Crude Rate	136.1	155.9	110.5	113.1	134.3
AS Rate	**106.7**	**107.0**	**84.8**	**100.7**	**104.7**
AS Rate - 95% LCL*	105.6	102.7	81.7	94.5	103.7
AS Rate - 95% UCL*	107.8	111.3	88.0	106.9	105.7

Table 1.1: Prostate Cancer (C61), number of new cases, Crude and European Age-Standardised (AS) Incidence Rates per 100,000 people, UK, 2011[12-15].

1.1.2.1.1 By age of diagnosis

Incidence of prostate cancer is strongly age-related, with a higher incidence rate in older people. In the UK between 2008 and 2010, about 75% of new diagnosed cases were from men by age of 65 or more and only 1% were diagnosed in the under 50s [2-5] (**Fig. 1.5**).

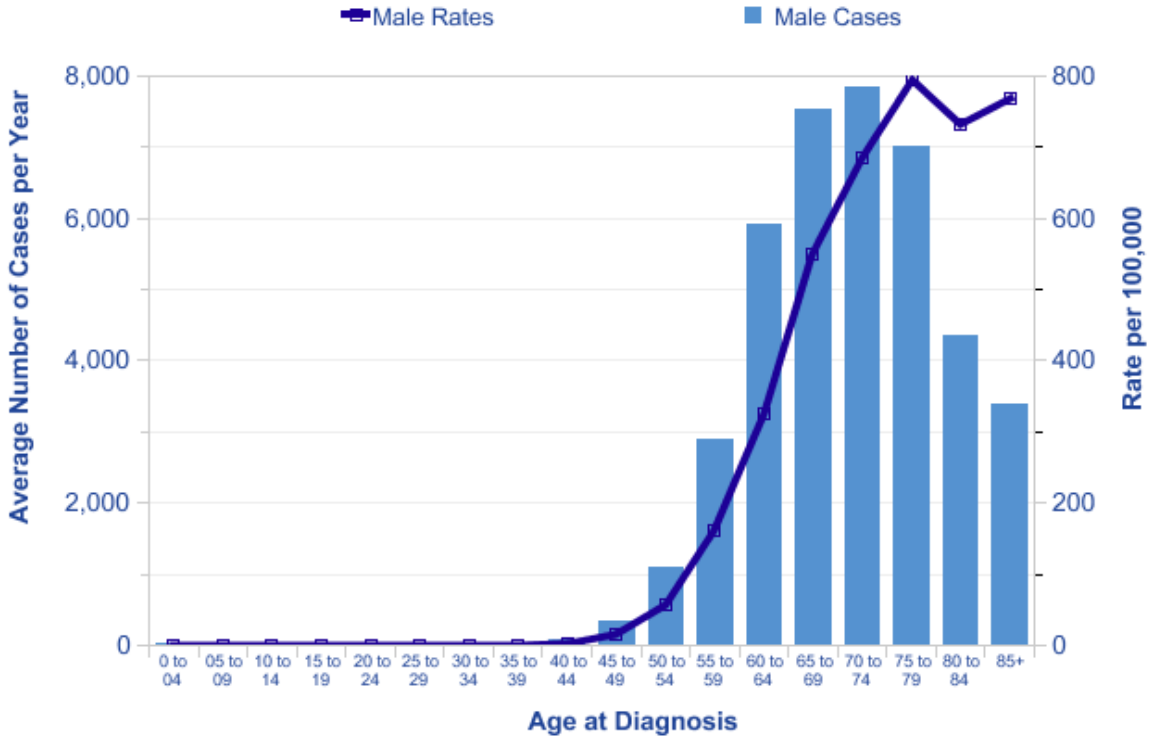

Figure 1.5: Prostate cancer, average number of cases per age of diagnosis, UK, 2008-10 [10].

1.1.2.1.2 Trends by the time

Incidence rate of prostate cancer has increased substantially during recent decades in many countries including Great Britain [16, 17]. Majority of this increase both in the UK and most other countries worldwide can be related to improved detection of prostate cancer during TURP (Trans Urethral Resection of Prostate) or PSA (Prostate Specific Antigen) testing [17, 18]. Prostate cancer incidence rate has increased overall in Great Britain from 1970s which shows a 218% rise between 1975-77 and 2008-2010 [3, 4] (**Fig. 1.6**).Two rapid increase can be seen in this chart: during early 1990s (44% increase between 1989-91 and 1994-96) and early 2000s (34% increase between 1997-99 and 2002-04); these periods related to introduction of PSA testing from the late 1980s [19-21] and increasing PSA testing rate around the late 1990s [22, 23]. During the last decade (between 1999-2001 and 2008-2010), incidence rates of prostate cancer have increased by 22% which may be related to increase detection rate through TURP [24-26].

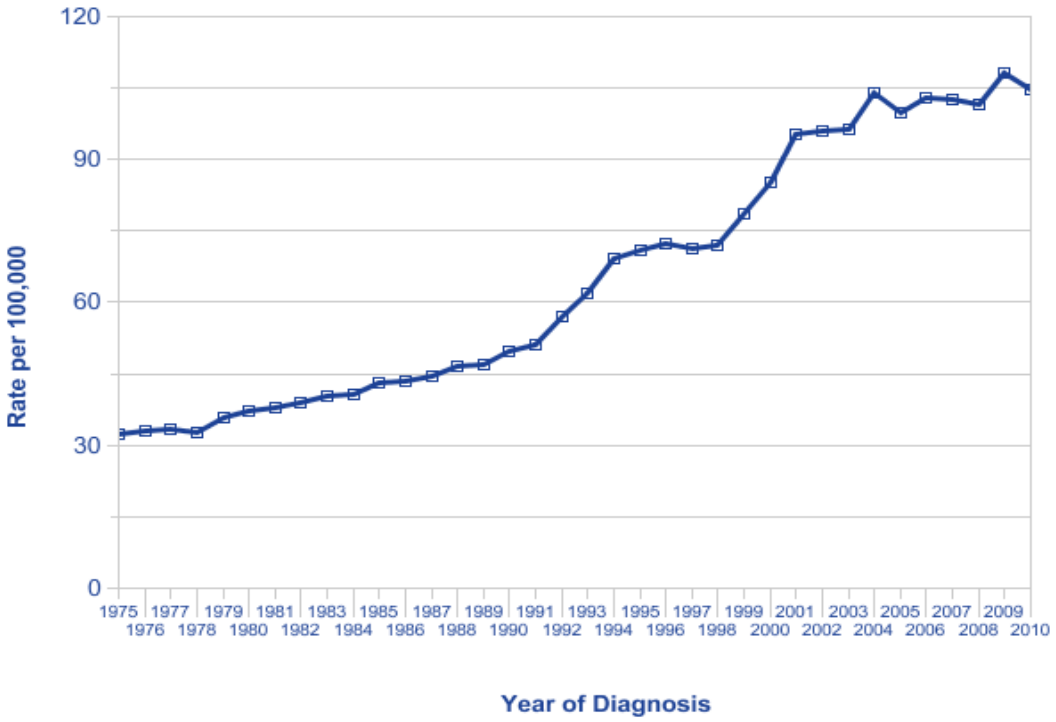

Figure 1.6: Prostate cancer, European age related incidence rates, males, Great Britain, 1975-2010 [10].

1.1.2.1.3 Life time risk

Life time risk is an estimation of risk which a new born child may be diagnosed with a type of cancer during his or her life-time. It is a summary of risk in the population. Genetic and lifestyle factors affect the risk of cancer. The life time risk of developing prostate cancer in the UK in 2010 was 1 in 8 [27].

1.1.2.1.4 Geographic variation worldwide

Prostate cancer is the 6th most common overall cancer with an estimated 900,000 new diagnosed cases in 2011. Rates of prostate cancer vary widely around the world; it is the least common cancer in South-central Asia, more common cancer in Europe and the most common cancer in Australia and New Zealand with around 25-fold variation around the world [10, 28] (**Fig. 1.7**). High risk of developing prostate cancer in black Caribbean and African American men and low risk in Asian men suggest that there may be ethnicity difference [29, 30].

1.1.2.1.5 Socio-economic factors

Incidence rate of prostate cancer is lower in more deprived men, so its incidence rate is strongly inversely correlated with deprivation and poverty [31]. These results are not unexpected, as levels of PSA are generally higher in wealthy people [32].

Figure 1.7: Prostate Cancer (C61), World Age-Standardised Incidence Rates, World Regions, 2011 Estimates [33].

1.1.2.2 Mortality

Prostate cancer is the 4th common cause of cancer death in the UK (2010) , accounting for 7% of all cancer death and the second leading cause of cancer death, after lung cancer in UK males (13% of male cancer death) [34-36]. In 2011, there were 10,793 deaths from prostate cancer in the UK (around 35 in every 100,000 men) [34-36] (**Table 1.2**).

	England	Scotland	Wales	Northern Ireland	UK
Deaths	**9,123**	**900**	**537**	**233**	**10,793**
Crude Rate	34.9	35.3	35.7	26.2	34.7
AS Rate	**23.8**	**21.9**	**21.9**	**21.7**	**23.7**
AS Rate - 95% LCL*	23.4	20.0	20.0	18.9	23.3
AS Rate - 95% UCL*	24.3	23.8	23.8	24.5	24.2

Table 1.2: Prostate cancer mortality rate, UK, 2011[12-15].

1.1.2.2.1 Age of death

Prostate cancer mortality is strongly related to age, with higher death rate in older men. In the UK between 2008 and 2010, around 93% of prostate cancer deaths were in men aged 65 and over and more than half (54%) were in 80s and over [34-36] (**Fig. 1.8**). Prostate cancer became the most common cause of cancer death in men aged 85 and over, with 31% of all prostate cancer deaths between 2008 and 2010, UK [34-36].

1.1.2.2.2 Trend over time

Like incidence rate, prostate cancer mortality rate has also increased in the UK from 1970s [34-36]. Mortality rate has risen from 20 deaths per 100,000 men in 1970s to a peak of 30 deaths per 100,000 men in 1990s; since then mortality rate has gradually fallen to 24 deaths per 100,000 men in 2008-2010 (**Fig. 1.9**). PSA test and improvement in cancer treatment may attribute the recent mortality reduction.

1.1.2.2.3 Geographic variation worldwide

Worldwide cancer mortality data was collected and distributed by WHO (World Health Organization) [37]. Prostate cancer is the 6th common cause of male cancer death worldwide (9th in both sexes). Mortality rate is the highest in the Caribbean men and the lowest in eastern and south-central Asian men by a variation of ten-fold [38] (**Fig. 1.10**).

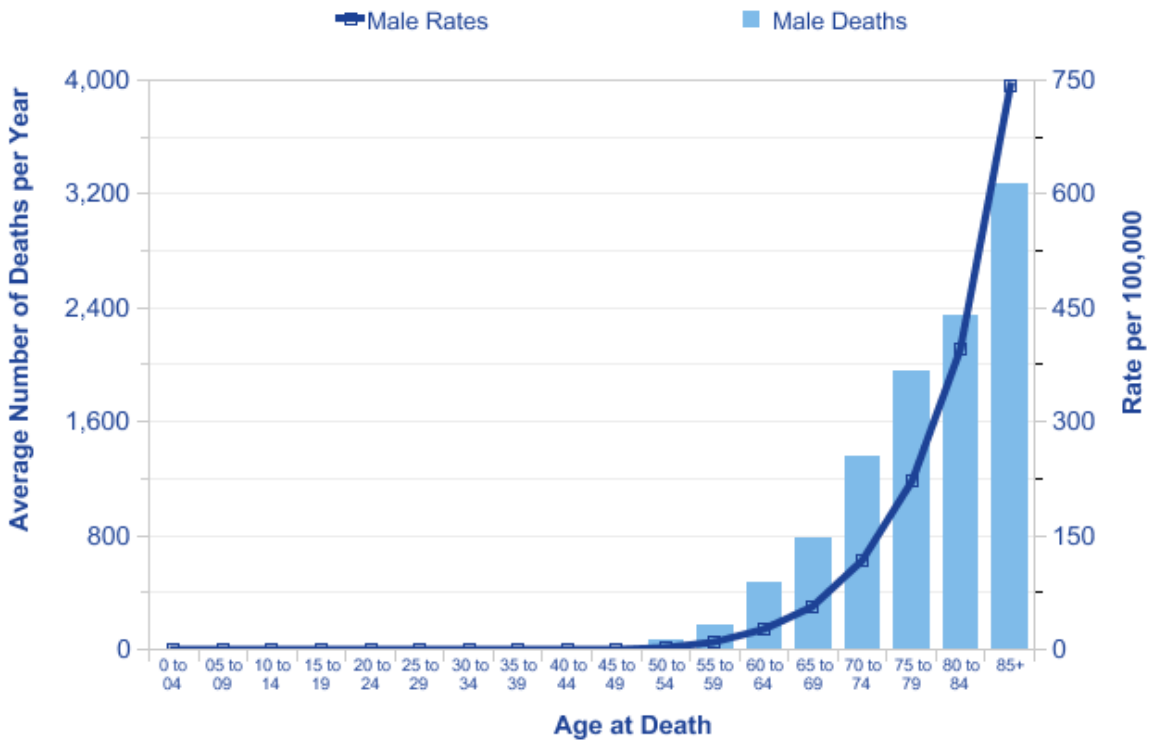

Figure 1.8: Prostate cancer mortality rate in age-specific groups, UK, 2010 [39].

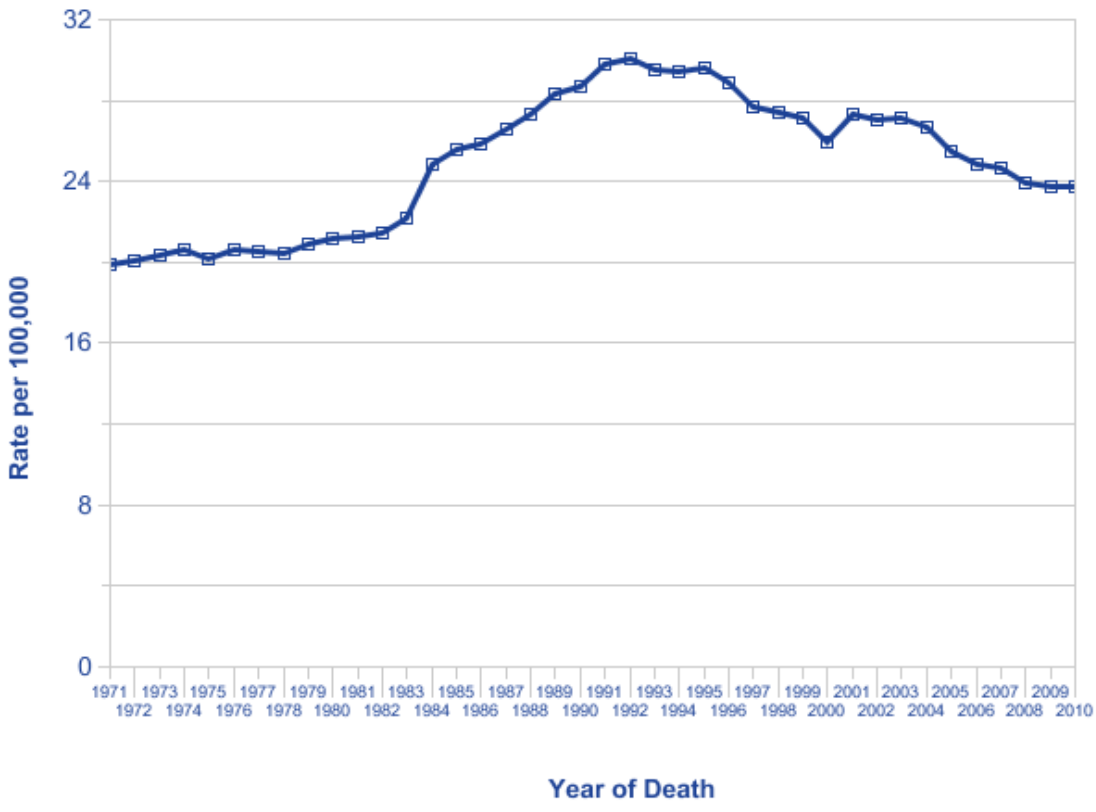

Figure 1.9: Prostate cancer mortality rate, UK, 1970-2010 [39].

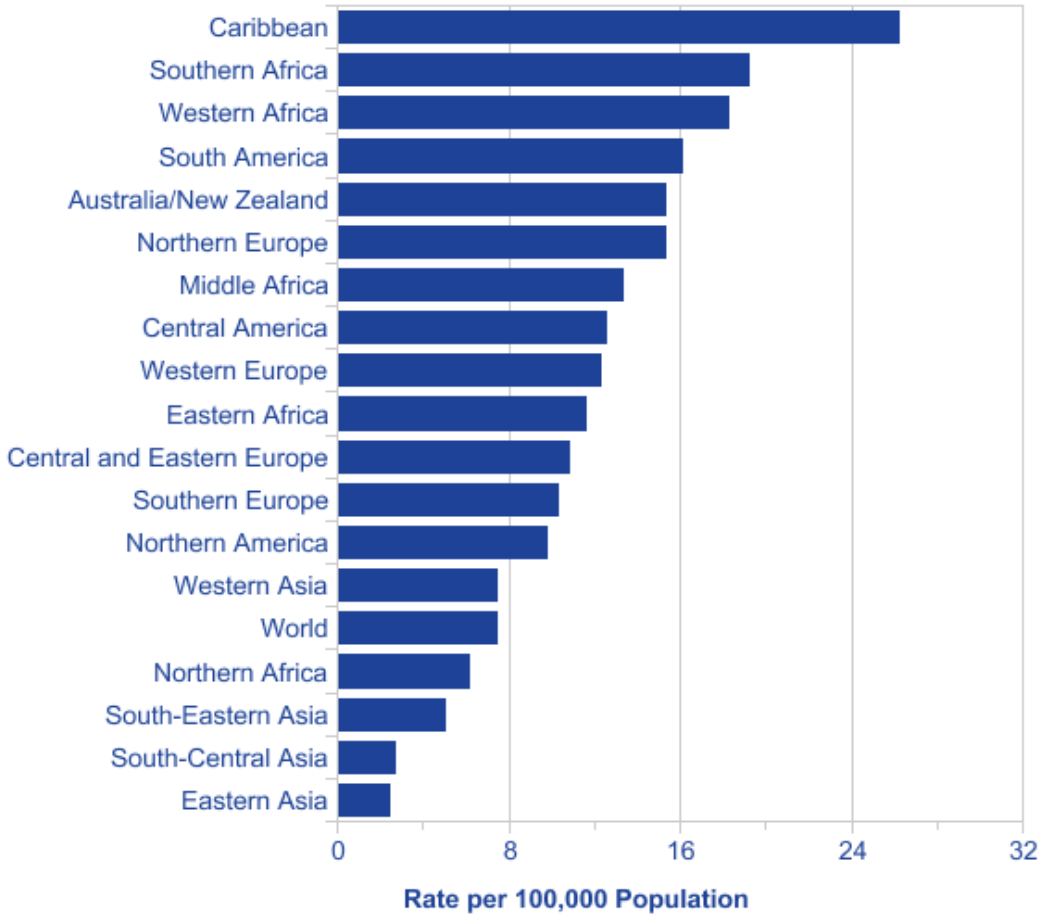

Figure 1.10: Prostate cancer mortality rate worldwide, 2011 [37].

1.1.2.3 Survival

Latest prostate cancer age-standardized relative survival rate in England and Wales between 2005 and 2009 revealed that 93.5% of men were expected to survive from prostate cancer in the first year of diagnosis which fell to 81.4% in the 5th year (**Table 1.3**) [40-42]. High survival rate was related to early detection of greater proportion of latent and slow growing tumours by TURP and PSA testing. Like most other cancers, relative survival for prostate cancer improves due to screening (PSA test), although some improvement may come from treatment. Five year survival rate increased from 31% in England and Wales during 1971-75 to 81.4% in England during 2005-9 [40, 43-45] (**Fig. 1.11**). Prostate cancer relative survival rate also strongly related to stage of the disease at the time of diagnosis. For cases without

metastasis, five year survival rate in England during 1999-2002 was 90% or higher but reduced to around 30% for metastatic cancers [46].

	Relative Survival (%)		
	1 Year	5 Year	10 Year
Sex	2005-2009	2005-2009	2007*
Male	93.5	81.4	68.5

Table 1.3: Prostate cancer one, five and ten year survival rates in England 2005-2009 and Wales 2007 [40, 47].

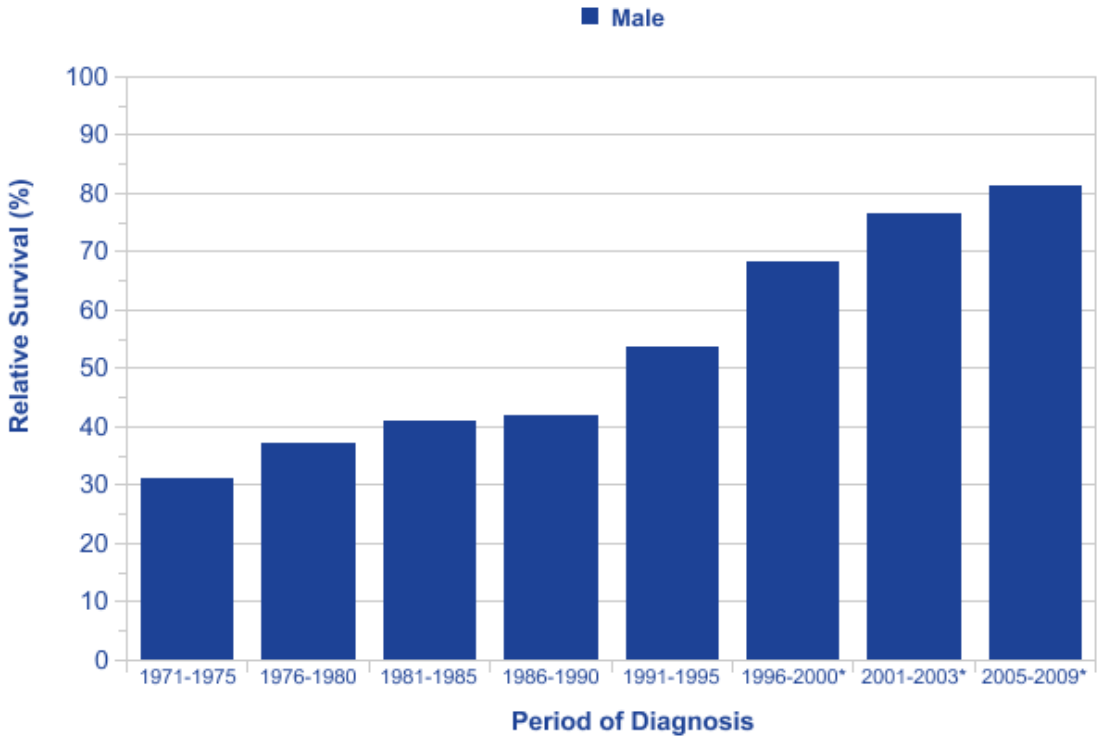

Figure 1.11: Prostate cancer relative survival rates, England and Wales 1971-1995, England 1996-2009 [48].

1.1.2.4 Risk factors

1.1.2.4.1 Family history

Past history of prostate cancer in first-degree relatives increases the risk of cancer by 120-150% [49-51]. Risk will increase in a man with affected father by 120-140% and with affected brother by 187-230%. The risk increase is higher when more than one first-degree relative is affected. Risk increase also reported in man with a second-degree affected relative by 90-150% [49-51]. Risk increase has been reported in men with mothers affected from breast cancer by 19-24%, but risk did not increase in men with sister diagnosed by breast cancer [52, 53]. Germ line mutation in BRCA2, breast cancer gene, can increase the overall risk of developing prostate cancer in men, up to five-fold and in men below 65 years old, by seven-fold [54]. It has been estimated that, about 5-9% of prostate cancer cases are associated with genes and family history [55].

1.1.2.4.2 Ethnicity

The latest England-wide data show that the black men have the highest prostate cancer risk , followed by the white ones, while Asian men (especially Chinese ethnicity) have the lowest risk [56]. A cohort study showed that risk increase related to black ethnicity is higher in younger ages, and black men may be diagnosed 3-5 years sooner than white men [30, 57, 58].

1.1.2.4.3 Other cancers

It has been shown that previous renal cell (kidney) carcinoma increase the risk of prostate cancer up to 69% [59, 60]. This associated risk was reported to be higher in cases with positive family history of prostate cancer [61]. Previous history of bladder cancer, melanoma and lung adenocarcinoma have been shown to increase prostate cancer risk by 14-151%, 15-50% and

56%, respectively [62-65]. Past history of thyroid cancer has also been shown to be related with increased prostate cancer risk [66].

1.1.2.4.4 Radiation

There were some evidences that exposure to gamma, x-ray and thorium-232 increased prostate cancer risk [67].

1.1.2.4.5 Insulin-like growth factor-1

High levels of insulin-like growth factor-1 (IGF-1) have been shown to be related to the increased risk of prostate cancer (38-83%) [68, 69]. Levels of IGF-2, IGFBP-1 and IGFBP-2 have not been shown to be related to prostate cancer [69, 70].

1.1.2.4.6 Factors associated with lower prostate cancer risk

World Cancer Research Fund/American Institute for Cancer Research (WCRF/AICR) reported that food containing higher level of lycopene (type of plant vitamin A) or selenium (a trace mineral) may protect against prostate cancer [71]. Men with high body levels of selenium and lycopene have shown to have a reduced prostate cancer risk by 26-71% and by 16-24%, respectively [72-75]. Some limited study in Asian population revealed that high intake of soy reduced risk of prostate cancer by 26-31% [76, 77]. Case-control and cohort studies showed that the exposure to warfarin (a vitamin K antagonist) was associated with a 17-31% reduction in prostate cancer risk [78-80]. Previous studies also showed that men, who were diagnosed by diabetes mellitus at least five to ten years earlier, had a 21% reduction in the risk of prostate cancer [81]. However it is still controversial that pathological events happening during the diabetes mellitus is the main reason or for example anti-cancer effects of anti-diabetes drugs [82].

1.2 Pathology of prostate cancer

1.2.1 Prostate anatomy

Prostate, an oval-shaped gland is a part of male reproductive and urinary system. Prostate surrounds the neck (base) of the bladder [83]. It is covered by a fibro muscular layer called prostate capsule which divide prostate to three different zones (**Fig. 1.12**); the peripheral zone (PZ) which consists about 70% of prostate volume, is the commonest location for prostatic intraepithelial neoplasia (PIN) and adenocarcinoma. The central zone makes up 25% of the total prostate mass, surrounds the ejaculatory ducts and accounts for only 2.5% of prostate cancers although these cancers tend to be more aggressive [84]. The transitional zone (TZ), which accounts for 5% of the prostate volume, is the primary site of benign prostatic hyperplasia (BPH).

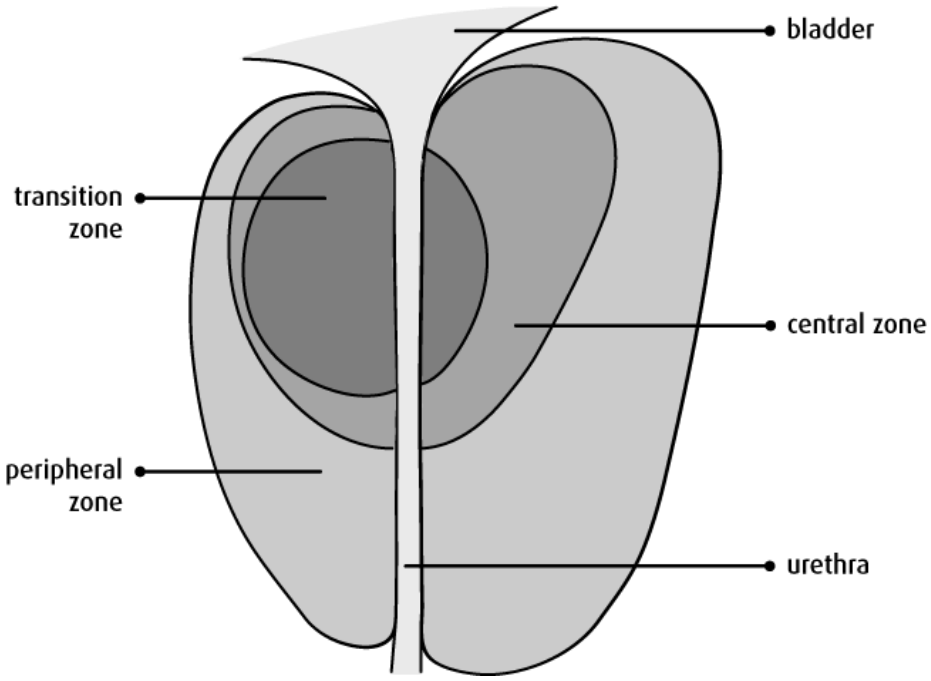

Figure 1.12: Schematic illustration of Prostate gland zones [85].

1.2.2 Normal prostate cells

Mainly, three different types of cells can be detected in prostate epithelium: Luminal cells, basal cells and neuroendocrine cells (**Fig. 1.13**). Basal lamina contains a series of stem cells which potentially work as a reservoir to generate all these three cell types [86].

Luminal cells have the highest population in prostate and secret prostatic proteins including PSA and prostatic acid phosphatase (PAP), two important prostate cancer biomarkers. Luminal cells are androgen dependent cells which express high level of androgen receptor (AR) [87]. Luminal cells are distinguished by the expression of cytokeratin (CK) 8 and 18, filament high molecular weight proteins. As 95% of prostate adenocarcinomas are originated from luminal cells, the levels of biomarkers such as PSA, CK8 and CK18 are expected to be increased in the cancer cells [88].

Basal cells, the second large population in prostate epithelial cells are located between luminal cells and basement membrane and express high molecular weight proteins like CK5 and CK14. Unlike luminal cells, basal cells neither secret any prostatic protein nor are dependent on androgen; so they do not go to apoptosis in androgen ablation situations [89, 90]. However, they express anti-apoptotic gene *Bcl-2* and free-radical scavenger GST-$\boldsymbol{\pi}$ which protect against DNA damage [91].

Neuroendocrine cells spread in all acini epithelium and ducts which can produce serotonin, thyroid stimulating hormone and Chromogranin A. They produce neuropeptides which are supportive factors in vitality and proliferation of luminal cell [91]. Neuroendocrine cells finally differentiate to androgen independent post-mitotic cells, which express neuropeptide Y [92]. Because of the immune-reactivity to neuropeptide Y in up to 75% of prostate cancers, it is supposed to have a main role in prostate cancer growth and expansion [93]. It has been proved in some studies that levels of neuroendocrine factors have a positive correlation with the advanced stage of prostate adenocarcinomas [94, 95].

Using specific biomarker such as $\alpha_2\beta_1$-integrin and $\alpha_2\beta_1^{hi}/CD133^+$, some research groups have confirmed the presence of the prostate stem cells within basal layer (about 1% of human prostate basal cells) [96] which have high potential to generate fully differentiated prostate epithelium *in vivo* [97, 98].

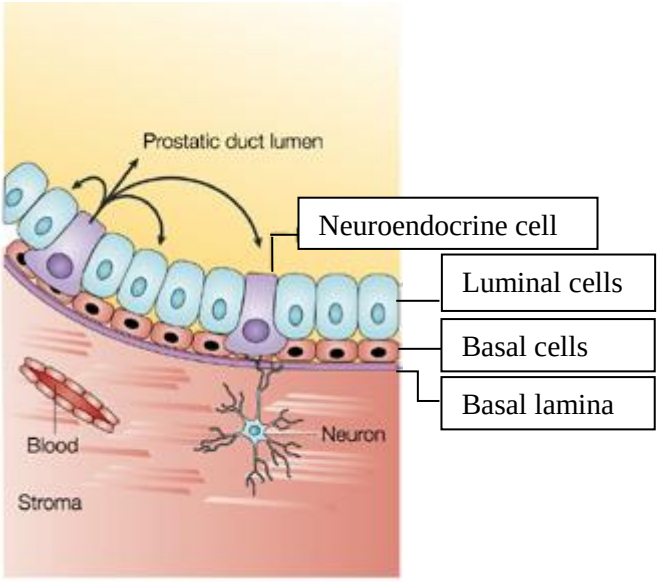

Figure 1.13: Schematic illustration of cells in human prostate epithelium [99]; three different types of cells can be detected in prostate epithelium: Luminal cells, basal cells and neuroendocrine cells. Basal lamina contains a series of stem cells with potential capability to generate all these three cell types.

1.2.3 Prostate cancer

1.2.3.1 Benign prostatic hyperplasia (BPH)

Non-malignant overgrowth of prostate cells is defined as BPH. Both BPH and prostate cancer are age-related and require androgen stimulation, so they are often found concurrently. However, BPH is not a precursor for prostate cancer [100]. BPH develops in transition zone, a ring of tissue around the urethra and its growth is inward toward the prostate's core, constantly tighten around the urethra and associate with lower urinary tract symptoms (LUTS). On the other hand, most of prostate carcinomas initiate from outer peripheral zone then invade to surrounding tissue. Although the pathogenesis of BPH is still poorly understood, some studies indicate that BPH relates to hormonal changes occurring in aged men [101]. Testis produces testosterone hormone which derives to 5-alpha-dihydrotestostron (DHT) and estrogen in target organs. It has been hypothesized that high level of DHT, which is involved in prostate growth, may trigger BPH initiation [102].

1.2.3.2 Prostatic Intraepithelial Neoplasia (PIN)

PIN is the earliest identifiable stage of prostate carcinogenesis and identified by abnormal proliferation of luminal epithelium cell with pre-existing of acini and ducts without any invasion to surrounding stroma [86]. It co-exists with cancer in more than 85% cases and unlike cancer which lacks of basal layer, PIN remains intact or fragmented [103]. PIN can be divided into two subgroups: low-grade and high-grade, according to their cellular crowding features, nuclear enlargement, chromatin patterns and nucleolar appearance [103]. Also basal layer shows frequent interruption in high-grade PIN but remain intact or rare interrupted in low-grades [104]. From the architectural point of view, high-grade PIN can be divided into four different groups: Tufting, Micropapillary, Cribriform and Flat [105]. Tufting is the most common pattern (97%), although multiple patterns can be found in most of the cases. Currently, the World

Health Organization (WHO) recommended using PIN term as a representative of high-grade PIN. Many studies described common properties of PIN and prostate cancer (epidemiologically, histologically and cytogenetically) and the importance of high-grade PIN as a biomarker or precursor for detection of potential prostate cancer [106].

1.2.3.3 Prostate cancer grading by Gleason scores

Combined Gleason scores are a grading system for prostate cancer proposed by Dr. David Gleason in 1960s which use to describe the degree of morphological changes in prostate cancer [107]. Nowadays, it is the most widely used method to evaluate the prognosis of men with prostate cancer.

In the Gleason grading, histological patterns were categorized at low magnification according to the extension of glandular differentiation and growth pattern of tumour in prostate stroma. Glandular patterns were classified from well-differentiated (grade 1) to anaplastic (grade 5) according to their morphological appearance (**Fig. 1.14**). Combined Gleason scores are the sum of the score of the major lesion and the score of the secondary lesion. Each lesion is measured by 5 different scores and thus the highest combined Gleason scores are 10 and the lowest are 2. The Gleason grading system has been simplified by compressing the scores into three groups: well differentiated (Gleason scores <6), moderately differentiated (Gleason scores 6-7) and poorly differentiated (Gleason scores 8-10). Combined Gleason scores were commonly used as prognostic indicator in prostate carcinomas and in correlation with all important pathologic parameter and clinical outcomes [103].

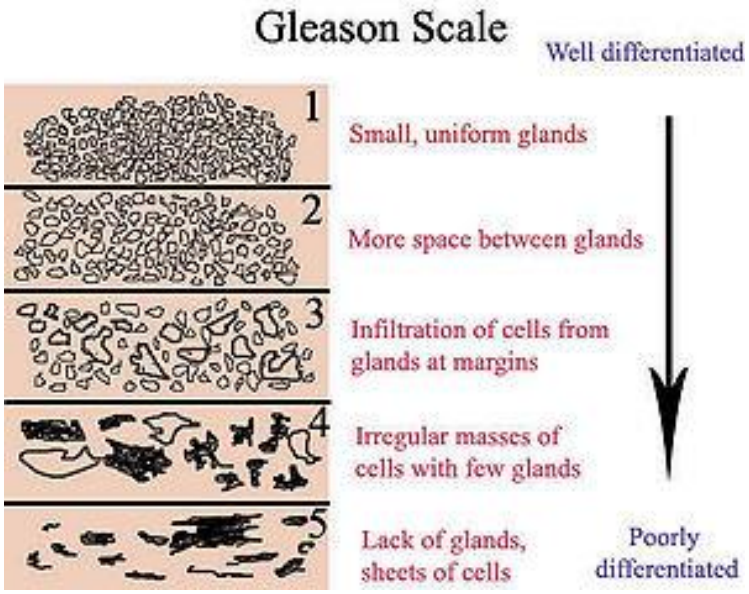

Figure 1.14: Schematic diagram of Gleason grading system [2].

1.2.4 Prostate cancer cell lines

To show the pathogenesis and malignant progression of prostate cancer a wide range of prostate cell lines have been studied, varied from benign PNT2, through less malignant LNCaP and moderately malignant 22RV1, to highly malignant DU145, PC3 and PC3-M.

1.2.4.1 PNT2

Normal human prostate cell line, initially derived from prostate epithelial cells of a dead 33 year old man and immortalized by transfecting with Simian virus 40 (SV40) [4, 5]. Their population doubling time is about 40 hours. They are androgen-dependent and express PSA, PAP, CK 8, 18 and 19 which are markers of differentiated luminal cells of prostate glands. There is no tumorigenic ability when inoculated in nude mice [108].

1.2.4.2 LNCaP

The LNCaP cells are derived from moderately-differentiated lymph node metastasis of prostate cancer [5]. Their population doubling time is 60 hours. They express high level of androgen receptor in nucleus and their growth rate increase in response to androgen. Animal studies show earlier tumour growth in male animals compare to females, due to possible higher sensitivity to androgen [3], however no metastatic spread detected in inoculated animals [109]. LNCaP cells express CK8, 18 and wild type TP53. In culture medium, they grow in clusters.

1.2.4.3 22RV1

22RV1 is a human prostate carcinoma epithelial cell line derived from a xenograft that was serially propagated in mice after castration-induced regression and relapse of the parental, androgen-dependent CWR22 xenograft. Their population doubling time is about 49-56 hours. 22RV1 cells express PSA, their growth is weakly stimulated by DHT and androgen receptor can be detected in its lysate by western blotting [110].

1.2.4.4 DU145

Moderately-differentiated prostate cancer cell line derived from brain metastasis [5]. Their population doubling time is about 34 hours. They are not hormone sensitive and express low level of PAP and do not express PSA, AR and human glandular kallikrein (hK2) [111]. DU145 cells express filament proteins, CK5, 8 and 18 which confirms its derivation from epithelial cells [112, 113] . Animal studies show metastasis in liver, spleen, lung, adrenal, kidney, lymph node and diaphragm when tumour cells inoculated in nude mice [114].

1.2.4.5 PC3 & PC3-M

PC3 and PC3-M cell lines initially derived from a poorly-differentiated bone marrow metastasis of prostate cancer [5, 115]. Their population doubling time is about 33 hours. They are androgen-independent, do not express PSA and show high rate of tumorigenicity and metastasis when they are inoculated in nude mice [116]. PC3-M cell line was established from the selection of the most aggressive sub-population from the parental PC3 cells [117].

1.2.5 Biomarkers and Oncogenes in prostate cancer

Current diagnosis and informed treatment decisions for prostate cancer are based on digital rectal examination (DRE), PSA and subsequent biopsies for histopathological staging [118]. In practice, each procedure has its shortcomings and, has led to the over-treatment of low-risk patients [119], unnecessary biopsies and non-essential radical prostatectomies [120, 121]. Major biomarkers can be used to assist decision-making on designing appropriate treatment strategy for individual patients, to detect advanced disease at an earlier stage, and to predict metastatic cancer and re-occurring disease following prostatectomy. A biomarker is defined by The National Cancer Institute as "a biological molecule found in the blood, other body fluids, or tissues that is a sign of a normal or abnormal process or of a condition or disease" [122]. So the ideal biomarker should be used to screen the disease and its progression, to identify high-risk individuals, to predict recurrence and to monitor response to treatments. It should be economical, consistent, non-invasive, easily accessible, and quickly quantifiable [123].

1.2.5.1 Prostatic Acid Phosphatase and Prostatic Specific Antigen

Prostatic acid phosphatase (PAP) is a dimer glycoprotein, produced predominately by prostate and was used as a serum biomarker to detect prostate cancer metastasis [124], but after development of PSA test, PAP replaced by PSA because of its low sensitivity in detecting localized disease [125].

PSA, a 33 kDa serine protease (human kallikrein-3), is secreted by the epithelial cells of the prostate. The 6 kb PSA gene is located in chromosome 19 and codes for a single chain 33 kDa glycoprotein [126]. It is secreted from the prostatic epithelium into the secretory ducts to contribute to the seminal fluid and to liquefy seminal coagulum by cleaving the protein semenogelin into small peptides hence increasing sperm motility [86]. However, the basal-cell layer disruption in prostate cancer, allows PSA to leak into the circulation resulting in elevated serum levels of PSA. Serum levels of PSA may be increased by non-cancerous BPH, prostatitis, diet alterations, some medications and certain environmental factors but rarely by other human malignancies [127, 128]. PSA levels cannot be used to clearly distinguish the difference between benign and malignant diseases; it cannot reflect different stages of the cancer; thus PSA test is not a very sensitive or specific method which may not be reliably used as foundations for making accurate therapeutic decisions [129]. Using the traditional cut-off point of PSA in screening studies (≥4 ng/mL) as an indicator for prostate biopsy, the sensitivity and specificity of PSA for detecting cancer have been estimated about 40-50% and 60-70%, respectively [130-132]. Other studies suggested that using a cut-off point ≥ 10 ng/ml to increase its sensitivity and specificity in prostate cancer detection to 72% and 95%, respectively [132]. Although, PSA is currently used as diagnostic and prognostic biomarkers for prostate cancer worldwide, some large clinical trials have casted some doubts on the effectiveness of screening the general population with PSA detection to identify the cancer patients [133, 134]. To increase the diagnostic accuracy of PSA test, it has been refined by measuring different molecular forms of PSA and rate of PSA increase as total PSA (tPSA). tPSA refers to the sum of free PSA (unbound) and bound PSA (complexed predominantly to α-1-antichymotrypsin) [135]. Whilst the level of tPSA is largely influenced by the level of free PSA, it still produces high false negatives or positives [136]. Although refinement of the tPSA assay can improve its diagnostic efficiency, tPSA still fail to fulfil the necessary standard of

an appropriate biomarker. These issues have highlighted the need of more accurate diagnostic and prognostic biomarkers for prostate cancer.

1.2.5.2 Over-detection and over-treatment of prostate cancer

With the widespread screening and aggressive diagnostic practices in recent years, more prostate cancer cases have been diagnosed and prostate cancer has now become the most commonly diagnosed solid male cancer in the developed countries. However prostate cancer autopsy studies showed that men with high prevalence rates of small, indolent tumours usually died from other causes which led to increased concern for the over-detection and over-treatment of prostate cancer [137]. Over-detection cannot only cause the cost burden to the patients; it can also lead to over-treatment and cause significant patient anxiety when facing the difficulty in choosing the alternative modalities. Over-treatment can cause considerably unnecessary decrements in quality of life, especially with regard to urinary incontinence and sexual dysfunction [138]. The recent results from the European Randomized Study of Screening for Prostate Cancer (ERSPC) revealed that among the 1,068 men in the screening program for PSA, it was estimated that for one life saved, 48 men were required to be treated [119]. Currently published results described the institutional experiences in active surveillance. Postponing selective therapy was suggested as a way to deal with men with low-grade, early-stage prostate cancer [139-144]. D'Amico defined low-risk prostate cancer as "Gleason score of $\leq$ 6 or $\leq$ 7 (3+4), PSA < 10 ng/ml and a tumour that is either non-palpable or only palpable in less than half of one lobe of the prostate (clinical stage T1c or T2a)" [145]. In those "active surveillance" studies, men were followed carefully with serial PSA assessments (every three months for two years at first; and then every six months), repeated biopsies (every six months for first year and then every 3-4 years) and in some cases other tests were employed to identify early signs of progression (such as MRI). Although active surveillance is becoming widely accepted [146], this strategy still relies on serial PSA assessments and repeat biopsies. In

addition to the invasive nature, repeated biopsies also carry other significant risks such as subsequent infection and short-term disturbances on quality of life [147, 148]. As the effectiveness of PSA screening is still under question, it is urgently needed to search for more sensitive and specific biomarkers.

1.2.5.3 Potential biomarkers

Blood, urine, semen and prostate tissue are the biomaterial sources that could be used to identify prostate cancer biomarkers. Serum proteomics analysis is a useful method for searching for biomarkers, but this method is facing the challenges presented by the wide range of protein concentrations. Another difficulty for using this method is to find low-abundance proteins due to the masking effects of high-abundance proteins. Other problems for serum proteomics include the interference produced by high levels of salts and other compounds, extreme variations among individuals and lack of reproducibility [149]. Semen is a relatively non-invasive material for analysing prostate biomarkers, in which proteins originated from prostate can be directly accessed; but it varies among different patients. Urine has become a popular source for identifying proteomic biomarker, due to its non-invasive nature. The problem for using urine is that the urine generally contains low concentration of biomolecules [123]. Genomic analysis is widely used for studying disease biomarkers. Genome wide analysis can stratify those people who have high cancer risk. Germ line genetic markers are widely used markers, their levels do not fluctuate over time and they are available for assay at any age [150]. Identifying biomarkers and understanding the key cancer-related pathways are essential for the development of new and improved diagnostic and predictive tools. A number of potential biomarkers have been identified and their predictive values for prostate cancer were studied. Apart from PSA, many other biomarkers have been reported and their diagnostic and prognostic significances were studied for prostate cancer [151]. These markers include, but not limited to: breast cancer mutated gene (*BRCA1*/*BRCA2*) (Tumour

suppressor) [152, 153], prostate cancer antigen 3 (*PCA3*) (non-coding RNA) [154, 155], *TMPRSS2-ERG* fusion gene (Transcription factor) [156, 157], early prostate cancer antigen 2 (*EPCA2*) (nuclear matrix protein) [158, 159], Interleukin-6 (IL-6) (Cytokine) [160], S100 family proteins (Calcium-binding protein family) [161, 162], Transforming growth factor β1 (*TGF β1*) (cytokine) [163, 164], Prostate Stem Cell Antigen (*PSCA*) (glycoprotein) [165, 166] and Cutaneous fatty acid binding protein (*C-FABP*) (cytoplasmic lipoprotein) [167, 168].

1.2.5.3.1 *BRCA1/2* gene mutation

BRCA1 and *BRCA2* are tumour suppressor genes. Germ-line *BRCA2/BRCA1* mutations produce a hereditary breast-ovarian cancer syndrome in affected families which also associated with higher prostate cancer risk (8.6-fold and 3.4-fold, respectively) in men ≤ 65 years [169, 170]. Studies revealed that a wide spectrum of pathogenic mutations in *BRCA2/1* conferred a more aggressive prostate cancer phenotype with a higher probability of locally advanced metastatic diseases. Furthermore *BRCA2* mutation was detected as a prognostic factor associated to poorer survival [153]. Mutation of germ-line *BRCA2/BRCA1* presented in 1.2% and 0.4% of prostate cancer cases [169, 170].

1.2.5.3.2 Prostate cancer antigen 3

Prostate cancer antigen 3 (*PCA3*) is a commercially available diagnostic marker. This non-coding RNA is only expressed in the prostate, and can be detected in urine and prostatic fluid. Since PCA3 test requires digital massage of the prostate prior to urine collection, it is considered more invasive than blood-based tests. It is over expressed in 95% of biopsies from prostate cancer patients compared to healthy or BPH patients with a high specificity [154]. A PCA3 level of >35 units in urine has been recorded with an average sensitivity of 66% and specificity of 76% for the diagnosis of prostate cancer compared to serum PSA (specificity of 47% and 65% sensitivity) [155]. Reliability of this test is depended on a full prostate massage

through DRE just before taking the urine sample, so it is not pleasure and varies due to examiner.

1.2.5.3.3 *TMPRSS2-ERG* gene fusion

TMPRSS2-ERG is the most frequent gene fusion present in prostate cancer, which has been greater than 90% specificity and 94% positive predictive value [156]. Unfortunately, a clinical diagnostic test is still not available for this marker and current evidence did not support the prognostic significance of *TMPRSS2-ERG* analysis with equivocal findings regarding outcomes [156]. *TMPRSS2-ERG* gene fusion has been found in patients with good prognosis [157], with no association to prostate cancer incidence or Gleason score [171].

1.2.5.3.4 Early prostate cancer antigen 2 (*EPCA2*)

Prostate cancer associated nuclear structural protein is expressed in prostate adenocarcinomas, can be detected in serum and its increased measurement in blood is correlated with tumour progression and poor prognosis [159]. Some studies implied that EPCA2 expression might occur early during the development of cancer so it may be used as a potential predictive marker for the onset of incidental prostate cancer. However tissue EPCA2 staining and plasma EPCA absorbance were not found to be correlated with tumour stage and Gleason scores in patients with prostate cancer [158].

1.2.5.3.5 Interleukin-6 (IL-6)

IL-6 is involved in the host immune defence mechanism (mediates B cell differentiation) as well as the modulation of growth and differentiation in various malignancies [172]. Overexpression of IL-6 was shown in relation with tumour progression through inhibition of cancer cell apoptosis, stimulation of angiogenesis, and promotion of drug resistance. Increased serum IL-6 concentration has been reported in association with advanced tumour

stages of various cancers (e.g., multiple myeloma, non-small cell lung carcinoma, colorectal cancer, renal cell carcinoma, prostate cancer, breast cancer and ovarian cancer) and short survival of the patients. In patients with high levels of IL-6, the response to treatment with chemotherapy and hormone therapy was worse than those with low levels of IL-6 [173]. Therefore, blocking IL-6 signalling may be considered as a potential therapeutic strategy (i.e., anti-IL-6 therapy) in those who have been characterized by pathological IL-6 overproduction. Further investigations in xenograft tumour models are needed to establish the therapeutic efficacy of anti-IL-6 therapy in human cancer [160].

1.2.5.3.6 S100 Protein family (Calcium-binding protein family)

The multi-gene calcium binding proteins, more commonly known as the S100 protein family, are involved in protein phosphorylation, enzyme activity and calcium homeostasis of cells. They are also involved in regulation of transcription factors, macrophage activators and modulators of cell proliferation [174]. Recently, it has been shown that they were involved in a variety of intracellular and extracellular functions including cell growth, cell-cell communication, energy metabolism and intracellular signal transduction [175]. Furthermore their different expression in neoplastic tissues was compared to normal tissue and their involvement in the metastasis process has been revealed [162]. At least seventeen S100 genes were recognized on human chromosome 1q21, a region frequently rearranged in several types of cancer [176]. Several proteins from this family, including S100A2, S100A4, S100A8, S100A9 and S100A11, are associated with prostate cancer recurrence and progression to higher pathological stages [161, 177]. Although S100A4 overexpression was detected in prostate cancer cell lines and tissues, it was not significantly associated with poor patient survival [178].

1.2.5.3.7 Transforming growth factor β1 (*TGF β1*)

TGF β1 involves in the regulation of cellular proliferation, chemotaxis, immune response, differentiation and angiogenesis. Increased expression of *TGF β1* in prostate cancer was correlated with severe tumour grade, invasion, metastasis (to regional lymph nodes and bone) and biochemical recurrence [164]. More validation is needed before *TGF β1* can be used as a prostate cancer biomarker [179].

1.2.5.3.8 Prostate Stem Cell Antigen (*PSCA*)

Prostate Stem Cell Antigen (*PSCA*) is a member of the Thy-1yLy-6 family of glycosyl-phosphatidyl-inositol, involved in regulation of cell proliferation. Its' up-regulation has been detected in both androgen-dependent and independent prostate cancer xenografts and is correlated with Gleason scores, advanced stage and metastatic progression [180, 181]. Exact biological function of *PSCA* is unknown; but its cell surface location makes it a putative target for therapy and diagnosis [123]. The expression of PSCA in prostate cancer supports the concept that cancers arise from transformation of basal cells [182]. But using PSCA as a serum marker need to develop better methods for detection and measurement [181].

1.2.5.3.9 Cutaneous fatty acid binding protein (*C-FABP*)

Cutaneous fatty acid protein (*C-FABP*) is also known as epidemic-FABP (E-FABP), psoriasis associated-FABP (PA-FABP), keratinocyte-FABP (K-FABP) or FABP5.Gene coding for C-FABP is located at chromosome 8q21.13. FABP5 is a 15 kDa cytosolic protein from fatty acid binding protein family with high affinity to bind with long chain fatty acids and other lipophilic substances like eicosanoid and retinoid [183]. C-FABP is expressed most abundantly in epidermal cells of the skin. However its wide expression has been detected in endothelial cell of placenta, skin, tongue, adipocyte, brain, intestine, kidney, liver, Clara and Goblet cells of lung, heart, skeletal muscle, testis, retina, lens, spleen, mammary gland, dendritic cell and

macrophage [184]. FABPs are involved in fatty-acid import, storage and export as well as cholesterol and phospholipid metabolism [185]. They have also been proposed to sequester and/or distribute ligands to regulate signalling processes and enzyme activities. Intracellular FABPs increase the solubility of fatty acids and facilitate the transport to organelles such as mitochondria or endoplasmic reticulum (**Fig. 1.15**) [184]. Presence of FABPs in the nucleus of some cell lines such as heart myocyte, hepatocyte, cancer cells and the cell lines transfected with FABP gene, leaded to the discovery of the interaction between the nuclear receptors and FABPs [186]. Overexpression of FABPs was reported to act in concert with PPARs and this activity is highly selective for particular FABP-PPAR pairs [187], which may indicate that individual FABPs initiate unique signalling pathway in nucleus and trigger specific gene expression, as shown in **Figure 1.15.**

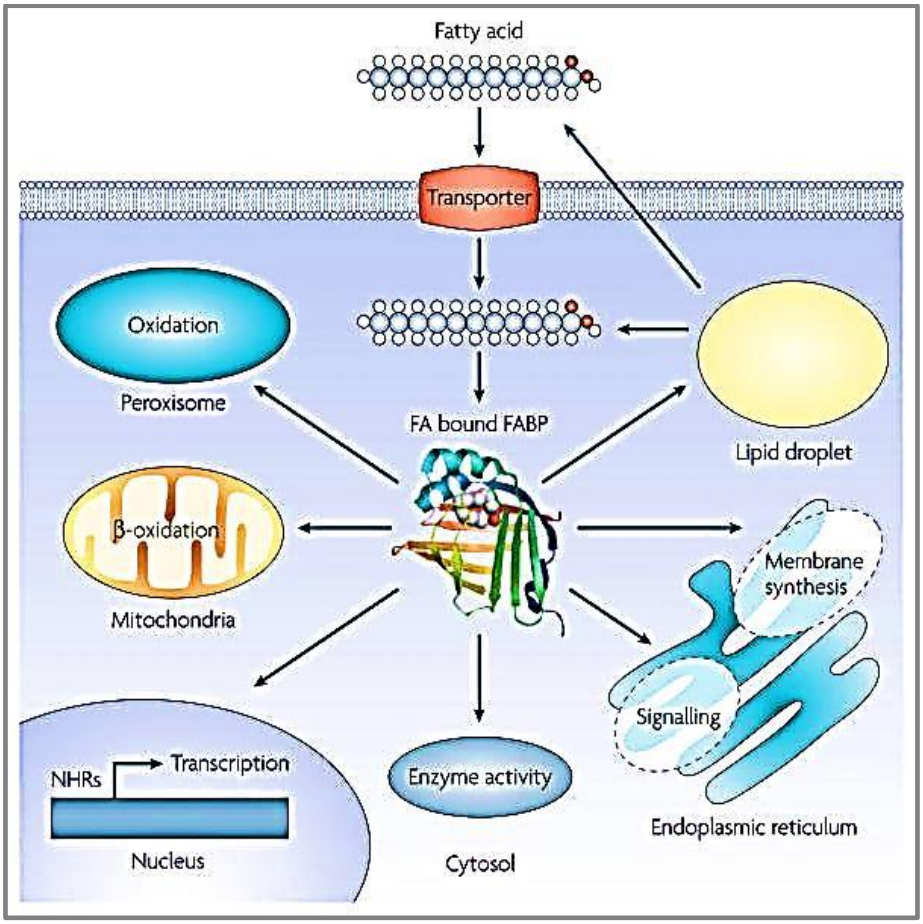

Figure 1.15: Putative intracellular functions of FABP [184]; FABPs involve in fatty-acid import, storage and export, oxidation (Perixosome), β-oxidation (Mitochondria), transcription (PPARs), enzyme activity (Cytosol) and signalling and membrane synthesis (Endoplasmic reticulum).

1.2.5.3.9.1 C-FABP and prostate cancer

Previous studies demonstrated that C-FABP is overexpressed in malignant prostate and breast cell lines and when transfected into the benign rat Rama 37 model cells, C-FABP induced metastasis of the DNA recipient cells, *in vivo* [188]. Further investigations revealed that over-expression of the C-FABP gene induced metastasis through up-regulation of the VEGF and thus VEGF might play a crucial role in this particular metastatic cascade [189]. Furthermore, it has been shown that suppression of C-FABP expression in highly malignant PC3-M cells

significantly reduced invasive capacity, *in vitro* [190] and inhibit the tumorigenicity, *in vivo* (nude mice model) [191] by decreasing VEGF and microvessel densities. On the other hand, inducing the *C-FABP* gene in less malignant, androgen-dependent LNCaP cells raised cell invasiveness and proliferation ability, *in vitro* and increased the tumorigenicity, *in vivo* (nude mice model) [167]. Higher levels of both nuclear and cytoplasmic C-FABP were detected in carcinoma tissues than those in normal and BPH tissues and the increased expression of C-FABP was significantly associated with a reduced patient survival time, thus it has been suggested as a prognostic biomarker to predict patients' outcome [168]. Recent studies showed that cancer promoting activity of C-FABP in prostate cancer is closely related to its ability to bind and transport extracellular fatty acids into the cancer cells [167]. It has been established that there is a fatty acid-initiated signalling pathway which may lead to malignant progression of prostatic cancer cells.

1.2.5.3.10 Peroxisome proliferator activated receptors (PPARs)

PPARs were originally identified in Xenopus frogs as receptors that induced the proliferation of peroxisomes in cells [192]. PPARs belong to the nuclear hormone receptor superfamily of ligand-inducible transcription factors [193]. They play essential roles in the regulation of cellular differentiation, development, metabolism (carbohydrate, lipid and protein) and tumorigenesis . PPARs regulate target gene expression by translocation from cytoplasm to nucleus and hetero-dimerization with retinoic X receptor (RXR) which binds to specific DNA binding domain known as peroxisome proliferator (hormone) response elements (PPREs) within enhancer sites of regulated genes (promoters) [194]. PPREs composed of direct repeat (DR) elements consisting of two hexanucleotides with a consensus sequence AGGTCA separated by a single nucleotide spacer and named DR1 (AGGTCA-A-AGGTCA). Alternatively, in DR2 motifs two hexanucleotides are separated by two nucleotide spacer and can also be recognized by PPARs [195]. Endogenous ligands for the

PPARs include free fatty acids and their derivations including eicosanoids and prostaglandins [196]. Three main isotypes of PPARs have been identified: PPARα (alpha) (NR1C1) (on chromosome 22q12-13.1) [197], PPARγ (gamma) (NR1C3) (on chromosome 3p25) [198], and PPARβ/δ (beta-delta) (NUC1) (on chromosome 6p21.1–p21.2) [199]. PPARα is highly expressed in tissues with high rates of mitochondrial fatty acid oxidation, such as liver, kidney, heart, muscle , adipose tissue and cells of arterial wall. It reduces triglyceride level and is involved in regulation of energy homeostasis. PPARβ/δ expresses in many tissues, particularly in brain, adipose tissue and skin, to enhance fatty acids metabolism. PPARγ is expressed on all major cells of the vasculature, including endothelial cells, VSMCs (Vascular Smooth Muscle Cells) and monocytes/macrophages, human coronary artery smooth muscle cells, umbilical artery smooth muscle cells, umbilical endothelial cells and aortic smooth muscle cells. It is predominately seen in adipose tissues where it plays a critical role in the regulation of adipocyte differentiation [200]. PPARγ causes insulin sensitization and enhances glucose metabolism. Three forms of PPARγ are transcribed by the same gene : **γ1** expresses in virtually all tissues, including heart, muscle, colon, kidney, pancreas and spleen; **γ2** expresses mainly in adipose tissue (30 amino acids longer) ; **γ3** expresses in macrophages, large intestine and white adipose tissue [201].

1.2.5.3.10.1 Intracellular PPARs regulatory pathway

All three isotypes of PPARs have been shown to modulate lipid metabolism. PPARα regulates the expression of genes involved in the peroxisomal and mitochondrial β-oxidation pathways such as Acyl-CoA oxidase, Enoyl-CoA hydratase/dehydrogenase multifunctional enzyme, Keto-Acyl-CoA thiolase, Malic enzyme, medium chain Acyl-CoA dehydrogenase and mitochondrial hydroxy methylglutaryl-CoA synthase. It also is regulated by FATP (Fatty Acid Transport Protein), FAT/CD36 (Fatty Acid Translocase), L-FABP (Liver Cytosolic Fatty Acid-Binding Protein) and UCP2 and UCP3 (Uncoupling Proteins-2

and 3). Hence activated PPARα leads to increased breakdown of triglycerides and fatty acids, increased cellular fatty acid uptake and reduced triglyceride and fatty acid synthesis [202]. PPARβ/δ is a potential downstream target of APC (Adenomatous Polyposis Coli), Beta-Catenin and TCF4 (T-Cell Factor-4) tumour suppressor pathway, which is involved in the regulation of growth promoting genes such as c-Myc and Cyclin-D1. PPARβ/δ plays an anti-apoptotic role in keratinocytes via transcriptional control of the Akt/PKB (Protein Kinase-B) signalling pathway. Both PI3K (Phosphatidylinositol-3 Kinase) and Integrin-linked kinase are target genes of PPARβ/δ [203]. Both PPARγ and PPARα are regulated by phosphorylation events. Activation of PPARγ inhibits monocyte and macrophage inflammatory responses by preventing the activation of nuclear transcription factors, such as NF-KappaB (Nuclear Factor-KappaB), AP-1 (Activating Protein-1) and STAT1 (Signal Transducer and Activator of Transcription-1) [204].

1.2.5.3.10.2 PPARs and cancer

Wide expression of PPARγ in many tumours and the ability of its ligands to inhibit cellular proliferation, promote differentiation, induce apoptosis and inhibit angiogenesis, highlight the importance the role of PPARγ in carcinogenesis. High expression levels of PPARγ have been detected in human mammary adenocarcinomas. PPARγ agonists have been reported to reduce growth and induce differentiation of malignant breast epithelial cells [205]. It has been shown that survival of patients with colorectal cancer was significantly longer in those with high level of PPARγ [206]. On the other hand, PPARγ has shown to have an important role in bladder tumorogenesis [207]. Inhibition of proliferation in lung carcinoma cells and non-small cell lung cancer (NSCLC) has been reported in association with PPARγ-dependent signals [208, 209]. It has been demonstrated that PPARγ ligands induced cell cycle arrest in pancreatic tumour cell lines [210].

Enhanced expression of PPARα has been reported in human hepatocellular carcinoma [211]. Previous studies revealed that PPARα expression correlated with a shorter survival time and poor chemo-response in patients with ovarian carcinoma [212]. Moreover, up-regulation of PPARα and its related proteins has been detected in human glioblastoma cells [213].

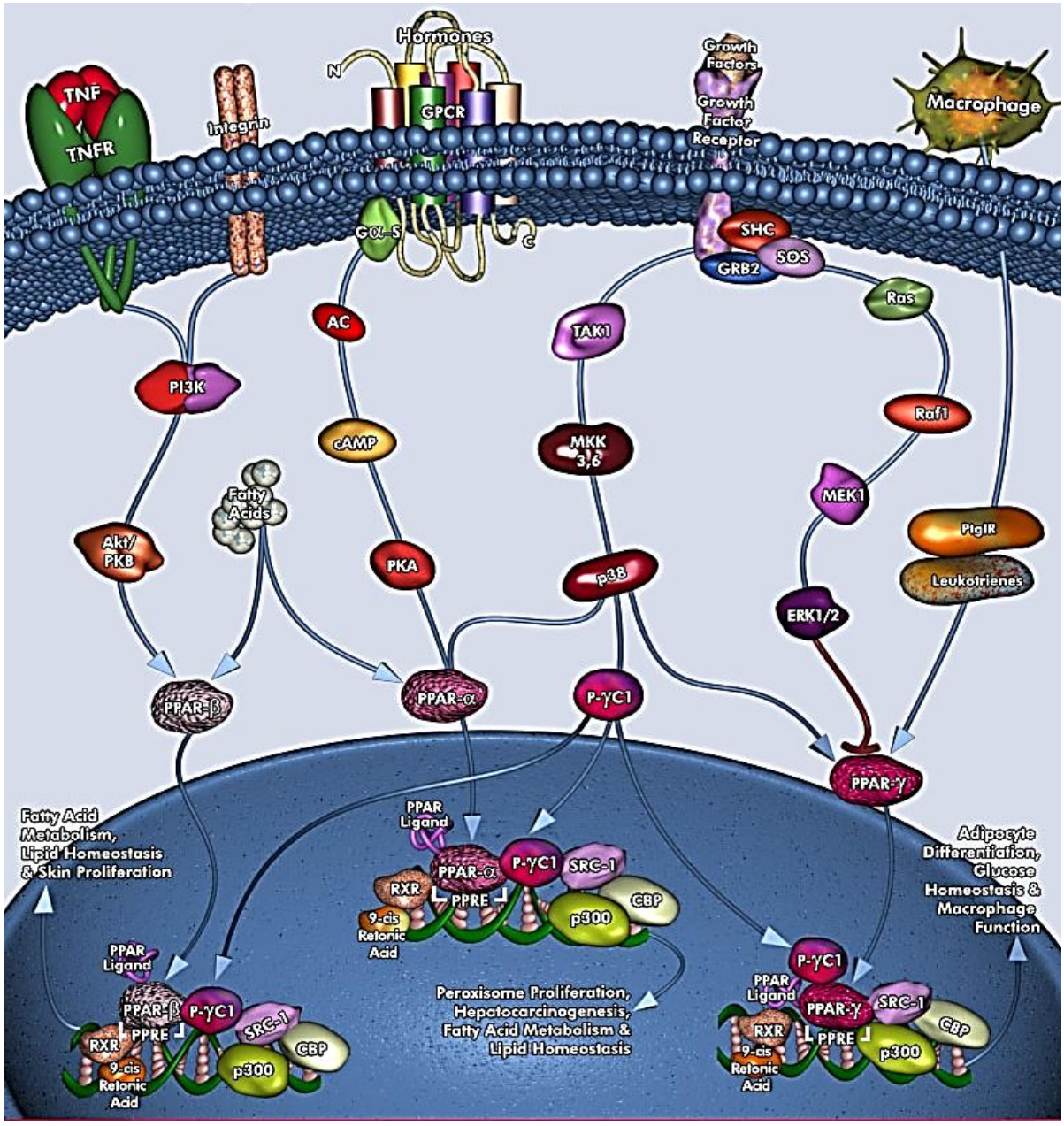

Figure 1.16: PPARs regulatory pathway [214].

PPARβ/δ has been identified as a target of the tumour suppressor APC in colorectal cancer cells [215]. Furthermore it has been showed that PPARβ/δ has regulatory effects on the genes which may increase cell proliferation and promote colon carcinogenesis [215]. Higher levels of PPARβ/δ have been detected in ovarian carcinomas, squamous cell carcinomas, breast tumours and endometrial carcinomas [212, 216-218]. Increased proliferation or inhibited apoptosis in presence of high PPARβ/δ has been shown in variety of human lung, breast, liver and prostate cancer cell lines [219]. Indeed, PPARβ/δ ligands have been reported to inhibit the proliferation of mouse and human keratinocytes [220].

1.2.5.3.11 Vascular endothelial growth factor (VEGF)

Process of new vascular network formation from pre-existent capillaries is called angiogenesis, which is one of the essential component of the tumour growth and the metastatic pathway [221]. During the process of vascularisation endothelial cells initially respond to changes in the local environment and migrate toward the growing tumour. The endothelial cells then migrate together to form tubular structures which are ultimately encapsulated by recruiting periendothelial support cells to establish a vascular network that facilitates tumour growth and metastasis [222]. Tumour angiogenesis is regulated by the production of angiogenic stimulators including the vascular endothelial growth factor (VEGF), basic fibroblast growth factor (FGF-2), acidic FGF (FGF-1), matrix metalloproteinases, insulin-like growth factor I, and angiopoietin-1 [223]. VEGF is a signalling protein being produced by cells to stimulate vasculogenesis and angiogenesis. VEGF belongs to a sub-family of growth factors (the platelet-derived growth factor family of cystine-knot growth factors). It has been divided to several sub- groups: VEGF-A (involve in angiogenesis by increasing endothelial cells mitosis and migration, creation of blood vessel lumen and creation fenestrations), VEGF-B (involved in embryonic angiogenesis), VEGF-C (involved in lymphangiogenesis), VEGF-D (involved in the development of

lymphatic vasculature surrounding lung bronchioles), VEGF-E (encoded by viruses and in the venom of some snakes) and a structurally related molecule named placental growth factor (PlGF) (important for vasculogenesis) [224]. Human VEGF is a 45 kDa homodimeric-binding glycoprotein which was firstly identified by Senger *et al.* at 1983. *VEGF* gene is located at chromosome 6p21.3 and consists of 8 exons separated by 7 introns [225]. As a key mediator of angiogenesis, *VEGF* is tightly regulated at both the transcriptional and post-transcriptional levels. VEGF regulation is complex as it is up-regulated by hypoxia, growth factors, steroid hormones and transcription factors [226].

1.2.5.3.11.1 VEGF and prostate cancer

There are some controversies regarding the relationship between VEGF expression and degree of malignancy of prostate cancer. It has been reported that expression of VEGF mRNA was significantly higher in PIN and poorly differentiated prostate carcinomas comparing to BPH and normal prostate tissues [227]. VEGF protein has been detected in 80% of prostate cancer, 18% of BPH, but not detected in normal prostate samples [228]. Hypoxia inducible factor (HIF)-1α, key regulator of VEGF, has been shown to be highly expressed in PIN lesions and in human prostate cancer [229]. The correlation between serum VEGF and micro vessel density (MVD) with the transition of a well differentiated tumour to a poorly differentiated tumour and prostate cancer metastasis has been confirmed [227, 230]. Studies on rat model cells revealed that C-FABP may stimulate the expression of the *VEGF* gene and promote angiogenesis to facilitate tumour formation and metastasis [189, 231]. Suppressing *C-FABP* gene in highly malignant prostatic cancer cells has reduced the expression of VEGF and down-regulated angiogenesis in the resultant cancer cells [168, 190]. Whereas increasing *C-FABP* expression in less malignant prostate cancer cells not only up-regulated VEGF level but also increased MVD [167]. Clinical studies showed that expression levels of VEGF in urine, serum or plasma were correlated with poor patient outcome, higher Gleason score or

metastasis [232, 233]. Furthermore anti-angiogenic treatment with VEGF inhibitors such as Bevacizumab, Sorafenib or Sunitinib reduced progression rate of prostate cancer and increased patient survival time [234]. Oestrogen has been reported to up-regulate the expression of VEGF in breast cancer cells via Specificity protein (Sp1/Sp3) transcription sites in the core VEGF promoter [235]. Similarly, androgen has mediated the up-regulation of VEGF expression in androgen dependent prostate cancer cells, through a Sp1/Sp3 binding site in the VEGF core promoter [236].

1.2.5.3.11.2 PPARs and angiogenesis

All PPARs are expressed in endothelial cells, where they also regulate cell proliferation, angiogenesis, inflammation, thrombosis and coagulation [237]. Experimental studies showed that PPAR*α* activation inhibits angiogenesis in vascular remodelling (proliferation, migration and tube formation) and in tumour cell growth [238]. PPAR*α* activation inhibited VEGF-induced endothelial cell migration and FGF-2-induced corneal angiogenesis *in vitro* and *in vivo* [239]. A significant correlation between expression of PPAR*α* and level of secreted VEGF has been reported in both normal and malignant endometrial tissues [240]. Treatment of implanted melanoma, glioblastoma and fibrosarcoma in mice with PPARα ligands, led to a reduction in tumour growth and microvessel density [239]. PPAR*β*/*δ* activation potently induces angiogenesis in human and murine vascular endothelial cells *in vitro* and *in vivo* [241]. In pancreatic tumours removed from patients, the expression levels of PPAR*β*/*δ* were strongly correlated with the advanced pathological tumour stage and increased risk of tumour recurrence and metastasis (via VEGF) [242]. Up-regulation of VEGF has been shown in poorly differentiated bladder cancer cells in relation to PPARβ/δ ligands [243]. PPARγ expression is associated with a vast number of cancers. It is found at higher levels in proliferating endothelial cells [244]. Up-regulation of VEGF (both mRNA and protein) has been reported in colorectal cancer cells after induction with both PPARβ/δ and PPARγ ligands [245]. VEGF

promoter contains PPRE sequences through which PPARγ ligands are capable of inducing VEGF and angiogenesis in endothelial/interstitial muscle cells [246]. Induction of VEGF was associated to increase activation of Akt and phosphorylation (activation) of ENOS (endothelial nitric oxide synthase) (NOS3) [247]. On the other hand, it has also been shown that PPARγ ligands repressed *VEGF* gene expression via PPREs in the *VEGF* gene promoter region, in human endometrial cells [248].

1.3 Aims and scope

1- Evaluation different expression levels of PPARβ/δ and PPARγ in correlation with C-FABP by RT-PCR in mRNA level and by Western blotting in protein level in different benign and malignant prostate cell lines.

2- Evaluation different expression levels of PPARβ/δ and PPARγ in correlation with C-FABP in benign and carcinoma prostate tissues using immunohistochemical staining.

3- Assessing the correlation of different expression levels of PPARβ/δ and PPARγ in prostate carcinoma tissues with different expression level of C-FABP, Gleason score (degree of malignancy), PSA level, AR index and patient's survival time using different statistical analysis methods.

4- Suppressing the most related PPAR to C-FABP in highly malignant prostate cancer cells, transiently and stably, using RNAi techniques.

5- Evaluation the silencing effects of dedicated PPAR on growth rate, invasiveness and anchorage-independent growth of prostate cancer cell, *in vitro*, using proliferation assay, invasion assay and soft agar assay.

6- Evaluation the silencing effects of dedicated PPAR on the tumorigenicity of prostate carcinoma tissues, *in vivo*, using nude mice model.

7- Evaluation the regulatory effects of C-FABP-PPAR axis on VEGF protein expression in cell extracts and medium, using Western blotting and ELISA, respectively. Assessing the biological activity of secreted VEGF by *in vitro* angiogenesis assay.

8- Evaluation the regulatory effects of C-FABP-PPAR pathway on VEGF expression through PPRE sequences in promoter region of VEGF, using Dual Luciferase Reporter assay.

1.3.1 Research Plan

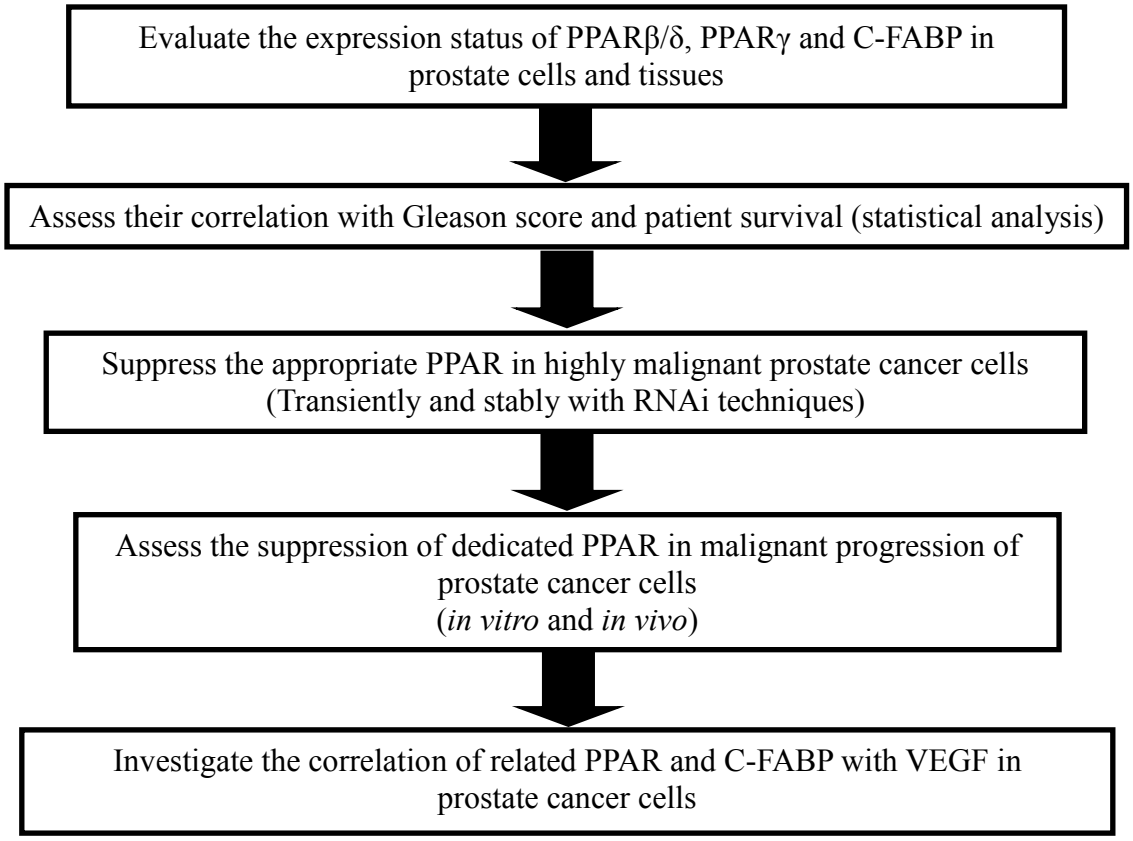

CHAPTER TWO:

MATERIALS AND METHODS

2 Materials and Methods

2.1 Materials

Reagents are listed in Appendix A, Buffers in Appendix B and Equipment in Appendix C.

2.2 Methodology

2.2.1 Cell culture

2.2.1.1 Routine cell culture

All human prostate cell lines were grown monolayer in routine medium (RM), in T75/T125 tissue culture flasks then kept in humidified incubator (Model TC2323 CO_2 incubator, Borolabs) at 37°C with 5% (v/v) CO_2. Cells were fed with fresh medium each 3-4 days. After reaching 80% of confluency, cells were passaged and sub-cultured in 1/10 fold. Old medium was removed; cells were washed twice with PBS. Trypsin 2.5% (v/v) in Versene was used to detach cells, 3ml/T75 flask and 5ml/T125. Cells were incubated with T/E 2-5 minutes till majority of them were rounded and detached. For deactivating T/E, equal volume of RM was added. Cell pallets were separated by centrifuging in 25 ml universals at 800 ×g for 3 minutes. Cell pallets were re-suspended with RM, and divided to flasks with suitable volume of medium.

2.2.1.2 Cell counts

Using Haemocytometer (Scientific Laboratory Supplies Ltd) cell numbers were counted. 20µl of suspended cells provided in **2.2.1.1** section were placed under the cover-slip. Mean of cells counted in four squares were considered as the number of cell $\times 10^4$ in 1 ml of cell suspension.

2.2.1.3 Cryopreservation/Cell Freezing

After reaching to 70% confluency, cells were detached (Section **2.2.1.1**), re-suspended in PBS and counted (section **2.2.1.2**). Using 3 minutes centrifuge at 1250 g, supernatant was separated and discarded. Pallet was re-suspended with Freezing medium (FM) containing 7.5% DMSO to reach the concentration of 1-1.5×10^6, then aliquot into 1 ml in Cryotubes (Nunc, Denmark). Cryotubes were placed in Cryobox (Nalgene, UK), filled by isopropanol and kept in -80°C freezer overnight before transferring into liquid nitrogen. In Cryobox, temperature decreases gradually (-1°C/minute) and prevents ice crystal formation during freezing process in the cells.

2.2.1.4 Cell Thawing

Frozen cells were removed from liquid nitrogen and thawed gradually first on ice and then in water bath (37°C). Then cells transferred into 25ml universal and diluted with 10ml RM, before centrifuged at 800 ×g for 3 minutes to discarding supernatant which contain cryoprotective DMSO (because of its toxic effect on cells in >4°C). The pellet was re-suspended and transferred into T75 flasks and maintained in humidified incubator with 5% CO_2 at 37°C.

2.2.2 Culturing of transfected cells

Transfected cells were grown and maintained in routine selective medium (RSM) which contain 100µg/ml Zeocin (Invitrogen, CA, USA). All the cell culture techniques were same as non-transfected ones expect using RSM.

2.2.3 Evaluating protein expressions in cell lines

Western blot was used for evaluating protein expressions. Protein extracts were loaded in a poly acrylamide gel electrophoresis (PAGE) system where separated according to their

molecular weight and charge ratio. Separated proteins then transferred to polyvinylidene difluoride (PVDF) membranes where protein expression identified using specific antibodies.

2.2.3.1 Protein extraction from cultured cells

When cell reached to 80% confluency, they were trypsinized (as described in section **2.2.1.1).** The pallet was incubated with CelLytic-M (100µl/5×10^6 cells) and protease inhibitor (1µl/5×10^6 cells) in a 1.5 ml micro-centrifuge tube on the roller for 15 minutes at room temperature. Then the mixture centrifuged at 8000 ×g for 20 minutes to separate cellular debris. The supernatant was kept in a fresh micro-centrifuge tube.

2.2.3.2 Bradford assay

Bio-Rad protein assay (Bio-Rad Laboratories GmbH, Munchen, Germany) was used to quantify the concentration of proteins extracted from cell lines. A concentration standard curve established using serial concentration of BSA (from 50µg/µl to 500µg/µl) in 50µl PBS. Appropriate volume of protein samples were also diluted within 50µl PBS. All controls and samples were incubated with 1ml of diluted (1/5) dye reagent, which filtered through Whatman 540 paper, for 15 minutes before measuring the absorbance at 595nm using the MultiSkan plate reader (BioTek Instruments, USA). Standard curve used to calculate the concentration of protein samples.

2.2.3.3 Western Blotting

2.2.3.3.1 Sodium Dodecyl Sulphate Poly Acrylamide Gel Electrophoresis (SDS-PAGE)

Proteins, extracted from cell lines and quantified using Bradford assay, were equalized with distilled water to reach the concentration of 20µg/10µl then 10µl of 2× sample loading buffer (SLB) was added. Prior to loading, mixture was heated at 95°C on hot plate (Techne, Ori-Block, USA) for 10 minutes to linearize proteins by breaking hydrogen band of tertiary

structure which made the antigen recognisable with antibody then chilled on ice for 2 minutes and spun down before loading in SDS gel. Electrophoresis was performed in 500ml of 1× running buffer (Next Gel™ Running Buffer, 20×, Amresco, USA) using Bio-Rad miniprotein system with 1mm spacers (Flowgen, Bio-Rad, Hemel, UK). Proteins were loaded in 12.5% polyacrylamide gel (Next Gel™ 12.5%, Amresco, USA) and ran at 100V for 60 minutes. Protein sizes were estimated using suitable protein marker (Lonza, Belgium).

2.2.3.3.2 Transfer proteins from SDS gel to PVDF membrane

Separated proteins were transferred from SDS gel to PVDF membrane (Immobilon-P, Transfer Membrane, Millipore, USA) using the Trans-Blot electrophoretic transfer system. Six sheets of Whatman 3mm filter paper and PVDF membrane were cut according to gel size and soaked in pre-chilled (4°C) 1× transfer buffer for 5 minutes. Then a pre-wet fiber-pad/paper/gel/membrane sandwich was assembled in the cassette. Air bubbles removed using glassy roller. Transferring was undertaken in a tank containing 750ml of chilled transfer buffer at 80V for 60-90 minutes at 4°C.

Efficacy of running and transferring was assessed at the end of each process by staining gel and membrane. Coomassie blue (Severn Biotech Ltd, UK) was used for staining the gel for one hour and washed with distilled water (slowly shaking) overnight before drying by vacuum gel-dryer (Flowgen, Nottingham, UK) at 70°C for 3 hours. Ponceau S 10% (Sigma, USA) was used for staining the membrane for 3 minutes and washed with TBS-T for 10 minutes to visualized protein bands.

2.2.3.3.3 Immunoblotting to detect protein expression

To prevent non-specific bindings of primary antibody, membranes were blocked with 10ml of 5% TBS-T-milk for one hour in room temperature on gently agitated shaker. Then they were incubated with appropriate concentration of primary antibody (**Table 2.1**) in room

temperature for one hour, followed by washes with 1× TBS-T four times for 10 minutes to remove unbound primary antibody. Then membranes were incubated with appropriate concentration of secondary antibody (**Table 2.1**) in room temperature for one hour followed by four times washing with 1× TBS-T for 10 minutes. Finally, for visualizing probed antibodies, they were incubated with ECL reagents (GE Healthcare, UK) for 2 minutes in room temperature before developing and fixing in dark room. Expressed proteins were recorded on Kodak film (GE Healthcare, UK) for a serial required times (0.5-15 minutes).

2.2.3.3.4 Correcting loading variations

To correct possible loading variation, expression of β-actin was evaluated in each membrane. After detecting the target protein, membrane was washed with 1× TBS-T for overnight. Then it was blocked with 10ml of 5% TBS-T-Milk for 30 minutes before incubating with β-actin antibody for 30 minutes in room temperature. Then membrane was washed four times with 1× TBS-T for 5 minutes followed by incubating with secondary antibody for 30 minutes in room temperature. It was washed four times with 1× TBS-T for 5 minutes before visualized by incubating with ECL reagents for 2 minutes. Membrane was developed and fixed in dark room and recorded on Kodak film. Expression level (EL) of each protein normalized by using this formula:

Normalized EL of target protein= EL of target protein/ EL of β-actin

Target Protein	Primary antibody	Secondary antibody
PPARβ/δ	Rabbit polyclonal anti-human PPAR delta (Thermo PA1-823A) (1:1000)	Swine polyclonal anti-rabbit Immunoglobulin/HRP (Dako) (1:20,000)
PPARγ	Rabbit polyclonal anti-human PPARγ (Santa Cruz sc-7196) (1:200)	Swine polyclonal anti-rabbit Immunoglobulin/HRP (Dako) (1:20,000)
C-FABP	Rabbit polyclonal anti-human E-FABP (Hycult HP-9030) (1:500)	Swine polyclonal anti-rabbit Immunoglobulin/HRP (Dako) (1:20,000)
VEGF	Mouse polyclonal anti-human VEGF (Thermo RB-9031-P1) (2µg/ml)	Rabbit polyclonal anti-mouse Immunoglobulin/HRP (Dako) (1:20,000)
β-actin	Mouse monoclonal anti β-actin (Sigma) (1:50,000)	Rabbit polyclonal anti-mouse Immunoglobulin/HRP (Dako) (1:20,000)

Table 2.1: Primary and secondary antibodies used for Western blotting.

2.2.4 Evaluating protein expression in tissues

2.2.4.1 Human tissue samples

Human prostate tissues were selected from an archival set with follow-up data held in Department of Molecular and Clinical Cancer Medicine (originally named Department of Pathology), University of Liverpool, UK. Patients who were originally diagnosed with prostate cancer, but died from other causes were excluded. Tissues were taken from 35 benign prostatic hyperplasia (BPH) patients and from 97 prostate adenocarcinoma patients with an average age of 67.5 and 73 years, respectively. All patients studied were treated by trans-urethral resection of the prostate (TURP) in the Royal Liverpool University Hospital during 6 years between 1995 and 2001. This study was approved by the National Science Ethics Committee in accordance with the Medical Research Council guidelines (project reference number: Ke; 02/019). Specimens had been fixed in 10% (v/o) formalin and embedded in paraffin wax. Cut histological sections were examined independently by two

qualified pathologists and classified as BPH and carcinomas and further classified according to their combined Gleason scores (GS) [107]. PSA levels at the initial diagnosis was obtained through telepath system and classified into two group low (<10ng/ml) and high (≥ 10ng/ml) [249].

2.2.4.2 Preparing tissue sections

Paraffin wax-embedded tissue blocks were pre-cooled in a container filled with ice and water. Using microtome (MICROM, Oxford, UK) tissues were cut at 4μm thickness and mounted on labelled Superior Adhesive Slides (Apex, Leica, UK), then dried overnight at 37°C.

2.2.4.3 Immunohistochemistry

Immunohistochemistry (IHC) refers to the process of detecting antigens (e.g., proteins) in cells of a tissue section by exploiting the principle of antibodies binding specifically to antigens in biological tissues [250]. Immunohistochemical staining is widely used in the diagnosis of abnormal cells such as those found in cancerous tumours. In this study, it was used to evaluate expression of different proteins in prostate cell lines.

For de-waxing the sections, they were washed twice in xylene (each 5 minutes) followed by two times rinsing in Industrial Methylated Spirits (IMS) (GENTA Environment Ltd., Tockwith, UK) (each 5 minutes) before transferred to fresh 3% H_2O_2/Methanol (15 minutes) to block endogenous peroxidase activity. Then sections were washed with running tap water for 30 seconds. Antigen retrieval achieved by incubating in 10 mM Sodium Citrate buffer (pH 6) on full power in the microwave for 15 minutes and allowed sections to rest in hot buffer for a further 15 minutes, for C-FABP, PPARγ and AR detection. For PPARβ/δ, antigen retrieval was performed by incubating sections in pressure cooker filled with ethylene diamine tetraacetic acid (EDTA) solution (pH 7) for 3 minutes. Then slides were washed three times with Tris Buffered Saline containing 0.025% Tween20 (TBS-T). For PPARγ and

PPARβ/δ, slides were racked into flat, humid chamber and incubated with appropriate concentration of primary antibody (**Table 2.2**) in 100µl of TBS-T in 4°C, overnight. For C-FABP and AR, they were racked into sequenzer (Immunohistochemistry Staining Trays, Shandon, UK) and incubated with appropriate concentration of primary antibody (**Table 2.2**) in 100µl of TBS-T in room temperature, for one hour. All slides were gone through 3 step washes with TBS-T (each one minute) in the sequenzer. Because PPARβ/δ and PPARγ antibodies were derived from gout , 100µl of diluted (10µg/ml) Linker (Anti-gout IgG, Vector, USA) in TBS-T were applied to slides for 30 minutes and followed by 3 washes with TBS-T (each 1 minute). Bound antibodies were detected with 200µl of EnVision™ FLEX/HRP (DakoCytomation, Ely, UK) for 1 hour then washed 3 times with TBS-T. 100µl of EnVision™ FLEX/DAB+ Chromogen (DakoCytomation, Ely, UK) used to visualize and stained of each section for 10 minutes, then slides were washed with distilled water for 4 minutes. Finally all slides counterstained with Haematoxylin solution (BWR international, London, UK) for 2 minutes, rinsed in 1% Acid/Alcohol, washed in water and briefly rinsed in Blue Scott till the blue colour appeared on slides. At the end, slides were rehydrated through four rinses in IMS and cleaned by three rinses in xylene, then mounted in DPX (Bios, Lancashire, UK).

Target Protein	Primary antibody
PPARβ/δ	Gout polyclonal Anti-human PPARβ (Santa Cruz sc1987) (1:100)
PPARγ	Gout polyclonal Anti-human PPARγ (Santa Cruz sc-1984) (1:50)
C-FABP	Rabbit polyclonal Anti-human E-FABP (Hycult HP-9030) (1:500)
Androgen Receptor	Mouse monoclonal Anti-human Androgen Receptor (Abcam ab-9474) (1:100)

Table 2.2: Primary antibodies used for immunohistochemical staining.

2.2.4.4 Controls for immunohistochemistry

To confirm the efficiency of immunohistochemical staining, specific tissues which showed high expression levels of dedicated antigen (according to the literatures) were used as positive control. Normal colorectal, colorectal adenocarcinoma and poorly differentiated prostate cancer tissues were used as positive control for PPARβ/δ, PPARγ and C-FABP, respectively.

Also in each experiment, the same sample was used as negative control which passed through all staining steps except the step of primary antibody. In that step, negative control samples were incubated with TBS-T only.

2.2.4.5 IHC scoring

Intensity and percentage of staining were evaluated in both cytoplasm and nucleus by two independent observers. Percentage of staining were scored as 1-3; 1: ≤ 30%, 2: 31-69%, 3: ≥70%. Intensity of obtained stains were scored as 1-3; 1: +, 2: ++, 3: +++. In cytoplasm, because of homogenous staining pattern, slides were scored only through intensity. For nuclear staining, final scores were obtained from multiplying the percentage and intensity scores (1-9). This method was similar to which used for scoring immunohisochemical detecting of ER in breast cancer [251]. Finally, slides classified as weakly positive, 1-3; moderately positive, 4-6; strongly positive, 7-9.

2.2.5 Evaluating RNA expressions in cell lines

2.2.5.1 Total RNA isolation

Prostate cells were cultured in 175 cm^2 flasks to 60-80% confluency (not more than 1×10^7) before harvesting and extracting their total RNA, using RNeasy Mini Kit (QIAGEN Sample & Assay Technologies, CA, USA). After washing pellet with PBS, cells were disrupted using

600µl of buffer RTL containing 1% β-Mercaptoethanol. Cell lysates then homogenized by centrifugation through a QIAshedder spin column placed in a 2ml collection tube for 2 minutes at full speed and precipitated in equal volume of 70% ethanol. Up to 700µl of solution were loaded in an RNeasy spin column sitting in a 2ml collection tube and centrifuged for 15 seconds in ≥8,000 ×g. The flow-through was discarded and column was washed with 700µl of Buffer RW1 which followed by centrifuged for 15 seconds in ≥8,000 ×g. To digest any DNA contamination, 10 µl of DNase I solution which diluted with 70 µl of buffer RDD was applied and left on benchtop for 15 minutes. The flow-through was discarded and column was washed with 500µl of Buffer RW1 which followed by centrifuged for 15 seconds in ≥8,000 ×g. To eliminate any carryover buffer, the RNeasy spin column was centrifuged at full speed for 1 minute. Finally, column was placed on a new collection tube and 30-50µl of RNase-free water were loaded directly to the membrane and centrifuged for 1 minute at ≥8,000 ×g to elute the RNA. The total RNA yield and purity was determined using NanoDrop ND-1000 spectrophotometer. Quality of each RNA sample was determined by $1.8 \leq 260/280 \text{ ratio} \leq 2$ [252, 253].

2.2.5.2 Reverse transcriptional polymerase chain reaction (RT-PCR)

This technique is commonly used in molecular biology to detect RNA expression levels by qualitatively detection of gene expression through creation of complementary DNA (cDNA) transcripts from RNA, then qPCR is used to quantitatively measure the amplification of DNA using fluorescent probes [254]. RT-PCR is currently the most sensitive method of RNA detection available [255]. In this study, it was applied to show the levels of PPARβ/δ and PPARγ gene expressions in prostate cell lines.

2.2.5.2.1 PCR primer design

Using PerlPrimer, primer design software (perlprimer.sourceforge.net/(, primers were designed spanning exon-exon junctions of PPARβ/δ and PPARγ genes and their specificities

were validated by the nucleotide Blast program (http://blast.ncbi.nlm.nih.gov/Blast.cgi?PROGRAM=blastn&PAGE_TYPE=BlastSearch&LINK_LOC=blasthome). Primers purchased from Invitrogen by Life Technologies Ltd. (Paisley, UK). β-actin primers were used as a house-keeping gene (**Table 2.3**).

Primers	Sequences
PPARβ/δ	Sense: 5'- AGGTTACCCTTCTCAAGTATGG-3' Antisense: 5'- CTTGTAGATCTCCTGGAGCAG-3'
PPARγ	Sense: 5'- CGCCGTGGCCGCAGATTTGA -3' Antisense: 5'- GCCTGTGGCATCCGCCCAAA -3'
β-actin	Sense: 5'- AGCCTCGCCTTTGCCGA -3' Antisense: 5'- CTGGTGCCTGGGGCG -3'

Table 2.3: RT-PCR primer's sequences.

2.2.5.2.2 Complementary DNA (cDNA) synthesis

In RT-PCR, the RNA template is first converted into a complementary DNA (cDNA) using a reverse transcriptase. The cDNA is then used as a template for exponential amplification using PCR. Total RNAs isolated from prostate cell lines were used to synthesize cDNA. For each cell line, 1µg of total RNA was mixed with 1µl of 50µM Oligo $(dt)_{20}$ primer and 1µl of dNTP mixture (10µM each dATP, dCTP, dGTP, dTTP at neutral pH) and volume was adjusted to 20µl with nuclease-free water. Mixtures were incubated in 65°C for 5 minutes followed by chilling on ice for 1 minute. Then 4µl of 5× first strand buffer and 2µl of 0.1M DTT were added and incubated at 42°C for 2 minutes followed by 1µl of SuperScript II Reverse Transcriptase and incubating at 42°C for 50 minutes. Finally, reaction were inactivated by heating at 70°C for 15 minutes [54]. β-actin RNA was used as a house-keeping gene.

2.2.5.2.3 RT-PCR

Polymerase Chain Reaction (PCR) was performed to amplify DNA template. Using the designed primers, PCR mixtures prepared as shown in **Table 2.4**:

Forward Primer (5µM)	1µl
Reverse Primer (5µM)	1µl
cDNA (for each cell lines)	1µl
Platinum®PCR SuperMix High Fidelity	22µl

Table 2.4: PCR Mixture.

Platinum ®PCR SuperMix High Fidelity (Invitrogen, Paisley, UK) contains anti-*Taq* DNA polymerase antibody, Mg^{++}, deoxyribonucleotide triphosphates, recombinant *Taq* DNA polymerase and *Pyrococcus* species GB-D thermostable polymerase.

Reactions were incubated in an automatic heat block thermal cycler (Peltier Thermal Cycler PTC-200) at 94°C for 2 minutes followed by 35 cycles of PCR amplification, each cycle includes of denaturing at 94°C for 30 seconds; annealing at 58 °C for 30 seconds and extension at 72°C for 1 minute. PCR was finalized by incubation at 72 °C for 5 minutes then maintained in 4°C [252]. PCR amplification products were analysed and visualized by 0.8% agarose gel electrophoresis (section: **2.2.6.5.7.3**).

2.2.6 Molecular biology

2.2.6.1 Small interfering RNA

Small interfering RNA (siRNA), sometimes known as short interfering RNA or silencing RNA, is a class of double-stranded RNA molecules, 20-25 base pairs in length. siRNAs have a well-defined structure: a short (usually 21-bp) double-stranded RNA (dsRNA)

with phosphorylated 5' ends and hydroxylated 3' ends with two overhanging nucleotides. siRNA plays many roles, but it is more notable in the RNA interference (RNAi) pathway, where it interferes with the expression of specific genes with complementary nucleotide sequence [256]. Since in principle, some genes can be knocked down by a synthetic siRNA with a complementary sequence, siRNAs are an important tool for validating gene function and drug targeting in the post-genomic era. Gene knockdown by transfection of exogenous siRNA is often unsatisfactory because the effect is only transient, especially in rapidly dividing cells. This may be overcome by creating an expression vector for the siRNA. The siRNA sequence is modified to introduce a short loop between the two strands. The resulting transcript is a short hairpin RNA (shRNA), which can be processed into a functional siRNA by dicer in its usual fashion [257].

2.2.6.2 Designing siRNA sequences

Three target sequences were chosen using Bioinformatics & Research Computing software (Whitehead siRNA selection program) (**Table 2.5**). Specificity of these sequences to PPARγ was confirmed by Blast search. Sequences were ordered from Ambion (by Life technologies, USA).

Position	Sequences
Sequence 1 (278-300)	Sense 5': GCCCUUCACUACUGUUGACUU mRNA: AA GCCCTTCACTACTGTTGACTT Antisense 5': GUCAACAGUAGUGAAGGGCUU
Sequence 2 (1209-1231)	Sense 5': GGCUUCAUGACAAGGGAGUUU mRNA: AA GGCTTCATGACAAGGGAGTTT Antisense 5':ACUCCCUUGUCAUGAAGCCUU
Sequence 3 (653-675)	Sense 5': UAAAUGUCAGUACUGUCGGUU mRNA: AATAAATGTCAGTACTGTCGGTT Antisense 5': CCGACAGUACUGACAUUUAUU

Table 2.5: PPARγ target and siRNA sequences.

2.2.6.3 Transient transfection

X-tremeGENE siRNA Transfection Reagent (Roche, Germany) was used for transient transfection. 1×10^5/well of PC-3M cells were pulled in 6-well plates 24 hours prior to transfection to reach the confluency of 30-60%. 1, 5 or 10 µl of X-tremeGENE siRNA Transfection Reagent (for each well) was diluted in 99, 95 and 90 µl of Opti-MEM I medium (Gibco, Invitrogen, Paisley, UK) to a final volume of 100 µl. Also1, 2 or 4µg/well of siRNAs was diluted in Opti-MEM I medium to a final volume of 100µl. After 15 minutes incubation in room temperature, diluted X-tremeGENE siRNA Transfection Reagent and siRNA were mixed by gently flicking the tubes and incubating in room temperature for another 15 minutes. Silencer® Negative Control #1 siRNA (Ambion, Inc., USA) was also diluted to use as scrambled RNA (control). Complex was overlaid drop-wise onto wells then distributed by gently rocking back and front. Dishes were incubated in normal cell culture conditions for 24, 48 and 72 hours. Proteins from cells were extracted (**2.2.3.1**) in different time points and expression of PPARγ was assessed in extracts (**2.2.3.3**). The most efficient siRNA was used to design shRNA for stable transfection in the most appropriate incubation time.

2.2.6.4 Designing short hairpin RNA (shRNA) sequences

The sequence which produced most suppression level for PPARγ (sequence 3) was chosen to design shRNA using siRNA Wizard™ Software (InvivoGen, USA) (**Table 2.6**). Specificity of these sequences to PPARγ was confirmed by Blast searching. Sequences were ordered from Ambion (by Life technologies, USA). Acc651 (GGTACC) and HindIII (AAGCTT) sequences were considered as restriction enzyme sites.

shRNA Sequences (oligos)		
PPARγ	Sense:	5' GTACCTCATAAATGTCAGTACTGTCGGTCAAGAGCCG ACAGTACTGACATTTATTTTTTGGAAA 3'
	Antisense	5' AGCTTTTCCAAAAAATAAATGTCAGTACTGTCGGCTC TTGACCGACAGTACTGACATTTATGAG 3'
Scramble	Sense	5' GTACCTCGGTAGAAATCGACGTATCTTTCAAGAGAAG ATACGTCGATTTCTACCTTTTTGGAAA 3'
	Antisense	5' AGCTTTTCCAAAAAGGTAGAAATCGACGTATCTTCTC TTGAAAGATACGTCGATTTCTACCGAG 3'

Table 2.6: PPARγ and negative control shRNA sequences.

2.2.6.5 Cloning silencing sequences into vector

2.2.6.5.1 Vector selection

psiRNA-h7SKGFPzeo plasmid (InvivoGen, USA) was chosen to perform the vector base approach of shRNA. psiRNA is specifically designed for cloning.

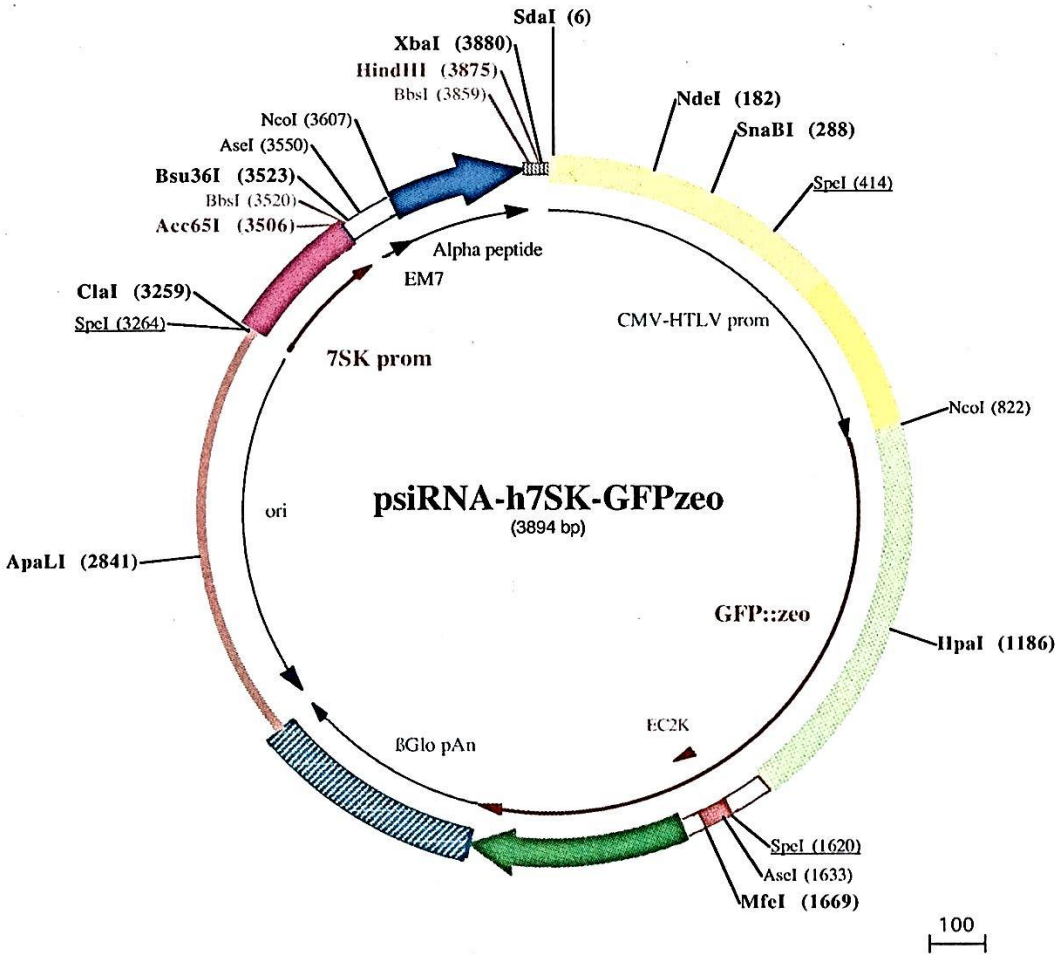

Figure 2.1: psiRNA-h7SK-GFPzeo vector map [258].

2.2.6.5.2 Annealing sense and anti-sense oligos

Oligonucleotides (forward and reverse) were dissolved first at a concentration of 100µM then more diluted to 25µM. After that annealing reaction was prepared by mixing the following components (**Table 2.7**). The reaction was incubated for 2 minutes at 80°C then stopped the heating and maintained in water bath till the temperature reached to 35°C. Annealed inserts were stored at -20°C.

Forward oligonucleotide (25µM)	2µl
Reverse oligonucleotide (25µM)	2µl
NaCl (0.5M)	6µl
H_2O to a final volume of	30µl

Table 2.7: Annealing reaction.

2.2.6.5.3 Competent cell preparation

E.coli GT116 strain, a *sbc*CD deletion mutant, which is more compatible with hairpin harbouring plasmids than standard laboratory strains, used for transformation. *E.coli* GT116 was provided as lyophilized cells, so first put them on ice for 5 minutes, then added 1ml of cold re-constitutive solution and kept on ice for 5 minutes. Solution was gently homogenised and cells were allowed completely rehydrate on ice for 25-30 minutes. Because re-constitutive cells can only be used once, a stock solution of *E.coli* GT116 strain was provided by inoculating 25 ml of LB medium (without antibiotic) with 25-100µl of re-constitutive cells. Overnight culture was aliquot in 20% glycerol, flash freezing in liquid Nitrogen and stored in -80°C.

For preparing competent cells, 1ml of overnight grown bacteria was put in a flask containing 100ml sterile SOB medium with 1ml of 2M magnesium salt, then incubated in 37°C for 90 minutes with shaking at 225 rpm . OD_{550} density was measured with spectrophotometer (Jenway, Genova, UK) in certain intervals (10-30 minutes) till OD reached 0.4. After that cultured medium was divided into 8 universals (12.5ml/tube) and cooled on ice for 10 minutes before being centrifuged at 4°C in 2000 ×g for 10 minutes. Then supernatants were discarded and pellets were re-suspended in 66ml (8.25ml/tube) RF1 buffer (RF1 calcium chloride/glycerol buffer) and kept on ice for 10 minutes before being centrifuged at 4°C in

2000 ×g for 10 minutes. Supernatants were discarded and pellets were re-suspended in 16ml (2ml/tube) RF2 buffer (RF2 calcium chloride/glycerol buffer) and pooled. Finally it has been dispensed into 1ml cryovials, flash freezing in liquid nitrogen and stored at -80°C.

2.2.6.5.4 Double digestion of plasmid DNA

After thawing psiRNA plasmid in ice, digestion reaction was prepared by mixing the following components (**Table 2.8**):

psiRNA-h7SK-GFPzeo plasmid (1µg)	~2µl
Enzyme buffer (2)	2µl
Hind III, restriction enzyme	1µl
Acc651, restriction enzyme	1µl
H_2O to a final volume of	20µl

Table 2.8: Double digestion reaction.

The reaction was incubate at 37°C water bath for one hour then put at 68°C for 10 minutes to inactivate enzymes. Enzyme digestion was confirmed by running the DNA samples on agarose gel (0.8%).

To purify digested plasmid, Wizard® SV Gel and PCR Clean-Up System (Promega, WI, USA) was used. After running the gel, band belong to digested plasmid was cut with sterile blade and put in a sterile microcetrifuge tube then Membrane Binding Solution was added to this (10µl/10µg of gel). Reaction was mixed by vortex and incubated at 50-65°C for 10 minutes before loaded in Wizard® SV Mini columns followed by 1 minute centrifuge in 10,000 ×g. After two step washing with 700 and 500µl of Membrane Wash Solution which removed by 5 minutes centrifuging at 10,000 ×g, 30-50µl of nuclease-free water was applied

directly to the centre of column then centrifuged for 1 minute at 14,000 rpm. Eluted DNA (plasmid) was used for ligation or stored in -20°C [259].

2.2.6.5.5 Ligation of shRNA insert into psiRNA

psiRNA-h7SK-GFPzeo plasmid was linearized and ligation ready. Silencing sequences (PPARγ and negative control) were annealed. Then ligation reaction was prepared by mixing the following components (**Table 2.9**), the reaction was incubated at 16°C overnight (or at 27°C for 2 hours).

Digested psiRNA	1µl (100ng)
Annealed shRNA insert	1µl
T_4 DNA Ligase	1µl (1unit)
10X ligation buffer	2µl
H_2O to a final volume of	20µl

Table 2.9: Ligation reaction.

2.2.6.5.6 Transformation

10µl of ligation product (no more than 50ng of supercoiled plasmid DNA) was introduced into pre-chilled Falcon 2059 tubes contained 200µl of *E.coli* GT116 competent cells, mixed by tapping gently and incubated on ice for 30 minutes. Alongside these transformation reactions, another tube was prepared containing only competent cell as control. All reactions were incubated in 42°C water-bath for exactly 90 seconds then placed on ice for 2 minutes. Then 800µl of freshly made SOC which pre-heated at 42°C were added to transformation product and incubated at 37°C for one hour with shaking at 225 rpm. Finally the transformed

mixtures were plated on LB-Zeocin agar plates each containing 100µg/ml Zeocin and incubated at 37°C overnight. Following incubation, colonies were picked and each grown in 10ml LB containing 100µg/ml Zeocin at 37°C with shaking, overnight. Plasmids were extracted using QIAGEN Plasmid mini-preparation kit (QIAGEN, USA). If more amount of plasmid needed, it grown in 10ml LB + Zeocin for 8 hours then 200µl of cultured product was diluted in 100ml LB + Zeocin and grown at 37°C with shaking overnight. In such cases plasmids were extracted using QIAGEN Plasmid midi-preparation kit (QIAGEN, USA).

2.2.6.5.6.1 Transformation efficiency

Transformation efficiency is the efficiency by which cells can take up extracellular DNA and express genes encoded by it. This is based on the competence of the cells. Many factors affect transformation efficiency of cells such as: plasmid size, forms of DNA, genotype of cell, growth of cell, method of transformation and damage to DNA [260-262]. It can be calculated by dividing the number of successful transformants or colony forming unit (cfu) by the amount of DNA (per µg) used during a transformation procedure.

2.2.6.5.7 Plasmid DNA preparation

QIAGEN plasmid preparation kits were used to extract and purified plasmid DNA [263, 264]. Preparation of up to 20µg plasmid DNA was performed using QIAGEN Plasmid mini-preparation kit (QIAGEN Sample & Assay Technologies, CA, USA) while for 20-100µg plasmid, QIAGEN Plasmid midi-preparation kit (QIAGEN Sample & Assay Technologies, CA, USA) was used.

2.2.6.5.7.1 Miniprep DNA extraction

Five millilitre of bacterial cell were harvested by centrifugation at > 6800 ×g for 3 minutes at room temperature. Pellets were collected and re-suspended with buffer P1 (250µl) in 1.5ml micro-centrifuge tubes. Then buffer P2 (250µl) was added and mixed thoroughly by inverting 4-6 times. After that, buffer N3 (350µl) was added and immediately mixed thoroughly by inverting tube 4-6 times. The mixture was centrifuged at 17,900 ×g for 10 minutes and the supernatant which containing plasmid DNA was applied to a QIAprep spin column. Column was centrifuged for 30-60 seconds before washed by buffer PB (500µl) followed by centrifuging 30-60 seconds. Next wash was done by applying buffer PE (750µl) and centrifuging for 30-60 seconds. Flow-through was discarded and the column was centrifuged for an additional 1 minute to remove residual wash buffer. Finally, the QIAprep spin column was placed into a clean micro-centrifuge tube and plasmid DNA was eluted by loading 30-50 µl buffer EB (10mM Tris-Cl, pH 8.5) which was let stand for 1 minute and centrifuged for 1 minute.

2.2.6.5.7.2 Midiprep DNA extraction

100-200ml of bacterial cell was harvested by centrifugation at > 6800 ×g 15 minutes at 4°C. Pellets were collected and re-suspended with buffer P1 (4ml) in PP bottles. Buffer P2 (4ml) was then added and mixed thoroughly by inverting sealed tube 4-6 times and incubated at room temperature (15-25°C) for 5 minutes. Pre-chilled buffer P3 (4ml) was added and immediately mixed thoroughly by inverting tube 4-6 times and incubated on ice for 5 minutes. The mixture centrifuged at ≥20,000 ×g for 30 minutes then the supernatant which containing plasmid DNA was transferred into a clean PP bottle and centrifuged again at ≥20,000 ×g for 30 minutes. Then supernatant was applied in a QIAGEN-tip 100 that equilibrated by applying buffer QBT (4ml) and allowed to enter the resin by gravity flow. At

this point, QIAGEN-tip 100 was washed with Buffer QC (10ml) twice before eluting DNA with buffer QF (5ml). The eluted DNA was collected in 15ml glass tube then DNA was precipitated by adding room-temperature isopropanol (3.5ml) which immediately centrifuged at ≥20,000 ×g for 30 minutes at 4°C. Supernatant was carefully decanted and DNA pellet was washed with 70% ethanol (2ml) and again centrifuged at 20,000 ×g for 10 minutes. DNA pellet was air-dried for 5-10 minutes then DNA was resolved in appropriate volume of TE Buffer (pH 8.0). DNA concentration was evaluated by NanoDrop spectrophotometer (Labtech International, Ringmer, UK). Extracted plasmid DNA was stored at -20°C.

2.2.6.5.7.3 Agarose gel analysis

To confirm the presence of shRNA insert, first the plasmid DNA was double digested (section **2.2.6.5.4**). Then a 0.8% agarose gel was prepared by dissolving 0.8g of agarose in 100ml of 0.5×TBE buffer using microwave. When the temperature reached to 50°C, Safe View (Nucleic Acid Stain) (NBS Biological Ltd., Cambridgeshire, UK) (5µl/100ml) was added for visualization and poured in cassette to set. Using undigested plasmid as control, samples were loaded in the gel. The gel was run at 80v in 0.5 × TBE buffer for one hour then visualized under UV light and subjected to densitometry for quantification using DNA molecular weight marker.

2.2.6.5.7.4 Sequencing analysis

Internal psiRNA-h7SK-GFPzeo plasmid primers [**OL559 primer** (forward):5'CGATAAGTAACTTGACCTAAGTG3'; **OL408 primer** (reverse):5'GCGTTACTATGGGAACATAC3'] were used to conduct sequencing the cloning site of plasmid. Plasmid DNAs were sent to Beckman Coulter Genomics, UK for sequencing. Sequence alignment was determined using BioEdit for searching Genbank (BLAST).

2.2.6.6 Stable transfection

X-tremeGENE HP DNA Transfection Reagent (Roche, Germany) was used for stable transfection. 1×10^5/well of PC-3M cells were put in 6-well plates 24 hours prior to transfection to reach the confluency of 30-60%. 1µl of X-tremeGENE HP DNA Transfection Reagent (for each well) was diluted in 99µl of Opti-MEM I medium (Gibco, Invitrogen, Paisley, UK) to a final volume of 100µl. Also 4µg/well of psiRNA with inserted shRNA was diluted in Opti-MEM I medium to a final volume of 100µl. After 15 minutes incubation in room temperature, diluted X-tremeGENE HP DNA Transfection Reagent and plasmid were mixed by gently flicking the tubes and incubate in room temperature for another 15 minutes. Complex was overlaid drop-wise onto wells then distributed by gently rocking back and forth. Dishes were incubated in normal cell culture conditions until cells were passaged (1-2 days). At that time, medium was replaced with those containing Zeocin^{TM} (100µg/ml) (Invitrogen, by Life technology, USA) which has been changed every three day. Zeocin^{TM} is a copper-chelated glycopeptide isolated from *Streptomyces verticillus.* When the antibiotic enters the cell, the copper cation is reduced from Cu^{2+} to Cu^{1+} and removed by sulfhydryl compounds in the cell. Upon removal of the copper, Zeocin^{TM} is activated and will bind DNA and cleave it which causing cell death [265]. Unsuccessfully transfected cells were killed by Zeocin^{TM} while successfully transfected cells were survived. After about one week, transfected cells were distributed into 9cm cell culture plates (petri dish) and cultured with selective medium containing Zeocin^{TM} for two weeks.

2.2.6.6.1 Ring cloning of transfected cells

When colonies reached to approximate diameter of 2-3 mm, single colonies were selected by ring cloning to generate single transfected cloned cell lines. Rings were created by cutting tops of 1ml pipette tips which then sterilized by autoclaving together with forceps and silicon

grease. Using the forceps, cloning rings were dipped in silicon grease and put over the colony. Small amount of silicon grease stacked the ring to plate and provided a watertight seal around the colony. Then 80µl of 2.5% Trypsin (v/v) in Versene (T/E) was added to each single colony and incubated for 2-3 minutes till cells became round and detached. T/E was deactivated by adding 160µl selective medium then cells from a clone transferred to 96-well plate. The medium was changed next day and colonies were grown in normal cell culture conditions.

2.2.7 In vitro assays

2.2.7.1 Proliferation assay

Proliferation is an important biological process for maintaining cell growth. Cell growth is defined as the increase in cell number and offset by the net cell loss by apoptosis and necrosis. The increased proliferation ability of cells is a characteristic hallmark in cancer malignancy. High proliferative activity can be occurred either from a high growth fraction or a short generation time. Especially in cancer cells, proliferation activity predicts the potential of tumorigenicity and metastasis. Thus it was necessary to determine the proliferation activity of knockdown cancer cell lines.

2.2.7.1.1 Growth curve preparation

Cells were grown in 175cm^2 flask up to 60-80% confluency then harvested and re-suspended in 10ml of complete culture medium. Using haemocytometer, a cell suspension containing 5×10^5/ml was prepared. A standard growth curve was prepared in a serial dilution as: 6.25×10^3/ml, 1.25×10^4/ml, 2.5×10^4/ml, 5×10^4/ml, 1×10^5/ml, 2.5×10^5/ml, 5×10^5/ml from which 200µl was placed in 96-well plate in triplicate. Each cell line needs its own standard curve. To measure proliferation activity of each cell line, same cell suspension containing 6.25×10^4/ml was prepared and 200µl (1.25×10^4 cells) was incubated in 96-well plate in

triplicate. As proliferation activity was assessed in 5 serial days, five similar set of cells were prepared. All plates were incubated at 37°C and 5% CO_2.

2.2.7.1.2 Cell number determination by MTT assay

MTT (3-(4, 5-dimethylthiazl-2-yl)-2, 5-diphenylterazolium bromide) is a yellow colour chemical reagent which can enter into the mitochondria of cells where then is converted by oxidative enzymes into a soluble blue dye as formazan that forms blue crystals in cell cytoplasm. Formazan crystals are dissolved by adding DMSO and prepare a blue solution which is directly proportional to the number of present cells. Optical density (OD) of dye will be measured at 570nm.

A MTT stock solution was prepared by concentration of 5mg/ml (in PBS) and stored in 4°C. Fifty µl of MTT was applied in each well of cells and incubated for 4 hours at 37°C. About 200µl of medium was removed from each well and 200µl of DMSO was loaded and incubated for 10min. The optical density of each well was measured at 570nm using the MultiSkan plate reader (BioTek Instruments, USA). Standard curve were established for each cell line by plotting OD against cell number. Then sample cell numbers were determined by extrapolating from standard curve.

2.2.7.2 Invasion assay

Invasiveness is one of the most important features of cancer cells, distinguishing benign and malignant lesions. Invasiveness and motility rate are indicators of tumour malignancy. A complex multi-stage process involves in prostate cancer cell metastasis. Invasion assay is an established method to measure invasive potential in cancer cells. The principal is those cells migrate along a chemoattractant gradient from an upper compartment through a porous membrane into the lower compartment. The BD BioCoat™ Growth Factor Reduced (GFR) Matrigel™ Invasion Chamber (BD Biosciences, USA) has been used for assessment of

metastatic potential of tumour cells [266] and different invasion aspects of cancer cells. BD Matrigel Matrix, a solubilized tissue basement membrane preparation, contains laminin, collagen type IV, heparin sulphate proteoglycan, entactin and growth factor [267]. PC3-M cells and transfected cells in an active growth phase with confluency less than 80% were maintained in serum free RPMI 1640 medium for 24 hours prior to setting up the invasion assay. After 24 hours starvation, cells were harvested and counted using haemocytometer to prepare a mixture containing 5×10^4 cells/ml in serum free medium.

At the meantime, chambers were brought out of -20°C freezer and allowed to come to room temperature. Then 0.5ml of warm medium (37°C) was applied to the interior of inserts and allowed to rehydrate for 2 hours in a humidified tissue culture incubator at 37°C, 5% CO_2 atmosphere. After rehydration, medium was carefully removed without disturbing the GFR Matrigel™ Matrix layer on the membrane. Finally, 2.5×10^4 cells in 0.5ml medium were loaded into every upper compartment of chambers while routine medium (with 10% (v/v) FCS) was placed 1ml per well in lower compartments. Negative control was set up for each cell line by using serum free medium in lower compartment. All cell lines were set as triplicate and assay was run in a humidified tissue culture incubator at 37°C, 5% CO_2 atmosphere for 24 hours. Then, cells which remain in upper side of filter were removed gently using cotton swabs and washed with PBS. The cells migrated to the lower part of filter were fixed and stained using 2% crystal violet for 10 minutes. After several washes with water, chambers were left at 37°C to dry. The number of stained cell in lower part were counted using light microscope (Leitz, labovert, Luton, UK) at 125× magnification. Photographs were taken using Olympus digital camera (Olympus C-4040) at 100× magnification.

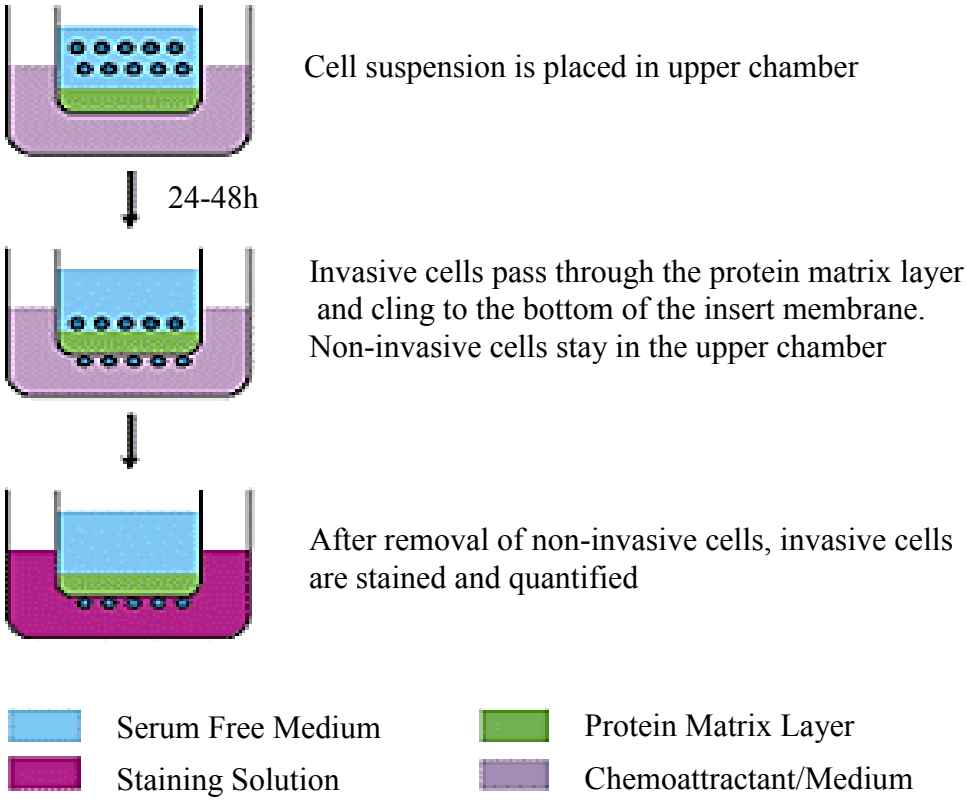

Figure 2.2: Invasion assay; performed in chambers with 8µm pore size which coated with Matrigel matrix.

2.2.7.3 Soft agar assay

Neoplastic transformation occurs via a series of genetic and epigenetic alterations which yield a cell population that is capable of proliferating independently of both external and internal signals that normally restrain growth. Basement membrane supports normal epithelial cells *in vivo* by providing a variety of physical and hormonal signals important for their homeostasis and phenotype differentiation. In suspension culture, many of these cells undergo apoptosis [268]. Alternatively, cancer cells are able to evade attachment regulated apoptosis (anoikis), leading to uncontrolled proliferation. Therefore, anchorage-independent growth is one of the hallmarks of cell transformation, which is considered the most accurate and stringent *in vitro* assay for detecting malignant transformation of cells, with normal cells typically not capable

of growth in semisolid matrices. The soft agar colony formation assay is a common method to monitor anchorage-independent growth, which measures proliferation in a semisolid culture media after 3-4 weeks by counting colonies [269]. So the more malignant a tumour cell, the greater the ability to produce colonies of cells in soft agar assay. In this study, parental and shRNA transfected PC3M cells were cultured in soft agar to evaluate their ability in colony formation.

The assay was carried out in 6-well plates which pre-coated 2ml of 2% (w/v) low-melting point agarose gel in routine and selective culture medium with 10% (v/v) FCS that solidified in refrigerator at 4°C for 20 minutes. In the meantime, parental and transfected cell lines were harvested and adjusted with routine and selective medium to 5000 cells/ml which then mix with 1ml of pre-warm 1% (w/v) low-melting point agarose gel and were placed on top of the present basement gel layer. Complex were again put in 4°C for 20 minutes for solidification before incubation at 37°C in humid incubator with 5% CO_2 atmosphere for 4-6 weeks. During this period, cells were feed with 200µl/well once a week. At the end of assay, colonies were stained by adding 0.5ml of 2% MTT (3-(4, 5-dimethylthiazl-2-yl)-2, 5-diphenylterazolium bromide) then incubated at 37°C, 5% CO_2 for 4 hours. Colonies larger than 150µm were counted using Gel Count (Oxford Optronix, UK).

2.2.7.4 Angiogenesis assays

Angiogenesis is a process of generating new capillary blood vessels. It is a fundamental component for a number of normal (reproduction and wound healing) and pathological processes (diabetic retinopathy, rheumatoid arthritis, tumour growth and metastasis) [270].

VEGF (Vascular endothelial growth factor) is also called VEGF-A, following the identification of several VEGF-related factors (VEGF-B, VEGF-C, VEGF-D, VEGF-E). VEGF significantly influence vascular permeability and is a strong angiogenesis protein in several bioassays and also plays a role in neovascularization under physiological conditions

[271]. In this study, expression levels of VEGF were assessed, in proteins extracted from cell lines by Western blotting (as section **2.2.3.3**) and in conditional medium (secreted VEGF) by ELISA. Activity of VEGF was also tested by evaluation of tube formation in *in vitro* angiogenesis assay.

2.2.7.4.1 Enzyme-linked immunosorbent assay for evaluating VEGF

The RayBio®Human VEGF ELISA (Enzyme-Linked Immunosorbent Assay) kit was used for quantitative measurement of human VEGF in the conditional media of 22RV1cells. This assay employs a specific human VEGF antibody coated in a 96-well plate. After loading standards and samples into wells, present VEGF was bound to wells by immobilized antibody. Biotinylated secondary antibody was added to each well after wash. Then after washing away unbounded biotinylated antibody, HRP-conjugated streptavidin was pipetted into each well to detect the secondary antibody. After another set of washing, the amount of bound VEGF was developed by adding the TMB substrate solution. Finally, the Stop Solution changed the colour from blue to yellow and the intensity of the colour was measured at 450nm [272].

2.2.7.4.1.1 Standard curve preparation

Four hundred microliter of diluent buffer were loaded in each tube then the recombinant human VEGF was diluted in 50mM sodium carbonate (PH: 7.6) to a concentration of 50ng/ml which then used to prepare serial dilutions as showed in **Figure 2.3**. Diluting buffer served as the zero standard (0pg/ml).

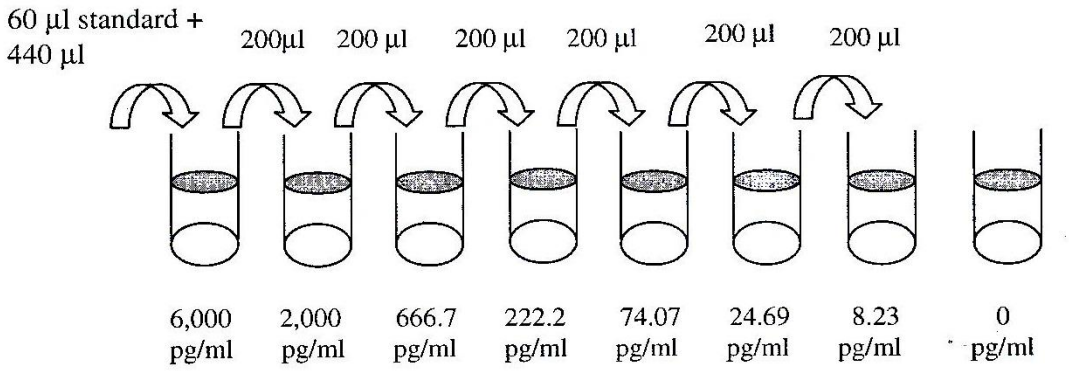

Figure 2.3: Serial dilutions for VEGF ELISA standard curve.

2.2.7.4.1.2 Human VEGF ELISA

1×10^6 cells were seed in $75cm^2$ culture flasks and cultured in growth factor deprived medium (phenol red-free RPMI 1640 containing 10% charcoal stripped FCS) for 48 hours. The conditional medium of each different treatments were collected then 100µl of each standard (**Fig. 2.3**) and samples were loaded into VEGF microplate wells. The plate covered by lead and incubated at room temperature for 2.5 hours (or overnight at $4^{\circ}C$) with gentle shaking. Supernatant was discarded and wells were washed four times with 300µl of wash solution provided by VEGF ELISA Kit. After that, 100µl of biotinylated secondary antibody was loaded into each well and incubated at room temperature for 1 hour which followed by four step wash as mentioned above. 100µl of HRP-Streptovidin solution was added to the wells and incubated for 45 minutes at room temperature. Finally for visualizing the VEGF level, after four washes, 100µl of TMB substrate reagent was loaded to each well and incubated for 30 minutes which followed by adding 50µl of 2M sulphuric acid to stop the reaction. The plate was immediately read at 450nm in the optical density plate reader and the expression level of VEGF secreted in conditional medium for each culture condition was quantified using standard curve. Results were the mean ± SD of three separate experiments.

2.2.7.4.2 *In vitro* angiogenesis assay

Millipore® *In Vitro* Angiogenesis Assay Kit was used for evaluation the tube formation of endothelial cells induced by secreted VEGF in conditional medium. When cultured on ECMatrix™, a solid gel of basement proteins prepared from the Engelbreth Holm-Swarm (EHS) mouse tumour pre-angiogenic factors, can provide the condition in which these endothelial cells rapidly align and form hollow tube-like structures [273].

2.2.7.4.2.1 Preparation of ECMatrix coated plate

ECMatrix and 10× diluent buffers were thawed overnight on ice in a 4°C refrigerator before mixing together (100µl of 10× diluent buffer with 900µl of ECMatrix) in a sterile micro-centrifuge tube. Undiluted ECMatrix is highly viscous, so it is necessary to cut off pipette tips with a sterile knife to ease pipetting and to prevent air bubble. All devices such as pipette tips, plates and tubes were precooled and experiment was carried out in cold room. 50µl of diluted ECMatrix was loaded in each well of 96-well plate then incubated at least for one hour at 37°C to solidify.

2.2.7.4.2.2 Angiogenesis assay

Human umbilical vein endothelial cells (HUVEC) were cultured to 60-80% confluency in 75cm^2 flask in EndoGRO basal medium added with Endo GRO LS supplement kit before harvesting and preparing a solution contain 10^4cells/100µl which was seeded on top of ECMatrix layer in each well. Then 100µl of conditional medium of each different treatment were loaded and plates were incubated at 37°C, 5%CO_2 for 6 hours. Recombinant human VEGF (10ng/ml) was used as positive control and each sample loaded as triplicate. Finally, cell-tubes were visualized by adding 50µl of 2% MTT for 10 minutes at room temperature and quantified under an inverted light microscope at 40 × magnification [274].

2.2.7.4.2.3 Quantitation of tube formation

Activated endothelial cells form cellular network (mesh like structure) from capillary tubes, which is a dynamic process, starting with cell migration and alignment, followed by development of capillary tubes, sprouting of new capillaries and terminate by formation of cellular networks. Although *in vitro* angiogenesis Assay is a qualitative assay, it is possible to quantitate by assigning a numerical value to each pattern. By this way, a numerical value is associated with progression of angiogenesis (**Table 2.10**). Five random field per well were examined and the values were averaged. Results of assays were statistically assessed using Student's t-test and the *p*-value less than 0.05 was considered as statistical significance.

Pattern	Value
Individual cells, well separated	0
Cells begin to migrate and align themselves	1
Capillary tubes visible. No sprouting	2
Sprouting of new capillary tubes visible	3
Closed polygons begin to form	4
Complex mesh structures develop	5

Table 2.10: Numerical values for degree of angiogenesis progression.

2.2.7.5 Dual-Luciferase®Reporter (DLR™) Assay

Genetic reporter systems are widely used to study eukaryotic gene expression and cellular physiology, receptor activity, transcription factors, intracellular signalling, mRNA processing and protein folding [41]. Dual reporters, the simultaneous expression and measurement of two individual reporter enzymes within a single system, are commonly used to improve experimental accuracy. Typically, the "experimental" reporter correlates with the effect of

specific experimental conditions, while the activity of co-transfected "control" serves as baseline response. Normalizing the activity of experimental reporter to the activity of internal control minimize experimental variability caused by difference of cell viability or transfection efficiency [275]. In the DLR™ Assay (Promega, WI, USA), the activities of firefly (*Photinus pyralis*) and *Renilla* (*Renilla reniformis*) luciferases are measured sequentially from a single sample. The firefly luciferase reporter is measured first by adding Luciferase assay reagent II (LAR II) to generate a stabilized luminescent signal, followed by adding Stop & Glo® reagent assay to produce a stabilized signal from the *Renilla* luciferase. Finally, by dividing the firefly luciferase activity to *Renilla* luciferase activity, luciferase expression of designated vector can be determined.

2.2.7.5.1 Luciferase Reporter Vector (pGL3-Promoter Vector)

The pGL3 Luciferase Reporter Vectors (Promega, WI, USA) are designed for quantitative analysis of factor which potentially regulates gene expression in mammalian. The pGL3 Vectors backbone contains a modified coding region for firefly (*Photinus pyralis*) luciferase, used to monitor transcriptional activity in transfected eukaryotic cells. The assay of this genetic reporter is rapid, sensitive and quantitative. pGL3 vectors contain numerous features that aid the characterization and mutagenesis of the putative regulatory sequences. This study based on promoter *VEGF* gene, so pGL3-promoter vector has been chosen. The pGL3-promoter vector contains SV40 promoter upstream of the luciferase gene. Inserts containing putative enhancer elements can be inserted in either orientation and upstream or downstream to the promoter-*luc* transcriptional unit (**Fig. 2.4**) [276].

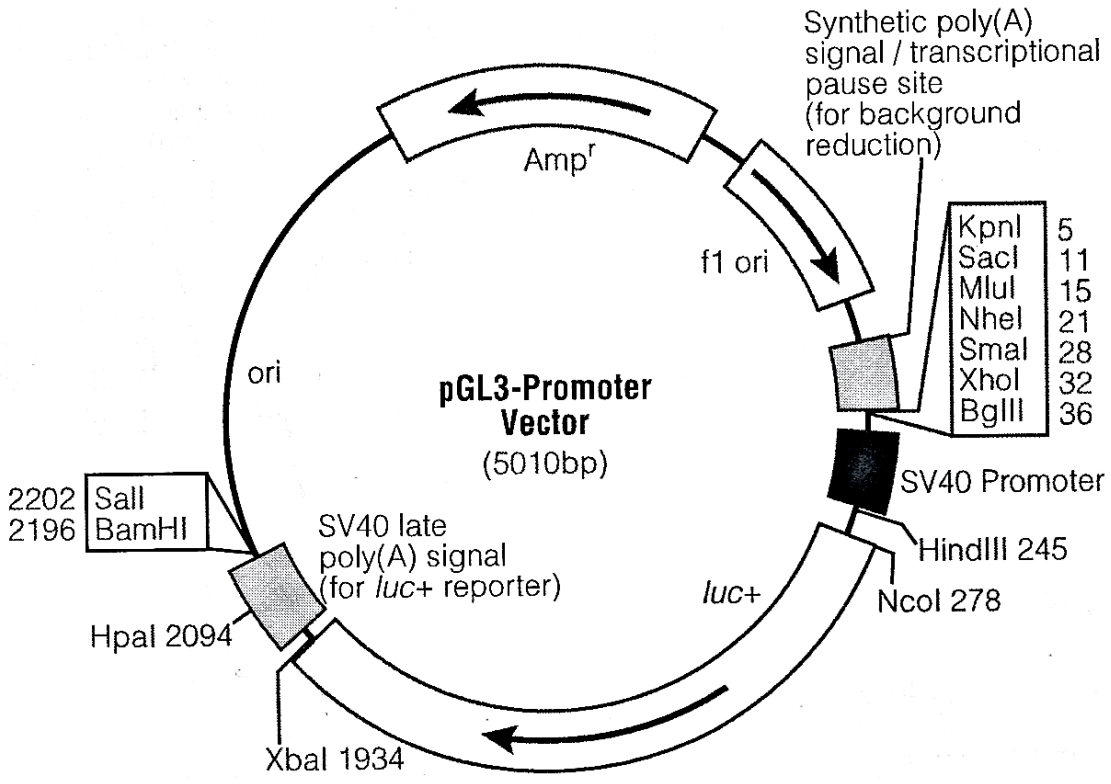

Figure 2.4: pGL3-Promoter Vector circle map.

2.2.7.5.2 Reporter constructs

Three promoter reporter constructs based on human VEGF promoter [277] were designed from whole VEGF promoter sequence (gi|224589818:43727945-43737944 Homo sapiens chromosome 6, GRCh37.p10 Primary Assembly) and constructed by Gen Script (Transforming Biology Research, NJ, USA). Main truncated promoter-reporter construct (Wild type) contained 5'flanking sequences extending -805 nucleotides from the transcriptional start site and including two peroxisome proliferative responsive elements (*PPRE*) (-796 to -790bp and -443 to -437bp) [248]. *PPRE* sequence (AGGCCA) [278] was mutated in Mutant1 constructs (ATGCAT) and in Mutant2 it made shorten to -393bp. KpnI (GGTACC) and XhoI (CTCGAG) sequences were added to each end of constructs as enzyme sites to be compatible for inserting in pGL3-promoter vector (complete constructs sequences shown in **Appendix D**).

2.2.7.5.3 Cell culture and transfection

22RV1, PC3-M, PC3-M-PPARγ-si-H and PC3-M-3 prostate cancer cell lines were cultured in normal cell culture condition up to 60-80% confluency before harvesting and seeding into 24-well plates. 5×10^4cells/well in 1ml medium was cultured overnight, then culture medium replaced with 900µl fresh medium, overlaid with 100µl of a transfection solution containing 1µg of each luciferase plasmids, 100ng of *Renilla* luciferase,1µl of X-treme GENE HP DNA Transfection Reagent (Roche, Germany) in Opti-MEM I medium (Gibco, Invitrogen, Paisley, UK). Transfection solution was incubated at least 15 minutes prior to overlaying in room temperature. In each set of experiment, cells were transfected with pGL3-promoter vector only, pGL3-promoter vector containing Wild type, Mutant1 or Mutant2, separately. After overnight transfection, reaction was stopped by refreshing medium, then after 6 hours recovery, cell were exposed to 0.5µM of Rosiglitazone (Sigma-Aldrich, UK) a synthetic PPARγ agonist, 20µM of GW9662 (Sigma-Aldrich, UK) a synthetic PPARγ antagonist, 2µM of wild type C-FABP recombinant protein, 2µM of single mutant C-FABP recombinant protein, 2µM of double mutant C-FABP recombinant protein or 0.1µM of Mithramycin A (Sigma-Aldrich, UK) as Sp1 inhibitor individually or as combination, overnight.

2.2.7.5.4 DLR™ Assay Protocol

After 16-24 hours treatment, culture medium was removed and cells were washed twice with PBS (phosphate buffer saline) before lysis with 100µl of 1× Passive Lysis Buffer. Cells were incubated with 1×PLB for 15 minutes in room temperature then cell lysates were collected in micro-centrifuge tubes and centrifuged in13, 000 rpm at 4°C for 30 seconds to separate the pellet. In the meantime, Luciferase Assay Reagent II (LARII) was prepared and loaded 100µl into the appropriate number of luminometer tubes to complete the desired number of DLR™ assays. Then 20µl of cell lysate was mixed to LARII by pipetting 2 or 3 times before first

measurement with Sirius Luminometer (Berthold detection system, Germany) which recorded firefly luciferase activity. Finally 100µl of Stop & Glo® assay reagent was added and vortex briefly to mix before second measurement with luminometer which represented *Renilla* luciferase activity. Pure luciferase expression of designated vector was calculated by dividing the firefly luciferase activity to *Renilla* luciferase activity and different expressions with different treatments were statistically assessed using Student`s t-test. *P*-value less than 0.05 were regarded as statistically significant.

2.2.8 *In vivo* tumorigenicity assay

2.2.8.1 Mice and cell lines

All the experiments were conducted in accordance to UKCCCR guideline under Home Office Licence: PPL 40/3578 to Prof. Y. Ke and the personal licence: PIL 40/10535 to Farzad S. Forootan. To investigate the tumorigenicity of suppressed PPARγ PC3-M cell lines, 30 male Balb/C immune-incompetent nude mice (6-8 week old) were purchased from Charles River Laboratories. They were weighted in their arrival and ranged between 18-21g. After one week settling down, they were divided to three groups of 10 and the following three cell lines were tested in them at same time:

Group 1: Control; PC3-M cells

Group 2: PC3-M-PPARγ-si-M (moderately suppressed PPARγ-PC3-M cells)

Group 3: PC3-M-PPARγ-si-H (highly suppressed PPARγ-PC3-M cells)

2.2.8.2 Mice inoculation

Cell lines for *in vivo* tumorigenicity assay, were cultured up to 80% confluency. On the day of inoculation, cells were harvested and re-suspended in PBS at the concentration of 5×10^6/ml. Cell suspensions were kept on ice before injecting 200µl (1×10^6 cells) subcutaneously in right or left flank region of each mice. Weight of mice and tumour size were measured twice a week using a calliper. Tumour volume were calculated by the following formula: Length×Width×Heigth×0.5236 [279] and primary tumours were weighted after autopsy.

2.2.8.3 Processing of primary tumour tissues

Primary tumours were removed by dissection and fixed in 10% formalin at least for 24 hours. The fixed tissue samples were trimmed and put in an embedding cassette and processed in Tissue-Tek VIP5 processor. Then processed tissues were embedded in paraffin wax at 60°C and cooled on ice. After solidification, blocks were cut using microtome (MICROM, Oxford, UK) and 4µm sections were mounted on labelled Superior Adhesive Slides (Apex, Leica, UK) prior to processing for immunohistochemistry.

2.2.8.4 Immunohistochemistry

To visualizing reduced expression of PPARγ in suppressed tissue, prepared sections were underwent immunohistochemical staining (section **2.2.4.3**) and scored by evaluating intensity and percentage of staining in both cytoplasm and nucleus (section **2.2.4.4**).

2.2.9 Statistical analysis

Statistical analysis was performed using the Statistical Package for Social Sciences (SPSS), version 20 (SPSS Inc., Chicago, IL., USA). In all statistical analyses, results were regarded as significant when *p* is smaller than 0.05.

2.2.9.1 Two-sided Fisher's exact test & Chi-square (χ^2)

2-sided Fisher exact test and χ^2 analysis are used to determine whether there is a significant difference between the expected frequencies and the observed frequencies in one or more categories. Correlation between PPARβ/δ and PPARγ, C-FABP and AR expression and the nature of prostate tissue (benign or malignant) were assessed by 2-sided Fisher exact test and χ^2 analysis. Two-sided Fisher's exact test was used when samples evaluated only for two parameters while χ^2 was used for assessing more than two parameters. A value of $p \leq 0.05$ was used to define the statistical significance.

2.2.9.2 Survival analysis

2.2.9.2.1 Kaplan-Meier curve

Correlation between survival and expression of individual factors was analysed by Kaplan-Meier survival test. In this study correlation between expression of PPARβ/δ, PPARγ, C-FABP (both in nucleus and cytoplasm), Androgen receptor, PSA level and Gleason score and patients' survival time were assessed by Kaplan-Meier curves.

2.2.9.2.2 Cox regression test

Cox regression test was used to analysis the effect of multiple factors on patient survival. Multiple effects of combined C-FABP with PPARγ or PPARβ/δ to patients' survival period were evaluated using Cox regression test.

2.2.9.2.3 Log Rank test

Log Rank test was used to assess the difference of survival time between different groups in Kaplan-Meier and Cox regression tests. It is a nonparametric test and appropriate to use when the data are right skewed and censored (technically, the censoring must be non-informative). A value of $p \leq 0.05$ was used to define the statistical significance.

2.2.9.3 Mann-Whitney U test

Man-Whitney U test is a nonparametric test of the null hypothesis that two populations are the same against an alternative hypothesis, especially that a particular population tends to have larger values than the other. Box plot is a convenient way of graphically depicting groups of numerical data through their quartiles. Box plot and Man-Whitney U test were used to assess the correlation between expression levels of PPARγ or PPARβ/δ and PSA level or AR index. A value of $p \leq 0.05$ was used to define the statistical significance.

2.2.9.4 Student's t-test

Student's t-test was used to evaluate the significant difference in average between two groups and is most commonly applied when the test statistic would follow a normal distribution. In this study, Student's t-test was used to compare any observed difference between experimental and control groups in proliferation assay, invasion assay, soft agar assay, *in vitro* angiogenesis assay , tumour volume in *in vivo* assay and difference in luciferase levels in DLR assay. A value of $p \leq 0.05$ was used to define the statistical significance.

CHAPTER THREE:

RESULTS

3 Results

3.1 Expression of PPARβ/δ, PPARγ and C-FABP at protein level in prostate cell lines

3.1.1 Expression of PPARβ/δ protein

The results of Western blot analysis of C-FABP and its possible receptors PPARβ/δ, PPARγ are shown in **Figure 3.1**. A single PPARβ/δ band of 52kDa was detected in benign PNT2 cells, weakly malignant LNCaP cells, and highly malignant PC3 and DU145 cells, but was barely detectable in the highly malignant PC3M cells (**Fig. 3.1, A**). When the densitometric level of PPARβ/δ in PNT2 was set at 1 (**Fig. 3.1, D**), the relative level in weakly malignant LNCaP cells was 0.66 ± 0.04; levels in highly malignant DU145, PC3-M and PC3 cells were 1.57 ± 0.15, 0.31 ± 0.03 and 0.61 ± 0.1, respectively. The changes in levels of PPARβ/δ did not appear to be related to changes in malignant characteristics.

3.1.2 Expression of PPARγ protein

A single PPARγ band of 57kDa was detected in all 5 cell lines by Western blotting (**Fig. 3.1, B**). When the densitometric level of PPARγ in PNT2 was set at 1 (**Fig. 3.1, E**), the level in weakly malignant LNCaP cells was 0.74 ± 0.09; levels in highly malignant DU145, PC3-M and PC3 cells were 1.14 ± 0.16, 2.73 ± 0.28 and 3.66 ± 0.23, respectively. Thus the level of PPARγ increased with increasing malignancy in these prostatic cells.

3.1.3 Expression of C-FABP protein

Western blots showed that C-FABP expression was not detected in benign PNT2 and weakly malignant LNCaP cells, but a strong 15kDa C-FABP band was detected in highly malignant cell lines DU145, PC3M, and PC3 (**Fig. 3.1, C**). When the densitometric level of C-FABP in PC3 was set at 1 (**Fig. 3.1, F**), levels expressed in other malignant PC3-M and DU145 cells

were reduced to 0.9 ± 0.07 and 0.59 ± 0.07, respectively. In contrast levels in the benign PNT2 and weakly malignant LNCaP cells were not detectable.

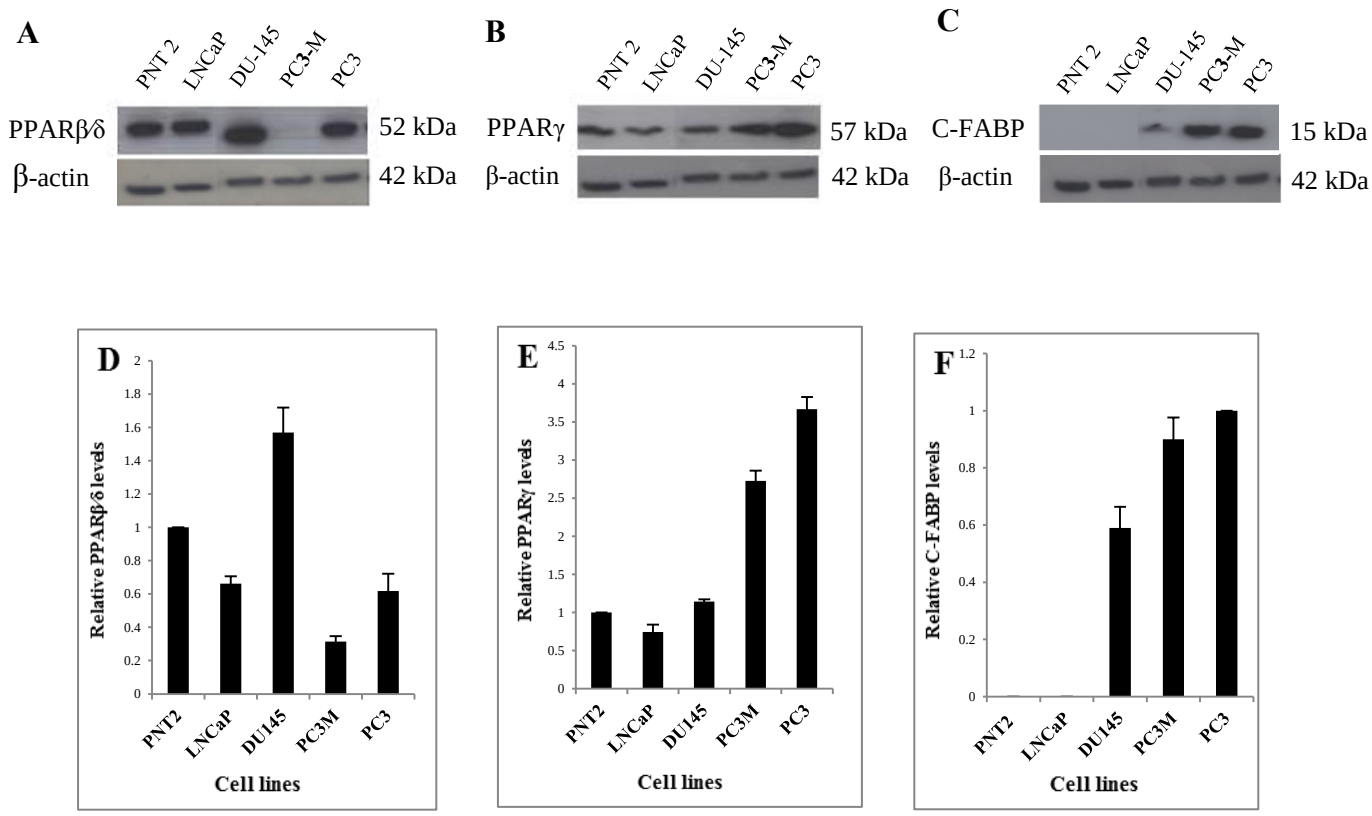

Figure 3.1: Measurement of levels of C-FABP and its possible nuclear receptors (PPARβ/δ and PPARγ) in prostate cell lines**.**

More accurate quantitative analysis on levels of PPARβ/δ (**A**), PPARγ (**B**) and C-FABP (**C**) were conducted by scanning the peak areas of the bands on the blots. To standardize the immune reactions, the same blot was incubated with an anti-β-actin antibody. Relative levels of each protein (**D:** PPARβ/δ**, E:** PPARγ and **F:** C-FABP) were measured by densitometric scanning of the intensities of the relevant protein bands and normalized to that of β-actin on the same blot. In **D** and **E**, the level of immunoreactive-proteins in PNT2 was set at 1; Levels expressed in other cell lines were obtained by comparison with that in PNT2. In **F**, the level of immunoreactive-proteins in PC3 was set at 1; Levels expressed in other cell lines were obtained by comparison with that in PC3. Results were obtained from 3 separate experiments (mean ± SD).

3.2 Expressions of *PPARβ/δ* and *PPARγ* at mRNA levels in prostate cell lines

RT-PCR used to evaluate mRNA expressions of *PPARβ/δ* and *PPARγ* in the total RNAs isolated from six prostate cell lines. RT-PCR products were analysed by agarose gel electrophoresis (**Fig. 3.2)**. RT-PCR showed a single *PPARβ/δ* band (481 bp) in benign PNT2 cells, moderately malignant 22RV1 cells, highly malignant PC3, PC3-M and DU145 cells, but was barely detectable in the weakly malignant LNCaP cells (**Fig. 3.2, A**). A single *PPARγ* band (463 bp) was detected prominently in PC3 and PC3-M cell lines, weakly in 22RV1 cells but was not found in DU145, LNCaP and PNT2 cell lines (**Fig. 3.2, B**). Expression levels of *β-actin* mRNA were used as a house-keeping gene (**Fig. 3.2, C**) to standardise the measurements.

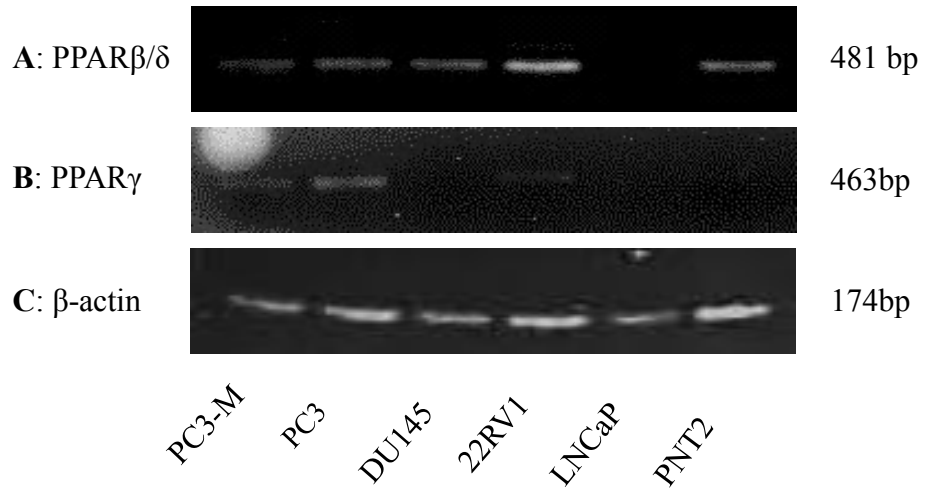

Figure 3.2: Detection of *PPARβ/δ*, *PPARγ* and *β-actin* mRNA in prostate cell lines**.**
RT-PCR results, analysed on a 0.8% agarose gel in 0.5×TBE buffer alongside 100 base pair ladder DNA marker revealed: **A**: Expressions of *PPARβ/δ* mRNA (481 bp), **B**: Expressions of *PPARγ* mRNA (463 bp), **C**: Expressions of *β-actin* mRNA (174 bp).

3.3 Expression of PPARβ/δ, PPARγ and C-FABP in prostate tissues

Immunehistochemical staining of 132 prostate tissue sections, including 35 BPH and 97 carcinoma samples were performed to detect PPARβ/δ, PPARγ and C-FABP proteins (in each experiment, some cases were excluded from the study because of technical reasons). Staining for PPARβ/δ in BPH and carcinomas was detected in both cytoplasm and nucleus (**Fig. 3.3, A-D**) (**Table 3.1-1**). Among 32 stained BPH cases, 28 (88%) were stained weakly and 4 (12%) moderately positive with PPARβ/δ antibody in both cytoplasm and nucleus (**Fig. 3.3, A**). Among 94 stained adenocarcinoma cases, both cytoplasmic and nuclear staining was observed. Cytoplasmic staining was weak in 32 (34%), moderate in 50 (53%) and strong in 12 (13%) cases and in the nucleus, staining was weak in 13 (14%), moderate in 65 (69%) and strong in 16 (17%) cases (**Fig. 3.3, B-D**). The levels of both cytoplasmic (χ^2 test, $p < 0.001$) and nuclear (χ^2 test, $p < 0.001$) staining for PPARβ/δ were significantly higher in carcinomas than those in BPH (**Table 3.1-1**).

Staining for PPARγ was detected in both cytoplasm and nucleus of cells in BPH and carcinoma tissues (**Fig. 3.3, E-H**) (**Table 3.1-2**). In 32 analysed BPH samples, cytoplasm was stained weakly in 31 (97%) and moderately in 1 (3%) cases; while nuclear staining was weak in 30 (94%) and moderate in 2 (6%) samples (**Fig. 3.3, E**). Among a total of 90 stained carcinomas, cytoplasm was stained weakly in 35 (39%), moderately in 45 (50%) and strongly in 10 (11%) cases; while nuclear staining was weak in 12 (13%), moderate in 57 (63%) and strong in 21 (24%) samples (**Fig. 3.3, F-H**). Staining for PPARγ in both cytoplasm (χ^2 test, $p < 0.001$) and nucleus (χ^2 test, $p < 0.001$) of carcinomas was significantly higher than those in BPH (**Table 3.1-2**).

Immunohistochemical staining for C-FABP was observed in both cytoplasm and nucleus of BPH and carcinoma cells (**Fig. 3.3, I-L**) (**Table 3.1-3**). Among 35 BPH cases, 33 (94%) were unstained and 2 (6%) stained weakly in the cytoplasm. In the nucleus, 25 (71%) were

unstained, 7 (20%) stained weakly, 5 (14%) stained moderately and 3 (8%) stained strongly (**Fig. 3.3, I**). Among 97 analysed adenocarcinomas, cytoplasmic and nuclear staining was observed in 94 (96%) and 88 (91%) of cases, respectively (**Fig. 3.3, J-L**). Cytoplasmic staining was weak in 23 (24%), moderate in 54 (56%) and strong in 17 (18%) cases. In the nucleus, 20 (21%) cases stained weakly, 32 (33%) moderately and 36 (37%) strongly. Intensities of both cytoplasmic (χ^2 test, $p < 0.001$) and nuclear (χ^2 test, $p < 0.001$) staining for C-FABP were significantly higher in carcinomas than those in BPH (**Table 3.1-3**).

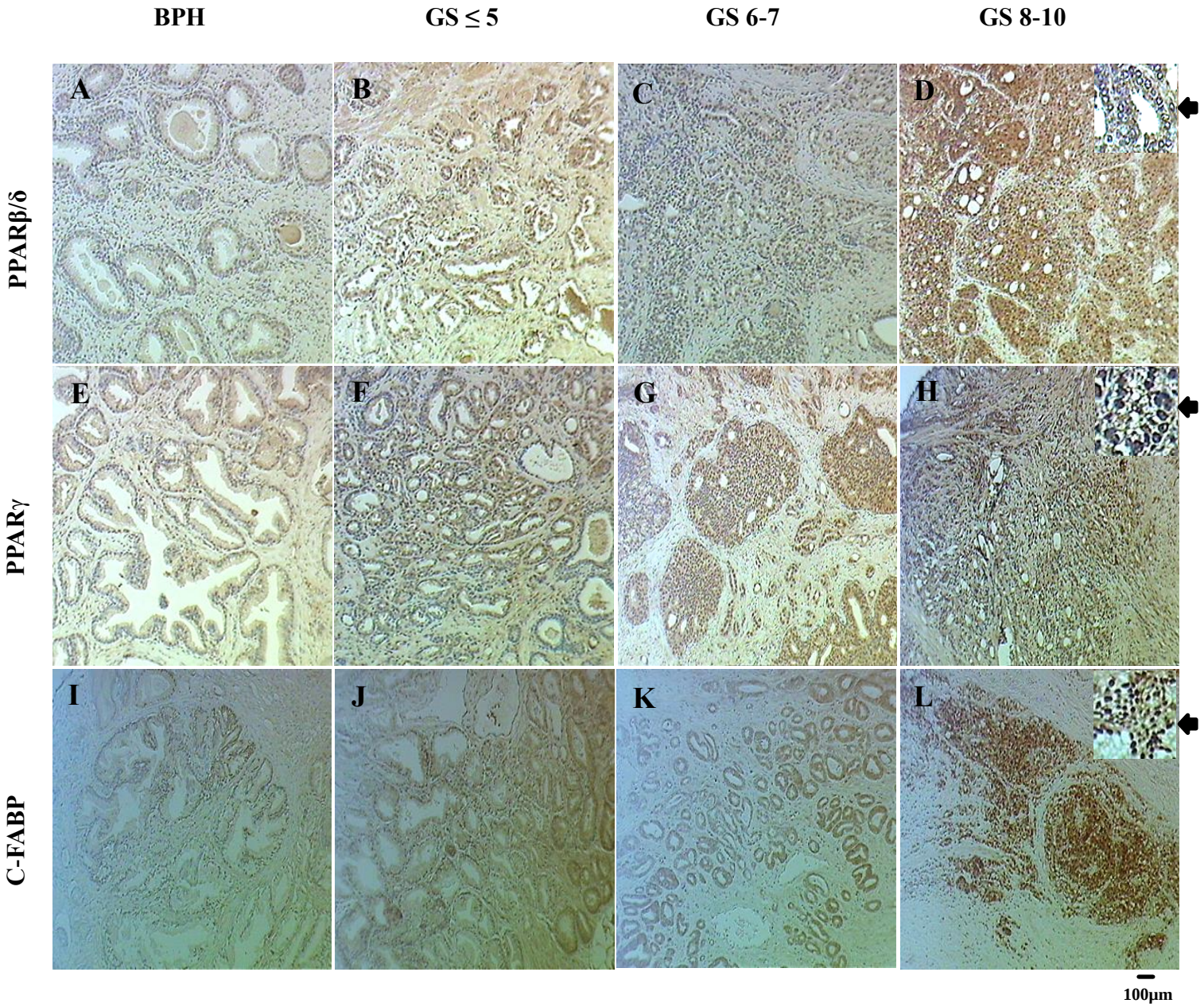

Figure 3.3: Immunohistochemical staining of BPH and prostatic carcinoma tissues with antibodies against PPARβ/δ, PPARγ, and C-FABP**.**

Carcinoma tissues were divided into weakly (GS ≤ 5), moderately (GS 6-7) and highly (GS 8-10) malignant groups according to their combined Gleason scores (GS). Cytoplasmic and nuclear staining is shown in the inserts (arrows). Original magnifications of images of representative slides were 100×; original magnifications of the inserts were 250×.

3.1-1: PPARβ/δ stain

Tissue	Cytoplasmic Stain intensities			No. Of cases	Nuclear stain intensity & Percentage score		
	+	++	+++		≤3	4-6	≥7
BPH	28	4	0	32•	28	4	0
Carcinomas (total)	32	50	12	94•	13	65	16
Scores* ≤5	6	6	2	14	4	9	3
Scores* 6-7	12	18	5	35	5	25	5
Scores* 8-10	14	26	5	45	6	31	8

3.1-2: PPARγ stain

BPH	31	1	0	32•	30	2	0
Carcinomas (total)	35	45	1	90•	12	57	21
Scores* ≤5	5	7	0	13	4	8	1
Scores* 6-7	13	18	1	34	4	21	9
Scores* 8-10	17	20	3	43	4	28	11

3.1-3: C-FABP stain

	0	+	++	+++		0	+	++	+++
BPH	33	2	0	0	35	25	7	5	3
Carcinomas (total)	3	23	54	17	97	9	20	32	36
Scores* ≤5	2	8	5	1	16	2	6	4	4
Scores* 6-7	0	12	17	8	37	4	7	12	14
Scores* 8-10	1	3	32	8	44	3	7	16	18

* Combined Gleason Scores

• Total BPH cases were 35 and total carcinoma cases were 97, but in each experiment, some cases were excluded from the study because of technical reasons.

Table 3.1: Cytoplasmic and nuclear expression of different PPARs and C-FABP in benign and malignant human prostate tissues.

3.4 Correlations between PPARβ/δ, PPARγ and C-FABP

When the relationship among the staining levels for PPARβ/δ, PPARγ and C-FABP in carcinomas was assessed, the increased level of PPARβ/δ in both cytoplasm and nucleus were not significantly correlated with either staining for PPARγ or C-FABP (Fisher's Exact test, $p > 0.05$). While increased nuclear staining for C-FABP was significantly correlated with increased nuclear staining for PPARγ (Fisher's Exact test, $p < 0.05$), increased cytoplamic staining for C-FABP was not significantly correlated with cytoplasmic staining for PPARγ (χ^2 test, $p > 0.05$). Interestingly, the increased cytoplasmic staining for C-FABP was significantly correlated with nuclear staining for PPARγ (Fisher's exact test, $p < 0.05$), whereas the increased cytoplasmic staining for PPARγ was not significantly correlated with nuclear staining for C-FABP (χ^2 test, $p > 0.05$). To correlate the staining for C-FABP and PPARs with GS, carcinomas were divided into low (≤5), moderate (6-7) and high (8-10) GS groups.

3.5 Correlation with Gleason score

Although expression levels of PPARβ/δ, PPARγ and C-FABP are higher in carcinoma tissues compare to benign, only increased nuclear PPARγ and cytoplasmic C-FABP staining significantly correlate with increased GS in patients.

3.5.1 Correlation of PPARβ/δ and Gleason score

Although cytoplasmic staining for PPARβ/δ was significantly correlated with its nuclear levels (χ^2 test, $p < 0.001$), neither nuclear (χ^2 test, $p > 0.05$) nor cytoplasmic (χ^2 test, $p > 0.05$) staining for PPARβ/δ was significantly correlated with increased GS in these cases.

3.5.2 Correlation of PPARγ and Gleason score

The increased cytoplasmic level of PPARγ was positively correlated with that in the nucleus (χ^2 test, $p < 0.001$). When correlation between staining for PPARγ and GS was assessed,

increased nuclear staining for PPARγ was significantly correlated with the higher GS of the carcinomas (Fisher's Exact test, $p \leq 0.05$), but the correlation between its cytoplasm staining and the increased GS was not significant (Fisher's Exact test, $p > 0.05$).

3.5.3 Correlation of C-FABP and Gleason score

The increased cytoplasmic level of C-FABP was positively correlated with that in the nucleus (χ^2 test, $p < 0.05$). When correlation between staining for C-FABP and GS was assessed, increased cytoplasmic staining for C-FABP was significantly correlated with the increased GS of the carcinomas (χ^2 test, $p < 0.05$), but the correlation between increased nuclear staining and high GS was not significant (χ^2 test, $p > 0.05$).

3.6 Correlations with patient survival

The level of PPARβ/δ, PPARγ or C-FABP and the duration of patients' overall survival time (the length of survival time from initial diagnosis) was plotted using Kaplan-Meier survival curves and the significance of the differences was assessed by Log Rank test (**Fig. 3.4,5**).

3.6.1 PPARβ/δ expression and patient survival

The median survival time for patients with strongly, moderately and weakly positive cytoplasmic staining for PPARβ/δ, was 47, 37 and 42 months, respectively (**Fig. 3.4, A**). For patients with a strongly positive nuclear staining for PPARβ/δ, the median survival time was 31 months (**Fig. 3.4, B**). This was shorter than 39 and 57 months for moderately and weakly stained cases, respectively. Correlation between the level of nuclear (Log Rank test, $p \geq 0.204$) and cytoplasmic (Log Rank test, $p \geq 0.532$) staining of PPARβ/δ and patient survival time was not statistically significant.

3.6.2 PPARγ expression and patient survival

When the correlation between nuclear staining for PPARγ (**Fig. 3.4, D**) and patient survival was assessed, the median survival time for the patients with weak nuclear staining was 48 months, this was reduced to 36 months (Log Rank test, $p \geq 0.422$) and significantly reduced to 12 months (Log Rank test, $p \leq 0.035$) for patients with moderate and strong staining, respectively. Overall, nuclear staining for PPARγ was significantly associated with patient survival (Log Rank test, $p \leq 0.044$). For cytoplasmic staining for PPARγ, although the median survival time for the cases with low staining (48 months) was not significantly (Log Rank test $p \geq 0.995$) different from those cases with moderate staining (48 months), it was significantly (Log Rank test, $p \leq 0.010$) reduced to 12 months for cases with strong staining. Similar to nuclear staining for PPARγ, overall reduced survival time was significantly associated with the increased cytoplasmic staining for PPARγ (Log Rank test, $p \leq 0.049$) (**Fig. 3.4, C**).

3.6.3 C-FABP expression and patient survival

For the patients with both strong and moderate staining for cytoplasmic C-FABP, the median survival time was 24 months, this was significantly shorter than that of 80 months for patients with weak staining and those unstained (Log Rank test, $p \leq 0.002$) (**Fig. 3.5, A).** The median survival time for patients with strongly, moderately and weakly positive nuclear staining for C-FABP, was 39, 34 and 48 months, respectively (**Fig. 3.5, B**). While increased cytoplasmic staining for C-FABP was significantly associated with a reduced patient survival time (Log Rank test, $p \leq 0.027$) (**Fig. 3.5, A),** no significant correlation between nuclear C-FABP levels and patient survival time was observed (Log Rank test, $p \geq 0.364$) (**Fig. 3.5, B)**.

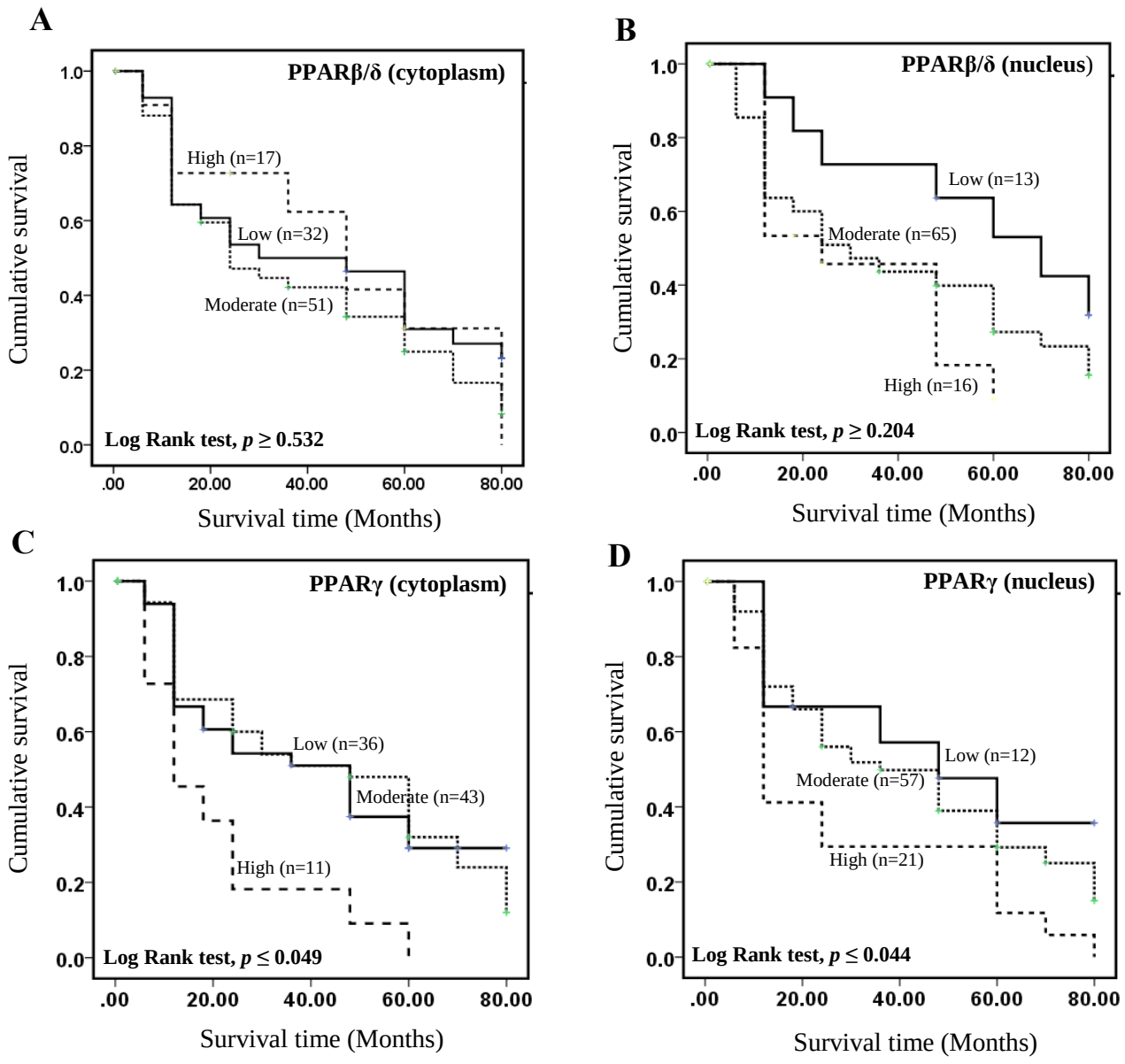

Figure 3.4: Kaplan-Meier survival curves of prostate cancer patients.

The cumulative survival of patients was plotted against time in months for different levels of 4 parameters. **A,** Different levels of cytoplasmic staining for PPARβ/δ: Weakly positive group (n=32); moderately positive group (n=51); and highly positive group (n=17). **B,** Different levels of nuclear staining for PPARβ/δ: Weakly positive group (n=13); moderately positive group (n=65); and highly positive group (n=16). **C**, Different levels of cytoplasmic staining for PPARγ: Weakly positive group (n=36); moderately positive group (n=43); and highly positive group (n=11). **D**, Different levels of nuclear staining for PPARγ: Weakly positive group (n=12); moderately positive group (n=57); and highly positive group (n=21).

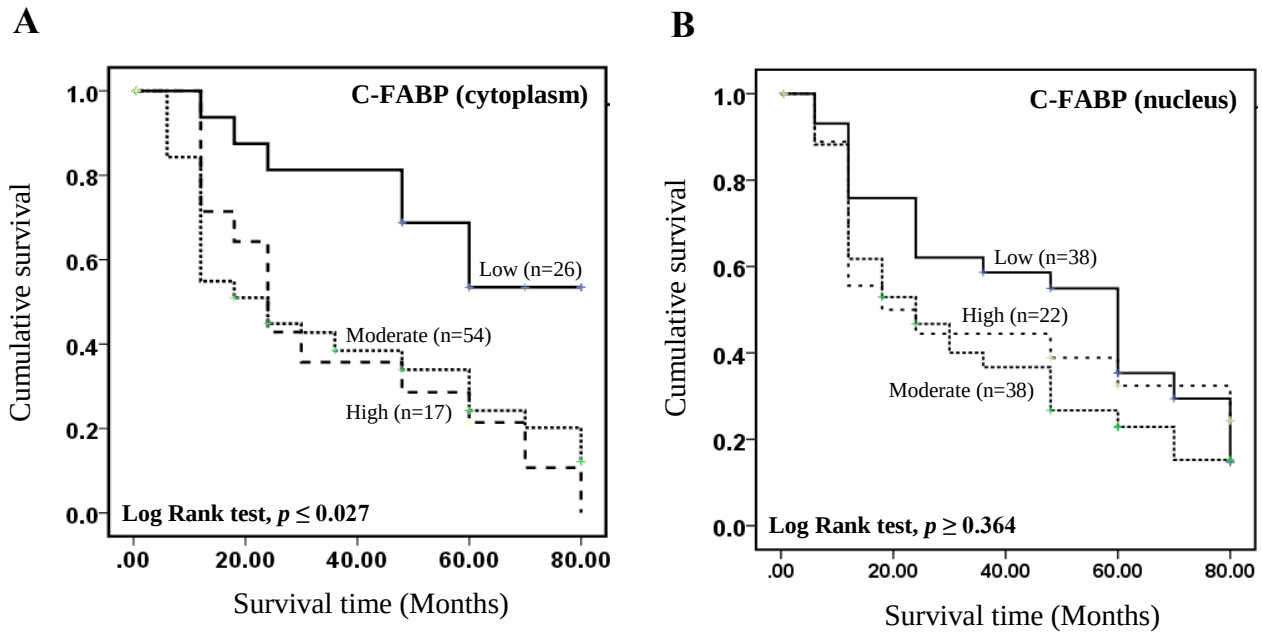

Figure 3.5: Kaplan-Meier survival curves of prostate cancer patients.

The cumulative survival of patients was plotted against time in months for different levels of 2 parameters. **A**, Different levels of cytoplasmic staining for C-FABP: Weakly positive group (n=26); moderately positive group (n=54); and highly positive group (n=17). **B,** Different levels of nuclear staining for C-FABP: Weakly positive group (n=38); moderately positive group (n=38); and highly positive group (n=22).

3.6.4 Gleason scores and patient survival

To assess the relationship between the GS and patient survival, 97 carcinoma cases were divided into three groups: weakly malignant with GS ≤ 5, moderately malignant with GS 6-7 and highly malignant with GS 8-10. The median survival time of patient with highly, moderately and weakly malignant carcinomas was 12, 60 and 80 months, respectively. The increased GS was significantly (Log Rank test $p \leq 0.0001$) associated with reduced survival time (**Fig. 3.6, A**).

3.6.5 Androgen receptor and patient survival

The correlation between patient survival time and staining for AR showed that the median survival time for patients with weak, moderate and strong staining was 60, 24 and 24 months, respectively. Overall survival time was not significantly reduced by the increased staining for AR (Log Rank test, $p \geq 0.052$) (**Fig. 3.6, B**).

3.6.6 Prostatic specific antigen and patient survival

The correlation between patient survival and blood PSA showed that the median survival time for patients with low (<10 ng/ml) and high (≥10 ng/ml) levels of PSA was 48 and 18 months, respectively (**Fig. 3.6, C**) but the difference was not statistically significant (Log Rank test, $p \geq 0.246$).

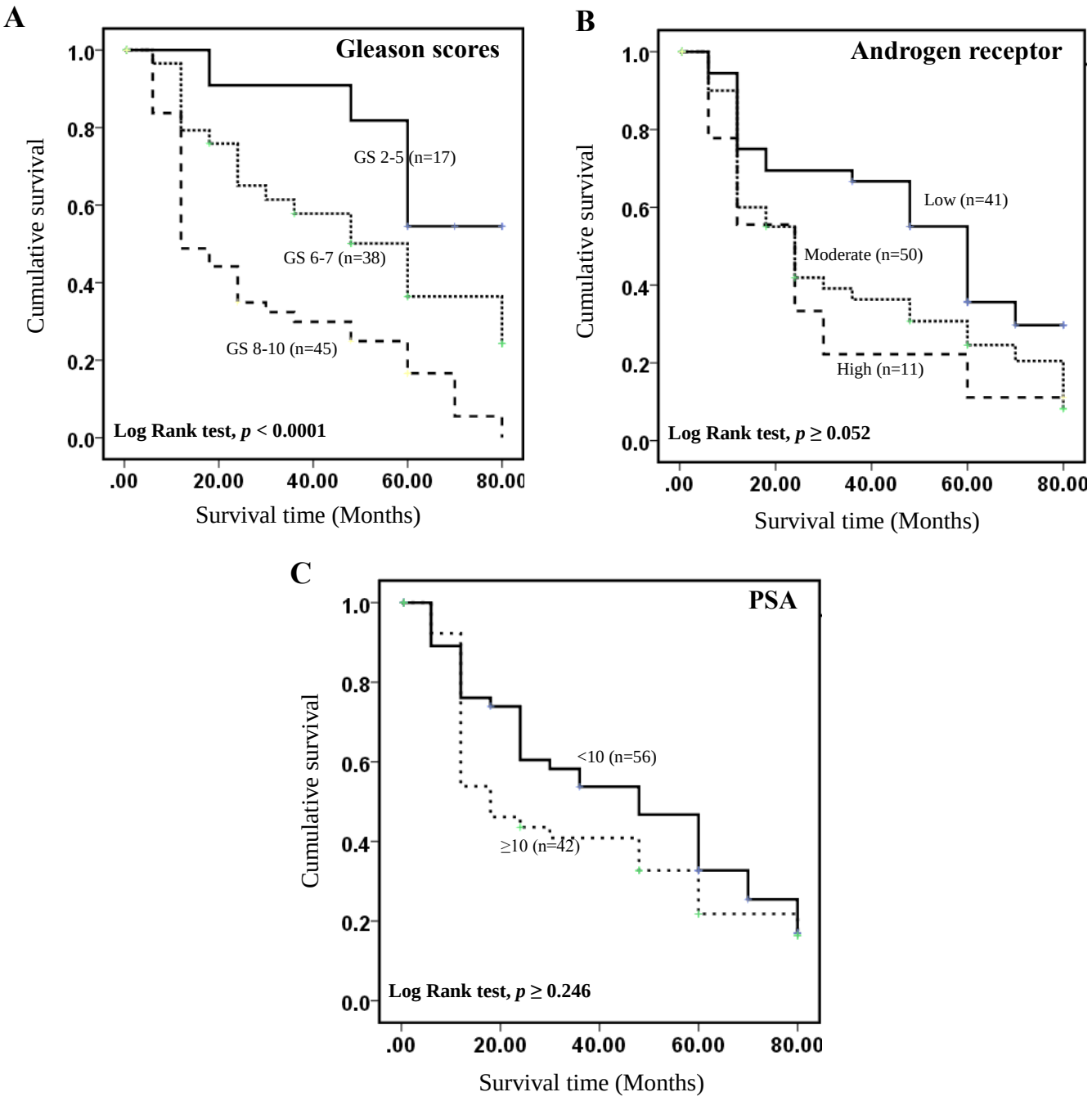

Figure 3.6: Kaplan-Meier survival curves of patients with prostatic cancer.

The cumulative survival of patients was plotted against time in months for different levels of 3 parameters. **A**, Different Gleason scores: Group 1, GS 2-5 (n=17); Group 2, GS 6-7 (n=38); Group 3, GS 8-10 (n=45). **B**, Different AR indices: Low group, or AR index1-3 (n=41); moderate group, or AR index 4-6 (n=50) and high group, or AR index 6-9 (n=11). **C**, Different levels of PSA: Group 1, PSA < 10 ng/ml (n=56) and Group 2, PSA ≥ 10 ng/ml (n=42).

3.6.7 Inter-relationship of C-FABP and PPARγ in predicting patient survival

To assess the possible effect of staining for C-FABP and PPARγ of both cytoplasm and nucleus in association with patients' survival, 90 carcinoma cases were divided into 4 groups: low C-FABP, low PPARγ; low C-FABP, high PPARγ; high C-FABP, low PPARγ and high C-FABP, high PPARγ. For cytoplasmic C-FABP and nuclear PPARγ, Kaplan-Meier plot **(Fig. 3.7, A)** showed that the median survival time for patients with high C-FABP, high PPARγ or high C-FABP, low PPARγ levels (33 & 30 months, respectively) were significantly shorter than whose had low C-FABP, low PPARγ or low C-FABP, high PPARγ levels (60 & 72 months, respectively) (Log Rank test, $p \leq 0.004$). Similar results were obtained when dividing up the carcinomas into cytoplasmic staining for C-FABP and cytoplasmic staining for PPARγ. Kaplan-Meier plot **(Fig. 3.7, B)** show that the median survival time for the patients with high C-FABP, high PPARγ or high C-FABP, low PPARγ levels (31 & 39 months, respectively) were significantly shorter than those had low C-FABP, low PPARγ or low C-FABP, high PPARγ levels (64 & 60 months, respectively) (Log Rank test, $p \leq 0.008$). When subjected to Cox's multivariate regression analysis, staining for cytoplasmic C-FABP still showed a significant association with patients' survival ($p \leq 0.048$), but increased staining for PPARγ in the nucleus was not significantly independently associated with clinical survival ($p \geq 0.143$) (**Table 3.2**) . Similar results were obtained when analysing cytoplasmic staining for C-FABP and cytoplasmic staining for PPARγ in relation to patients' survival ($p \geq 0.362$). Overall these results show that the significant association of staining for PPARγ with patient survival was confounded by that of staining for C-FABP when tested together. These results suggest that nuclear PPARγ staining is dependent on cytoplasmic C-FABP staining when they used as prognostic marker in prostate cancer patients. When nuclear staining of C-FABP and nuclear staining of PPARγ was analysed

(results are not shown), high level of C-FABP and high level of PPARγ was not significantly associated with shorter patients' survival (Log Rank test, $p \geq 0.195$).

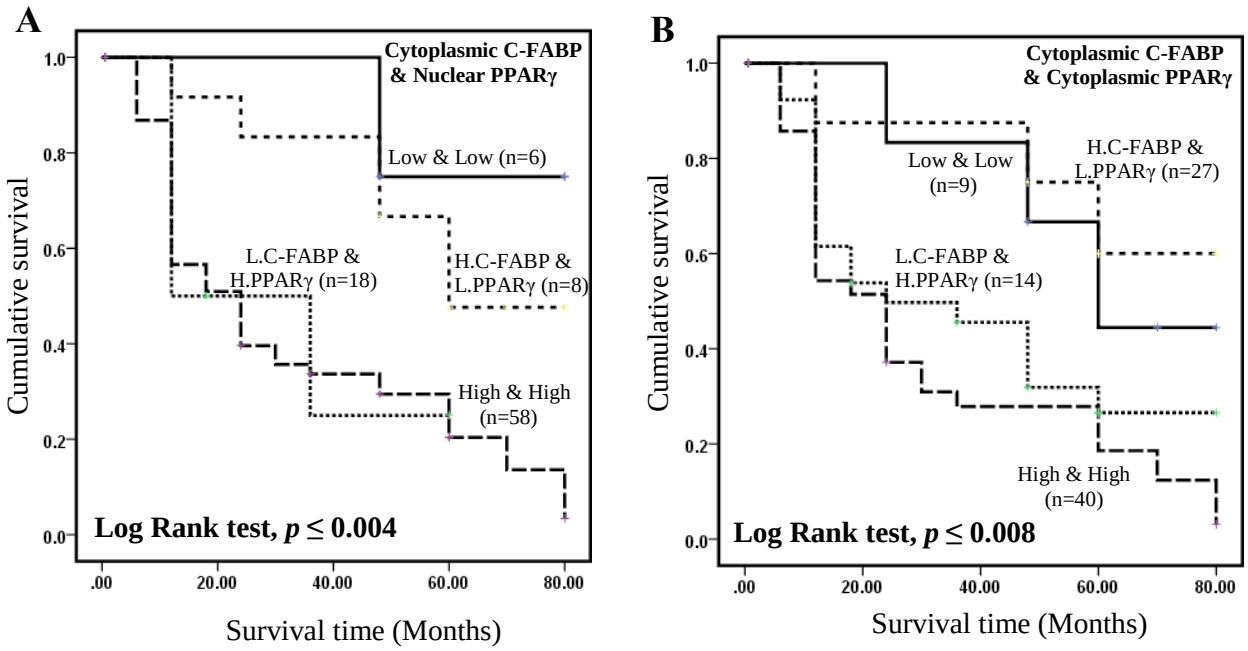

Figure 3.7: Kaplan-Meier survival curves of patients with prostatic cancer.

The cumulative survival of patients was plotted against time in months for different levels of 2 parameters. **A**, Different levels of joint nuclear staining for PPARγ and cytoplasmic staining for C-FABP: low C-FABP, low PPARγ group (n=6); low C-FABP, high PPARγ group (n=18); high C-FABP, low PPARγ group (n=8); high C-FABP, high PPARγ group (n=58). **B**, Different levels of joint cytoplasmic staining for PPARγ and cytoplasmic staining for C-FABP: low C-FABP, low PPARγ group (n=9); low C-FABP, high PPARγ group (n=14); high C-FABP, low PPARγ group (n=27); high C-FABP, high PPARγ group (n=40).

	Univariate analysis (Log Rank test, *p* value)	**Multivariate analysis** (Cox Regression test, *p* value)
C-FABP(cytoplasm)	≤ 0.027	≤ 0.048
PPARγ (nucleus)	≤ 0.044	≥ 0.143
PPARγ (cytoplasm)	≥ 0.059	≥ 0.362
PPARβ⁄δ (nucleus)	≥ 0.204	**---------**

Table 3.2: Multiple Cox regression test between levels of C-FABP and PPARs with patients' survival. To test whether each protein can be used independently or even dependent to the other as prognostic biomarker in predicting patient's survival time, data subjected to multiple Cox regression test. *p* value ≤ 0.05 consider as significant.

3.7 Correlations between PPARβ/δ, PPARγ and PSA level and AR index

3.7.1 Correlation of PPARβ/δ and PSA level

The correlation between levels of PSA and cytoplasmic expression of PPARβ/δ is shown in **Fig. 3.8, A**. In the patients with weak, moderate and strong cytoplasmic PPARβ/δ staining, the median PSA was 8.3ng/ml, 6.7ng/ml and 11.6ng/ml, respectively. Box plot analysis showed no significant difference between levels of PSA in the patients with different levels of cytoplasmic PPARβ/δ (Mann-Whitney U test, $p \geq 0.807$).

The correlation between levels of PSA and nuclear expression of PPARβ/δ is shown in **Fig. 3.8, B**. In the patients with weak, moderate and strong nuclear PPARβ/δ staining, the median PSA was 2.5ng/ml, 11.5ng/ml and 7.5ng/ml, respectively. Box plot analysis showed no significant difference between levels of PSA in the patients with different levels of nuclear PPARβ/δ (Mann-Whitney U test, $p \geq 0.188$).

3.7.2 Correlation of PPARγ and PSA level

The correlation between levels of PSA and cytoplasmic expression of PPARγ is shown in **Fig. 3.8, C**. In the patients with weak, moderate and strong cytoplasmic PPARγ staining, the median PSA was 8.6ng/ml, 7.6ng/ml and 10.4ng/ml, respectively. Box plot analysis showed no significant difference between levels of PSA in the patients with different levels of cytoplasmic PPARγ (Mann-Whitney U test, $p \geq 0.731$).

The correlation between levels of PSA and nuclear expression of PPARγ is shown in **Fig. 3.8, D**. In the patients with weak, moderate and strong nuclear PPARγ staining, the median PSA was 3.5ng/ml, 9ng/ml and 11ng/ml, respectively. Box plot analysis showed no significant difference between levels of PSA in the patients with different levels of nuclear PPARγ (Mann-Whitney U test, $p \geq 0.15$).

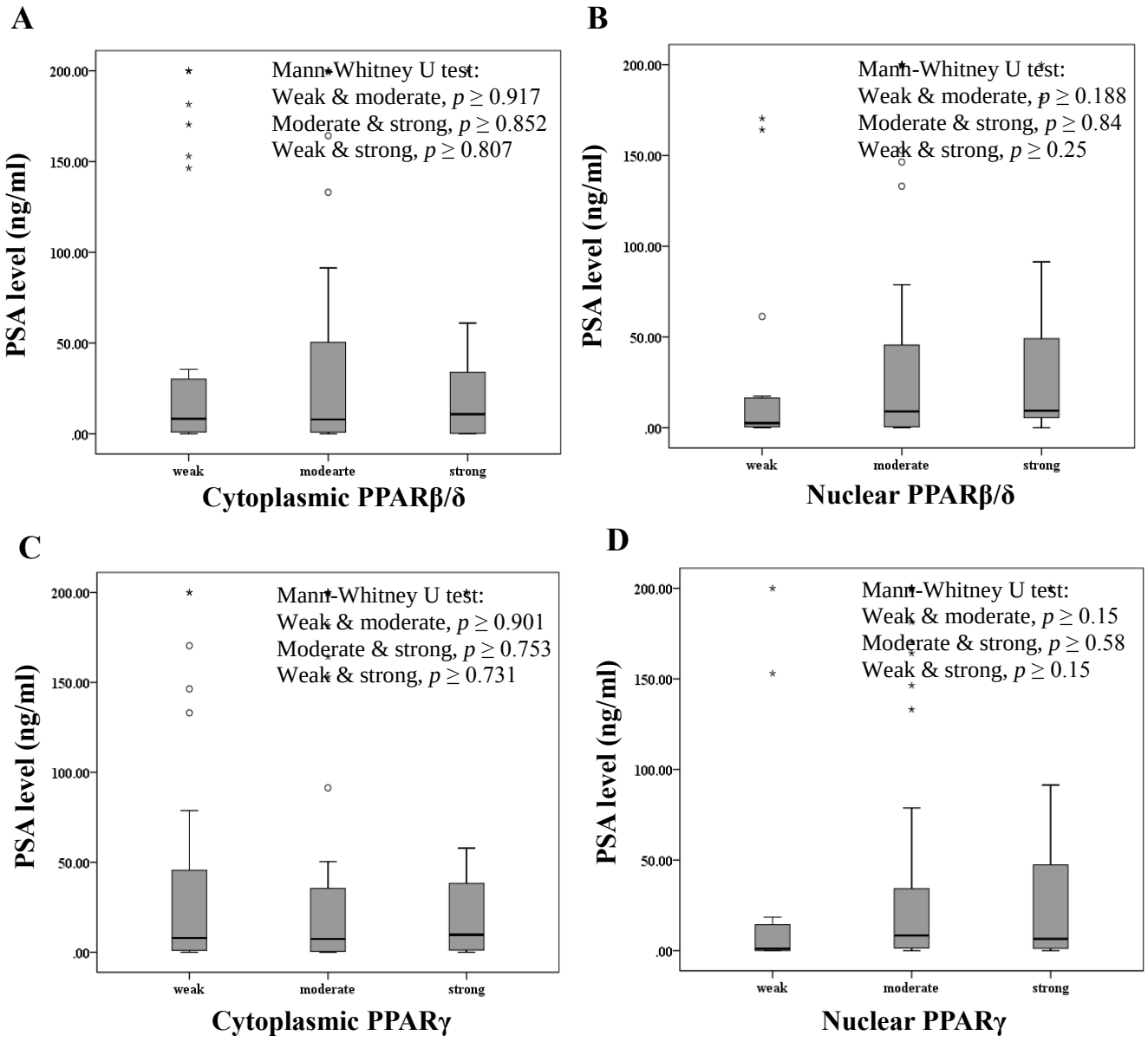

Figure 3.8: Box plot analysis of correlation between different levels of PSA with cytoplasmic and nuclear PPARβ/δ and PPARγ staining.

A: Correlation between different levels of PSA in three groups of prostate cancer patients with different cytoplasmic staining of PPARβ/δ; weakly positive (n=43), moderately positive (n=45) and strongly positive (n=12). **B**: Correlation between different levels of PSA in three groups of prostate cancer patients with different nuclear staining of PPARβ/δ; weakly positive (n=11), moderately positive (n=63) and strongly positive (n=27). **C**: Correlation between different levels of PSA in three groups of prostate cancer patients with different cytoplasmic staining of PPARγ; weakly positive (n=37), moderately positive (n=46) and strongly positive (n=11). **D**: Correlation between different levels of PSA in three groups of prostate cancer patients with different nuclear staining of PPARγ; weakly positive (n=15), moderately positive (n=58) and strongly positive (n=21).

3.7.3 Correlation of PPARβ/δ and AR index

The correlation between AR index (**section 2.2.4.5**) and cytoplasmic expression of PPARβ/δ is shown in **Fig. 3.9, A**. In the patients with weak, moderate and strong cytoplasmic PPARβ/δ staining, the median AR index was 4, 4.1 and 4, respectively. Box plot analysis showed no significant difference between AR indexes in the patients with different levels of cytoplasmic PPARβ/δ (Mann-Whitney U test, $p \geq 0.525$).

The correlation between AR index and nuclear expression of PPARβ/δ is shown in **Fig. 3.9, B**. In the patients with weak, moderate and strong nuclear PPARβ/δ staining, the median AR index was 4, 3.9 and 3.8, respectively. Box plot analysis showed no significant difference between AR indexes in the patients with different levels of nuclear PPARβ/δ (Mann-Whitney U test, $p \geq 0.59$).

3.7.4 Correlation of PPARγ and AR index

The correlation between AR index and cytoplasmic expression of PPARγ is shown in **Fig. 3.10, A**. In the patients with weak, moderate and strong cytoplasmic PPARγ staining, the median AR index was 3.9, 4 and 4.1, respectively. Box plot analysis showed no significant difference between AR indexes in the patients with different levels of cytoplasmic PPARγ (Mann-Whitney U test, $p \geq 0.195$).

The correlation between AR index and nuclear expression of PPARγ is shown in **Fig. 3.10, B**. In the patients with weak, moderate and strong nuclear PPARγ staining, the median AR index was 2, 4.2 and 4, respectively. Although median AR index were increased in those with moderately or strongly nuclear PPARγ staining compare to weakly staining group, Box plot analysis showed no statistical difference in AR indexes between two groups of weakly and moderately nuclear PPARγ staining (Mann-Whitney U test, $p \geq 0.23$) or weakly and strongly nuclear PPARγ staining (Mann-Whitney U test, $p \geq 0.08$).

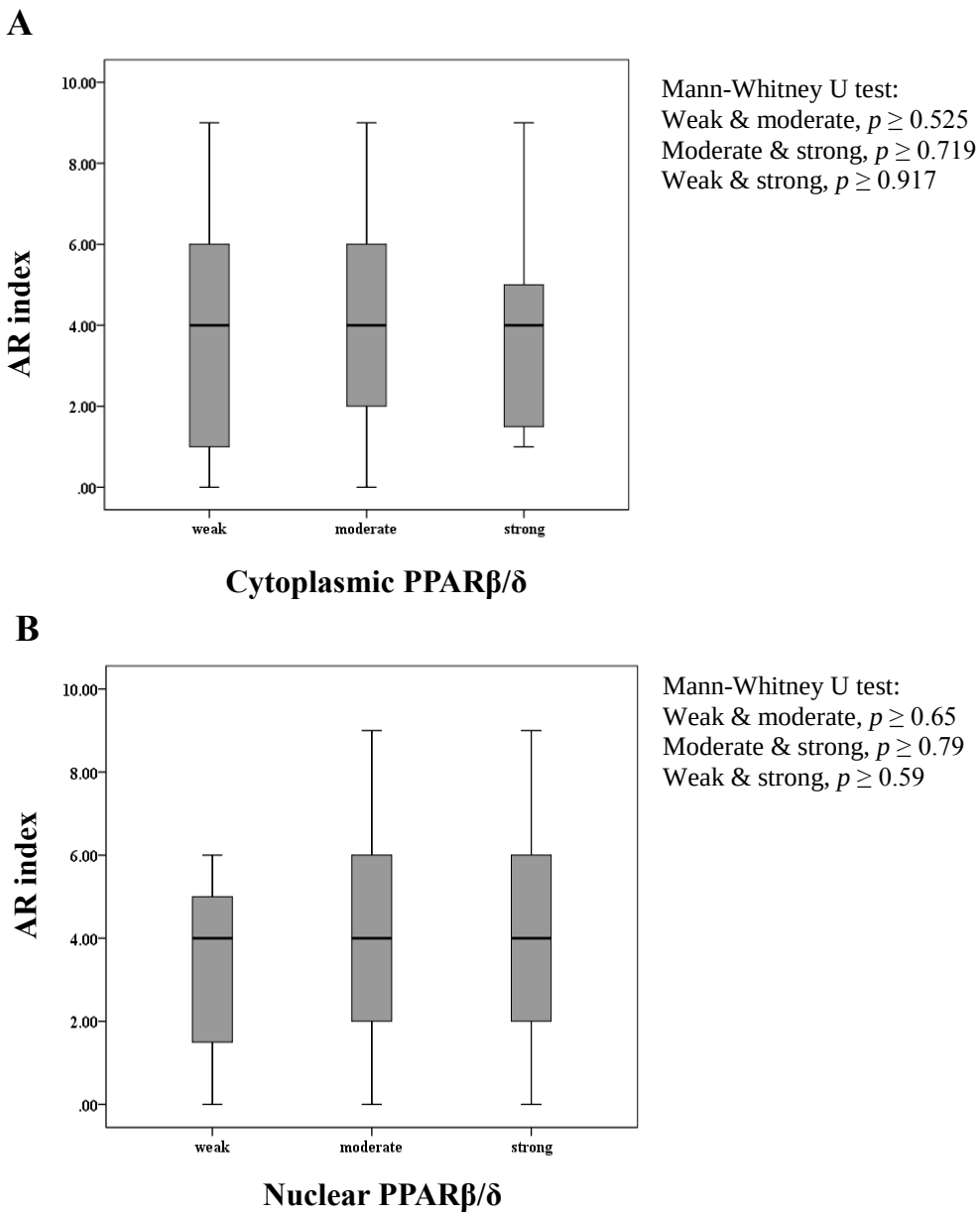

Figure 3.9: Box plot analysis of correlation between different AR indexes with cytoplasmic and nuclear PPARβ/δ staining.

A: Correlation between different AR indexes in three groups of prostate cancer patients with different cytoplasmic staining of PPARβ/δ; weakly positive (n=43), moderately positive (n=45) and strongly positive (n=12).

B: Correlation between different AR indexes in three groups of prostate cancer patients with different nuclear staining of PPARβ/δ; weakly positive (n=15), moderately positive (n=55) and strongly positive (n=26).

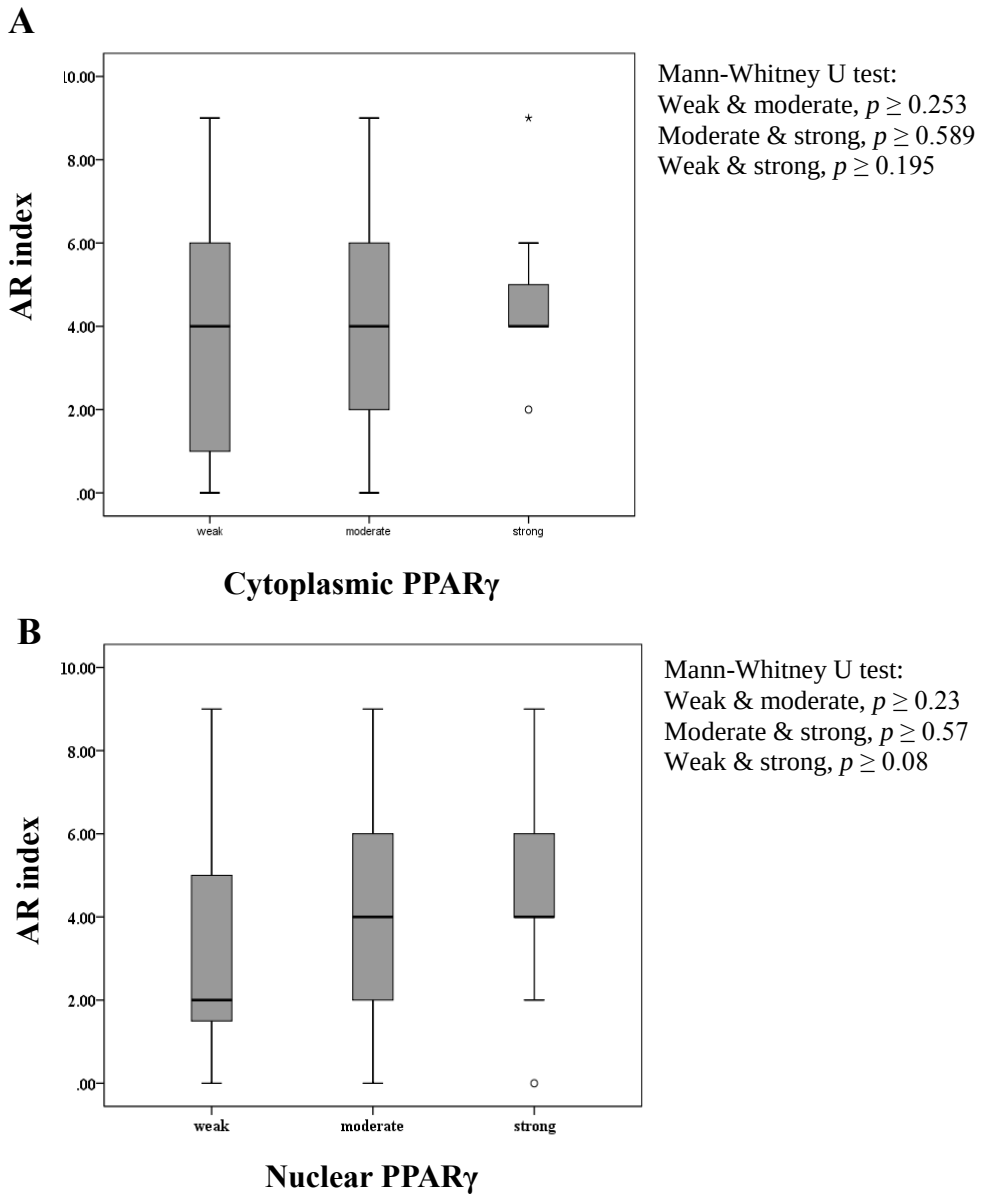

Figure 3.10: Box plot analysis of correlation between different AR indexes with cytoplasmic and nuclear PPARγ staining.

A: Correlation between different AR indexes in three groups of prostate cancer patients with different cytoplasmic staining of PPARγ; weakly positive (n=11), moderately positive (n=63) and strongly positive (n=27).

B: Correlation between different AR indexes in three groups of prostate cancer patients with different nuclear staining of PPARγ; weakly positive (n=15), moderately positive (n=55) and strongly positive (n=26).

3.8 Suppression of PPARγ expressions by siRNA

Highly malignant prostate cancer cells, PC3-M, express high level of PPARγ (**Fig. 3.1, B**). Using RNAi technique, PPARγ expression was suppressed in PC3-M cells transiently. After identifying the most efficient siRNA sequence by transient transfection, stable transfection was performed to investigate whether suppression of tumorigenicity of prostate cancer cells can be achieved by reducing PPARγ expression.

3.8.1 Selection of most efficient siRNA for PPARγ suppression

Three 21-nt sequences within the PPARγ cDNA for RNAi were designed to form double-strand siRNA constructs. PC3-M cells were transiently transfected with different concentrations of each siRNA in combination with different concentrations of transfection reagent for 24, 48 or 72 hours (section **2.2.6.3**). Using Western blot, expression levels of PPARγ were evaluated in protein extracts of the cancer cells with different combination of siRNA and transfection reagent. The highest suppression efficiency for PPARγ was achieved by siRNA-3 (2µg/ml) in combination with 2.5µl/ml of X-tremeGENE siRNA Transfection Reagent in 24 hours incubation , which reduced PPARγ expression up to 88% from the level detected in parental cells (**Fig. 3.11, 3.12**). Thus siRNA-3 was selected as the most efficient sequence to design shRNA for stable transfection.

A

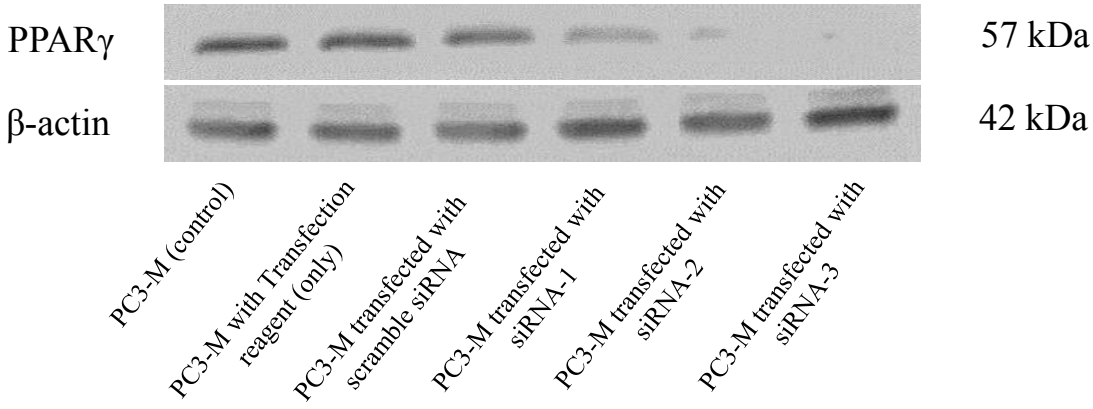

B

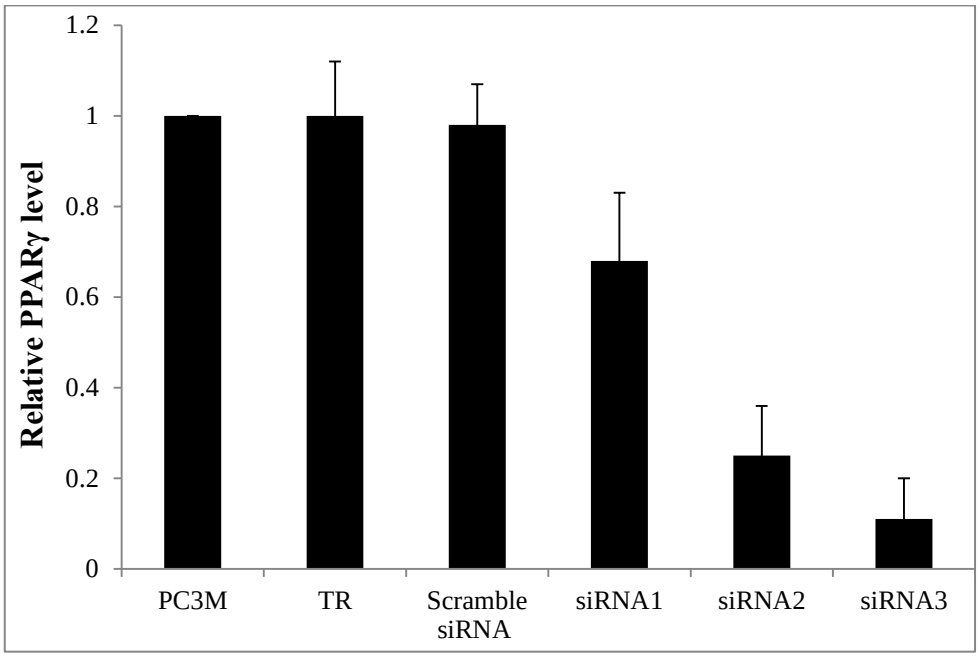

Figure 3.11: Expression levels of PPARγ in PC3-M cells after transient transfection with different siRNAs.

A: Detecting of PPARγ protein expression by Western blotting. The anti-β-actin antibody was used to correct possible loading errors in the same blot.

B: The relative expression levels of PPARγ. The expression level of PPARγ in parental PC3-M cells was set as 1.0. The levels of PPARγ in other cells were calculated by relating to the level of PPARγ expressed in parental PC3-M. Results were obtained from three different measurements (mean ± SD).

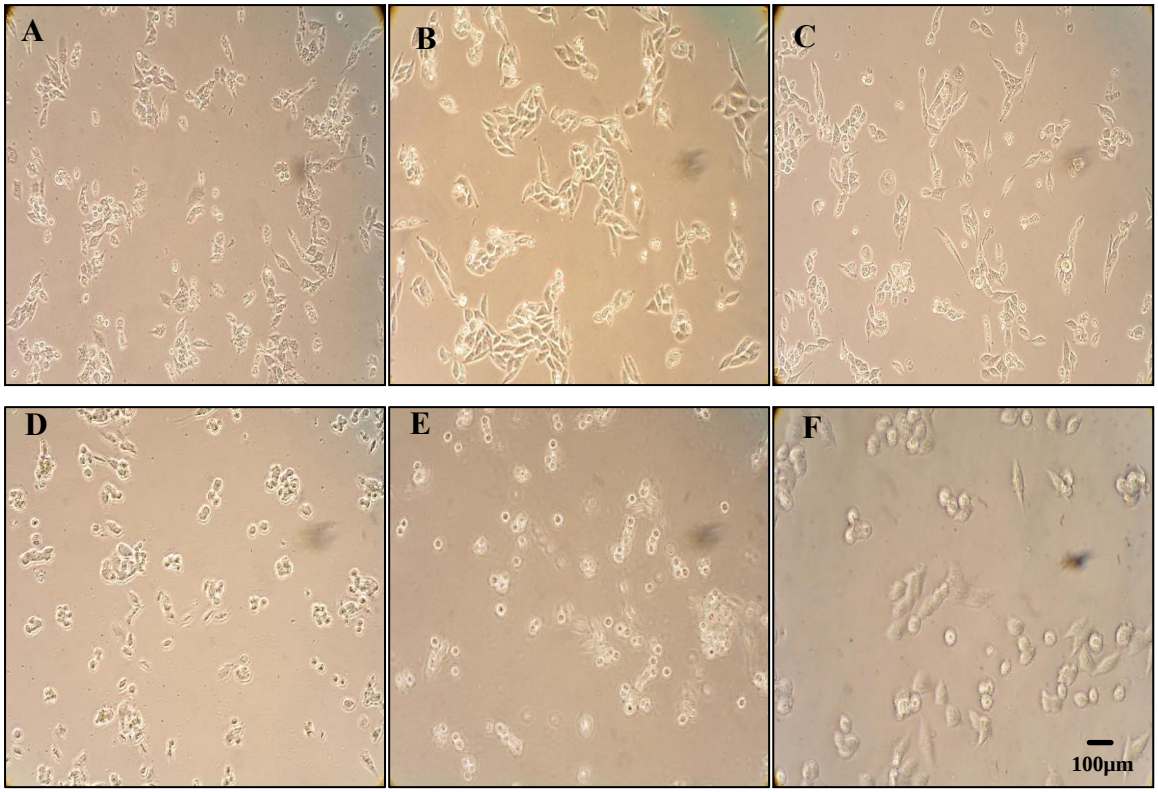

Figure 3.12: Different morphological patterns in PC3-M cells, after 24 hours transient transfection with different siRNAs.

A: Parental PC3-M cells; **B**: PC3-M cells treated only with X-tremeGENE siRNA Transfection Reagent; **C**: PC3-M cells transfected by scramble siRNA (negative control); **D**: PC3-M cells transfected by siRNA-1; **E**: PC3-M cells transfected by siRNA-2; **F**: PC3-M cells transfected by siRNA-3. Original magnifications of images were ×100.

3.9 Establishment of stably PPARγ-suppressed PC3-M cell lines

Using siRNA-3 sequence as template, shRNA was designed and used in stable transfection (section **2.2.6.4**). psiRNA-h7SKGFPzeo plasmid was double digested with Hind III and Acc651 restriction enzymes. Digestion was confirmed by electrophoresis in low-melting temperature agarose gel (1%) (**Fig. 3.13**). Appropriate band of digested plasmid was cut, purified (section **2.2.6.5.4**), then ligated with annealed oligonucleotides (forward and reverse) of shRNA (sections **2.2.6.5.2** and **2.2.6.5.5**). Ligation products were transformed into *E.coli* GT116 competent cells (section **2.2.6.5.6**) and plated onto the LB-zeocin agar plates each containing 100μg/ml zeocin and incubated at 37°C, overnight. Transformation efficiency for *PPARγ*-suppressed plasmid and the control scrambled RNA-plasmid were 1500 and 3800 cfu, respectively.

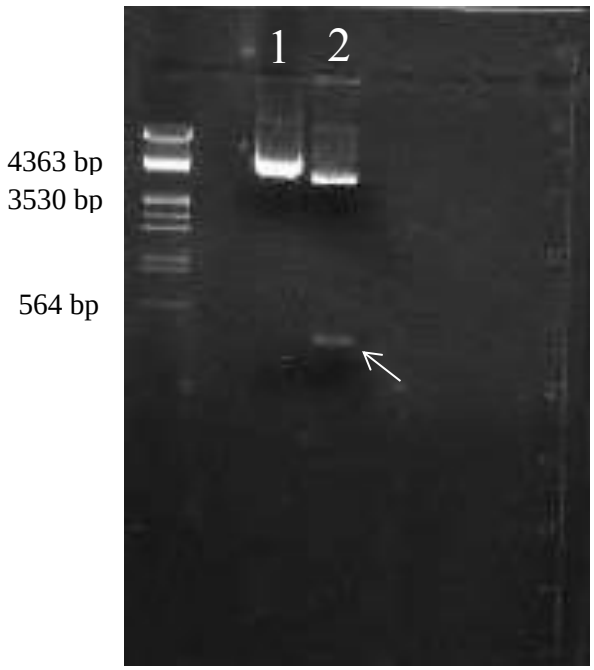

Figure 3.13: Digestion of psiRNA-h7SKGFPzeo plasmid.
Electrophoresis was performed in Low-melting temprature agarose gel (1%) to confirm the successful cleavage of the plasmid DNA. Undigested psiRNA-h7SKGFPzeo plasmid was loaded in well **1** and digested one in well **2**. The extra small band (arrow) was the 369 bp fragment of plasmid which was replaced by shRNA in ligation process.

Five single clones of transformed bacteria with *PPARγ*-suppressed plasmid and two clones from scramble shRNAs were picked up and grown in LB medium containing 100μg/ml Zeocin. Plasmid DNAs were extracted and purified from the bacterial cells using QIAGEN Plasmid mini-preparation kit (section **2.2.6.5.7.1**). Plasmids were double digested with Hind III and Acc651 restriction enzymes and the presence of inserted oligonucleotides were confirmed by electrophoresis in agarose gel (**Fig. 3.14**). Finally, plasmid DNAs from three different clones (1-3) were sent for sequencing analysis (section **2.2.6.5.7.4**) using internal plasmid primers [OL559 primer (forward); OL408 primer (reverse)]. Plasmids from clone 1 in which habituation of correct DNA insert was confirmed by sequencing analysis, was chosen for DNA amplification and the subsequent stable transfection (**Table 3.3**).

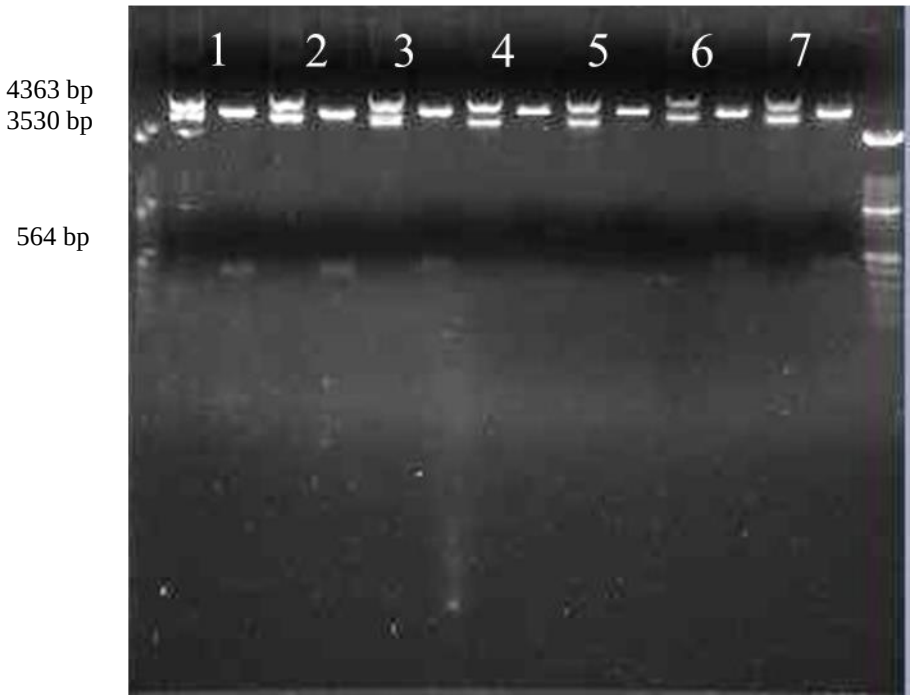

Figure 3.14: Confirmation of the correct DNA insertion.

Mini-preparation of DNA was made from 5 colonies harbouring *PPARγ*-suppressed DNA constructs and 2 colonies harbouring scramble-shRNA plasmids. DNA from each clone was double digested using *Hind III* and *Acc651* restriction enzymes and an undigested plasmid DNA sample was loaded in parallel with the digested sample as control. As shown in the figure, the first 5 pairs of samples (1-5) were DNAs isolated from clones harbouring *PPARγ*-suppressed constructs and the last 2 pairs of samples (6-7) were DNAs isolated from colonies harbouring scramble-shRNA plasmids.

Forward

5’ NNAATGAATCCTTGGTTAATAGCTTGTGCGCCGCCTGGGTACCTCATAAATGT
CAGTACTGTCGGTCAAGAGCCGACAGTACTGACATTTATTTTTTGGAAAAGCTTCTAGA
CTTAATTAACCTGCAGGCGTTACATAACTTACGGTAAATGGCCCGCCTGGCTGACCGCC
CAACGACCCCCGCCCATTGACGTCAATAATGACGTATGTTCCCATAGTAACGCCAATAG
GGACTTTCCATTGACGTCAATGGGTGGAGTATTTACGGTAAACTGCCCACTTGGCAGTA
CATCAAGTGTATCATATGCCAAGTACGCCCCCTATTGACGTCAATGACGGTAAATGGCC
CGCCTGGCATTATGCCCAGTACATGACCTTATGGGACTTTCCTACTTGGCAGTACATCTA
CGTATTAGTCATCGCTATTACCATGATGATGCGGTTTTGGCAGTACATCAATGGGCGTG
GATAGCGGTTTGACTCACGGGGATTTCCAAGTCTCCACCCCATTGACGTCAATGGGAGT
TTGTTTTGACTAGTAAATCAACGGGACTTTCCAAAATGTCGTAACAACTCCGCCCCATTG
ACGCAAATGGGCGGTAGGCGTGTACGGTGGGAGGTCTATATAAGCAGAGCTCGTTTAG
TGAACCGTCAGATCAGCTTCGAGGGGCTCGCATCTCTCCTTCACGCGCCCGCCGCCCTA
CCTGAGGCCGCCATCCACGCCGGTTGAGTCGCGTTCTGCCGCCTCCCGCCTGTGGTGCCT
CCTGAACTGCGTCCGCCGTCTAGGTAAGTTTAAAGCTCAGGTCGAGACCGGGCCTTTGT
CCGGCGCTCCCTTGGAGCCTACCTAGACTCANCCGGCTCTCCACGCTTTGCCTGAANCCT
GCTTGCTCACTCTACGTCTTTNGTTCGTTTTCTGTNCTGCNCCGTTACAGATCCCAGCCA
CCATNGNGTTCTAAGGANAANAAACTCTTACTGGNGNTGTCCCATTTCTGGTGAACTGG
ATNGTGATGTGAATGGCNNCAATTNNCTGTNNCTGGGAAAGTGAAGAANNGCACTTNT
GGAACTGANNCTGAATTCATTGACANNAGAAACTGCNNNGCTTGCCANNNTGGGACAC
CTGACTAAGGT 3’

Reverse

5’ NNNNGNNAGGGCGGGNNNGTTGGGCGGTCAGCCAGGCGGGCCATTTACCGT
AAGTTATGTAACGCCTGCAGGTTAATTAAGTCTAGAAGCTTTTCCAAAAAATAAATGTC
AGTACTGTCGGCTCTTGACCGACAGTACTGACATTTATGAGGTACCCAGGCGGCGCACA
AGCTATATAAACCTGAAGGAAATCTCAACTTTACACTTAGGTCAAGTTACTTATCGTAC
TAGAGCTTCAGCAGGAAATTTAACTAAAATCTAATTTAACCAGCATAGCAAATATCATT
TATTCCCAAAATGCTAAAGTTTGAGATAAACGGACTTGATTTCCGGCTGTTTTGACACTA
TCCAGAATGCCTTGCAGATGGGTGGGGCATGCTAAATACTGCAGCACTAGTATCGATTA
AGAACATGACCAAAATCCCTTAACGTGAGTTTTCGTTCCACTGAGCGTCAGACCCCGTA
GAAAAGATCAAAGGATCTTCTTGAGATCCTTTTTTTCTGCGCGTAATCTGCTGCTTGCAA
ACAAAAAAACCACCGCTACCAGCGGTGGTTTGTTTGCCGGATCAAGAGCTACCAACTCT
TTTTCCGAAGGTAACTGGCTTCAGCAGAGCGCAGATACCAAATACTGTTCTTCTAGTGT
AGCCGTAGTTAGGCCACCACTTCAAGAACTCTGTAGCACCGCCTACATACCTCGCTCTG
CTAATCCTGTTACCAGTGGCTGCTGCCAGTGGCGATAAGTCGTGTCTTACCGGGTTGGA
CTCAAGACGATAGTTACCGGATAAGGCGCAGCGGTCGGGCTGAACGGGGGGTTCGTGC
ACACAGCCCAGCTTGGAGCGAACGACCTACACCGAACTGAGATACCTACAGCGTGAGC
TATGAGAAAGCGCCACGCTTCCCGAAGGGAGAAAGGCGGACAGGTATCCGGTAAGCGG
CAGGGTCGGAACAGGAGAGCGCACGAGGGAGCTTCCAGGGGGAAACGCCTGGTATCTT
TATAGTCCTGTCGGGTTTCGCCACCTCTGACTTGAGCGTCGATTTTTGTGATGCTCGTCA
GGGGGGCGGAACCTATGGAAAAACGCCAGCAACGCGGCCTTTTTACGGTTCCTGGCCTT
TTGCTGGCCTTTTGCTCCNATGCATAAAAAAACCNGCCGAACCGGGTTTTTAATTAAAN
NNNNGCANANCAAAACTTTAACCTCCAAATCAAGCCTNNNNNTGAATCCTTTNNNNNN
AGNNNNAAA 3’

Table 3.3: A part of psiRNA-h7SKGFPzeo plasmid sequence map.

To check and confirm the correct insertion of shRNA, plasmid was sequenced using internal plasmid primers by Beckman Coulter Genomics, UK. Sequence alignment was performed using BioEdit for searching Genbank and the alignment results proved that the insertion was accurate.

3.9.1 Stable transfection

PC3-M cells were transfected using plasmids extracted from clone 1 (2μg/ml) with X-tremeGENE HP DNA Transfection Reagent (2.5μl/ml). After 36 hours, culture medium was replaced with fresh medium containing Zeocin^{TM} (100μg/ml). A week later, transfected cells were transferred into 9cm cell culture plates (petri dish) and continued to grow until single clones appeared and visualized with naked eye (2-3 weeks). Then, using ring cloning method (section **2.2.6.6.1**), ten single clones of *PPARγ*-suppressed transfectants and five of scramble-transfectants were picked up and transferred onto a 96-well plate. The medium was changed next day and colonies were grown in normal cell culture conditions.

Using Western blotting, expression levels of PPARγ were evaluated in different transfectants. A single PPARγ band of 57kDa was detected in parental and transfectant cells (**Figure 3.15, A**). When the densitometric level of PPARγ in PC3-M cells (parental) was set at 1 (**Figure 3.15, B**), the level in scramble (control) cells was 0.98 ± 0.11; levels in clone 1, clone 2, clone 3 and clone 4 cells were 0.86 ± 0.09, 0.64 ± 0.08, 0.48 ± 0.11 and 0.18 ± 0.06, respectively. Levels of PPARγ suppressed by 52% and 82% in clone 3 and clone 4 cells, respectively; whereas there was no significant change in its level in scramble cells. Thus clone 3 and clone 4 cell lines were selected as moderately and highly *PPARγ*-suppressed transfectants (derived from PC3-M cells), respectively. For future investigation, highly *PPARγ*-suppressed transfectants is named as **PC3-M-PPARγ-si-H** and moderately *PPARγ*-suppressed transfectants is named as **PC3-M-PPARγ-si-M**. Also scramble cells were used as control.

A

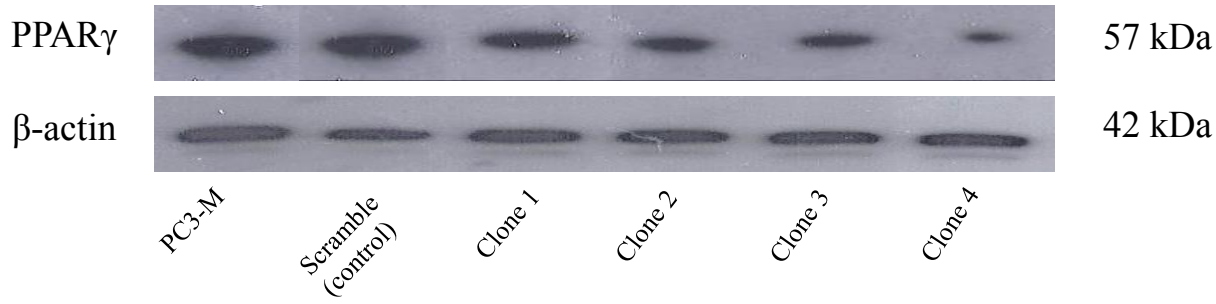

B

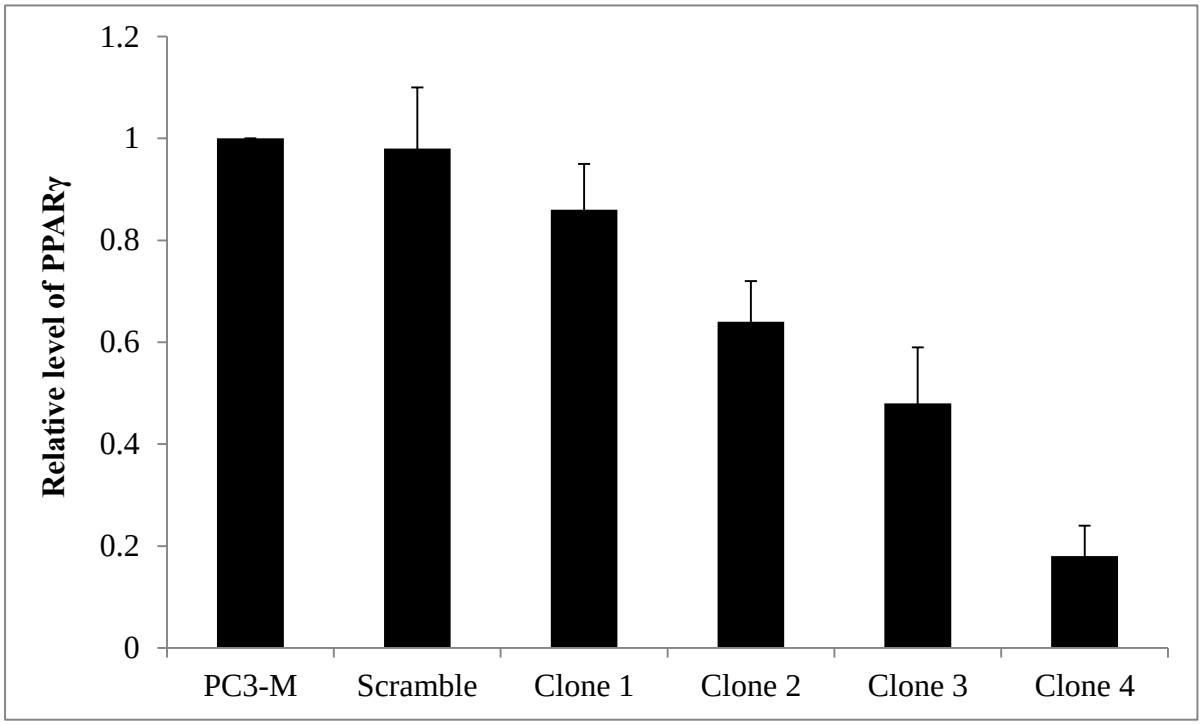

Figure 3.15: Effect of shRNA on levels of PPARγ expression in PC3-M-derived transfectants.

A: Detecting of PPARγ protein expression by Western blotting. The anti-β-actin antibody was used to correct possible loading errors in the same blot.

B: Relative levels of PPARγ in different transfectants. The expression level of PPARγ in parental PC3-M cells was set as 1.0. The levels of PPARγ in control and other 4 transfectant clones were calculated by relating to that in parental PC3-M cells. Results were obtained from three different measurements (mean ± SD).

3.10 Effect of *PPARγ* suppression on tumour cells *in vitro*

3.10.1 Effect of *PPARγ* suppression on cellular proliferation

To find whether suppression of *PPARγ* would affect on the growth rate of PC3-M cells, proliferation assay was performed on control and transfectants cell lines over 5 days (120 hours). Standard curve of each tested cell line is shown in **Fig. 3.16** (section **2.2.7.1.1**).

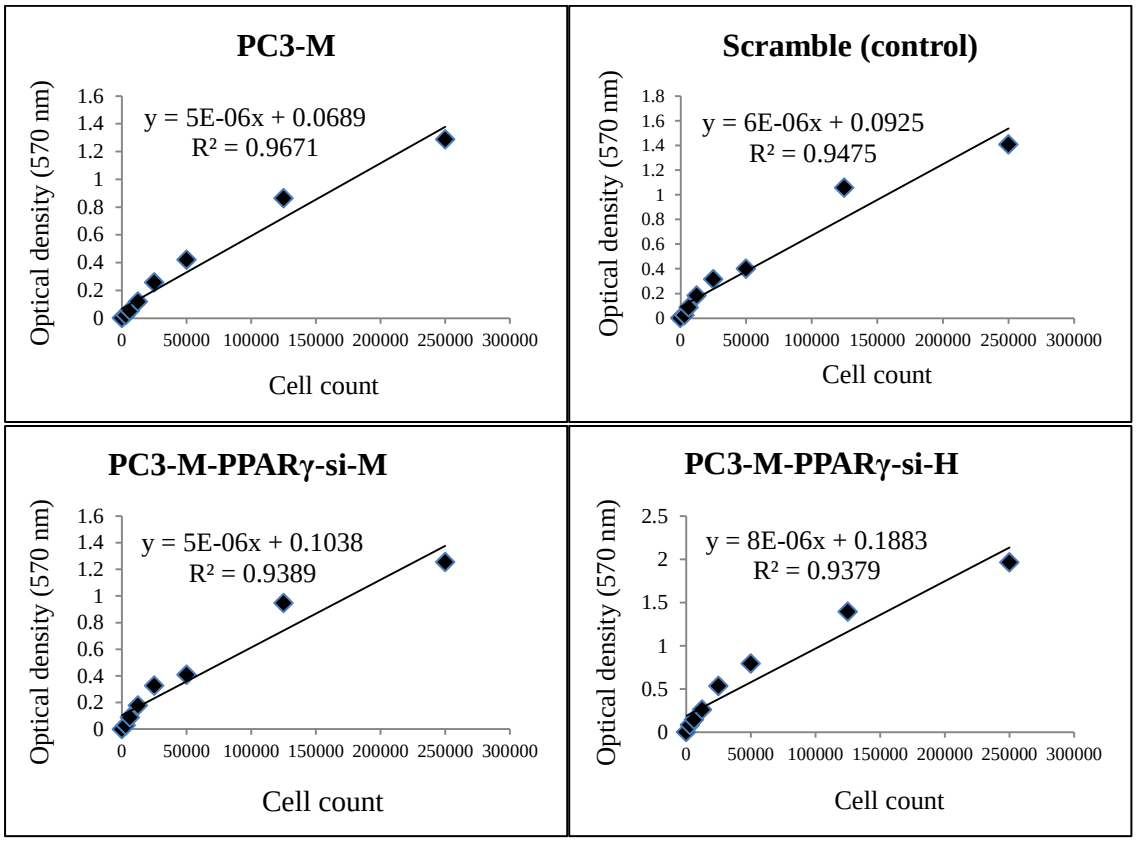

Figure 3.16: Standard curves of parental PC3-M and different transfected cell lines.
Using linear regression analysis, Standard curves were established for each cell line by plotting absorbance (OD at 570 nm) (Y axis) against the cell numbers (X axis). The curve equation and regression of each standard curve is presented in diagram.

The density of culture cells were determined by extrapolating from the standard curve and cell counts were obtained by MTT assays (section **2.2.7.1.2**). Overall, growth rate of parental cells and control (scramble) exhibited very similar growth pattern. In the first 48 hours, no significant difference was detected between different cell lines. But from the 3rd day onward, growth rates were significantly reduced in both PC3-M-PPARγ-si-H cells and PC3-M-PPARγ-si-M cells compare to controls. At the end of the 5th day, cell numbers in PC3-M and scramble groups raised to 262,000 ± 14,000 and 283,000 ± 9810, respectively; whereas in PC3-M-PPARγ-si-H cells and PC3-M-PPARγ-si-M cells, numbers reached to 134,000 ± 19,040 and 224,000 ± 15,200, respectively (**Table 3.4**). Cell proliferation rate of PC3-M-PPARγ-si-H cells (Student's test, $p \leq 0.0009$) and PC3-M-PPARγ-si-M cells (Student's test, $p \leq 0.004$) were significantly reduced by 53% and 21%, respectively, compare to control cells (**Fig. 3.17**).

Cell line	Mean number of cells ± SD	*p* Value
PC3-M	262,000 ± 14,000	——
Scramble (control)	283,000 ± 9810	≥ 0.44
PC3-M-PPARγ-si-M	224,000 ± 15,200	≤ 0.004
PC3-M-PPARγ-si-H	134,000 ± 19,040	≤ 0.0009

Table 3.4: Cell counts of parental and transfected PC3-M cells at the 5th day of proliferation assay. Using Student's t-test, *p* values were obtained by comparing data from test groups to parental group.

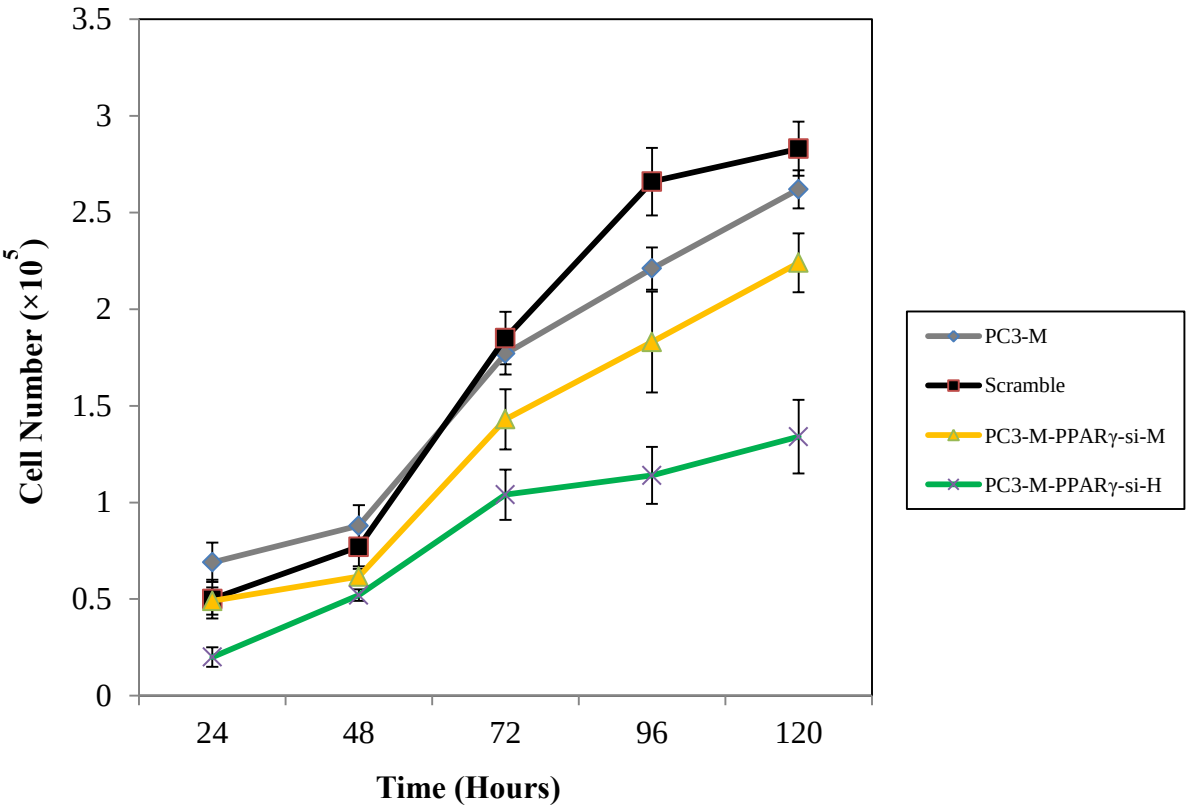

Figure 3.17: The impact of *PPARγ* silencing on the proliferation rate of transfectant cells. The growth rates of parental, scramble (control), PC3-M-PPARγ-si-M and PC3-M-PPARγ-si-H cells during 5 days experimental period. Cell count of each sample was calculated by comparing serially diluted standard from standard curve. Results were obtained from three separate measurements (mean ± SE).

3.10.2 Effect of PPARγ suppression on invasiveness of prostate cancer cell

The effect of *PPARγ* suppression on invasiveness of parental and transfectant cells was assessed using BD Matrigel coated invasion chambers (section **2.2.7.2**). Transfected cells in an active growth phase with confluency less than 80% were maintained in serum-free RPMI 1640 medium for 24 hours prior to setting up the invasion assay. After 24 hours starvation, cells were harvested and counted to prepare a mixture containing 5×10^4 cells in serum-free medium. Chambers were rehydrated for 2 hours before 2.5×10^4 cells in 0.5ml medium were loaded into every upper compartment of chambers. Routine medium (with 10% (v/v) FCS) was placed 1ml / well in lower compartments. All cell lines were set as triplicate and assay was run in a humidified tissue culture incubator for 24 hours. Finally, remaining cells in upper part were removed by gently using cotton swabs and washed with PBS. Migrated cells were fixed and stained using 2% crystal violet for 10 minutes and counted in nine random fields using light microscope at 125 × magnifications. Mean number of invaded cells in scramble (control), PC3-M-PPARγ-si-M and PC3-M-PPARγ-si-H group was 54 ± 4, 11 ± 2 and 6 ± 1, respectively. Invasiveness of PC3-M-PPARγ-si-H cell (Student's t-test, $p \leq 0.0002$) and PC3-M-PPARγ-si-M cell (Student's t-test, $p \leq 0.0003$) was reduced by 88.9% and 79.7%, respectively, in comparison with the control cell (**Fig. 3.18**) (**Table 3.5**).

Cell line	Mean number of migrated cells ± SD	*p* Value
Scramble (control)	54 ± 4	-------
PC3-M-PPARγ-si-M	11 ± 2	≤ 0.0003
PC3-M-PPARγ-si-H	6 ± 1	≤ 0.0002

Table 3.5: Number of invaded cells per field in invasion assay.
Differences of invasiveness between different groups were assessed by Student's t-test. *p* values were obtained by comparing data in test groups to control group.

A

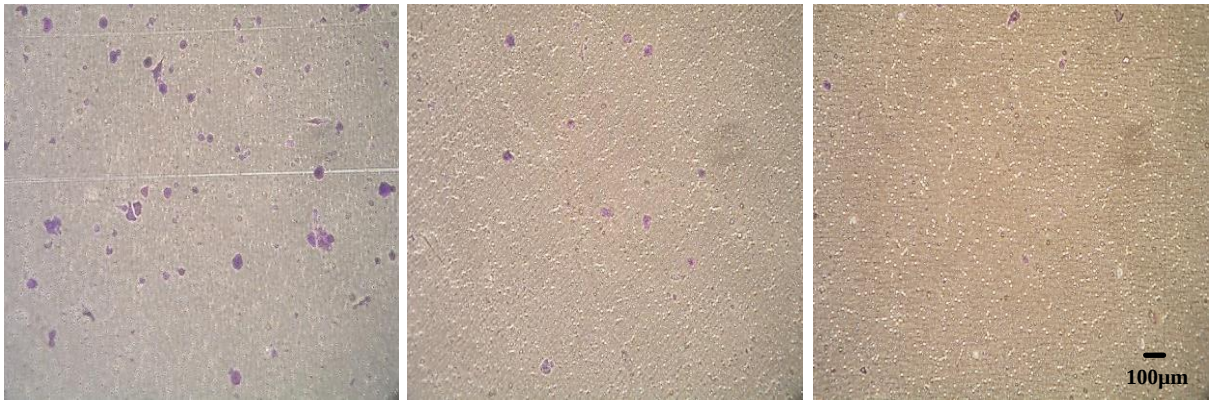

B

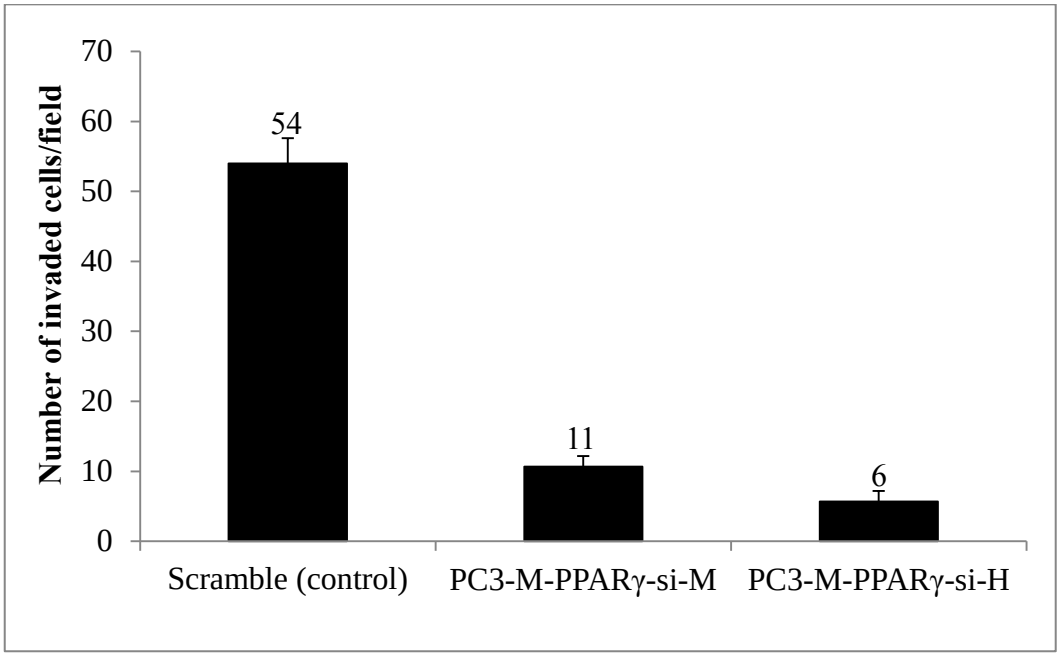

Figure 3.18: The impact of *PPARγ* silencing on invasiveness of transfectants.

A: Representative fields of invasion assay; cells were fixed and stained by crystal violet (2%). Original magnifications of images were ×100.

B: Number of invaded cells per field in invasion assay; cells were incubated in BD Matrigel coated invasion chambers with serum-free medium for 24 hours. Normal culture medium used as chemo-attractant. Results were obtained from three separate measurements (mean ± SE).

3.10.3 Effect of *PPARγ* suppression on anchorage-independent growth of prostate cancer cells

To investigate the effect of *PPARγ* suppression on tumorigenicity of transfectant cells, their anchorage-independent growth rates in the soft agar colony-formation were assessed. Scramble cells were used as control. Assay was set as triplicate and cells were grown for 4 weeks. Colonies were stained by adding 0.5ml of 2% MTT for 4 hours. Colonies larger than 150µm were counted using Gel Count. The number of colonies produced in soft agar after 4 weeks by scramble (control), PC3-M-PPARγ-si-M and PC3-M-PPARγ-si-H were 756 ± 64, 80 ± 14 and 45 ± 9, respectively. Colony formation potency of PC3-M-PPARγ-si-H cells (Student's t-test, $p \leq 0.0015$) and PC3-M-PPARγ-si-M cells (Student's t-test, $p \leq 0.0012$) were reduced by 94.1% and 89.5%, respectively, in comparison to control cells (**Fig. 3.19**) (**Table 3.6**).

Cell line	Mean number of colonies ± SD	*p* Value
Scramble (control)	756 ± 64	-------
PC3-M-PPARγ-si-M	80 ± 14	≤ 0.0012
PC3-M-PPARγ-si-H	45 ± 9	≤ 0.0015

Table 3.6: Colony counts of transfected cells at 4th week of soft agar assay.
Differences of number of colonies between different groups were assessed by Student's t-test. *p* values were obtained by comparing sample groups to control group data.

A

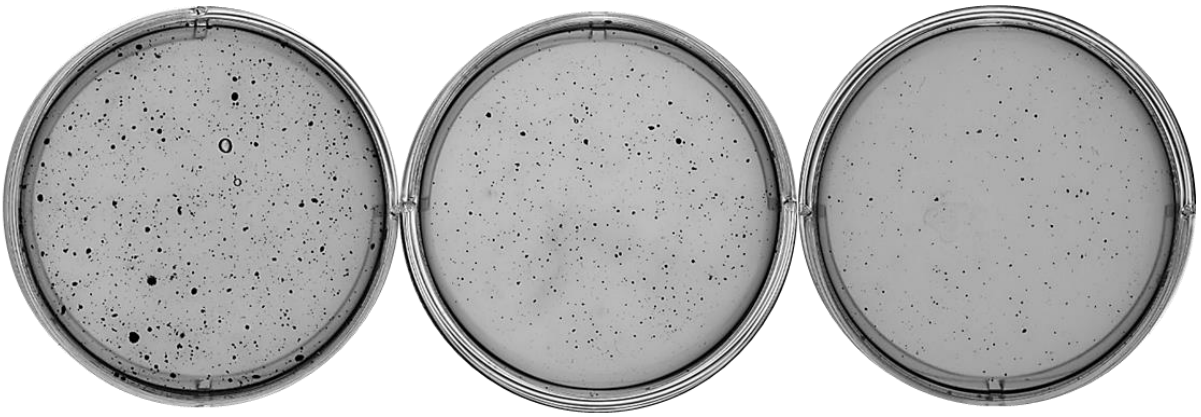

Scramble (control) PC3-M-PPARγ-si-M PC3-M-PPARγ-si-H

B

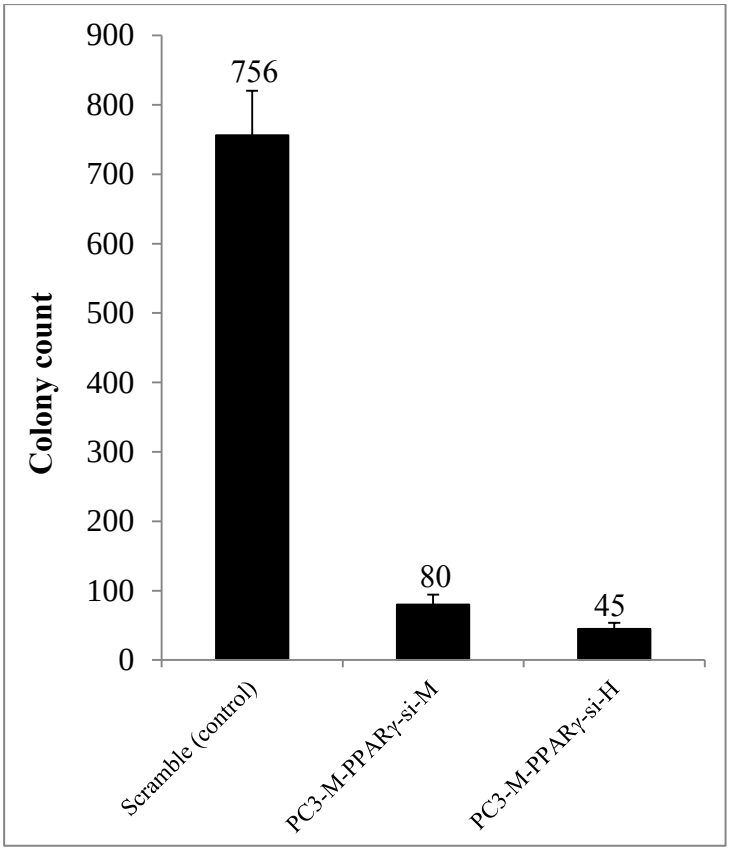

Figure 3.19: The impact of *PPARγ* silencing on the anchorage-independent growth of tranfectant cells.

A: Representative plates of soft agar colony formation with different transfectants.

B: Colony counts of different transfectants; Results were obtained from three separate measurements (mean ± SE).

3.11 Effect of *PPARγ* suppression on tumorigenicity of prostate cancer cells *in vivo*

To evaluate the effect of *PPARγ* suppression on the tumorigenicity of PC3-M cells *in vivo*, parental and transfected cells were harvested and re-suspended in PBS (1×10^6 cells/200 µl). Thirty male Balb/C immune-incompetent nude mice were divided into three equal groups and cells were injected subcutaneously into their flanks (section **2.2.8.2**). Weight of mice and tumour sizes were measured twice a week using a calliper. The median latent period for group inoculated with PC3-M-PPARγ-si-H cells was 21 days which was significantly longer than those inoculated with parental cells [6 days (ranged 5-14)] and with PC3-M-PPARγ-si-M cells [11 days (ranged 7-19)]. After three weeks, only 1 out of 10 (10%) of mice which inoculated with PC3-M-PPARγ-si-H cells produced tumour whereas all mice (100%) inoculated with parental cells and 7 out of 10 (70%) inoculated with PC3-M-PPARγ-si-M cells produced tumour (**Table 3.7**). At the end point of this experiment, average volume of tumours produced by control cells (250.6 mm^3 ± 60) was significantly larger than those produced by PC3-M-PPARγ-si-M cells (19.5 mm^3 ± 14.6) (Student's t-test, $p \leq 0.008$) and PC3-M-PPARγ-si-H cells (2 mm^3) (Student's t-test, $p \leq 0.0009$) (**Fig. 3.20**). At autopsy (three weeks after inoculation), average weight of the tumours produced by parental cells was 275 mg ± 105 which was significantly higher than those produced by PC3-M-PPARγ-si-M cells (26.5 mg ± 12.6) (Student's t-test, $p \leq 0.002$) and PC3-M-PPARγ-si-H cells (4 mg) (Student's t-test, $p \leq 0.0003$). Representative nude mice from each group, corresponding tumour mass, H&E and immunohistochemical staining of tumour tissues were shown in **Figure 3.21**. Primary tumours were fixed in 10% formalin for 24 hours before processed and paraffin embedded. Expression levels of PPARγ protein were evaluated in all primary tumours by immunohistochemical staining then intensity and percentage of nuclear staining were scored (section **2.2.4.3** and **2.2.4.4**) (**Table 3.8**). When tumour sections were stained with anti-PPARγ antibody, the intensity of nuclear staining in both test groups were much weaker than

that of control group which indicate that reduced PPARγ was responsible for reduction of tumour mass. In control group, 5 (50%) sections stained moderately positive in the nucleus and 5 (50%) sections stained strongly positive in the nucleus (**Figure 3.21**). Among a total of 7 stained sections from PC3-M-PPARγ-si-M group, 2 (29%) stained weakly positive in the nucleus and 5 (71%) stained moderately positive in the nucleus. Nuclear expression of PPARγ in the only tumour that produced by PC3-M-PPARγ-si-H cells was weakly positive. No significant difference in cytoplasmic expression of PPARγ in different primary tumours was detected. Intensity of staining for PPARγ in tumours produced by PC3-M-PPARγ-si-H cells (χ^2 test, $p \leq 0.002$) or PC3-M-PPARγ-si-M cells (χ^2 test, $p \leq 0.02$) was significantly weaker compare to those produced by parental cells.

Cell lines	No. of inoculated mice	Incidence of tumours [I]		Median of latent period (range) [II]	Tumour weight (mg) [III]
		No.	%		
PC3-M-PPARγ-si-H	10	1	10	21	4
PC3-M-PPARγ-si-M	10	7	70	11 (7-19)	26.5 ± 12.6
PC3-M (control)	10	10	100	6 (5-14)	275 ± 105

Table 3.7: Incidence, latent period and weight of tumours developed by parental and transfectant cells in nude mice.

I: Tumour incidence calculated by the percentage of number of the mice with tumour/total number of inoculated animals.

II: Latent period is the number of days from the inoculation time to the time of first appearance of tumour.

III: Tumour weight was measured at autopsy in 21st day after inoculation of parental and transfectant cells.

Origin of tissue (mice groups)	No. of cases	Nuclear stain intensity & percentage score		
		≤ 3	4-6	≥ 9
Control	10	0	5	5
PC3-M-PPARγ-si-M	7	2	5	0
PC3-M-PPARγ-si-M	1	1	0	0

Table 3.8: Nuclear expression of PPARγ in different primary tumours resected from nude mice.

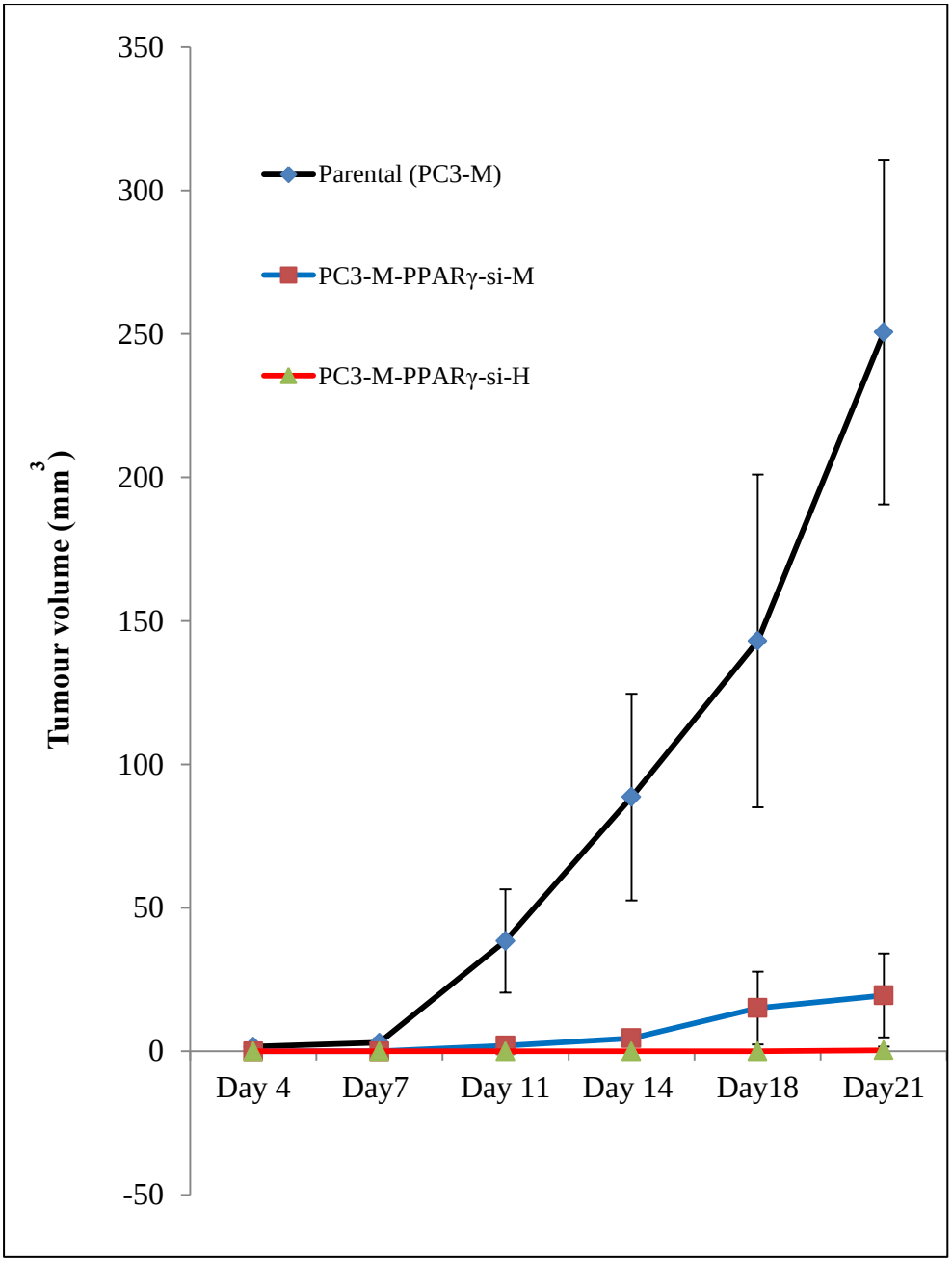

Figure 3.20: Average tumour volume of each test group.

Parental and transfectant cells were inoculated subcutaneously into the flank of nude mice of each test group (10 animals in each group). Weight of mice and tumour size were measured twice a week using a calliper. Tumour volume was calculated by the following formula: Length×Width×Heigth×0.5236.

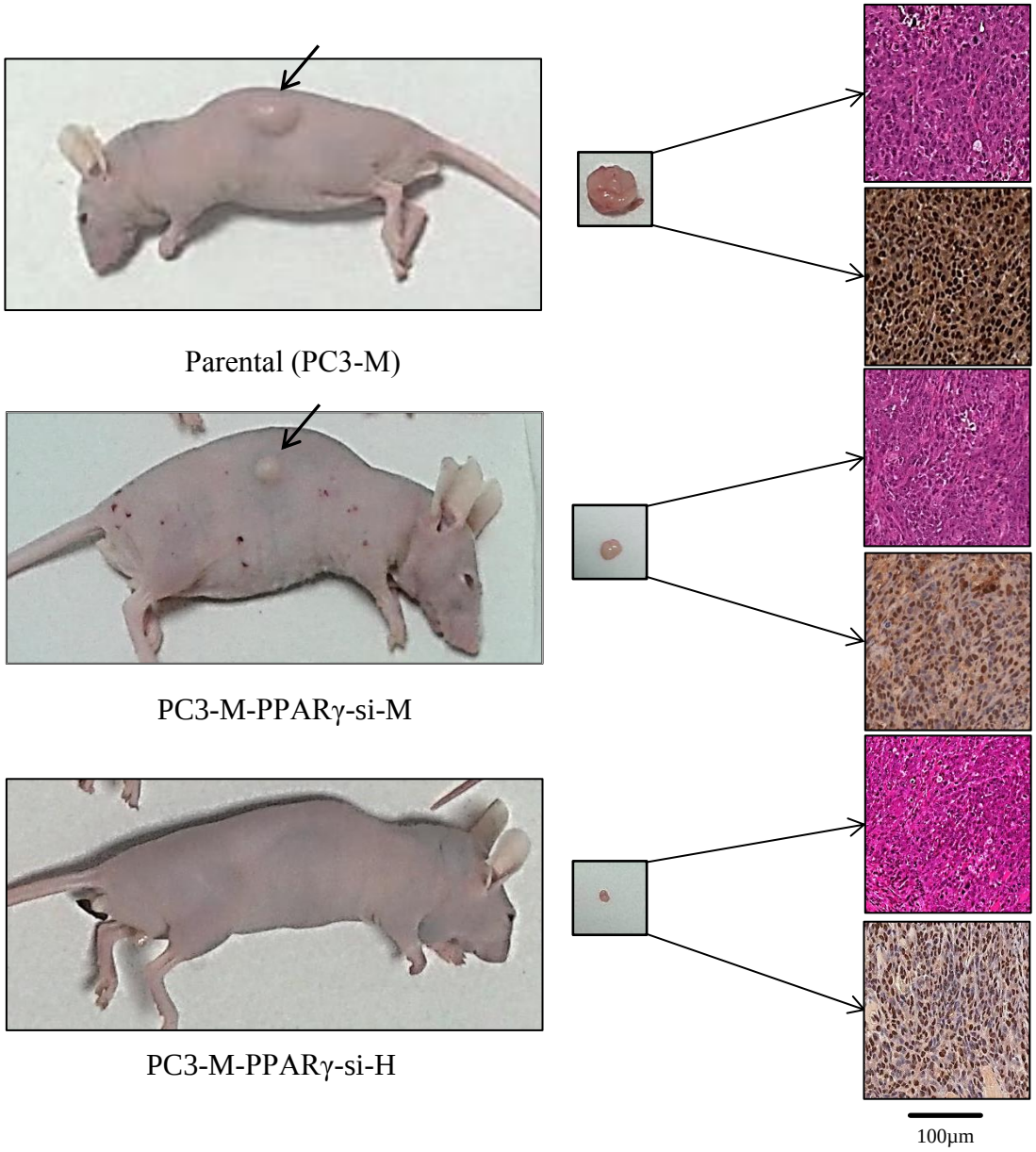

Figure 3.21: Representative mice and corresponding tumour mass of each test group.
The tumour produced by parental cells and PC3-M-PPARγ-si-M cells were pointed by an arrow but the one developed by PC3-M-PPARγ-si-H cells was barely visible. Presence of tumour cells in all tumour masses has been confirmed by H&E staining. Immunohistochemical staining with PPARγ antibody (1/50) showed significant difference between the expressions of PPARγ in test groups compare to the control. Original magnifications of images of representative slides were 250×.

3.12 Interaction of C-FABP and PPARγ and its effects on regulation of VEGF expression

To investigate the possible interaction between C-FABP and PPARγ and its effect on regulation of VEGF in prostate cancer cells, moderately malignant 22RV1 cell line was subjected to different treatments, so the effect of the interaction of C-FABP and PPARγ could be assessed. Prior to the treatment, the level of C-FABP and PPARγ in 22RV1 and PC3-M cells were detected with Western blot. Both C-FABP and PPARγ levels appeared to be much lower in 22RV1 cells than in PC3-M cells (**Fig. 3.22, A**). Further quantitative analysis showed that the level of C-FABP in PC3-M was 5.4-fold higher than that in 22RV1. The level of PPARγ in PC3-M cells was also higher (3.2-fold) than that in 22RV1 cells (**Fig. 3.22, B**).

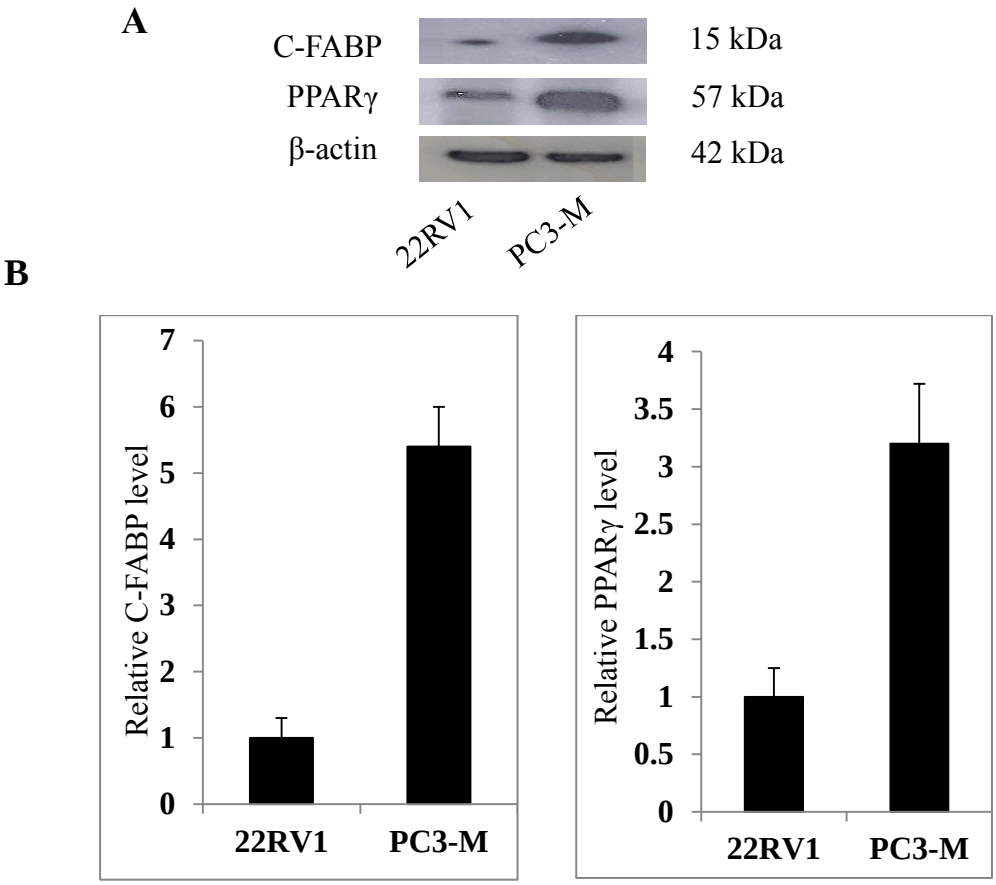

Figure 3.22: Levels of C-FABP and PPARγ in PC3-M and 22RV1 cells.

A: Western blot analysis of C-FABP and PPARγ expressed in 22RV1 and PC3-M cells. The anti-β-actin antibody was used to correct possible loading errors in the same blot.

B: Relative expression of C-FABP and PPARγ. The levels of both proteins in 22RV1 cells were set as 1.0. Levels in PC3-M cells were calculated by relating to those in 22RV1. Results were obtained from three different measurements (mean ± SE).

3.12.1 C-FABP and PPARγ up-regulated VEGF expression

In order to study the possible role of C-FABP on up-regulation of VEGF (through PPARγ), the 60% confluent 22RV1 cells were treated with Rosiglitazone (PPARγ synthetic agonist) (0.5 µM) [248] or C-FABP recombinant protein (2 µM) [167, 280], overnight. The level of VEGF was assessed before and after treatments. Using Western blotting, different levels of VEGF expressed in protein extracted from 22RV1 cells before and after treatments were analysed. Two VEGF bands of 19 & 22kDa were detected in untreated and treated cells (**Fig. 3.23, A**). When the densitometric level of VEGF in untreated 22RV1 cells was set at 1, levels in those treated with Rosiglitazone and recombinant C-FABP were 1.41 ± 0.12 and 1.36 ± 0.08, respectively (**Fig. 3.23, B**). Levels of VEGF in the protein extracted from cells showed 41% and 36% increment after exposing to Rosiglitazone and recombinant C-FABP, respectively.

When the levels of secreted VEGF in conditional media of 22RV1 cells before and after treatments were analysed by ELISA, VEGF was detected in all culture media from treated and untreated cells (**Fig. 3.24, B**). While the amount of VEGF produced by 22RV1 cells without any treatment, was detected about 120 ± 8.3 pg/ml, in those which treated with Rosiglitazone (0.5 µM) and recombinant C-FABP (2 µM) were increased to 915 ± 37.8 pg/ml (7.6 times) and 756 ± 25.6 pg/ml (6.3 times), respectively. Statistical analysis showed a significant difference between the levels of secreted VEGF in those treated with Rosiglitazone (Student's t-test, $p \leq 0.0003$) or recombinant C-FABP (Student's t-test, $p \leq 0.0005$) and VEGF level of untreated cells. The relative level of VEGF was greater in conditional media compare to cell lysates (especially for those treated with Rosiglitazone or recombinant C-FABP) and both sets of experiment followed a similar pattern.

Biological activity of secreted VEGF from 22RV1 cells which exposed to different treatments were evaluated by endothelial tube formation assay (*in vitro* angiogenesis assay). The tube formation ability of HUVEC cells were strongly promoted and well-assembled

organizations formed in those treated with Rosiglitazone (**Fig. 3.25, D)** or recombinant C-FABP (**Fig. 3.25, F)**, similar to positive control (cells were treated with recombinant human VEGF, 10ng/ml) **(Fig. 3.25, A)**. Conditional medium from the untreated 22RV1 cells caused partially visible sprouting of new capillary tubes **(Fig. 3.25, C)**. The average numerical values associated with tube formation showed a significant increase in cells treated with Rosiglitazone (2-fold) and recombinant C-FABP (1.8-fold) compare to untreated cells (**Fig. 3.26**). Comparing to untreated cells, the network formation value in cells treated with Rosiglitazone (Student's t-test, $p \leq 0.003$) or recombinant C-FABP (Student's t-test, $p \leq 0.006$) was significantly higher.

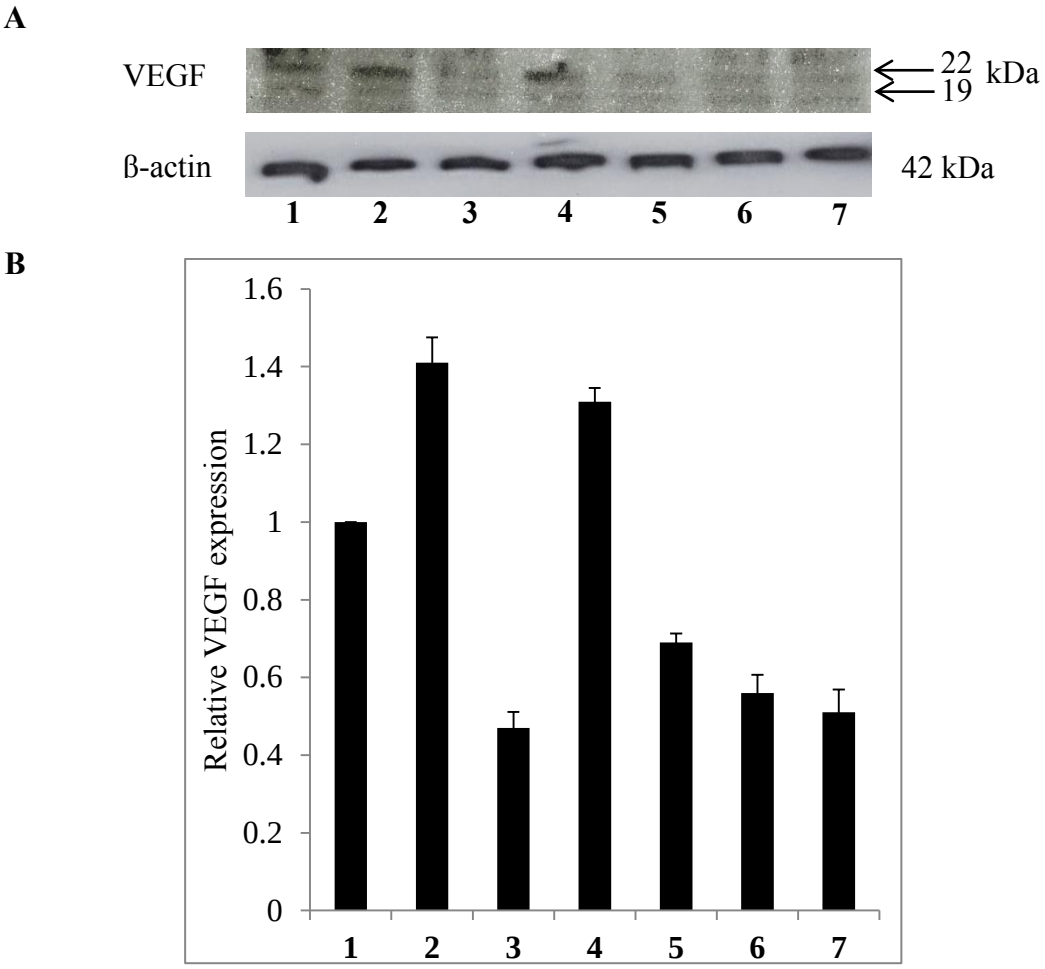

Figure 3.23: Levels of VEGF protein in 22RV1 cells exposed to different treatments.

A: VEGF levels in 22RV1 cells treated overnight in different conditions were analysed by Western blotting (according to the instruction of manufacture, antibody reacts with two splice variant of VEGF antigen by molecular weight of 19 & 22 kDa); **1**: 22RV1 cells without any treatment, **2**: 22RV1 cells treated with Rosiglitazone (PPARγ agonist) (0.5 μM), **3**: 22RV1 cells treated with GW9662 (PPARγ antagonist) (20 μM), **4**: 22RV1 cells treated with C-FABP recombinant protein (2 μM), **5**: 22RV1 cells treated with a mixture of C-FABP recombinant protein (2 μM) & GW9662 (20 μM), **6**: 22RV1 cells treated with single mutant C-FABP protein (2 μM), **7**: 22RV1 cells treated with double mutant C-FABP protein (2 μM). The anti-β-actin antibody was used to correct possible loading errors in the same blot.

B: Relative levels of VEGF. The level of VEGF in untreated 22RV1 cells was set as 1.0; levels in other cells were calculated by relating to level that in untreated 22RV1 cells. Results were obtained from three different measurements (mean ± SE).

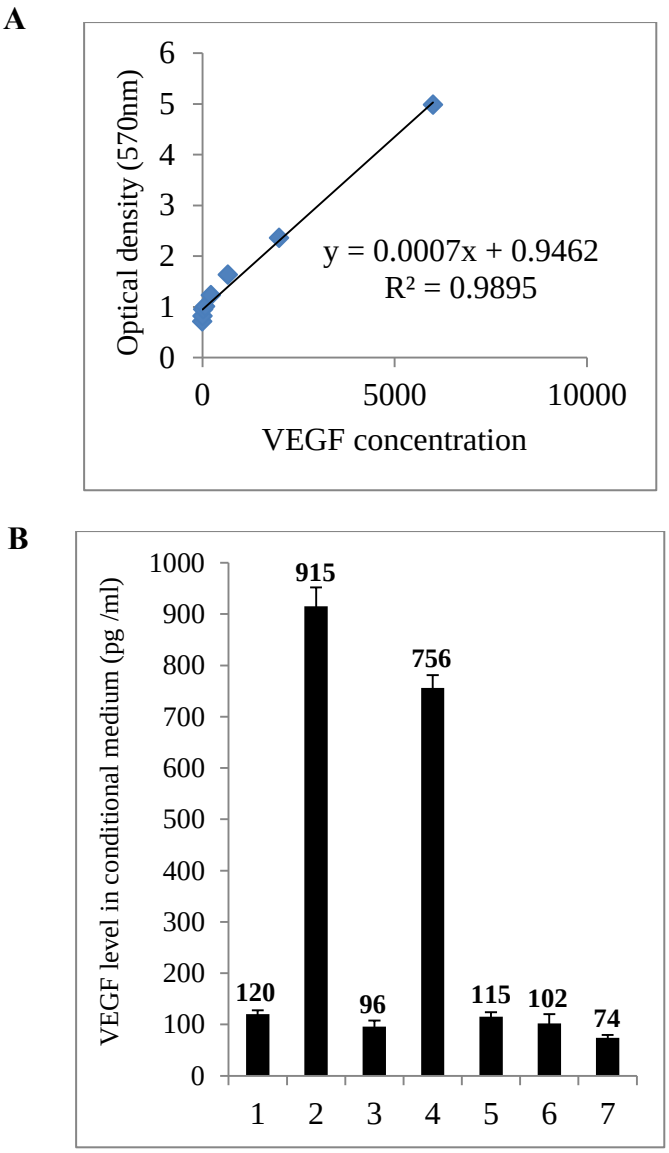

Figure 3.24: Levels of secreted VEGF in conditional media of 22RV1 cells exposed to different treatments.

A: Standard VEGF curve generated by ELISA. The quantity of VEGF was determined by comparing to serially-diluted concentrations of the standard curve.

B: VEGF levels in conditional media of 22RV1 cells treated overnight with different conditions were analysed by ELISA; **1**: 22RV1 cells without any treatment, **2**: 22RV1 cells treated with Rosiglitazone (PPARγ agonist) (0.5 µM), **3**: 22RV1 cells treated with GW9662 (PPARγ antagonist) (20 µM), **4**: 22RV1 cells treated with C-FABP recombinant protein (2 µM), **5**: 22RV1 cells treated with a mixture of C-FABP recombinant protein (2 µM) & GW9662 (20 µM), **6**: 22RV1 cells treated with single mutant C-FABP protein (2 µM), **7**: 22RV1 cells treated with double mutant C-FABP protein (2 µM). Results were obtained from three different measurements (mean ± SE).

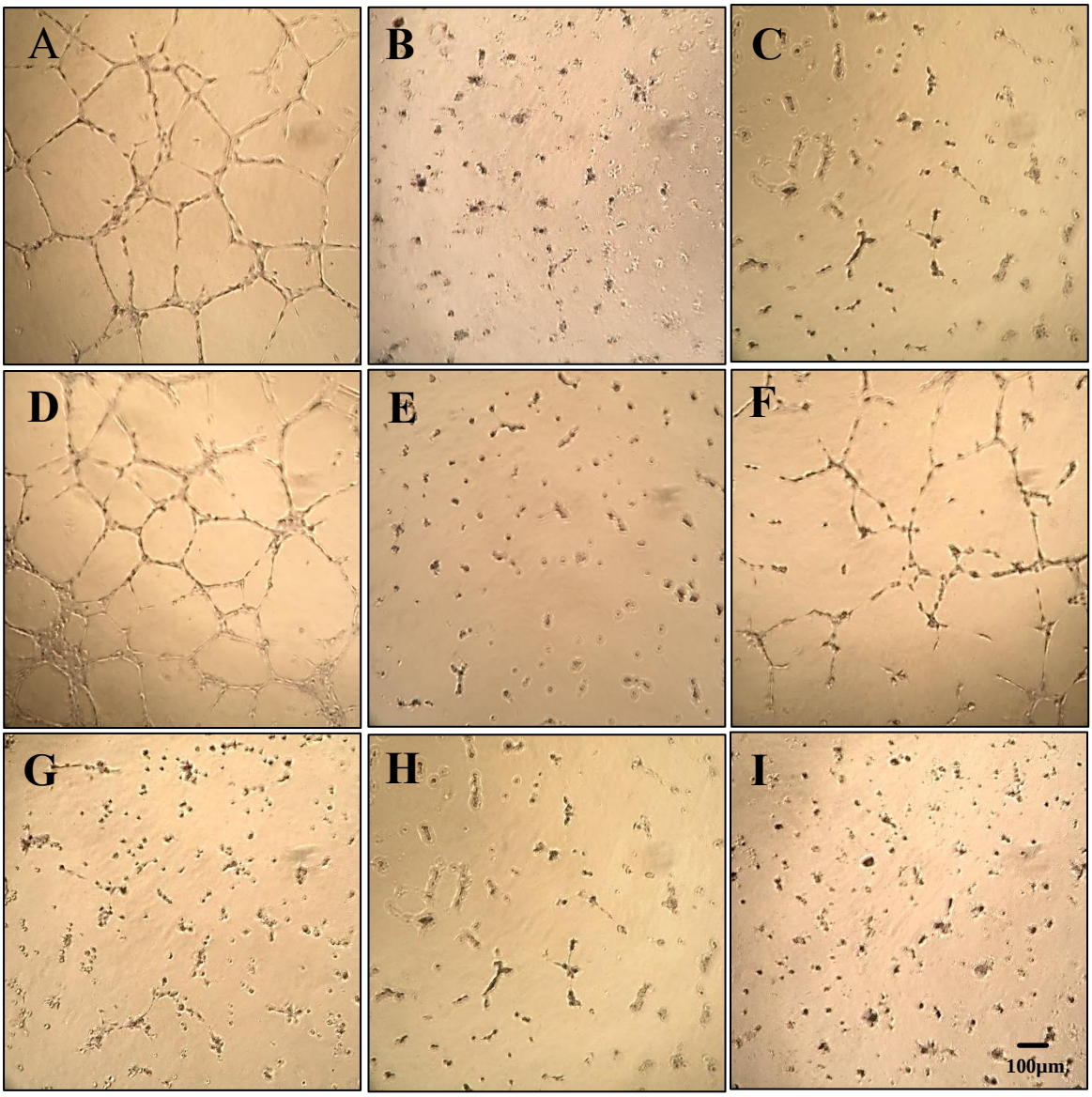

Figure 3.25: HUVEC cells network formation on ECMatrix, exposed to conditional media of 22RV1 cells with different treatments.

After 6 hours incubation of endothelial cells with conditional media from 22RV1 cell culture media exposed to different treatments, network structures were visualized by MTT (2%). Original magnifications of images of representative slides were 250×. **A**: Positive control (recombinant human VEGF, 10ng/ml); **B**: Negative control (normal culture medium); **C**: The medium of 22RV1 cells without any treatment; **D**: The medium of 22RV1 cells treated with Rosiglitazone (PPARγ agonist) (0.5 µM); **E**: The medium of 22RV1 cells treated with GW9662 (PPARγ antagonist) (20 µM); **F**: The medium of 22RV1 cells treated with C-FABP recombinant protein (2 µM); **G**: The medium of 22RV1 cells treated with a mixture of C-FABP recombinant protein (2 µM) & GW9662 (20 µM); **H**: The medium of 22RV1 cells treated with single mutant C-FABP protein (2 µM); **I**: The medium of 22RV1 cells treated with double mutant C-FABP protein (2 µM).

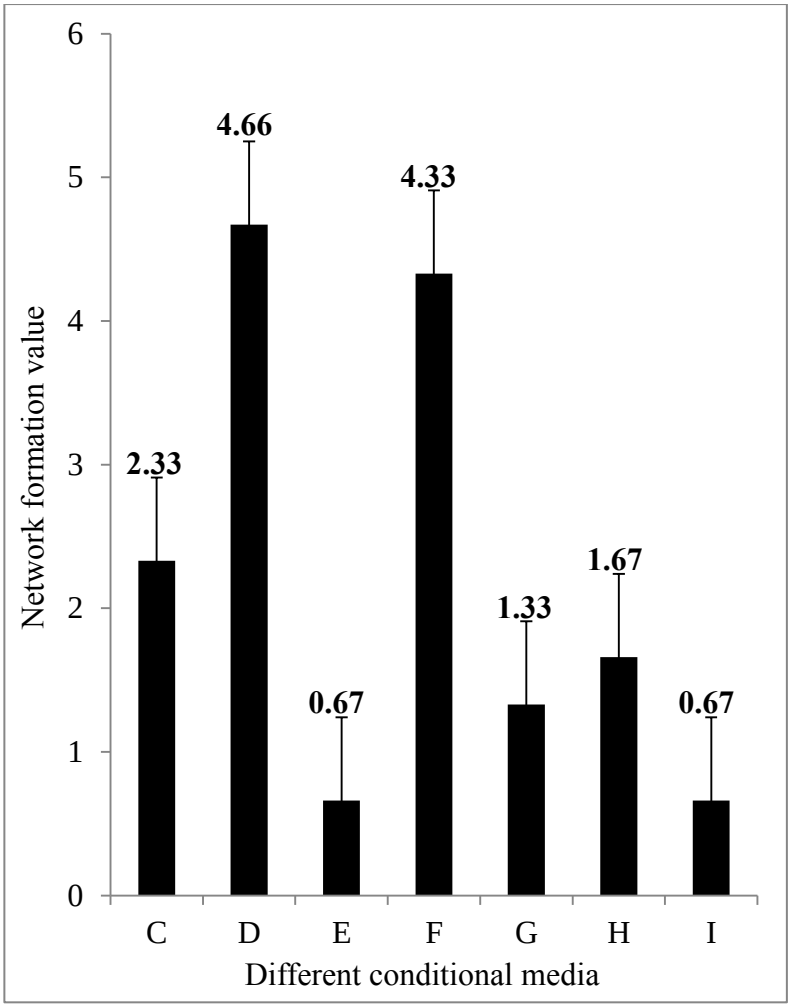

Figure 3.26: Relative values of HUVEC cells network formation under 22RV1 cells' conditional media exposed to different treatments.

The effects of conditional media (from 22RV1 cells subjected to different treatments) on HUVEC cells network formation were assessed and quantified according the cell network pattern. Three individual assays were performed for each treatment and the values of five random fields in each assay were averaged (mean ± SD). **C**: The medium of 22RV1 cells without any treatment (2.33 ± 0.66); **D**: The medium of 22RV1 cells treated with Rosiglitazone (0.5 µM) (4.66 ± 0.67); **E**: The medium of 22RV1 cells treated with GW9662 (20 µM) (0.67 ± 0.66); **F**: The medium of 22RV1 cells treated with C-FABP recombinant protein (2 µM) (4.33 ± 0.67); **G**: The medium of 22RV1 cells treated with a mixture of C-FABP recombinant protein (2 µM) & GW9662 (20 µM) (1.33 ± 0.67); **H**: The medium of 22RV1 cells treated with single mutant C-FABP recombinant protein (2 µM) (1.67 ± 0.66); **I**: The medium of 22RV1 cells treated with double mutant C-FABP recombinant protein (2 µM) (0.67 ± 0.66).

3.12.2 Suppression of C-FABP or PPARγ down-regulated VEGF expression

In order to study the possible role of C-FABP suppression on down-regulation of VEGF (through PPARγ), the 60% confluent 22RV1 cells were treated with GW9662 (PPARγ synthetic antagonist) (20 μM) [167] , single mutant C-FABP recombinant protein (2 μM) or double mutant C-FABP recombinant protein (2 μM) [167, 280], overnight. Western blot was used to assess the level of VEGF in cellular extracts of 22RV1 cells before and after treatments. Two VEGF bands of 19 & 22 kDa were detected in untreated and treated cells (**Fig. 3.23, A**). When the level of VEGF in untreated 22RV1 cells was set at 1, level in those treated with GW9662, single mutant and double mutant recombinant C-FABP were 0.47 ± 0.08, 0.56 ± 0.08 and 0.49 ± 0.12, respectively (**Fig. 3.23, B**). Levels of VEGF in the cell extracts was reduced by 53%, 44% and 51% after treatment with GW9662, single mutant or double mutant recombinant C-FABP, respectively.

When the levels of secreted VEGF in conditional medium of 22RV1 cells before and after treatments were analysed by ELISA, VEGF was detected in all culture media from treated and untreated cells (**Fig. 3.24, B**). While the amount of VEGF produced by 22RV1 without any treatment was about 120 ± 8.3 pg/ml, the amount of VEGF in those treated with GW9662 (20 μM), single and double mutant recombinant C-FABP (2 μM) were 96 ± 12.1 pg/ml, 102 ± 18.4 pg/ml and 74 ± 6.2 pg/ml, respectively. Thus treating with GW9662, single and double mutant recombinant C-FABP produced 20%, 15% and 39% reductions in secreted VEGF level. The amount of VEGF in media of cells treated with GW9662 (Student's t-test, $p \leq 0.02$) and double mutant recombinant C-FABP (Student's t-test, $p \leq 0.0009$) was significantly reduced in comparison with that of the untreated cells. The level of VEGF in medium of cells treated with single mutant recombinant C-FABP was not statistically different (Student's t-test, $p \geq 0.1$) from that in control.

Biological activity of secreted VEGF from 22RV1 cells was evaluated by endothelial tube formation assay (*in vitro* angiogenesis assay). HUVEC cells remained randomly separated without any sign of formation of complex mesh likes structures after treatment with GW9662 **(Fig. 3.25, E)** or double mutant recombinant C-FABP **(Fig. 3.25, I)**, similar to that of the negative control (cells were treated with normal culture medium) **(Fig. 3.25, B)**. Conditional medium of cells treated with single mutant recombinant C-FABP only induced some visible capillary tubes without any sprouting (**Fig. 3.25, H)**. Conditional medium from the untreated 22RV1 cells caused partially visible sprouting of new capillary tubes **(Fig. 3.25, C)**. The average numerical values associated with tube formation showed a prominent reduction in cells treated with GW9662 or double mutant recombinant C-FABP in comparison to untreated 22RV1 cells (72%) (**Fig. 3.26**). Comparing with the untreated cells, the network formation value in cells treated with GW9662 (Student's t-test, $p \leq 0.01$) and double mutant recombinant C-FABP (Student's t-test, $p \leq 0.01$) were significantly lower; whereas the difference between the value of the cells treated with single mutant recombinant C-FABP and that of control was not statistically different (Student's t-test, $p \geq 0.11$).

3.12.3 Suppression of PPARγ neutralized up-regulatory effect of C-FABP on VEGF expression

To study the possible effect of PPARγ inhibition in counteracting up-regulatory effect of C-FABP on VEGF, 60% confluent 22RV1 cells were treated with GW9662 (PPARγ synthetic antagonist) (20 µM) , C-FABP recombinant protein (2 µM) or a combination of C-FABP recombinant protein with GW9662, overnight. Western blot detected two VEGF bands of 19 & 22 kDa in cellular extracts of untreated and treated 22RV1 cells (**Fig. 3.23, A**). When the level of VEGF in untreated 22RV1 cells was set at 1, levels in those treated with GW9662, recombinant C-FABP and mixture of recombinant C-FABP with GW9662 were 0.47 ± 0.08, 1.36 ± 0.08 and 0.69 ± 0.04, respectively (**Fig. 3.23, B**). Although level of VEGF showed 36% increment after treating with recombinant C-FABP, 31% decrement was detected after treating with a mixture of recombinant C-FABP with GW9662.

When the level of secreted VEGF was analysed by ELISA, VEGF was detected in all culture media from treated and untreated 22RV1 cells (**Fig. 3.24, B**). While the amount of VEGF produced by untreated 22RV1 cells was 120 ± 8.3 pg/ml, the amount of VEGF in cells treated with GW9662 (20 µM), recombinant C-FABP (2 µM) and mixture of recombinant C-FABP with GW9662 were 96 ± 12.1 pg/ml, 756 ± 25.6 pg/ml and 105 ± 9.6 pg/ml, respectively. Although treatment with recombinant C-FABP produced 6.3-fold increase in secreted VEGF level, combination of recombinant C-FABP with GW9662 produced 12.5% reduction in secreted VEGF level. The amount of VEGF in media of cells treated with GW9662 (Student's t-test, $p \leq 0.02$) and recombinant C-FABP (Student's t-test, $p \leq 0.0005$) was significantly different from that of the untreated cells. The level of VEGF in medium of cells treated with mixture of recombinant C-FABP and GW9662 was not statistically different (Student's t-test, $p \geq 0.05$) from that in control.

Biological activity of secreted VEGF from 22RV1 cells was evaluated by endothelial tube formation assay (*in vitro* angiogenesis assay). The tube formation ability of HUVEC cells was strongly enhanced and well-assembled organizations formed in those treated with C-FABP recombinant protein (**Fig. 3.25, F).** Conditional medium from treated cells with combination of recombinant C-FABP with GW9662 only induced some visible capillary tubes without any sprouting (**Fig. 3.25, G)**. Conditional medium from the untreated 22RV1 cells caused partially visible sprouting of new capillary tubes **(Fig. 3.25, C)**. The average numerical values associated with tube formation showed a significant increase in the cells treated with recombinant C-FABP (1.8-fold); whereas in those treated with combination of recombinant C-FABP and GW9662 showed about 42% reduction from control level (**Fig.3.26**). Comparing with untreated cells, the network formation value in cells treated with recombinant C-FABP (Student's t-test, $p \leq 0.006$) was significantly higher; whereas the difference between the value of the cells treated with mixture of C-FABP recombinant protein and GW9662 and that of control was not statistically different (Student's t-test, $p \geq 0.05$) .

3.12.4 Effects of *C-FABP* and *PPARγ* on *VEGF* activity through *PPRE*s

To investigate whether the activated PPARγ (by fatty acids transported via C-FABP) up-regulated VEGF through binding to the *PPRE*s in promoter region of the *VEGF* gene, a luciferase reporter gene system was employed to test the relationship between the presence or absence of *PPRE* and the level of VEGF expression. pGL3-promoter luciferase vector was used to make three DNA constructs: In construct A (Wild type), 805bp segment of VEGF promoter region containing two *PPRE*s was cloned upstream of the luciferase reporter gene. In construct B (Mutant1) a segment of DNA from the same region with mutated sequences to replace two *PPRE*s was inserted into upstream of the reporter gene. In construct C (Mutant2), a 393bp section of DNA from VEGF promoter region in which both *PPRE*s were deleted was cloned upstream of reporter gene. Thus three constructs harbouring a section of VEGF promoter in the upstream of luciferase gene, were made; one contains two *PPRE*s, the other one contains two mutated *PPRE* sequences and the last one contains no *PPRE*. In addition, pGL3-promoter vector alone was used as control. Four different prostate cancer cell lines including: 22RV1 cells, PC3-M cells, PC3-M-3 cells (*C-FABP* knockdown PC3-M cells) [168] and PC3-M-PPARγ-si-H cells (*PPARγ*-suppressed PC3-M cells) were used to perform transient transfection with three luciferase gene constructs, respectively. Different levels of luciferase activity were measured in co-transfected prostate cancer cell lines before exposing to any treatment (**Fig. 3.27)**. When the level of luciferase activity in 22RV1 cells transfected with control plasmid was set as 1, levels in those transfected with Wild type, Mutant1 and Mutant2 plasmids were 2.62 ± 0.26, 2.41 ± 0.25 and 1.29 ± 0.17, respectively. When the level of luciferase activity in PC3-M cells transfected with control plasmid was set as 1, levels in those transfected with Wild type, Mutant1 and Mutant2 plasmids were 3.3 ± 0.12, 2 ± 0.14 and 1 ± 0.21, respectively. When the level of luciferase activity in PC3-M-PPARγ-si-H cells transfected with control plasmid was set as 1, levels in those transfected with Wild

type, Mutant1 and Mutant2 plasmids were 2.16 ± 0.22, 1.75 ± 0.24 and 0.99 ± 0.23, respectively. When the level of luciferase activity in PC3-M-3 cells transfected with control plasmid was set as 1, levels in those transfected with Wild type, Mutant1 and Mutant2 plasmids were 2.5 ± 0.32, 1.71 ± 0.31 and 0.99 ± 0.2, respectively.

Luciferase activity in 22RV1, PC3-M, PC3-M-PPARγ-si-H and PC3-M-3 cells which transfected with Wild type showed 262%, 330%, 216% and 250% increase, respectively; whereas levels in the same set of cell lines transfected with Mutant2 plasmid only increased by 29%, 21%, 24% and 31%, respectively. After being transfected with Muatnt1 plasmid, levels of luciferase activity raised 241%, 200%, 175% and 171% in 22RV1, PC3-M, PC3-M-PPARγ-si-H and PC3-M-3 cells, respectively.

Then transfected cell lines were treated with Rosiglitazone (PPARγ agonist) (0.5μM), GW9662 (PPARγ antagonist) (20μM), C-FABP recombinant protein (2μM), single mutant C-FABP recombinant protein (2μM), double mutant C-FABP recombinant protein (2μM) and Mithramycin A (Sp1 inhibitor) (0.1μM) to investigate their effects on the luciferase activity.

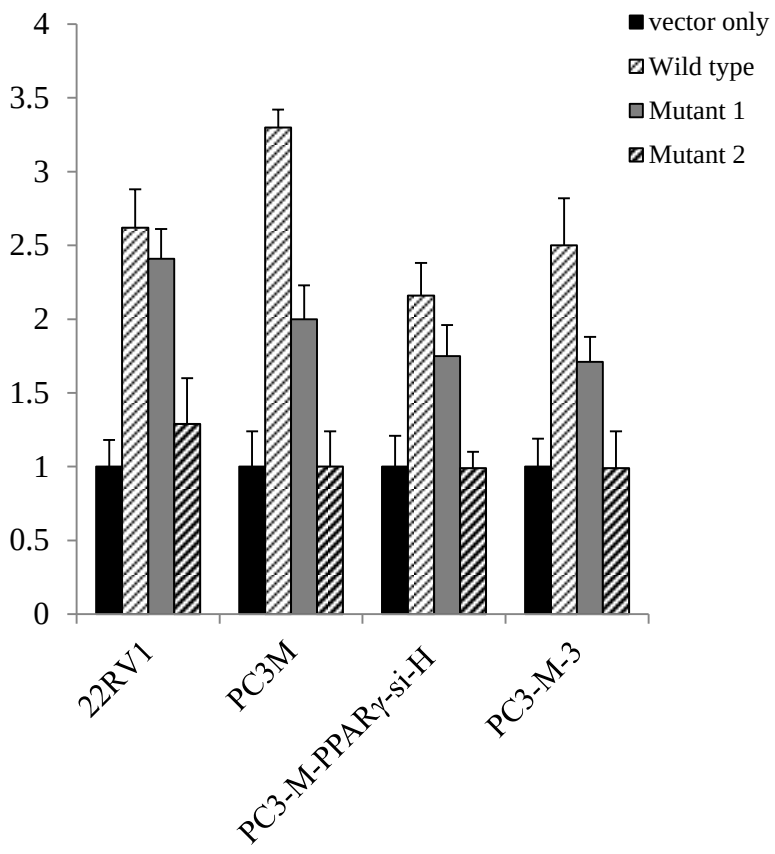

Figure 3.27: Luciferase activity in different prostate cancer cell lines transfected with different luciferase reporter gene constructs.

VEGF-promoter luciferase and *Renilla* luciferase plasmids were co-transfected into 22RV1, PC3-M, PC3-M-PPARγ-si-H and PC3-M-3 cell lines. Luciferase activity of transfected cells with control (pGL3-promoter) was set as 1. Levels in other cells were calculated by relating to that of the control. Results were obtained from three different measurements (mean ± SD).

3.12.4.1 *PPARγ* regulated *VEGF*-promoter activity

Different levels of luciferase activity were measured in co-transfected prostate cancer cell lines before and after subjecting them to different treatments.

When the level of luciferase activity in 22RV1 cells transfected with control plasmid was set as 1, levels in those transfected with Wild type, Mutant1 and Mutant2 plasmids were 2.62 ± 0.26, 2.41 ± 0.25 and 1.29 ± 0.17, respectively; after treating with Rosiglitazone (PPARγ agonist) (0.5μM) luciferase activity in the same set of transfectants detected as 4.25 ± 0.35, 2.33 ± 0.50 and 1.42 ± 0.26, respectively (**Fig. 3.28, A**). Comparing with the control, the luciferase level in cells transfected with Wild type and treated with Rosiglitazone (Student's t-test, $p \leq 0.0003$) was significantly higher; whereas the difference between the levels in the cells transfected with Mutant1 (Student's t-test, $p \geq 0.44$) and Mutant2 (Student's t-test, $p \geq 0.25$) and that of control was not statistically significant.

When the level of luciferase activity in PC3-M cells transfected with control plasmid was set as 1, levels in those transfected with Wild type, Mutant1 and Mutant2 plasmids were 3.3 ± 0.12, 2 ± 0.14 and 1 ± 0.21, respectively; after treating with GW9662 (PPARγ antagonist) (20μM) luciferase activity in the same transfectants was reduced to 2.23 ± 0.12, 1.70 ± 0.22 and 1.15 ± 0.32, respectively. When the level of luciferase activity in PC3-M-PPARγ-si-H cells transfected with control plasmid was set as 1, levels in those transfected with Wild type, Mutant1 and Mutant2 plasmids were 2.16 ± 0.22, 1.75 ± 0.24 and 0.99 ± 0.23, respectively (**Fig. 3.28, B**). Comparing with untreated control cells, the luciferase level in PC3-M cells transfected with Wild type and treated with GW9662 (Student's t-test, $p \leq 0.002$) was significantly lower; whereas the difference between levels of the cells transfected with Mutant1 (Student's t-test, $p \geq 0.08$) or Mutant2 (Student's t-test, $p \geq 0.27$) and that of the control was not statistically significant. No significant difference was detected between levels of luciferase in transfected PC3-M cells treated with GW9662 and that in PC3-M-PPARγ-si-H cells.

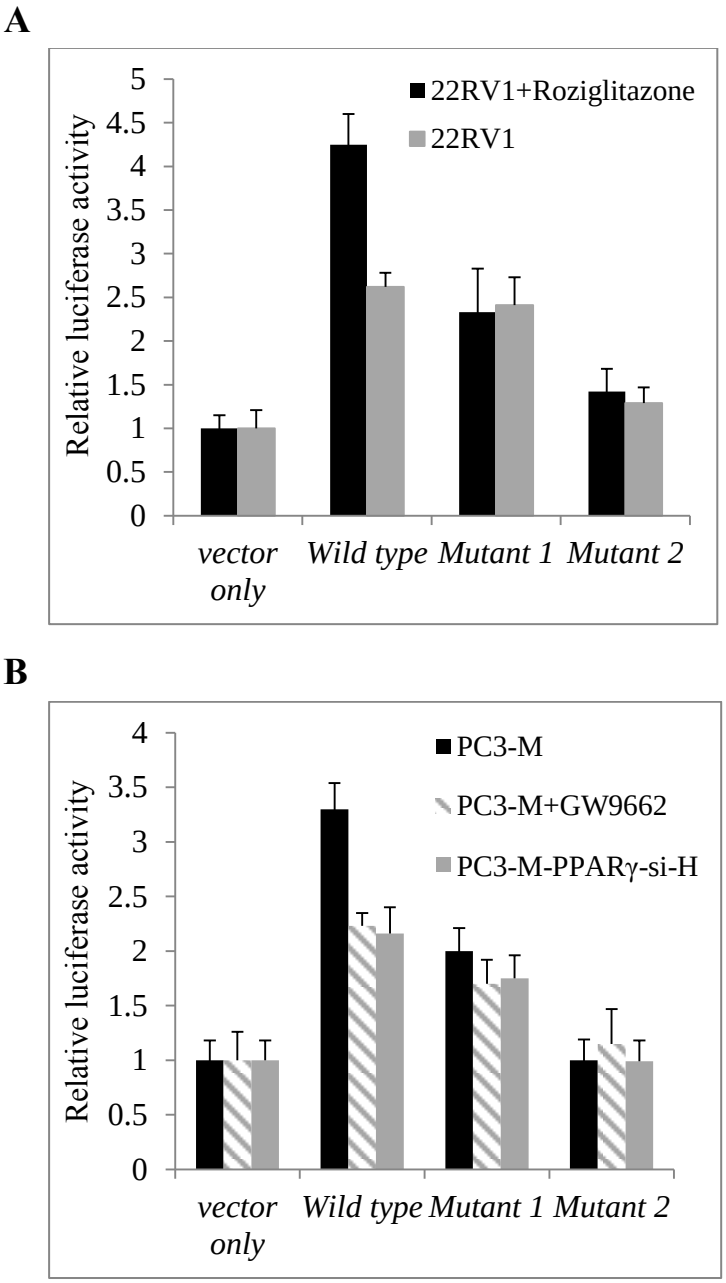

Figure 3.28: Effects of *PPARγ* on *VEGF*-promoter activity in prostate cancer cells.
VEGF-promoter luciferase and *Renilla* luciferase plasmids were co-transfected into 22RV1, PC3-M and PC3-M-PPARγ-si-H cells. Luciferase activity of transfected cells with vector only (pGL3-promoter) was set as 1. Levels in other cells were calculated by relating to the control. Results were obtained from three different measurements (mean ± SD). **A**: Luciferase activity level in transfected 22RV1 cells before and after Rosiglitazone (0.5µM) treatment; **B**: Luciferase activity levels in transfected PC3-M cells before and after GW9662 (20µM) treatment. Luciferase activity levels in transfected PC3-M-PPARγ-si-H cells without any treatment.

3.12.4.2 C-FABP regulated *VEGF*-promoter activity

Different luciferase activity levels were measured in co-transfected prostate cancer cell lines before and after different treatments.

When the level of luciferase activity in 22RV1 cells transfected with control plasmid was set as 1, levels in those transfected with Wild type, Mutant1 and Mutant2 plasmids were 2.62 ± 0.26, 2.41 ± 0.25 and 1.29 ± 0.17, respectively; after treating with recombinant C-FABP, luciferase activity levels in the same transfectants were increased to 4.23 ± 0.41, 2.04 ± 0.32 and 1.26 ± 0.40, respectively. After treating with recombinant double mutant C-FABP, luciferase level in 22RV1 cells transfected with Wild type, Mutant1 and Mutant2 were 2.29 ± 0.35, 2.14 ± 0.32 and 1.1 ± 0.41, respectively (**Fig. 3.29, A**). Comparing with untreated cells, the luciferase level in 22RV1 cells transfected with Wild type and treated with recombinant C-FABP (Student's t-test, $p \leq 0.004$) was significantly higher; whereas the difference between the value of the cells transfected with Mutant1 (Student's t-test, $p \geq 0.44$) or Mutant2 (Student's t-test, $p \geq 0.09$) and that of the control was not statistically significant. No significant difference was detected between luciferase level in transfected 22RV1 cells treated with recombinant double mutant C-FABP and that in the control (Student's t-test, $p \geq 0.33$).

When the level of luciferase activity in PC3-M cells transfected with control plasmid was set as 1, levels in those transfected with Wild type, Mutant1 and Mutant2 plasmids were 3.3 ± 0.12, 2 ± 0.14 and 1 ± 0.21, respectively; level of luciferase activity in the same transfectants in PC3-M-3 cells were 2.15 ± 0.12, 1.71 ± 0.22 and 0.99 ± 0.32, respectively (**Fig. 3.29, B**). Comparing with PC3-M cells, the luciferase level in PC3-M-3 cells transfected with Wild type (Student's t-test, $p \leq 0.001$) was significantly lower; whereas the difference between the level of the cells transfected with Mutant1 (Student's t-test, $p \geq 0.07$) or Mutant2 (Student's t-test, $p \geq 0.48$) and that of control was not statistically significant.

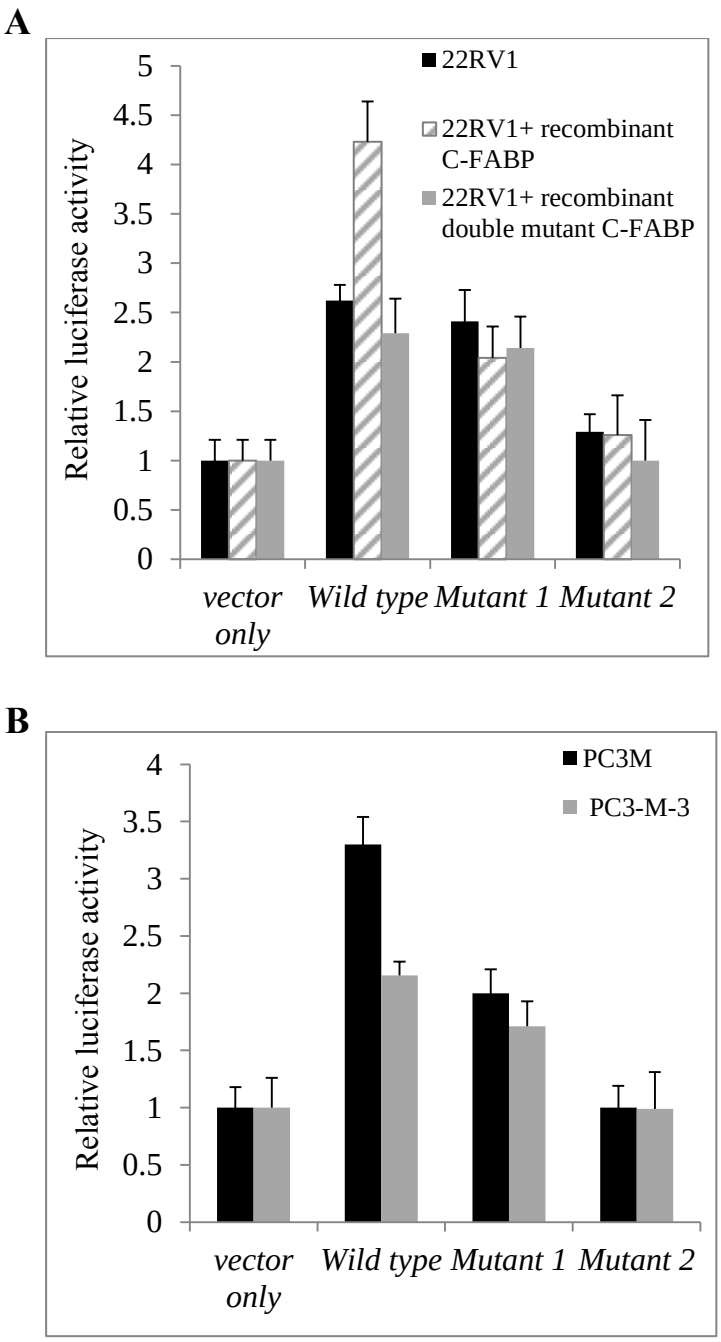

Figure 3.29: Effects of C-FABP on *VEGF*-promoter activity in prostate cancer cells.
VEGF-promoter luciferase and *Renilla* luciferase plasmids were co-transfected into 22RV1, PC3-M and PC3-M-3 cells. Luciferase activity level of the transfected cells with control (pGL3-promoter) was set as 1. Levels in other cells were calculated by relating to the control. Results were obtained from three different measurements (mean ± SE). **A**: Luciferase activity in transfected 22RV1 cells before and after treatment with recombinant C-FABP (2µM) or recombinant double mutant C-FABP (2µM); **B**: Luciferase activity in transfected PC3-M and PC3-M-3 cells without any treatment.

3.12.4.3 Combined effects of C-FABP and *PPARγ* on *VEGF*-promoter activity

Different luciferase activity levels were measured in co-transfected prostate cancer cell lines before and after different treatments.

Levels of luciferase activity in all untreated and treated 22RV1 cells transfected with Wild type plasmid were increased in comparison to control group (**Fig. 3.30, A**). When the luciferase activity of transfected cells with control plasmid was set as 1, levels of those treated with Rosiglitazone (0.5µM), recombinant C-FABP (2µM) and combination of Rosiglitazone and recombinant C-FABP were 4.25 ± 0.12, 4.13 ± 0.22 and 4.36 ± 0.32, respectively. Level in untreated 22RV1 cells was 2.62 ± 0.26. The luciferase levels in cells transfected with Wild type and treated with either Rosiglitazone (Student's t-test, $p \leq 0.0003$), recombinant C-FABP (Student's t-test, $p \leq 0.004$) or combination of Rosiglitazone and recombinant C-FABP (Student's t-test, $p \leq 0.001$) were significantly higher in comparison to untreated control cells; whereas they were not significantly different when compared to each other (Student's t-test, $p \geq 0.17$).

Levels of luciferase activity in PC3-M and PC3-M-3 cells transfected with Wild type plasmid were enhanced compare to control group (**Fig. 3.30, B**). When the level of luciferase activity of PC3-M cells transfected with control plasmid was set as 1, levels in cells transfected with Wild type was 3.3 ± 0.18. Levels in PC3-M cells treated with GW9662 (20µM), untreated PC3-M-3 cells and PC3-M-3 cells treated with GW9662 (20µM) were 2.05 ± 0.24, 2.23 ± 0.21, 1.95 ± 0.19, respectively.

Comparing to untreated PC3-M cells, the luciferase levels in PC3-M cells treated with GW9662 (Student's t-test, $p \leq 0.001$), untreated PC3-M3 cells (Student's t-test, $p \leq 0.001$) and PC3-M-3 cells treated with GW9662 (Student's t-test, $p \leq 0.0004$) were significantly lower; whereas these levels were not significantly different when compared to each other (Student's t-test, $p \geq 0.25$).

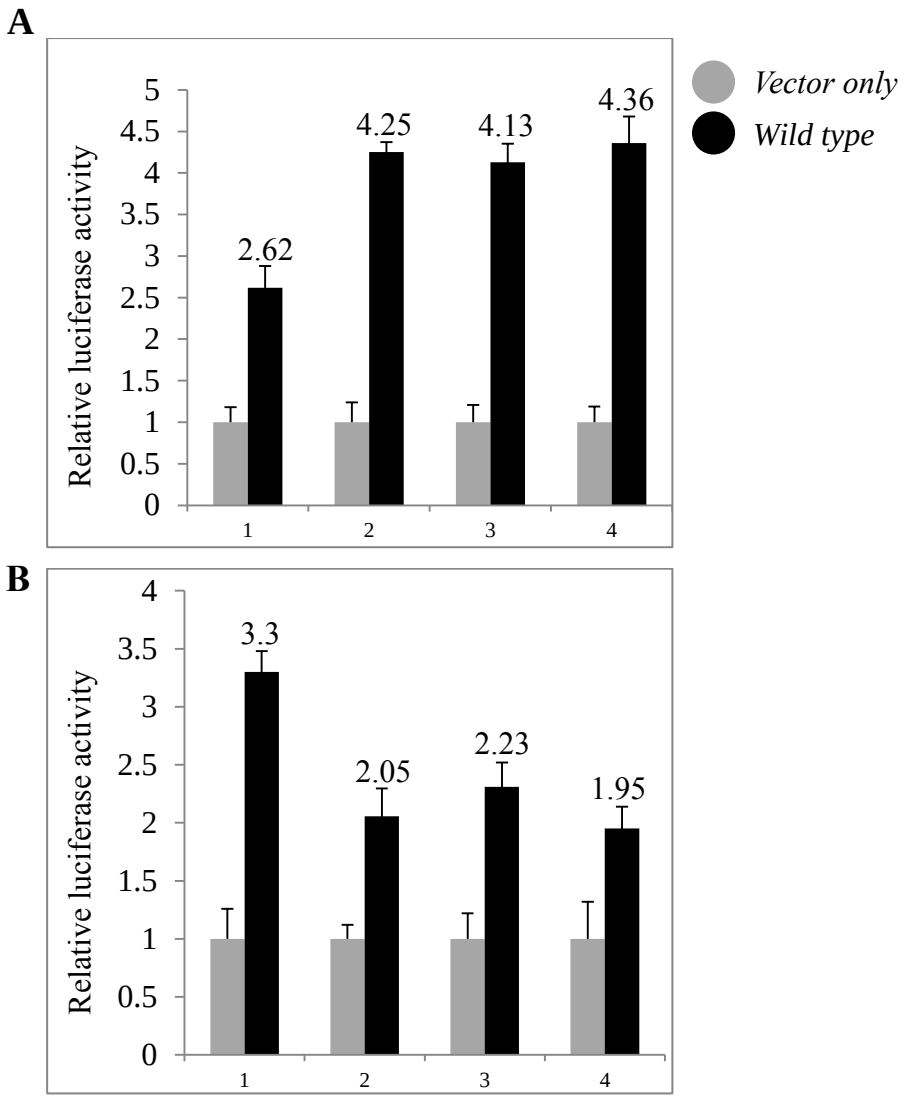

Figure 3.30: Combined effects of C-FABP and *PPARγ* on *VEGF*-promoter activity in prostate cancer cells. VEGF-promoter luciferase and *Renilla* luciferase plasmids were co-transfected into 22RV1, PC3-M and PC3-M-3 cells. Luciferase activity level of transfected cells with control plasmid (pGL3-promoter) was set as 1. Levels in other cells were calculated by relating to control. Results were obtained from three different measurements (mean ± SE). A: Luciferase activity in 22RV1 transfectant cells (transfected with Wild type or Control) before and after treating with Rosiglitazone (0.5μM) and C-FABP recombinant protein (2μM) either individually or combined; (1) 22RV1 transfectants, (2) 22RV1 transfectants + Rosiglitazone, (3) 22RV1 transfectants + C-FABP recombinant protein, (4) 22RV1 transfectants + Rosiglitazone & C-FABP recombinant protein; B: Luciferase activity in PC3-M and PC3-M-3 transfectant cells before and after GW9662 (20μM) treatment; (1) PC3-M transfectants, (2) PC3M transfectants + GW9662, (3) PC3-M-3 transfectants, (4) PC3-M-3 transfectants + GW9662.

3.12.5 Effects of Sp1 (Androgen binding site) on *VEGF*-promoter activity

Different levels of luciferase activity were measured in co-transfected prostate cancer cell lines before and after subjecting them to different treatments.

When the level of luciferase activity in androgen-dependent 22RV1 cells transfected with control plasmid was set as 1, levels in those transfected with Wild type, Mutant1 and Mutant2 plasmids were 2.62 ± 0.26, 2.41 ± 0.25 and 1.29 ± 0.17, respectively. After treating with Mithramycin A (Sp1 inhibitor) (0.1μM) luciferase activity in the same set of transfectants was reduced to 1.73 ± 0.11, 1.19 ± 0.24 and 0.97 ± 0.31, respectively (**Fig. 3.31, A**). Comparing with the untreated control, after treating with Mithramycin A the luciferase level in cells transfected with Wild type (Student's t-test, $p \leq 0.007$) and Mutant1 (Student's t-test $p \leq 0.001$) were significantly lower; whereas the difference between the level in cells transfected with Mutant2 (Student's t-test, $p \geq 0.101$) and that in control cells was not statistically significant.

When the level of luciferase activity in androgen-independent PC3-M cells transfected with control plasmid was set as 1, levels in those transfected with Wild type, Mutant1 and Mutant2 plasmids were 3.3 ± 0.12, 2 ± 0.14 and 1 ± 0.21, respectively. After treating with Mithramycin A level of luciferase activity in the same transfectants were 3.2 ± 0.23, 1.7 ± 0.11, 0.95 ± 0.25, respectively (**Fig. 3.31, B**). After treating with Mithramycin A the difference between the luciferase levels in PC3-M cells transfected with Wild type (Student's t-test, $p \geq 0.27$), Mutant1 (Student's t-test, $p \geq 0.06$) or Mutant2 (Student's t-test $p \geq 0.40$) and that of control was not statistically significant.

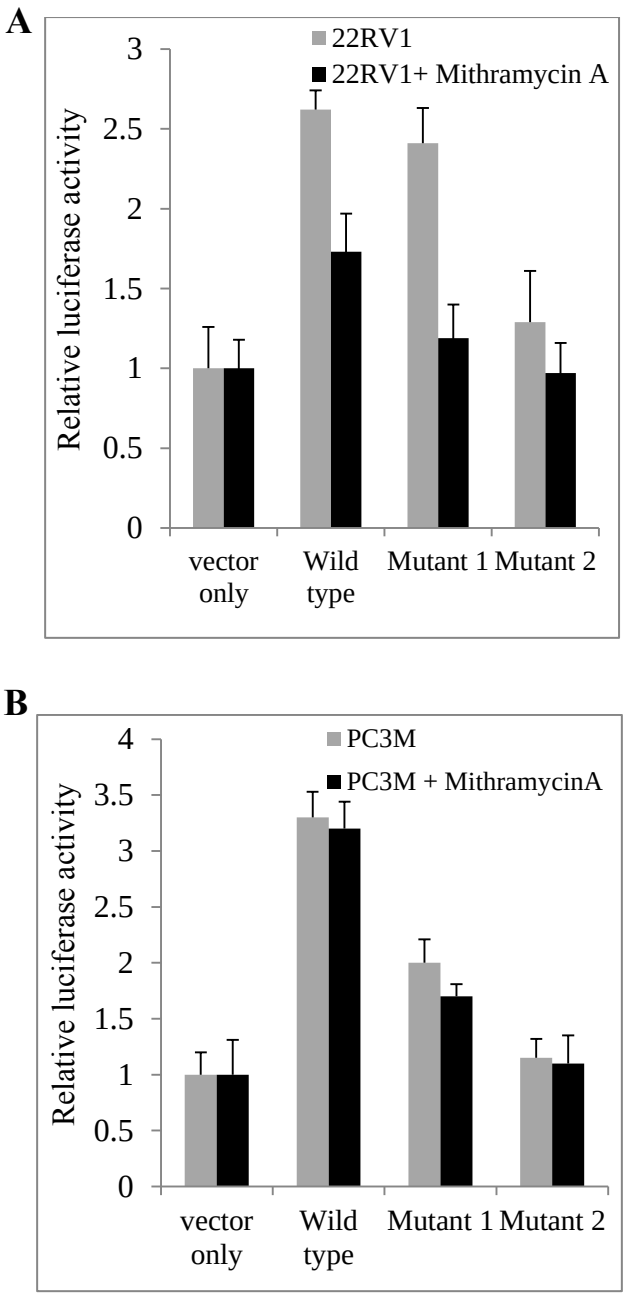

Figure 3.31: Effects of Sp1 binding site on *VEGF*-promoter activity in prostate cancer cells. VEGF-promoter luciferase and *Renilla* luciferase plasmids were co-transfected into 22RV1 and PC3-M cells. Luciferase activity level of transfected cells with control plasmid (pGL3-promoter) was set as 1. Levels in other cells were calculated by relating to the control. Results were obtained from three different measurements (mean ± SE). A: Luciferase activity in 22RV1 transfectants before and after Mithramycin A (Sp1 inhibitor) (0.1µM) treatment; B: Luciferase activity in PC3-M transfectants before and after Mithramycin A treatment.

3.12.5.1 Combined effects of Sp1 and *PPARγ* on *VEGF*-promoter activity

Different levels of luciferase activity were measured in co-transfected prostate cancer cells before and after subjecting them to different treatments.

When the level of luciferase activity in 22RV1 cells transfected with control plasmid (pGL3-promoter) was set as 1, levels in those transfected with Wild type plasmid and treated with Mithramycin A (Sp1 inhibitor) (0.1μM), GW9662 (PPARγ antagonist) (20μM) and combination of Mithramycin A with GW9662 were 1.73 ± 0.11, 2.09 ± 0.12 and 1.68 ± 0.35, respectively. The level in untreated 22RV1 cells was 2.62 ± 0.26 (**Fig. 3.32**). Comparing with the untreated control, the luciferase level in cells transfected with Wild type and treated with Mithramycin A (Student's t-test, $p \leq 0.007$), GW9662 (Student's t-test, $p \leq 0.026$) and combination of Mithramycin A with GW9662 (Student's t-test, $p \leq 0.011$) was significantly lower; whereas the difference between the level in the cells treated with combination of Mithramycin A with GW9662 to the level of those treated with Mithramycin A (Student's t-test, $p \geq 0.416$) or GW9662 (Student's t-test, $p \geq 0.085$) was not statistically significant.

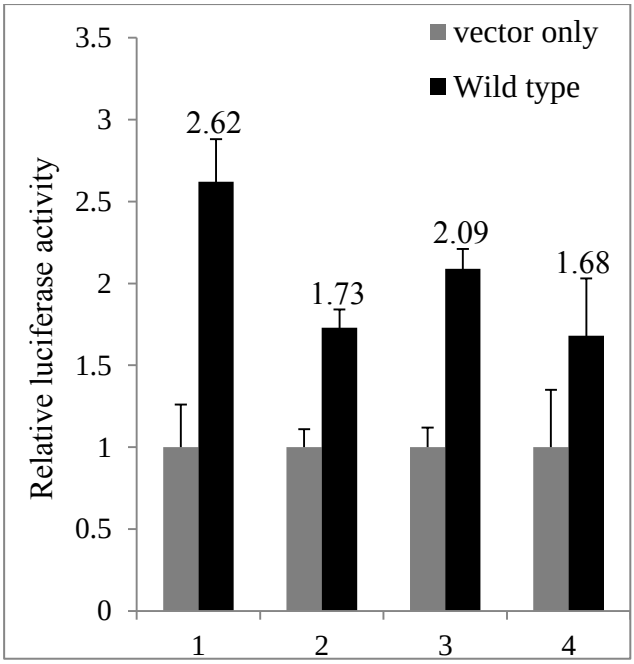

Figure 3.32: Combined effects of Sp1 binding site and *PPARγ* on *VEGF*-promoter activity in prostate cancer cells. VEGF-promoter luciferase and *Renilla* luciferase plasmids were co-transfected into 22RV1 cells. Luciferase activity of transfected cells with control plasmid (pGL3-promoter) was set as 1. Levels in other cells were calculated by relating to the control. Results were obtained from three different measurements (mean ± SE). Luciferase activity in transfected 22RV1 cells before and after treating with Mithramycin A (0.1µM) and GW9662 (20µM), either individually or combined; (1) 22RV1 transfectants, (2) 22RV1 transfectants + Mithramycin A, (3) 22RV1 transfectants + GW9662, (4) 22RV1 transfectants + Mithramycin A & GW9662.

CHAPTER FOUR:

DISCUSSION

4 Discussion

C-FABP is a 15 kDa cytosolic protein that belongs to the fatty acid binding protein family [281] and binds to long chain fatty acids with high affinity. In addition to skin, C-FABP is detected in endothelial cells of placenta, heart, skeletal muscle, small intestine, renal medulla and in Clara and goblet cells of lung [282]. Apart from prostate cancer [188], C-FABP has been implicated in malignancies of bladder and pancreas [283-285] and its expression is associated with poor survival in breast cancer [286] and glioblastoma [287]. Recently, the molecular mechanisms involved in cancer-promoting activity of C-FABP in prostate cancer were investigated. Based on the currently available evidences, it was hypothesized that there may be a fatty acid-initiated signalling pathway that leads to the malignant progression of prostate cancer cells. This pathway may work through following route: Increased level of C-FABP transports a large amount of intracellular fatty acids into the cancer cells and the excessive amount of fatty acids may generate enhanced signals through their nuclear PPAR receptors to trigger a chain of molecular events that ultimately leads to the increased activities of down-stream cancer-promoting genes which facilitate angiogenesis and inhibit apoptosis and thereby enhance the malignant progression [288, 289]. Although this hypothesis was partly justified by the results of some recent studies [167], more evidence is needed to fully demonstrate the existence of the hypothesized signalling pathway in prostate cancer cells. This current work investigated the detailed molecular mechanisms involved in each step of connections of the hypothesized pathway and discovered a C-FABP (fatty acids)-PPARγ-VEGF axis that promotes the malignant progression of the cancer cells. Thus the results in this study provided more evidence to justify the original hypothesis.

4.1 C-FABP and PPARγ were overexpressed in prostate cancer cells and tissues

There are three nuclear PPARs (PPARα, PPARβ/δ and PPARγ) that could act as fatty acid receptors [290]. Previous studies were shown weak expression of PPARα in prostate cell lines and tissues. Moreover no significant difference has been detected in expression levels of PPARα between benign and malignant prostate cell lines or tissues [200, 291]. Thus, PPARα is unlikely to be involved in activities exerted by C-FABP in prostate cancer.

Although results from this study revealed that PPARβ/δ is expressed in cultured prostate cells, its level was not demonstrably different between benign and malignant cell lines (**Fig. 3.1**, **A**). However, expression of PPARβ/δ in tissue samples appeared to be different from that in the cell lines. While staining for PPARβ/δ was detected in BPH and carcinoma cases, levels detected in malignant tissues were significantly higher than those in BPH (**Table 3.1-1**). These results suggested that expression of PPARβ/δ in cultured cell lines measured by Western blot may not reflect the levels in human tissues measured by immunohistochemical staining. However, increased nuclear staining for PPARβ/δ was not significantly correlated with increased cytoplasmic staining for C-FABP, indicating that elevated PPARβ/δ may not be directly related to C-FABP and hence to fatty acid stimulation in prostate cancer cells.

In contrast to the other PPARs, patterns of expression level for PPARγ in cell lines measured by Western blot and in tissues measured by immunohistochemistry were very similar to those of C-FABP (**Fig. 3.1**, **B-C**). The levels of C-FABP and PPARγ in malignant cells were significantly higher than those in benign PNT2 cells and elevated levels of PPARγ and C-FABP were associated with increasing malignancy of the prostatic cancer cells (**Fig. 3.1**, **E-F**). Similarly in immunohistochemical analysis, the staining levels for PPARγ and C-FABP were significantly higher in carcinomas than in BPH and the enhanced staining levels in the carcinomas were significantly associated with GS (**Table 3.1-2&3**). Furthermore, increased cytoplasmic staining for C-FABP was significantly correlated with increased nuclear staining

for PPARγ in the carcinomas. These findings are in line with our separate work, in which we found that C-FABP acted with PPARγ in a coordinated manner to promote malignant progression in prostatic cancer cells [292] and hence, PPARγ is more likely to be the receptor for the fatty acids transported by C-FABP than PPARβ/δ.

4.2 Increased expression levels of C-FABP and PPARγ were associated with poor patient survival

In prostate cancer management, a major problem is the lack of reliable biomarkers to predict the aggressiveness or potential therapeutic response of an individual prostate cancer. Results in this work suggested that AR (**Fig. 3.6**, **B**) and PSA (**Fig. 3.6**, **C**) are not significant prognostic markers in this tested patient group although the number of patients is relatively small. It is also suggested that PSA, the most commonly employed biomarker cannot be used to predict patient outcomes, as previously suggested to be unreliable [293]. Current results showed that increased levels of nuclear PPARγ and cytoplasmic C-FABP (**Table 3.1-2&3**) were significantly correlated with GS and significantly associated with reduced survival time (**Fig. 3.4**, **D**) (**Fig. 3.5, A**). These findings suggested that increased levels of nuclear PPARγ and cytoplasmic C-FABP may be alternative biomarkers for reduced cellular differentiation (GS), as well as reliable prognostic factors to predict patient survival. Multivariate survival analysis revealed that prognostic value of nuclear PPARγ expression in prostate cancer patients is dependent on prognostic value of cytoplasmic C-FABP (**Table 3.2**). Assessment of the conjoined expression levels of C-FABP and PPARγ showed that in 75% of cases, expression pattern of PPARγ (either in the nucleus or in cytoplasm) was detected the same as cytoplasmic expression of C-FABP (either high or low) (**Fig. 3.7**, **A** & **B**). So conjoined cytoplasmic C-FABP and nuclear PPARγ expression may, together, have better prognostic value than each of the individual parameters. In contrast, no correlation was found between cytoplasmic or nuclear levels of PPARβ/δ and patient survival (**Fig. 3.4**, **A&B**). Increased

levels of PPARβ/δ were not significantly associated with increased Gleason scores. Therefore, PPARβ/δ was not considered to be a suitable biomarker to assess the degree of malignancy in prostate cancer or a marker that would predict patients' outcome.

Results in this work also showed that the level of staining for PPARγ in the cytoplasm was also increased. Although this increase was not correlated with an increased GS, it was significantly associated with a shorter patients' survival time. While the increase of C-FABP in the cytoplasm is significantly associated with GS or patients' survival, the increased nuclear C-FABP is not significantly associated with either factor (**Fig. 3.5, B**). This result suggested that transporting fatty acids to PPARγ through C-FABP may be a short delivery process, after which C-FABP may return to the cytoplasm, rather than staying on the nuclear membrane.

As a steroid hormone receptor, activated PPARγ should be theoretically localized in the nuclear membrane. However, many previous studies revealed that the cellular distribution of PPARγ was predominantly cytoplasmic in a number of cancer types [294-297]. The reason for the cytoplasmic staining for PPARγ is not known and current opinions on this are inconsistent [298, 299]. In line with previous study [300], results in this work showed that the level of PPARγ expressed in the cytoplasm of prostatic carcinoma cells is significantly higher than that in BPH. More study is needed to understand the biological significance of the increase in cytoplasmic PPARγ and its interaction with C-FABP in prostate cancer cells.

4.3 Suppression of *PPARγ* reduced the tumorigenicity of prostate cancer cells

Troglitazone (classic PPARγ agonist) was shown to exhibit some levels of anticancer effect through PPARγ-independent pathways [82, 301]. On the other hand although most TZDs are potent PPARγ agonists, they also have some degrees of affinity to PPARα or PPARβ/δ [302, 303]. Moreover, it was shown that TZDs had inhibitory effects on cholesterol biosynthesis, independently from PPARγ-related pathways [304]. Thus when assessing the possible key role

of PPARγ in the fatty acid-initiated signalling pathway, particularly its function on tumorigenicity, it is more appropriate to use RNAi gene knock down technique than using PPARγ antagonists suppression method due to their possible non-specific effects. Since the discovery of RNAi technique [305] , it has been used to evaluate the biological activity of many genes in plants, fungi and animals [306]. Previous studies revealed that RNAi could successfully silence the expression of genes in cancer cells and reduced subsequent protein expressions [307, 308]. In this work, RNAi was used to suppress the expression of *PPARγ* in highly malignant prostate cancer cells, PC3-M and the stablely *PPARγ*-suppressed PC3-M derived sub-lines were established (**Fig. 3.15**). Effects of *PPARγ*-suppression on proliferation rate, invasiveness and anchorage-independent growth of prostate cancer cells were evaluated by proliferation assay (**Fig. 3.17**) (**Table 3.4**), invasion assay (**Fig. 3.18**) (**Table 3.5**) and soft agar assay (**Fig. 3.19**) (**Table 3.6**), respectively. Nude mice model was used to investigate the effect of *PPARγ*-suppression in tumorigenicity of prostate cancer cells, *in vivo* (**Fig. 3.20-21**) (**Table 3.7-8**). Anchorage-independent growth, invasiveness and growth rate are three important criteria in tumorigenesis and capability of metastasis in cancer cells [309]. Results of this work showed that suppression of *PPARγ* in highly malignant prostate cancer cells produced a significant reduction in growth rate (up to 55%), invasiveness (up to 90%) and anchorage-independent growth (up to 95%). Furthermore, by inoculating the *PPARγ*-suppressed PC3-M cells into nude mice, it was shown that suppression of *PPARγ* in PC3-M cells could significantly reduce the sizes of tumours formed in nude mice by 99% in highly suppressed group and by 92% in moderately suppressed group. Tumour incidence was decrease by 30% in moderately suppressed group and by 90% in highly suppressed group. Latent period of those inoculated with highly suppressed group was significantly longer than in control (3.5-fold). These results suggested that *PPARγ* played a determined role in tumour growth in nude mice. Similarly previous studies showed that suppression of *C-FABP* expression in PC3-M

cells significantly reduced invasiveness *in vitro* [190] and inhibited the tumorigenicity *in vivo* [191]. Combining the results from this study and those of the previous studies suggested that C-FABP and PPARγ may be functioning in a co-ordinated manner to promote the malignant progression of human prostate cancer cells. Thus the results obtained from this study support our original hypothesis [191, 292, 310]. Understanding the detailed molecular mechanisms on how C-FABP and PPARγ co-ordinately functioning in prostate cancer cells may provide a novel opportunity for developing new therapeutic approaches to regulate the malignant phenotype and to switch prostatic cancer cells from an aggressive to indolent behaviour, as previously proposed [311, 312].

4.4 C-FABP promoted biological activity of VEGF through PPARγ in prostate cancer cells

There are some evidences indicated that increased level of PPARγ in several cancers including breast, prostate, pancreas and colon carcinoma could stimulate angiogenesis through up-regulation of VEGF or other pro-angiogenic factors [245, 247, 313, 314]. Moreover it has been shown that overexpression of the *C-FABP* gene in prostate cancer cells induced metastasis through up-regulation of the *VEGF*[189]; while suppression of *C-FABP* inhibited the tumorigenicity by decreasing VEGF expression in prostate cancer tissues[191]. Moderately malignant prostate cancer cells, 22RV1, which expresses low levels of C-FABP and PPARγ (**Fig. 3.22**) was used to study the effect of both C-FABP and PPARγ on the expression level of VEGF. 22RV1 cells were exposed to different treatments and then the expression level of VEGF was evaluated both in cell extracts (**Fig. 3.23**) and in the conditional media (for secreted VEGF) (**Fig. 3.24**). To find out whether the VEGF produced by the cancer cells is biologically active, the angiogenesis activity of secreted VEGF in conditional media was assessed by a HUVEC assay (**Fig. 3.25-26**).

As showed in **Fig. 3.23**, levels of VEGF in cell extracts were increased by 41% and 36% after the cells were treated with PPARγ agonist (Rosiglitazone) and wild type recombinant C-FABP, respectively. After the same treatments, levels of secreted VEGF in conditional media were increased by 7.6-times and 6.3-times, respectively (**Fig. 3.24**). Treatments of prostate cancer cells with Rosiglitazone and C-FABP recombinant protein increased the angiogenesis activity of secreted VEGF in the conditional media by 2-fold and 1.8-fold, respectively (**Fig. 3.25-26**). These increments can be blocked by the anti-VEGF antibody [167], indicating that the increased angiogenesis was the result of the increased VEGF production.

On the other hand, after treating 22RV1 cells with PPARγ antagonist (GW9662) and recombinant double mutant C-FABP which is incapable of binding to fatty acids, levels of VEGF in cell extracts were reduced by 55% and 50%, respectively (**Fig. 3.23**). Similarly, in conditional media, they were reduced by 20% and 40%, respectively (**Fig. 3.24**). The angiogenesis activity of secreted VEGF was reduced by 70% after 22RV1 cells were treated by either GW9662 or double mutant recombinant C-FABP (**Fig. 3.25-26**).

Further analysis showed that there was no significant difference between level of VEFG or angiogenesis index obtained by stimulation with PPARγ agonist and those with recombinant C-FABP. Similarly, differences between reduced level of VEGF obtained by treating the cells with GW9662 and that by double mutant recombinant C-FABP was not statistically significant.

Like other FABPs, the biological function of C-FABP is to bind and to transport intracellular fatty acids into cells. When its fatty acid-binding motif was changed by mutating 2 of the 3 key amino acids (double mutant C-FABP), it lost the ability of binding or transporting fatty acids [167]. The result showed that stimulating 22RV1 cells with the wild type recombinant C-FABP increased VEGF and angiogenesis activity, but when the cells were stimulated with the double mutated recombinant C-FABP which was deprived of fatty acid-binding ability,

reduced the level of VEGF and angiogenesis. These results indicated that the VEGF up-regulation was produced by the increased cellular intake of large amount of fatty acids transported by the wild type recombinant C-FABP. When the ability of binding and transporting fatty acids was deprived, the double mutated recombinant C-FABP did not only incapable of inducing VEGF, it also blocked, at least partially, the biological activity of the wild type C-FABP and prevented its promotion on VEGF expression. Although it is not clear how C-FABP delivers fatty acids to their receptor and thus to activate the receptor, it is likely that the presence of an excessive amount of double mutated C-FABP may competitively inter-react with the fatty acid receptor to suppress the wild type C-FABP to deliver the fatty acids to their nuclear receptors and hence to prevent the down-stream activity. This result suggested that the double mutated recombinant C-FABP can act as an inhibitor to suppress the tumorigenicity-promoting activity of the wild type C-FABP.

The results of this study also showed that like C-FABP, PPARγ agonist can promote the up regulation of VEGF and increase the angiogenesis, whereas the PPARγ antagonist can reduce the VEGF level of the cancer cells and suppress angiogenesis. This result suggested that the suppression of tumorigenicity of prostate cancer cells by knocking down PPARγ gene with RNAi was achieved through, at least partially, inhibiting the biological activity of VEGF. Thus up-regulating VEGF expression must be an immediate consequence of the PPARγ when it is activated by its legends, such as fatty acids which are transported by FABPs, particularly C-FABP in prostate cancer cells. The result also showed that the wild type C-FABP plus PPARγ antagonists could not induce the up-regulation of the VEGF expression, or in another word, the biological activity of C-FABP was blocked by the PPARγ antagonists. This result suggested that C-FABP promoted VEGF expression and angiogenesis by PPARγ (through the stimulation of the fatty acids transported by C-FABP). When PPARγ was blocked with its antagonists, it did not respond to stimulation signal produced by fatty acids, even when high

level of fatty acids was available. These results suggested that there is a C-FABP- PPARγ-VEGF axis in prostate cancer which can facilitate the malignant progression of the cancer cells. Identification of this axis provided a novel target to suppress the malignant progression of prostate cancer cells.

4.5 C-FABP-PPARγ up-regulated *VEGF* expression in prostate cancer cells via acting with the *PPRE*s in the promoter region of *VEGF* gene

The results in this study combined with the results in some of our previous studies suggested that large amount of fatty acids transported by the elevated level of C-FABP may stimulate and activate their nuclear receptor PPARγ which triggers a chain of molecular events that lead to the up-regulation of some down-stream cancer-promoting genes, and a major such gene is *VEGF* [167, 168, 189, 190, 231]. Although it was demonstrated that androgen can mediate the up-regulation of VEGF expression in androgen-dependent cells through the Sp1/Sp3 binding site in *VEGF* core promoter [236], it was not previously known how PPARγ exactly up-regulated VEGF in prostate cancer cells. Some studies showed that regulatory effect of PPARγ ligands on *VEGF* gene expression in human endometrial cells was modulated through *PPRE*s in the promoter region of *VEGF* gene [248]. Could PPARγ up-regulate VEGF expression and promote angiogenesis in prostate cancer cells through acting with the *PPRE*s in the promoter region of *VEGF* gene, as it does in endometrial cells?

To answer this question, a luciferase reporter gene system was employed to test the relationship between the presence or absence of *PPRE* and the level of VEGF expression when prostate cancer cells were treated with PPARγ agonists or antagonists. Although the promoter region of *VEGF* gene is relatively long and contains many sequences of *PPRE*s, the efficiency in promoting the reporter gene expression generated by the full length (2274bp) and the efficiency produced by a truncated (790bp) segment of *VEGF* promoter region were very similar [248]. Thus in this study, a truncated DNA segment containing 2 *PPRE*s, rather

than the full-length of the promoter region, was used to assess whether PPARγ up-regulates *VEGF* gene through *PPREs* in promoter region. The pGL3-promoter-luciferase plasmid was used to make 3 reporter-gene constructs by ligating (to the up-stream of the 5'- end) 3 different DNA fragments from the *VEGF* promoter region: Construct A (Wild type) containing a 805bp segment of VEGF promoter region which includes 2 *PPRE*s; Construct B (Mutant1) containing a 805bp segment of DNA from the same region with both *PPREs* mutated; and construct C (Mutant2) containing a 393bp sequence of DNA from *VEGF* promoter region in which both *PPREs* were deleted. Following cell lines were chosen to perform transient transfection experiments: 22RV1 cells, a moderately malignant cell line which expresses relatively low levels of C-FABP and PPARγ [110]; PC3-M cells, which expresses very high levels of C-FABP and PPARγ [5, 115]; PC3-M-3 cells, a PC3-M-derived cell line established by knocking down *C-FABP* gene [168]; and PC3-M-PPARγ-si-H, a PC3-M- derived cell line established by suppressing *PPARγ* expression (section **3.8.1**).

When Wild type and the control plasmids were co-transfected into the 22RV1 cells, which expressed low levels of PPARγ and C-FABP, and treated with PPARγ agonist (Rosiglitazone), the relative level of luciferase activity was significantly increased from 2.62 to 4.25; whereas in cells transfected with other constructs which did not contain *PPRE*s, the luciferase activity was not remarkably changed (**Fig. 3.28, A**). Similarly, when the co-transfected highly malignant PC3-M cells, which expressed high levels of both PPARγ and C-FABP, were treated with a PPARγ antagonist (GW9662), the luciferase level was remarkably reduced to the level similar to that in Mutant1 transfectants or that in PPARγ-suppressed cells (PC3-M-PPARγ-si-H).These results suggested that increased VEGF expression in prostate cancer cells was due to the interaction between PPARγ with the *PPRE*s in *VEGF* promoter region to activate and up-regulate VEGF expression.

When the co-transfected 22RV1 cells (with control vector and Wild type, Mutant1 and Mutant2 plasmids, respectively) were treated with wild type recombinant C-FABP, the level of luciferase activity of the Wild type transfectants was increased by 62% (**Fig. 3.29, A**). No increment was observed in either Mutant1 or Mutant2 transfectants (**Fig. 3. 29, A**). This result suggested that C-FABP can promote VEGF expression only at the presence of *PPRE*s. When the same transfectants were treated with the mutant C-FABP which is incapable of binding fatty acids, no increment was observed in any of the 3 transfectants. This result indicated that it was the fatty acids transported by C-FABP that activated PPARγ and up-regulated *VEGF* through *PPRE*s. This was further confirmed by the result that when C-FABP was knocking down (PC3-M-3 cells), the luciferase activity was reduced by 35% compared to the co-transfected PC3-M cells, as the suppressed C-FABP expression (**Fig. 3.29, B**).

After treating 22RV1 co-transfectants (transfected with Wild type) with PPARγ agonist (Rosiglitazone) and recombinant C-FABP, levels of luciferase activity of VEGF promoter were increased by 60% and 55%, respectively **(Fig. 3.30, A);** while subjecting them to a combination of both treatments could only raise the level of luciferase activity to 65% (**Fig. 3.30, A**). There was no significant difference between the level of luciferase activity obtained by combined PPARγ agonist and recombinant C-FABP treatment and that obtained by each of individual treatment. This result suggested that in 22RV1 cells expressing low levels of PPARγ and C-FABP, both PPARγ agonist and recombinant C-FABP can effectively increase VEGF expression. Alternatively, levels of luciferase activities in PC3-M co-transfectants (transfected with Wild type) treated with PPARγ antagonist (GW9662), the untreated PC3-M-PPARγ-si-H co-transfectants (transfected with Wild type) and PC3-M-3 co-transfectants (transfected with Wild type) were reduced by 32.5%, 35% and 34%, respectively (**Fig. 3.28, B**) (**Fig. 3.29, B**). This result suggested that in PC3-M transfectant cells, which expressed high levels of both PPARγ and C-FABP, suppressing the biological activity of PPARγ by

either its antagonist or knocking down its mRNA by RNAi (as seen in PC3-M-PPARγ-si-H cells) can reduce the level of *VEGF* expression. Furthermore, suppression of *C-FABP* expression in PC3-M cells can also reduce the level of VEGF (as seen in PC3-M-3). The difference between the level of luciferase activity in the untreated *C-FABP*-knockdown PC3-M-3 cells and that in the cells treated with PPARγ antagonist was not significantly different. This result indicated that when VEGF was already reduced by suppressing C-FABP, little further reduction can be achieved by further treatment with PPARγ antagonist. Combined these results together, it is clear that both C-FABP and PPARγ may be involved in an identical signalling pathway which regulated VEGF promoter activity in prostate cancer cells. Based on these results, the detailed route of the proposed fatty acid-C-FABP-PPARγ-VEGF axis that leading to a facilitated malignant progression of the prostate cancer cells can be shown by following illustration (**Fig. 4.1**):

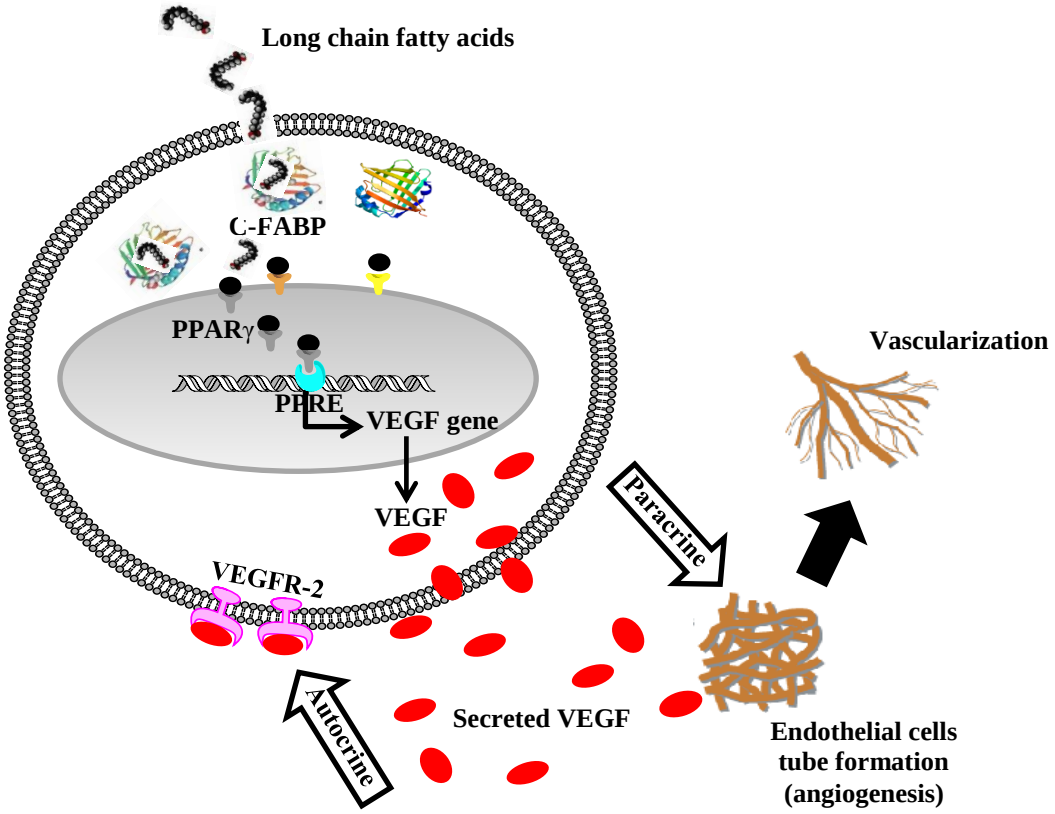

Figure 4.1: Schematic illustration of "C-FABP (fatty acids)-PPARγ-VEGF" axis.
The excessive amount of intracellular fatty acids was transported by over-expressed C-FABP into the cancer cells to activate their nuclear receptors PPARγ which then up-regulated *VEGF* gene through acting with *PPRE*s in the promoter region of *VEGF*. Secreted VEGF promoted angiogenesis by facilitating vasculature network formation (paracrine pathway). It also directly promoted tumorigenicity by stimulating VEGFR-2 (autocrine pathway).

4.6 Androgen regulated *VEGF* activity in androgen-dependant prostate cancer cells through Sp1 (Androgen binding site) in promoter region of VEGF

When 22RV1 cells were co-transfected with different constructs, Wild type, Mutant1 and Mutant2 produced increases in relative luciferase activities (**Fig. 3.27**) by 260%, 240%, and 30%, respectively. The increment produced by Wild type was similar to that by Mutant1. Mutant1 or Mutant2 did not contain *PPRE*s and luciferase activities did not change when the Mutant1 or Mutant2 transfectants were stimulated with PPARγ agonist (Rosiglitazone). Thus these increment caused by Mutant1 was not produced by the *PPREs* in the promoter region. This result suggested that there are some other elements, rather than *PPREs,* in the promoter region of the *VEGF* gene which can up-regulate *VEGF* expression in the 22RV1 prostate cancer cells. When PC3-M cells were transfected with different DNA constructs, both Wild type and Mutant1 produced increase in luciferase activity. While 3.3-fold increment was seen when Wild type was transfected, Mutant1 produced a 2-fold increase when compared with control. Mutant1 also produced some increments in PC3-M-PPARγ-si-H and PC3-M-3 transfectants. This result further confirmed that except *PPRE*s, there are some other elements in the promoter region of *VEGF* gene that can modulate the VEGF expression in the highly malignant PC3-M cells (**Fig. 3.27**).

The occurrence and development of prostate cancer has been related to the level of circulating male hormone. Thus androgen receptor played a key role in the carcinogenesis of prostate cells [315-317]. Prostate cancer cells are generally sensible to the initial androgen blockade treatment, but in the majority of cases, cancer relapses in about 2 years after the initial androgen blockade therapy with a more aggressive form (named castration resistant prostate cancer) (CRPC). The growth and expansion of castration resistant prostate cancer does not completely depend on androgen supply anymore, but in large number of circumstances, continuation of androgen blockade therapy can still suppress the malignant

progression [318, 319]. The molecular pathology involved in how the androgen-dependent cancer cells were transformed to androgen-independent or castration resistant cells is not fully understood. Currently several hypothesized mechanisms were proposed to explain this transition, and the most common theory to explain this transition is the androgen receptor (AR) sensitivity amplification theory [320, 321]. This hypothesis proposed that when the cancer cells is deprived of androgen supply in the initial round of therapy, cells try to maximise their survival ability by increasing the sensitivity of AR to make use the small amount of androgen escaped from the blockage and thus some survived cells with an increased ability of using micro-quantity of androgen become dominant and castration resistant [322, 323]. Some studies also suggested that mutations of AR gene could increase sensitivity to androgen stimulation [324, 325]. Although each current theory can explain certain aspects of this complicated molecular pathology process, no single theory can satisfactorily explain every aspects of the process of transition in the cancer cells from androgen-dependent to androgen-independent form. For example, if AR amplification theory is true, then re-expression of AR in AR-negative cells should increase the malignancy, but several studies on the highly malignant PC3 cells showed that the forced re-expression of AR in PC3 cells actually reduced the malignancy of cells [326-328].

In previous study, an important molecular mechanism involved in VEGF regulation was the androgen-AR initiated Specificity-protein-1 or Specificity-protein-3 (Sp1/Sp3) pathways in androgen-dependent prostate cancer cells. Sp1/Sp3 binding sites are located in the promoter region of *VEGF* and their regulatory effect on VEGF activity was shown in breast cancer [235], retinoblastoma cancer [329], bronchiolo-alveolar cancer [330] and pancreatic cancer [331]. Oestrogen has been reported to up-regulate the expression of VEGF in breast cancer cells via acting with Sp1/Sp3 transcription sites in the core VEGF promoter [235]. Similarly, androgen could

mediate the up-regulation of VEGF expression in androgen-dependent prostate cancer cells through Sp1/Sp3 binding sites in the VEGF core promoter region [236].

To investigate the possible regulatory effect of Sp1 transcription binding site on VEGF activity in androgen-dependent prostate cancer cells in comparison with androgen-independent cells, 22RV1 cells and PC3-M cells were transiently transfected with the three luciferase gene constructs. After treating 22RV1 co-transfectants (transfected with Wild type) with GW9662 and Mithramycin A, levels of luciferase activity were reduced by 21% and 34%, respectively (**Fig. 3.31, A**). Comparing with GW9662, Mithramycin A produced more than 1.6-times reduction in luciferase activity. Subjecting them to a combination of both treatments could reduce the level of luciferase activity to only 36% (**Fig. 3.32**). Thus level of luciferase activity in 22RV1 co-transfectants significantly reduced after treating with Sp1 inhibitor and PPARγ antagonist. These results indicated that in androgen-dependent 22RV1 cells, both the C-FABP-PPARγ and the androgen-Sp1 pathways played important roles in up-regulating the expression level of VEGF and the androgen-Sp1 route appeared to be even more important than the C-FABP-PPARγ route. Alternatively, when PC3-M co-transfectants (transfected with Wild type) was treated with the Sp1 inhibitor (Mithramycin A), the level of luciferase activity was hardly reduced by only 3% (**Fig. 3.31, B**). While level of luciferase activity in 22RV1 co-transfectants (transfected with Mutant1) was decreased by 51% after Mithramycin A treatment (**Fig. 3.31, A**); level in PC3-M co-transfectants (transfected with Mutant1) were only reduced by 15% after the same treatment (**Fig. 3.31, B**). While significant reduction in luciferase activity in PC3-M co-transfectants was achieved by GW9662 treatment (**Fig. 3.28, B**), no significant reduction was detected in the level of luciferase activity in PC3-M co-transfectants after treating with Sp1 inhibitor. These results suggested that in the androgen-independent PC3-M cells, the androgen-Sp1 pathway is not important anymore in up-regulating VEGF expression. The extremely high level of VEGF

expression in these cells was caused mainly through C-FABP-PPARγ route. It seemed that in the early stage of prostate cancer when the cancer cells are still responsive to androgen stimulation, the androgen-Sp1 pathway played a dominant role in promoting VEGF expression. As the cells gradually reduced their dependency on androgen supply and until ultimately loss responsive ability to androgen, the role of androgen-Sp1 pathway is gradually reduced and ultimately disappeared completely in AR-negative, androgen-independent cells (**Fig. 4.2**).

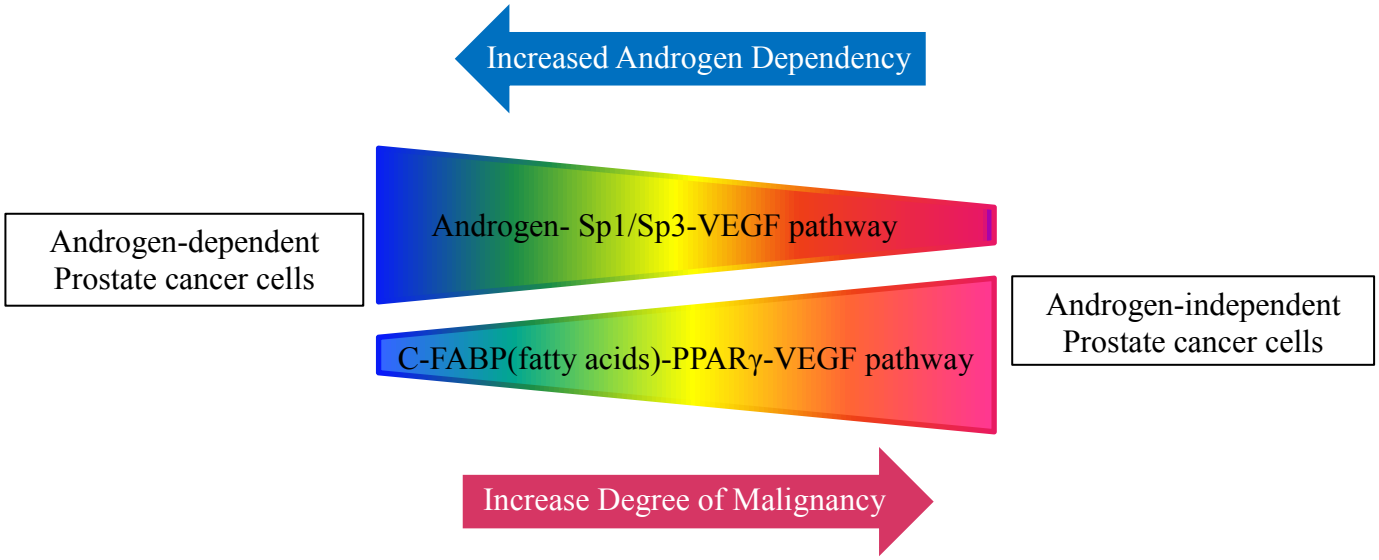

Figure 4.2: Schematic illustration of inter-relationship between androgen-Sp1/Sp3 and C-FABP (fatty acids)-PPARγ signalling route in up-regulating VEGF in androgen-dependant and androgen-independent prostate cancer cells.

VEGF is a potent angiogenic factor which promotes vasculature formation of vessel network that is essential for growing and expansion of the cancer cells. VEGF can also directly promote malignancy of the cancer cells through an autocrine mechanism to simulate the receptor highly expressed on the surface of the prostate cancer cells (VEGFR-2)[332, 333]. Based on the results in this study and relevant results from other studies, I propose the following alternative hypothesis to explain the molecular mechanism involved in the crucial transition of the prostate cancer cells from androgen-dependant to androgen-independent state: When the cancer cells are deprived of androgen supply in the initial round of chemotherapy, the cells are desperate to seek for new sources of energy supply and under the heavy selection pressure, most of the cancer cells died due to starvation. However, some of the cancer cells may have survived under the heavy selection pressure by switching their reliance on androgen to fatty acids (transported by C-FABP) as an alternative energy source. These cells may be the so-called castration resistant cells. Although these cells can still use androgen, and although further androgen blockade will kill some more cells, it can also make some other cells more resistant to androgen deprivation by increasing and eventually, completely relying on fatty acids as their energy source. As the consequence of the increased demand of fatty acids and hence the high level of C-FABP during this process, the C-FABP-PPARγ-VEGF axis gradually increases its functional activity and eventually replace the androgen-Sp1/Sp3 pathway to become the dominant route to promote further malignant progression. Consequentially, cancer cells will ultimately become totally androgen-independent after their androgen supply is repeatedly blocked. This hypothesis is further supported by the fact that a fatty acid synthase (FASN) greatly increased in prostate cancer cells [334-337]. Based on this alternative hypothesis, disrupting the C-FABP-PPARγ-VEGF axis and cutting off the alternative energy supply of the cancer cells, rather than only blocking the last drop of

androgen, should be the correct way to kill the AR-negative androgen-independent cancer cells.

4.7 Conclusion

Based on the data achieved in this study, several important finding have been established:

1- Overexpression of C-FABP and PPARγ in highly malignant prostate cancer cells and poorly differentiated tissues suggest that increased C-FABP may interact with PPARγ in a co-ordinated mechanism to facilitate malignant progression in prostate carcinoma.

2- Association the elevated levels of C-FABP and PPARγ with shorten patient survival and related statistical studies suggest that prognostic value of PPARγ is dependent to C-FABP in prostate carcinomas and they may employ as prognostic biomarkers in prostatic cancer patients.

3- Suppression of *PPARγ* can inhibit the growth rate, invasiveness and anchorage-independent growth in prostate cancer cells, *in vitro.*

4- Suppression of *PPARγ* expression can reduced the incidence, volume and growth rate of prostate carcinoma *in vivo* which suggested that PPARγ can be used as a therapeutic target in prostate cancer.

5- Both C-FABP and PPARγ regulate the VEGF expression and biological activity in prostate cancer in co-ordinated manner; which suggest that may be both C-FABP and PPARγ are involved in the same signalling network which integrated in the regulation of the VEGF activity in prostate cancer cells.

6- *C-FABP-PPARγ* axis affects on *VEGF* promoter activity through *PPRE* elemants in prostate cancer cells. Although regulatury effects of androgen on VEGF activity has been shown to undergo through Sp1/Sp3 on VEGF promoter in androgen-dependent prostate cancer cells, it has been suggested that *C-FABP-PPARγ* axis may compensate this role in androgen-independent prosate carcinoma.

Last but not least, it was suggested that C-FABP, together with fatty acids, PPARγ and VEGF should be considered as key factors in a proposed fatty acid signalling pathway that promotes metastasis of prostatic cancer cells. Therefore, the *C-FABP-PPARγ* axis may be a novel therapeutic target for prostatic cancer.

References

5 References

1. J Maddams DB, [...], and H Møller. Cancer prevalence in the United Kingdom: estimates for 2008. *Br J Cancer* 2009;101(3):541–7.
2. Humphrey PA. Gleason grading and prognostic factors in carcinoma of the prostate. *Mod Pathol* 2004;17(3):292-306.
3. Zheng X, Cui XX, Gao Z, Zhao Y, Lin Y, Shih WJ, et al. Atorvastatin and celecoxib in combination inhibits the progression of androgen-dependent LNCaP xenograft prostate tumors to androgen independence. *Cancer Prev Res (Phila)* 2010;3(1):114-24.
4. Cussenot O, Berthon P, Berger R, Mowszowicz I, Faille A, Hojman F, et al. Immortalization of human adult normal prostatic epithelial cells by liposomes containing large T-SV40 gene. *J Urol* 1991;146(3):881-6.
5. Sobel RE, Sadar MD. Cell lines used in prostate cancer research: a compendium of old and new lines--part 1. *J Urol* 2005;173(2):342-59.
6. http://www.cancerresearchuk.org/cancer-info/cancerstats/incidence/uk-cancer-incidence-statistics.
7. All Cancers (C00-C97 Excl. C44) Average Number of New Cases per Year and Age-Specific Incidence Rates, UK, 2009-2011,http://www.cancerresearchuk.org/cancer-info/cancerstats/incidence/age/.
8. All Cancers Excluding Non-Melanoma Skin Cancer (C00-C97 Excl. C44), European Age-Standardised Incidence Rates, Great Britain, 1975-2011,http://www.cancerresearchuk.org/cancer-info/cancerstats/incidence/all-cancers-combined/.
9. Jemal A, Bray F, Center MM, Ferlay J, Ward E, Forman D. Global Cancer Statistics. *Ca-a Cancer Journal for Clinicians* 2011;61(2):69-90.
10. Ferlay J, Parkin DM, Steliarova-Foucher E. Estimates of cancer incidence and mortality in Europe in 2008. *Eur J Cancer* 2010;46(4):765-81.
11. Jemal A, Bray F, Center MM, Ferlay J, Ward E, Forman D. Global cancer statistics. *CA Cancer J Clin* 2011;61(2):69-90.
12. Data were provided by the Office for National Statistics on request, July 2013. Similar data can be found here: http://www.ons.gov.uk/ons/rel/vsob1/cancer-statistics-registrations--england--series-mb1-/index.html.
13. Data were provided by ISD Scotland on request, May 2013. Similar data can be found here: http://www.isdscotland.org/Health-Topics/Cancer/Publications/index.asp.
14. Data were provided by the Welsh Cancer Intelligence and Surveillance Unit on request, June 2013. Similar data can be found here: http://www.wales.nhs.uk/sites3/page.cfm?orgid=242&pid=59080.
15. Data were provided by the Northern Ireland Cancer Registry on request, June 2013. Similar data can be found here: http://www.qub.ac.uk/research-centres/nicr/CancerData/OnlineStatistics/.
16. Hsing AW, Tsao L, Devesa SS. International trends and patterns of prostate cancer incidence and mortality. *Int J Cancer* 2000;85(1):60-7.
17. Bray F, Lortet-Tieulent J, Ferlay J, Forman D, Auvinen A. Prostate cancer incidence and mortality trends in 37 European countries: an overview. *Eur J Cancer* 2010;46(17):3040-52.
18. Quinn M, Babb P. Patterns and trends in prostate cancer incidence, survival, prevalence and mortality. Part I: international comparisons. *BJU Int* 2002;90(2):162-73.
19. Brewster DH, Fraser LA, Harris V, Black RJ. Rising incidence of prostate cancer in Scotland: increased risk or increased detection? *BJU Int* 2000;85(4):463-72; discussion 72-3.
20. Pashayan N, Powles J, Brown C, Duffy SW. Incidence trends of prostate cancer in East Anglia, before and during the era of PSA diagnostic testing. *Br J Cancer* 2006;95(3):398-400.

21. UK National Screening Committee. Screening for Prostate Cancer. Review against programme appraisal criteria for the UK National Screening Committee (UK NSC). London: UKNSC; 2010.
22. Melia J, Moss S. Survey of the rate of PSA testing in general practice. *Br J Cancer* 2001;85(5):656-7.
23. Melia J CP, Johns L,et al. Report to the Department of Health. Study to assess the rate of PSA testing in men with no previous diagnosis of prostate cancer (Mapping of PSA testing: Part II). 2003.
24. Potosky AL, Miller BA, Albertsen PC, Kramer BS. The role of increasing detection in the rising incidence of prostate cancer. *JAMA* 1995;273(7):548-52.
25. Smith DP, Supramaniam R, Marshall VR, Armstrong BK. Prostate cancer and prostate-specific antigen testing in New South Wales. *Med J Aust* 2008;189(6):315-8.
26. Carsin AE, Drummond FJ, Black A, van Leeuwen PJ, Sharp L, Murray LJ, et al. Impact of PSA testing and prostatic biopsy on cancer incidence and mortality: comparative study between the Republic of Ireland and Northern Ireland. *Cancer Causes Control* 2010;21(9):1523-31.
27. Lifetime risk was calculated by the Statistical Information Team at Cancer Research UK, 2012.
28. Ferlay J SH, Bray F, et al. GLOBOCAN 2008 v1.2, Cancer incidence and mortality worldwide: IARC CancerBase No. 10 [Internet]. Lyon, France: International Agency for Research on Cancer; 2010. Available from http://globocan.iarc.fr. Accessed. May 2011.
29. U.S. Cancer Statistics Working Group. United States Cancer Statistics: 1999– 2007 Incidence and Mortality Web-based Report. Atlanta: U.S. Department of Health and Human Services, Centers for Disease Control and Prevention and National Cancer Institute; 2010. Available at: www.cdc.gov/uscs.
30. Metcalfe C, Patel B, Evans S, Ibrahim F, Anson K, Chinegwundoh F, et al. The risk of prostate cancer amongst South Asian men in southern England: the PROCESS cohort study. *BJU Int* 2008;102(10):1407-12.
31. NCIN. Cancer Incidence by Deprivation, England, 1995-2004. London: NCIN; 2008.
32. Williams N, Hughes LJ, Turner EL, Donovan JL, Hamdy FC, Neal DE, et al. Prostate-specific antigen testing rates remain low in UK general practice: a cross-sectional study in six English cities. *BJU Int* 2011;108(9):1402-8.
33. Jemal A, Center MM, DeSantis C, Ward EM. Global patterns of cancer incidence and mortality rates and trends. *Cancer Epidemiol Biomarkers Prev* 2010;19(8):1893-907.
34. Office for National Statistics Mortality Statistics: Deaths registered in 2010, England and Wales. London: National Statistics; 2011. Mortality Statistics: Deaths registered in 2010, England and Wales.
35. General Register Office for Scotland. 2010 Deaths Time Series Data: Deaths in Scotland in 2010. Deaths Time Series Data, Deaths in Scotland in 2010.
36. Northern Ireland Statistics and Research Agency Registrar General Annual Report 2010.
37. World Health Organisation.Global Health Observatory Data Repository.
38. Ferlay J SH, Bray F, Forman D, Mathers C, Parkin DM. GLOBOCAN 2008 v1.2, Cancer Incidence and Mortality Worldwide: IARC CancerBase No. 10 [Internet]. Lyon, France: .
39. http://www.cancerresearchuk.org/cancer-info/cancerstats/types/prostate/mortality/uk-prostate-cancer-mortality-statistics.
40. For data for 2005-2009: Office for National Statistics (ONS). Cancer survival in England: Patients diagnosed 2005-2009 and followed up to 2010. London: ONS; 2011.
41. Kricka LJ, Stanley PE. Bioluminescence and chemiluminescence literature. The 1990 literature: Part I. *J Biolumin Chemilumin* 1991;6(3):203-20.
42. Welsh Cancer Intelligence and Surveillance Unit (WCISU). Cancer Survival Trends in Wales 1985-2004. Cardiff: WCISU; 2010.

43. For data for 1996-2003: Rachet B, Maringe C, Nur U, et al. Population-based cancer survival trends in England and Wales up to 2007. Lancet Oncol 2009;10:351-369. Age-standardised figures were provided by the author on request.
44. For data for 1971-1990: Coleman MP, Babb P, Damiecki P, et al. Cancer Survival Trends in England and Wales, 1971-1995: Deprivation and NHS Region. Series SMPS No 61. London: ONS; 1999.
45. For data for 1991-1995: Office for National Statistics (ONS). Cancer Survival: England and Wales, 1991-2001, twenty major cancers by age group. London: ONS; 2005.
46. South West Public Health Observatory (SWPHO). SWPHO Briefing 4: Prostate cancer survival by stage. Bristol: SWPHO; 2008.
47. For data for 2007: Coleman MP, et al. Research commissioned by Cancer Research UK, London School of Hygiene and Tropical Medicine. 2010.
48. http://www.cancerresearchuk.org/cancer-info/cancerstats/types/prostate/survival/prostate-cancer-survival-statistics.
49. Bruner DW, Moore D, Parlanti A, Dorgan J, Engstrom P. Relative risk of prostate cancer for men with affected relatives: systematic review and meta-analysis. *Int J Cancer* 2003;107(5):797-803.
50. Johns LE, Houlston RS. A systematic review and meta-analysis of familial prostate cancer risk. *BJU Int* 2003;91(9):789-94.
51. Kicinski M, Vangronsveld J, Nawrot TS. An epidemiological reappraisal of the familial aggregation of prostate cancer: a meta-analysis. *PLoS One* 2011;6(10):e27130.
52. Hemminki K, Chen B. Familial association of prostate cancer with other cancers in the Swedish Family-Cancer Database. *Prostate* 2005;65(2):188-94.
53. Chen YC, Page JH, Chen R, Giovannucci E. Family history of prostate and breast cancer and the risk of prostate cancer in the PSA era. *Prostate* 2008;68(14):1582-91.
54. lifetechnology Ib. First-Strand cDNA synthesis using SuperScriptII RT, User's Instruction. 2010.
55. Hemminki K, Czene K. Age specific and attributable risks of familial prostate carcinoma from the family-cancer database. *Cancer* 2002;95(6):1346-53.
56. National Cancer Intelligence Network and Cancer Research UK. Cancer Incidence and Survival by Major Ethnic Group E-hwnouvar. 2009.
57. Karami S, Young HA, Henson DE. Earlier age at diagnosis: another dimension in cancer disparity? *Cancer Detect Prev* 2007;31(1):29-34.
58. Metcalfe C, Evans S, Ibrahim F, Patel B, Anson K, Chinegwundoh F, et al. Pathways to diagnosis for Black men and White men found to have prostate cancer: the PROCESS cohort study. *Br J Cancer* 2008;99(7):1040-5.
59. Liu H, Hemminki K, Sundquist J. Renal cell carcinoma as first and second primary cancer: etiological clues from the Swedish Family-Cancer Database. *J Urol* 2011;185(6):2045-9.
60. Neuzillet Y, Lechevallier E, Coulange C. [Renal cancer and second cancer: critical review of the literature]. *Prog Urol* 2007;17(1):35-40.
61. Zhang H, Bermejo JL, Sundquist J, Hemminki K. Prostate cancer as a first and second cancer: effect of family history. *Br J Cancer* 2009;101(6):935-9.
62. Lehnert M, Kraywinkel K, Pesch B, Holleczek B, Bruning T. New malignancies following cancer of the urinary bladder: analysis of German cancer registry data. *Eur J Cancer Care (Engl)* 2012;21(3):398-402.
63. Kellen E, Zeegers MP, Dirx M, Houterman S, Droste J, Lawrence G, et al. Occurrence of both bladder and prostate cancer in five cancer registries in Belgium, The Netherlands and the United Kingdom. *Eur J Cancer* 2007;43(11):1694-700.
64. Hayat MJ, Howlader N, Reichman ME, Edwards BK. Cancer statistics, trends, and multiple primary cancer analyses from the Surveillance, Epidemiology, and End Results (SEER) Program. *Oncologist* 2007;12(1):20-37.

65. Bradford PT, Freedman DM, Goldstein AM, Tucker MA. Increased risk of second primary cancers after a diagnosis of melanoma. *Arch Dermatol* 2010;146(3):265-72.
66. Subramanian S, Goldstein DP, Parlea L, Thabane L, Ezzat S, Ibrahim-Zada I, et al. Second primary malignancy risk in thyroid cancer survivors: a systematic review and meta-analysis. *Thyroid* 2007;17(12):1277-88.
67. Cogliano VJ, Baan R, Straif K, Grosse Y, Lauby-Secretan B, El Ghissassi F, et al. Preventable exposures associated with human cancers. *J Natl Cancer Inst* 2011;103(24):1827-39.
68. Renehan AG, Zwahlen M, Minder C, O'Dwyer ST, Shalet SM, Egger M. Insulin-like growth factor (IGF)-I, IGF binding protein-3, and cancer risk: systematic review and meta-regression analysis. *Lancet* 2004;363(9418):1346-53.
69. Roddam AW, Allen NE, Appleby P, Key TJ, Ferrucci L, Carter HB, et al. Insulin-like growth factors, their binding proteins, and prostate cancer risk: analysis of individual patient data from 12 prospective studies. *Ann Intern Med* 2008;149(7):461-71, W83-8.
70. Rowlands MA, Gunnell D, Harris R, Vatten LJ, Holly JM, Martin RM. Circulating insulin-like growth factor peptides and prostate cancer risk: a systematic review and meta-analysis. *Int J Cancer* 2009;124(10):2416-29.
71. World Cancer Research Fund / American Institute for Cancer Research (WCRF/AICR). Food N, Physical Activity, and the Prevention of Cancer: a Global Perspective. Washington DC: AICR; 2007. http://www.wcrf.org/cancer_research/cup/second_expert_report.php.
72. Hurst R, Hooper L, Norat T, Lau R, Aune D, Greenwood DC, et al. Selenium and prostate cancer: systematic review and meta-analysis. *Am J Clin Nutr* 2012;96(1):111-22.
73. Dennert G, Zwahlen M, Brinkman M, Vinceti M, Zeegers MP, Horneber M. Selenium for preventing cancer. *Cochrane Database Syst Rev* 2011(5):CD005195.
74. Key TJ, Appleby PN, Allen NE, Travis RC, Roddam AW, Jenab M, et al. Plasma carotenoids, retinol, and tocopherols and the risk of prostate cancer in the European Prospective Investigation into Cancer and Nutrition study. *Am J Clin Nutr* 2007;86(3):672-81.
75. Etminan M, Takkouche B, Caamano-Isorna F. The role of tomato products and lycopene in the prevention of prostate cancer: a meta-analysis of observational studies. *Cancer Epidemiol Biomarkers Prev* 2004;13(3):340-5.
76. Yan L, Spitznagel EL. Soy consumption and prostate cancer risk in men: a revisit of a meta-analysis. *Am J Clin Nutr* 2009;89(4):1155-63.
77. Hwang YW, Kim SY, Jee SH, Kim YN, Nam CM. Soy food consumption and risk of prostate cancer: a meta-analysis of observational studies. *Nutr Cancer* 2009;61(5):598-606.
78. Pottegard A, Friis S, Hallas J. Cancer risk in long-term users of vitamin K antagonists: a population-based case-control study. *Int J Cancer* 2013;132(11):2606-12.
79. Pengo V, Noventa F, Denas G, Pengo MF, Gallo U, Grion AM, et al. Long-term use of vitamin K antagonists and incidence of cancer: a population-based study. *Blood* 2011;117(5):1707-9.
80. Tagalakis V, Tamim H, Blostein M, Collet JP, Hanley JA, Kahn SR. Use of warfarin and risk of urogenital cancer: a population-based, nested case-control study. *Lancet Oncol* 2007;8(5):395-402.
81. Zhang F, Yang Y, Skrip L, Hu D, Wang Y, Wong C, et al. Diabetes mellitus and risk of prostate cancer: an updated meta-analysis based on 12 case-control and 25 cohort studies. *Acta Diabetol* 2012;49 Suppl 1:S235-46.
82. Weng JR, Chen CY, Pinzone JJ, Ringel MD, Chen CS. Beyond peroxisome proliferator-activated receptor gamma signaling: the multi-facets of the antitumor effect of thiazolidinediones. *Endocr Relat Cancer* 2006;13(2):401-13.
83. McNeal JE. Origin and development of carcinoma in the prostate. *Cancer* 1969;23(1):24-34.
84. Cohen RJ, Shannon BA, Phillips M, Moorin RE, Wheeler TM, Garrett KL. Central zone carcinoma of the prostate gland: a distinct tumor type with poor prognostic features. *J Urol* 2008;179(5):1762-7; discussion 7.
85. Canadian Cancer Society website hwccec-ic-tpa-a-pro.

86. Foster CS, Bostwick DG, Bonkhoff H, Damber JE, van der Kwast T, Montironi R, et al. Cellular and molecular pathology of prostate cancer precursors. *Scand J Urol Nephrol Suppl* 2000(205):19-43.
87. Denmeade SR, Lin XS, Isaacs JT. Role of programmed (apoptotic) cell death during the progression and therapy for prostate cancer. *Prostate* 1996;28(4):251-65.
88. Okada H, Tsubura A, Okamura A, Senzaki H, Naka Y, Komatz Y, et al. Keratin profiles in normal/hyperplastic prostates and prostate carcinoma. *Virchows Arch A Pathol Anat Histopathol* 1992;421(2):157-61.
89. Bonkhoff H, Remberger K. Widespread distribution of nuclear androgen receptors in the basal cell layer of the normal and hyperplastic human prostate. *Virchows Arch A Pathol Anat Histopathol* 1993;422(1):35-8.
90. Harper ME, Glynne-Jones E, Goddard L, Mathews P, Nicholson RI. Expression of androgen receptor and growth factors in premalignant lesions of the prostate. *J Pathol* 1998;186(2):169-77.
91. Abate-Shen C, Shen MM. Molecular genetics of prostate cancer. *Genes Dev* 2000;14(19):2410-34.
92. Bui M, Reiter RE. Stem cell genes in androgen-independent prostate cancer. *Cancer Metastasis Rev* 1998;17(4):391-9.
93. Ruscica M, Dozio E, Motta M, Magni P. Role of neuropeptide Y and its receptors in the progression of endocrine-related cancer. *Peptides* 2007;28(2):426-34.
94. Ather MH, Abbas F. Prognostic significance of neuroendocrine differentiation in prostate cancer. *Eur Urol* 2000;38(5):535-42.
95. Abrahamsson PA. Neuroendocrine differentiation in prostatic carcinoma. *Prostate* 1999;39(2):135-48.
96. Lang SH, Frame FM, Collins AT. Prostate cancer stem cells. *J Pathol* 2009;217(2):299-306.
97. Richardson GD, Robson CN, Lang SH, Neal DE, Maitland NJ, Collins AT. CD133, a novel marker for human prostatic epithelial stem cells. *J Cell Sci* 2004;117(Pt 16):3539-45.
98. Collins AT, Habib FK, Maitland NJ, Neal DE. Identification and isolation of human prostate epithelial stem cells based on alpha(2)beta(1)-integrin expression. *J Cell Sci* 2001;114(Pt 21):3865-72.
99. Bok RA, Small EJ. Bloodborne biomolecular markers in prostate cancer development and progression. *Nat Rev Cancer* 2002;2(12):918-26.
100. Sausville J, Naslund M. Benign prostatic hyperplasia and prostate cancer: an overview for primary care physicians. *Int J Clin Pract* 2010;64(13):1740-5.
101. Wise GJ, Md EO. Hormonal treatment of patients with benign prostatic hyperplasia: pros and cons. *Curr Urol Rep* 2001;2(4):285-91.
102. Roehrborn CG. Clinical management of lower urinary tract symptoms with combined medical therapy. *BJU Int* 2008;102 Suppl 2:13-7.
103. Bostwick DG. The pathology of early prostate cancer. *CA Cancer J Clin* 1989;39(6):376-93.
104. Foster CS, Ke Y. Stem cells in prostatic epithelia. *Int J Exp Pathol* 1997;78(5):311-29.
105. Berry PA, Maitland NJ, Collins AT. Androgen receptor signalling in prostate: effects of stromal factors on normal and cancer stem cells. *Mol Cell Endocrinol* 2008;288(1-2):30-7.
106. Ayala AG, Ro JY. Prostatic intraepithelial neoplasia: recent advances. *Arch Pathol Lab Med* 2007;131(8):1257-66.
107. Gleason DF, Mellinger GT. Prediction of prognosis for prostatic adenocarcinoma by combined histological grading and clinical staging. *J Urol* 1974;111(1):58-64.
108. Berthon P, Cussenot O, Hopwood L, Leduc A, Maitland N. Functional expression of sv40 in normal human prostatic epithelial and fibroblastic cells - differentiation pattern of nontumorigenic cell-lines. *Int J Oncol* 1995;6(2):333-43.

109. Tuxhorn JA, McAlhany SJ, Dang TD, Ayala GE, Rowley DR. Stromal cells promote angiogenesis and growth of human prostate tumors in a differential reactive stroma (DRS) xenograft model. *Cancer Res* 2002;62(11):3298-307.
110. Sramkoski RM, Pretlow TG, 2nd, Giaconia JM, Pretlow TP, Schwartz S, Sy MS, et al. A new human prostate carcinoma cell line, 22Rv1. *In Vitro Cell Dev Biol Anim* 1999;35(7):403-9.
111. Carpten J, Nupponen N, Isaacs S, Sood R, Robbins C, Xu J, et al. Germline mutations in the ribonuclease L gene in families showing linkage with HPC1. *Nat Genet* 2002;30(2):181-4.
112. Nabha SM, Glaros S, Hong M, Lykkesfeldt AE, Schiff R, Osborne K, et al. Upregulation of PKC-delta contributes to antiestrogen resistance in mammary tumor cells. *Oncogene* 2005;24(19):3166-76.
113. van Bokhoven A, Varella-Garcia M, Korch C, Johannes WU, Smith EE, Miller HL, et al. Molecular characterization of human prostate carcinoma cell lines. *Prostate* 2003;57(3):205-25.
114. Bastide C, Bagnis C, Mannoni P, Hassoun J, Bladou F. A Nod Scid mouse model to study human prostate cancer. *Prostate Cancer Prostatic Dis* 2002;5(4):311-5.
115. Kaighn ME, Narayan KS, Ohnuki Y, Lechner JF, Jones LW. Establishment and characterization of a human prostatic carcinoma cell line (PC-3). *Invest Urol* 1979;17(1):16-23.
116. Shevrin DH, Gorny KI, Kukreja SC. Patterns of metastasis by the human prostate cancer cell line PC-3 in athymic nude mice. *Prostate* 1989;15(2):187-94.
117. Kozlowski JM, Fidler IJ, Campbell D, Xu ZL, Kaighn ME, Hart IR. Metastatic behavior of human tumor cell lines grown in the nude mouse. *Cancer Res* 1984;44(8):3522-9.
118. Whittington K, Connors B, King K, Assinder S, Hogarth K, Nicholson H. The effect of oxytocin on cell proliferation in the human prostate is modulated by gonadal steroids: implications for benign prostatic hyperplasia and carcinoma of the prostate. *Prostate* 2007;67(10):1132-42.
119. Schroder FH, Hugosson J, Roobol MJ, Tammela TL, Ciatto S, Nelen V, et al. Screening and prostate-cancer mortality in a randomized European study. *N Engl J Med* 2009;360(13):1320-8.
120. Moyer VA, Force USPST. Screening for prostate cancer: U.S. Preventive Services Task Force recommendation statement. *Ann Intern Med* 2012;157(2):120-34.
121. Schroder FH. Stratifying risk--the U.S. Preventive Services Task Force and prostate-cancer screening. *N Engl J Med* 2011;365(21):1953-5.
122. Institute NC. NCI Dictionary of Cancer Terms. http://www.cancer.gov/dictionary?cdrid=45618. 2013.
123. Velonas VM, Woo HH, Remedios CG, Assinder SJ. Current status of biomarkers for prostate cancer. *Int J Mol Sci* 2013;14(6):11034-60.
124. Gutman AB, Gutman EB. An " Acid " Phosphatase Occurring in the Serum of Patients with Metastasizing Carcinoma of the Prostate Gland. *J Clin Invest* 1938;17(4):473-8.
125. Hernandez J, Thompson IM. Prostate-specific antigen: a review of the validation of the most commonly used cancer biomarker. *Cancer* 2004;101(5):894-904.
126. Armbruster DA. Prostate-specific antigen: biochemistry, analytical methods, and clinical application. *Clin Chem* 1993;39(2):181-95.
127. Liu Y, Hegde P, Zhang F, Hampton G, Jia S. Prostate cancer - a biomarker perspective. *Front Endocrinol (Lausanne)* 2012;3:72.
128. Bodey B, Bodey B, Jr., Kaiser HE. Immunocytochemical detection of prostate specific antigen expression in human primary and metastatic melanomas. *Anticancer Res* 1997;17(3C):2343-6.
129. Hessels D, Schalken JA. Urinary biomarkers for prostate cancer: a review. *Asian J Androl* 2013;15(3):333-9.
130. Mistry K, Cable G. Meta-analysis of prostate-specific antigen and digital rectal examination as screening tests for prostate carcinoma. *J Am Board Fam Pract* 2003;16(2):95-101.

131. Lin MW, Ho JW, Harrison LC, dos Remedios CG, Adelstein S. An antibody-based leukocyte-capture microarray for the diagnosis of systemic lupus erythematosus. *PLoS One* 2013;8(3):e58199.
132. Schroder FH, van der Cruijsen-Koeter I, de Koning HJ, Vis AN, Hoedemaeker RF, Kranse R. Prostate cancer detection at low prostate specific antigen. *J Urol* 2000;163(3):806-12.
133. Andriole GL, Crawford ED, Grubb RL, 3rd, Buys SS, Chia D, Church TR, et al. Prostate cancer screening in the randomized Prostate, Lung, Colorectal, and Ovarian Cancer Screening Trial: mortality results after 13 years of follow-up. *J Natl Cancer Inst* 2012;104(2):125-32.
134. Roobol MJ, Zhu X, Schroder FH, van Leenders GJ, van Schaik RH, Bangma CH, et al. A Calculator for Prostate Cancer Risk 4 Years After an Initially Negative Screen: Findings from ERSPC Rotterdam. *Eur Urol* 2013;63(4):627-33.
135. Connolly D, Black A, Murray LJ, Napolitano G, Gavin A, Keane PF. Methods of calculating prostate-specific antigen velocity. *Eur Urol* 2007;52(4):1044-50.
136. Capitanio U, Ahyai S, Graefen M, Jeldres C, Shariat SF, Erbersdobler A, et al. Assessment of biochemical recurrence rate in patients with pathologically confirmed insignificant prostate cancer. *Urology* 2008;72(6):1208-11; discussion 12-3.
137. Draisma G, Etzioni R, Tsodikov A, Mariotto A, Wever E, Gulati R, et al. Lead time and overdiagnosis in prostate-specific antigen screening: importance of methods and context. *J Natl Cancer Inst* 2009;101(6):374-83.
138. Wei JT, Dunn RL, Sandler HM, McLaughlin PW, Montie JE, Litwin MS, et al. Comprehensive comparison of health-related quality of life after contemporary therapies for localized prostate cancer. *J Clin Oncol* 2002;20(2):557-66.
139. Klotz L, Zhang L, Lam A, Nam R, Mamedov A, Loblaw A. Clinical results of long-term follow-up of a large, active surveillance cohort with localized prostate cancer. *J Clin Oncol* 2010;28(1):126-31.
140. van den Bergh RC, Roemeling S, Roobol MJ, Aus G, Hugosson J, Rannikko AS, et al. Outcomes of men with screen-detected prostate cancer eligible for active surveillance who were managed expectantly. *Eur Urol* 2009;55(1):1-8.
141. Ruutu M, Rannikko A. Words of wisdom. Re: Active surveillance for the management of prostate cancer in a contemporary cohort. Dall'Era MA, Konety BR, Cowan JE, Shinohara K, Stauf F, Cooperberg MR, Meng MV, Kane CJ, Perez N, Master VA, Carroll PR. Cancer 2008;112:2664-70. *Eur Urol* 2009;55(1):244-5.
142. Kakehi Y, Kamoto T, Shiraishi T, Ogawa O, Suzukamo Y, Fukuhara S, et al. Prospective evaluation of selection criteria for active surveillance in Japanese patients with stage T1cN0M0 prostate cancer. *Jpn J Clin Oncol* 2008;38(2):122-8.
143. Carter HB, Kettermann A, Warlick C, Metter EJ, Landis P, Walsh PC, et al. Expectant management of prostate cancer with curative intent: an update of the Johns Hopkins experience. *J Urol* 2007;178(6):2359-64; discussion 64-5.
144. Soloway MS, Soloway CT, Eldefrawy A, Acosta K, Kava B, Manoharan M. Careful selection and close monitoring of low-risk prostate cancer patients on active surveillance minimizes the need for treatment. *Eur Urol* 2010;58(6):831-5.
145. D'Amico AV, Whittington R, Malkowicz SB, Schultz D, Schnall M, Tomaszewski JE, et al. A multivariate analysis of clinical and pathological factors that predict for prostate specific antigen failure after radical prostatectomy for prostate cancer. *J Urol* 1995;154(1):131-8.
146. Conference NS-o-t-S. Role of Active Surveillance in the Management of Men With Localized Prostate Cancer[http://consensus.nih.gov/2011/prostate.htm]
Page. 2011.
147. Nam RK, Saskin R, Lee Y, Liu Y, Law C, Klotz LH, et al. Increasing hospital admission rates for urological complications after transrectal ultrasound guided prostate biopsy. *J Urol* 2013;189(1 Suppl):S12-7; discussion S7-8.

148. Nam RK, Saskin R, Lee Y, Liu Y, Law C, Klotz LH, et al. Increasing hospital admission rates for urological complications after transrectal ultrasound guided prostate biopsy. *J Urol* 2010;183(3):963-8.
149. Wu CC, Yates JR, 3rd. The application of mass spectrometry to membrane proteomics. *Nat Biotechnol* 2003;21(3):262-7.
150. Huang PY, Best OG, Belov L, Mulligan SP, Christopherson RI. Surface profiles for subclassification of chronic lymphocytic leukemia. *Leuk Lymphoma* 2012;53(6):1046-56.
151. Fleshner NE, Lawrentschuk N. Risk of developing prostate cancer in the future: overview of prognostic biomarkers. *Urology* 2009;73(5 Suppl):S21-7.
152. Edwards SM, Evans DG, Hope Q, Norman AR, Barbachano Y, Bullock S, et al. Prostate cancer in BRCA2 germline mutation carriers is associated with poorer prognosis. *Br J Cancer* 2010;103(6):918-24.
153. Castro E, Goh C, Olmos D, Saunders E, Leongamornlert D, Tymrakiewicz M, et al. Germline BRCA mutations are associated with higher risk of nodal involvement, distant metastasis, and poor survival outcomes in prostate cancer. *J Clin Oncol* 2013;31(14):1748-57.
154. Salagierski M, Schalken JA. Molecular diagnosis of prostate cancer: PCA3 and TMPRSS2:ERG gene fusion. *J Urol* 2012;187(3):795-801.
155. van Gils MP, Hessels D, van Hooij O, Jannink SA, Peelen WP, Hanssen SL, et al. The time-resolved fluorescence-based PCA3 test on urinary sediments after digital rectal examination; a Dutch multicenter validation of the diagnostic performance. *Clin Cancer Res* 2007;13(3):939-43.
156. Hessels D, Smit FP, Verhaegh GW, Witjes JA, Cornel EB, Schalken JA. Detection of TMPRSS2-ERG fusion transcripts and prostate cancer antigen 3 in urinary sediments may improve diagnosis of prostate cancer. *Clin Cancer Res* 2007;13(17):5103-8.
157. Saramaki OR, Harjula AE, Martikainen PM, Vessella RL, Tammela TL, Visakorpi T. TMPRSS2:ERG fusion identifies a subgroup of prostate cancers with a favorable prognosis. *Clin Cancer Res* 2008;14(11):3395-400.
158. Zhao Z, Zeng G, Zhong W. Serum early prostate cancer antigen (EPCA) as a significant predictor of incidental prostate cancer in patients undergoing transurethral resection of the prostate for benign prostatic hyperplasia. *Prostate* 2010;70(16):1788-98.
159. Zhao Z, Ma W, Zeng G, Qi D, Ou L, Liang Y. Preoperative serum levels of early prostate cancer antigen (EPCA) predict prostate cancer progression in patients undergoing radical prostatectomy. *Prostate* 2012;72(3):270-9.
160. Guo Y, Xu F, Lu T, Duan Z, Zhang Z. Interleukin-6 signaling pathway in targeted therapy for cancer. *Cancer Treat Rev* 2012;38(7):904-10.
161. Ke Y, Jing C, Barraclough R, Smith P, Davies MP, Foster CS. Elevated expression of calcium-binding protein p9Ka is associated with increasing malignant characteristics of rat prostate carcinoma cells. *Int J Cancer* 1997;71(5):832-7.
162. Gupta S, Hussain T, MacLennan GT, Fu P, Patel J, Mukhtar H. Differential expression of S100A2 and S100A4 during progression of human prostate adenocarcinoma. *J Clin Oncol* 2003;21(1):106-12.
163. Qin J, Wu SP, Creighton CJ, Dai F, Xie X, Cheng CM, et al. COUP-TFII inhibits TGF-beta-induced growth barrier to promote prostate tumorigenesis. *Nature* 2013;493(7431):236-40.
164. Shariat SF, Shalev M, Menesses-Diaz A, Kim IY, Kattan MW, Wheeler TM, et al. Preoperative plasma levels of transforming growth factor beta(1) (TGF-beta(1)) strongly predict progression in patients undergoing radical prostatectomy. *J Clin Oncol* 2001;19(11):2856-64.
165. Madu CO, Lu Y. Novel diagnostic biomarkers for prostate cancer. *J Cancer* 2010;1:150-77.
166. Beckett ML, Cazares LH, Vlahou A, Schellhammer PF, Wright GL, Jr. Prostate-specific membrane antigen levels in sera from healthy men and patients with benign prostate hyperplasia or prostate cancer. *Clin Cancer Res* 1999;5(12):4034-40.

167. Bao Z, Malki MI, Forootan SS, Adamson J, Forootan FS, Chen D, et al. A novel cutaneous Fatty Acid-binding protein-related signaling pathway leading to malignant progression in prostate cancer cells. *Genes Cancer* 2013;4(7-8):297-314.
168. Morgan EA, Forootan SS, Adamson J, Foster CS, Fujii H, Igarashi M, et al. Expression of cutaneous fatty acid-binding protein (C-FABP) in prostate cancer: potential prognostic marker and target for tumourigenicity-suppression. *Int J Oncol* 2008;32(4):767-75.
169. Kote-Jarai Z, Leongamornlert D, Saunders E, Tymrakiewicz M, Castro E, Mahmud N, et al. BRCA2 is a moderate penetrance gene contributing to young-onset prostate cancer: implications for genetic testing in prostate cancer patients. *Br J Cancer* 2011;105(8):1230-4.
170. Leongamornlert D, Mahmud N, Tymrakiewicz M, Saunders E, Dadaev T, Castro E, et al. Germline BRCA1 mutations increase prostate cancer risk. *Br J Cancer* 2012;106(10):1697-701.
171. de Muga S, Hernandez S, Salido M, Lorenzo M, Agell L, Juanpere N, et al. CXCR4 mRNA overexpression in high grade prostate tumors: lack of association with TMPRSS2-ERG rearrangement. *Cancer Biomark* 2012;12(1):21-30.
172. Paul W. IL-6: a multifunctional regulator of immunity and inflammation. *Jpn J Cancer Res* 1991;82(12):1458-9.
173. Zhang GJ, Adachi I. Serum interleukin-6 levels correlate to tumor progression and prognosis in metastatic breast carcinoma. *Anticancer Res* 1999;19(2B):1427-32.
174. Donato R. Intracellular and extracellular roles of S100 proteins. *Microsc Res Tech* 2003;60(6):540-51.
175. Donato R. S100: a multigenic family of calcium-modulated proteins of the EF-hand type with intracellular and extracellular functional roles. *Int J Biochem Cell Biol* 2001;33(7):637-68.
176. Ilg EC, Schafer BW, Heizmann CW. Expression pattern of S100 calcium-binding proteins in human tumors. *Int J Cancer* 1996;68(3):325-32.
177. Rehman I, Cross SS, Catto JW, Leiblich A, Mukherjee A, Azzouzi AR, et al. Promoter hyper-methylation of calcium binding proteins S100A6 and S100A2 in human prostate cancer. *Prostate* 2005;65(4):322-30.
178. Zhang Y. Functional characterization of three novel candidate biomarkers and therapeutic targets for prostate cancer (PhD thesis). June 2010.
179. Kattan MW, Shariat SF, Andrews B, Zhu K, Canto E, Matsumoto K, et al. The addition of interleukin-6 soluble receptor and transforming growth factor beta1 improves a preoperative nomogram for predicting biochemical progression in patients with clinically localized prostate cancer. *J Clin Oncol* 2003;21(19):3573-9.
180. Reiter RE, Gu Z, Watabe T, Thomas G, Szigeti K, Davis E, et al. Prostate stem cell antigen: a cell surface marker overexpressed in prostate cancer. *Proc Natl Acad Sci U S A* 1998;95(4):1735-40.
181. Ramirez ML, Nelson EC, Evans CP. Beyond prostate-specific antigen: alternate serum markers. *Prostate Cancer Prostatic Dis* 2008;11(3):216-29.
182. Bonkhoff H, Remberger K. Differentiation pathways and histogenetic aspects of normal and abnormal prostatic growth: a stem cell model. *Prostate* 1996;28(2):98-106.
183. Zimmerman AW, Veerkamp JH. New insights into the structure and function of fatty acid-binding proteins. *Cell Mol Life Sci* 2002;59(7):1096-116.
184. Furuhashi M, Hotamisligil GS. Fatty acid-binding proteins: role in metabolic diseases and potential as drug targets. *Nat Rev Drug Discov* 2008;7(6):489-503.
185. Haunerland NH, Spener F. Fatty acid-binding proteins--insights from genetic manipulations. *Prog Lipid Res* 2004;43(4):328-49.
186. Schroeder F, Petrescu AD, Huang H, Atshaves BP, McIntosh AL, Martin GG, et al. Role of fatty acid binding proteins and long chain fatty acids in modulating nuclear receptors and gene transcription. *Lipids* 2008;43(1):1-17.

187. Tan NS, Shaw NS, Vinckenbosch N, Liu P, Yasmin R, Desvergne B, et al. Selective cooperation between fatty acid binding proteins and peroxisome proliferator-activated receptors in regulating transcription. *Mol Cell Biol* 2002;22(14):5114-27.
188. Jing C, Beesley C, Foster CS, Rudland PS, Fujii H, Ono T, et al. Identification of the messenger RNA for human cutaneous fatty acid-binding protein as a metastasis inducer. *Cancer Res* 2000;60(9):2390-8.
189. Jing C, Beesley C, Foster CS, Chen H, Rudland PS, West DC, et al. Human cutaneous fatty acid-binding protein induces metastasis by up-regulating the expression of vascular endothelial growth factor gene in rat Rama 37 model cells. *Cancer Res* 2001;61(11):4357-64.
190. Adamson J, Morgan EA, Beesley C, Mei Y, Foster CS, Fujii H, et al. High-level expression of cutaneous fatty acid-binding protein in prostatic carcinomas and its effect on tumorigenicity. *Oncogene* 2003;22(18):2739-49.
191. Forootan SS, Bao ZZ, Forootan FS, Kamalian L, Zhang Y, Bee A, et al. Atelocollagen-delivered siRNA targeting the FABP5 gene as an experimental therapy for prostate cancer in mouse xenografts. *Int J Oncol* 2010;36(1):69-76.
192. Dreyer C, Krey G, Keller H, Givel F, Helftenbein G, Wahli W. Control of the peroxisomal beta-oxidation pathway by a novel family of nuclear hormone receptors. *Cell* 1992;68(5):879-87.
193. Mangelsdorf DJ, Thummel C, Beato M, Herrlich P, Schutz G, Umesono K, et al. The nuclear receptor superfamily: the second decade. *Cell* 1995;83(6):835-9.
194. Wakabayashi S, Shigekawa M, Pouyssegur J. Molecular physiology of vertebrate Na+/H+ exchangers. *Physiol Rev* 1997;77(1):51-74.
195. Venkatachalam G, Kumar AP, Yue LS, Pervaiz S, Clement MV, Sakharkar MK. Computational identification and experimental validation of PPRE motifs in NHE1 and MnSOD genes of human. *BMC Genomics* 2009;10 Suppl 3:S5.
196. Berger J, Moller DE. The mechanisms of action of PPARs. *Annu Rev Med* 2002;53:409-35.
197. Sher T, Yi HF, McBride OW, Gonzalez FJ. cDNA cloning, chromosomal mapping, and functional characterization of the human peroxisome proliferator activated receptor. *Biochemistry* 1993;32(21):5598-604.
198. Greene ME, Blumberg B, McBride OW, Yi HF, Kronquist K, Kwan K, et al. Isolation of the human peroxisome proliferator activated receptor gamma cDNA: expression in hematopoietic cells and chromosomal mapping. *Gene Expr* 1995;4(4-5):281-99.
199. Yoshikawa T, Brkanac Z, Dupont BR, Xing GQ, Leach RJ, Detera-Wadleigh SD. Assignment of the human nuclear hormone receptor, NUC1 (PPARD), to chromosome 6p21.1-p21.2. *Genomics* 1996;35(3):637-8.
200. Braissant O, Foufelle F, Scotto C, Dauca M, Wahli W. Differential expression of peroxisome proliferator-activated receptors (PPARs): tissue distribution of PPAR-alpha, -beta, and -gamma in the adult rat. *Endocrinology* 1996;137(1):354-66.
201. Tyagi S, Gupta P, Saini AS, Kaushal C, Sharma S. The peroxisome proliferator-activated receptor: A family of nuclear receptors role in various diseases. *J Adv Pharm Technol Res* 2011;2(4):236-40.
202. Ogata T, Miyauchi T, Sakai S, Irukayama-Tomobe Y, Goto K, Yamaguchi I. Stimulation of peroxisome-proliferator-activated receptor alpha (PPAR alpha) attenuates cardiac fibrosis and endothelin-1 production in pressure-overloaded rat hearts. *Clin Sci (Lond)* 2002;103 Suppl 48:284S-8S.
203. Boitier E, Gautier JC, Roberts R. Advances in understanding the regulation of apoptosis and mitosis by peroxisome-proliferator activated receptors in pre-clinical models: relevance for human health and disease. *Comp Hepatol* 2003;2(1):3.
204. Chawla A, Barak Y, Nagy L, Liao D, Tontonoz P, Evans RM. PPAR-gamma dependent and independent effects on macrophage-gene expression in lipid metabolism and inflammation. *Nat Med* 2001;7(1):48-52.

205. Mueller E, Sarraf P, Tontonoz P, Evans RM, Martin KJ, Zhang M, et al. Terminal differentiation of human breast cancer through PPAR gamma. *Mol Cell* 1998;1(3):465-70.
206. Ogino S, Shima K, Baba Y, Nosho K, Irahara N, Kure S, et al. Colorectal cancer expression of peroxisome proliferator-activated receptor gamma (PPARG, PPARgamma) is associated with good prognosis. *Gastroenterology* 2009;136(4):1242-50.
207. Mansure JJ, Nassim R, Chevalier S, Szymanski K, Rocha J, Aldousari S, et al. A novel mechanism of PPAR gamma induction via EGFR signalling constitutes rational for combination therapy in bladder cancer. *PLoS One* 2013;8(2):e55997.
208. Han S, Sidell N, Fisher PB, Roman J. Up-regulation of p21 gene expression by peroxisome proliferator-activated receptor gamma in human lung carcinoma cells. *Clin Cancer Res* 2004;10(6):1911-9.
209. Han S, Roman J. Rosiglitazone suppresses human lung carcinoma cell growth through PPARgamma-dependent and PPARgamma-independent signal pathways. *Mol Cancer Ther* 2006;5(2):430-7.
210. Elnemr A, Ohta T, Iwata K, Ninomia I, Fushida S, Nishimura G, et al. PPARgamma ligand (thiazolidinedione) induces growth arrest and differentiation markers of human pancreatic cancer cells. *Int J Oncol* 2000;17(6):1157-64.
211. Kurokawa T, Shimomura Y, Bajotto G, Kotake K, Arikawa T, Ito N, et al. Peroxisome proliferator-activated receptor alpha (PPARalpha) mRNA expression in human hepatocellular carcinoma tissue and non-cancerous liver tissue. *World J Surg Oncol* 2011;9:167.
212. Davidson B, Hadar R, Stavnes HT, Trope CG, Reich R. Expression of the peroxisome proliferator-activated receptors-alpha, -beta, and -gamma in ovarian carcinoma effusions is associated with poor chemoresponse and shorter survival. *Hum Pathol* 2009;40(5):705-13.
213. Benedetti E, Galzio R, Laurenti G, D'Angelo B, Melchiorre E, Cifone MG, et al. Lipid metabolism impairment in human gliomas: expression of peroxisomal proteins in human gliomas at different grades of malignancy. *Int J Immunopathol Pharmacol* 2010;23(1):235-46.
214. QIAGEN sathwqcpgappdp. PPAR pathway.
215. He TC, Chan TA, Vogelstein B, Kinzler KW. PPARdelta is an APC-regulated target of nonsteroidal anti-inflammatory drugs. *Cell* 1999;99(3):335-45.
216. Nijsten T, Geluyckens E, Colpaert C, Lambert J. Peroxisome proliferator-activated receptors in squamous cell carcinoma and its precursors. *J Cutan Pathol* 2005;32(5):340-7.
217. Glazer RI, Yuan H, Xie Z, Yin Y. PPARgamma and PPARdelta as Modulators of Neoplasia and Cell Fate. *PPAR Res* 2008;2008:247379.
218. Tong BJ, Tan J, Tajeda L, Das SK, Chapman JA, DuBois RN, et al. Heightened expression of cyclooxygenase-2 and peroxisome proliferator-activated receptor-delta in human endometrial adenocarcinoma. *Neoplasia* 2000;2(6):483-90.
219. Peters JM, Shah YM, Gonzalez FJ. The role of peroxisome proliferator-activated receptors in carcinogenesis and chemoprevention. *Nat Rev Cancer* 2012;12(3):181-95.
220. Bility MT, Zhu B, Kang BH, Gonzalez FJ, Peters JM. Ligand activation of peroxisome proliferator-activated receptor-beta/delta and inhibition of cyclooxygenase-2 enhances inhibition of skin tumorigenesis. *Toxicol Sci* 2010;113(1):27-36.
221. Folkman J. Angiogenesis in cancer, vascular, rheumatoid and other disease. *Nat Med* 1995;1(1):27-31.
222. Hanahan D, Folkman J. Patterns and emerging mechanisms of the angiogenic switch during tumorigenesis. *Cell* 1996;86(3):353-64.
223. Zetter BR. Angiogenesis and tumor metastasis. *Annu Rev Med* 1998;49:407-24.
224. Ferrara N. Vascular endothelial growth factor: basic science and clinical progress. *Endocr Rev* 2004;25(4):581-611.
225. Vincenti V, Cassano C, Rocchi M, Persico G. Assignment of the vascular endothelial growth factor gene to human chromosome 6p21.3. *Circulation* 1996;93(8):1493-5.

226. Josko J, Mazurek M. Transcription factors having impact on vascular endothelial growth factor (VEGF) gene expression in angiogenesis. *Med Sci Monit* 2004;10(4):Ra89-98.
227. Huss WJ, Hanrahan CF, Barrios RJ, Simons JW, Greenberg NM. Angiogenesis and prostate cancer: identification of a molecular progression switch. *Cancer Res* 2001;61(6):2736-43.
228. Ferrer FA, Miller LJ, Andrawis RI, Kurtzman SH, Albertsen PC, Laudone VP, et al. Vascular endothelial growth factor (VEGF) expression in human prostate cancer: in situ and in vitro expression of VEGF by human prostate cancer cells. *J Urol* 1997;157(6):2329-33.
229. Zhong H, De Marzo AM, Laughner E, Lim M, Hilton DA, Zagzag D, et al. Overexpression of hypoxia-inducible factor 1alpha in common human cancers and their metastases. *Cancer Res* 1999;59(22):5830-5.
230. Weidner N, Carroll PR, Flax J, Blumenfeld W, Folkman J. Tumor angiogenesis correlates with metastasis in invasive prostate carcinoma. *Am J Pathol* 1993;143(2):401-9.
231. Chen HJ, Treweeke AT, Ke YQ, West DC, Toh CH. Angiogenically active vascular endothelial growth factor is over-expressed in malignant human and rat prostate carcinoma cells. *Br J Cancer* 2000;82(10):1694-701.
232. Bok RA, Halabi S, Fei DT, Rodriquez CR, Hayes DF, Vogelzang NJ, et al. Vascular endothelial growth factor and basic fibroblast growth factor urine levels as predictors of outcome in hormone-refractory prostate cancer patients: a cancer and leukemia group B study. *Cancer Res* 2001;61(6):2533-6.
233. Duque JL, Loughlin KR, Adam RM, Kantoff PW, Zurakowski D, Freeman MR. Plasma levels of vascular endothelial growth factor are increased in patients with metastatic prostate cancer. *Urology* 1999;54(3):523-7.
234. Hwang C, Heath EI. Angiogenesis inhibitors in the treatment of prostate cancer. *J Hematol Oncol* 2010;3:26.
235. Stoner M, Wormke M, Saville B, Samudio I, Qin C, Abdelrahim M, et al. Estrogen regulation of vascular endothelial growth factor gene expression in ZR-75 breast cancer cells through interaction of estrogen receptor alpha and SP proteins. *Oncogene* 2004;23(5):1052-63.
236. Eisermann K, Broderick CJ, Bazarov A, Moazam MM, Fraizer GC. Androgen up-regulates vascular endothelial growth factor expression in prostate cancer cells via an Sp1 binding site. *Mol Cancer* 2013;12:7.
237. Bishop-Bailey D, Hla T. Endothelial cell apoptosis induced by the peroxisome proliferator-activated receptor (PPAR) ligand 15-deoxy-Delta12, 14-prostaglandin J2. *J Biol Chem* 1999;274(24):17042-8.
238. Varet J, Vincent L, Mirshahi P, Pille JV, Legrand E, Opolon P, et al. Fenofibrate inhibits angiogenesis in vitro and in vivo. *Cell Mol Life Sci* 2003;60(4):810-9.
239. Panigrahy D, Kaipainen A, Huang S, Butterfield CE, Barnes CM, Fannon M, et al. PPARalpha agonist fenofibrate suppresses tumor growth through direct and indirect angiogenesis inhibition. *Proc Natl Acad Sci U S A* 2008;105(3):985-90.
240. Nickkho-Amiry M, McVey R, Holland C. Peroxisome proliferator-activated receptors modulate proliferation and angiogenesis in human endometrial carcinoma. *Mol Cancer Res* 2012;10(3):441-53.
241. Piqueras L, Reynolds AR, Hodivala-Dilke KM, Alfranca A, Redondo JM, Hatae T, et al. Activation of PPARbeta/delta induces endothelial cell proliferation and angiogenesis. *Arterioscler Thromb Vasc Biol* 2007;27(1):63-9.
242. Abdollahi A, Schwager C, Kleeff J, Esposito I, Domhan S, Peschke P, et al. Transcriptional network governing the angiogenic switch in human pancreatic cancer. *Proc Natl Acad Sci U S A* 2007;104(31):12890-5.
243. Fauconnet S, Lascombe I, Chabannes E, Adessi GL, Desvergne B, Wahli W, et al. Differential regulation of vascular endothelial growth factor expression by peroxisome proliferator-activated receptors in bladder cancer cells. *J Biol Chem* 2002;277(26):23534-43.

244. Panigrahy D, Singer S, Shen LQ, Butterfield CE, Freedman DA, Chen EJ, et al. PPARgamma ligands inhibit primary tumor growth and metastasis by inhibiting angiogenesis. *J Clin Invest* 2002;110(7):923-32.
245. Rohrl C, Kaindl U, Koneczny I, Hudec X, Baron DM, Konig JS, et al. Peroxisome-proliferator-activated receptors gamma and beta/delta mediate vascular endothelial growth factor production in colorectal tumor cells. *J Cancer Res Clin Oncol* 2011;137(1):29-39.
246. Yamakawa K, Hosoi M, Koyama H, Tanaka S, Fukumoto S, Morii H, et al. Peroxisome proliferator-activated receptor-gamma agonists increase vascular endothelial growth factor expression in human vascular smooth muscle cells. *Biochem Biophys Res Commun* 2000;271(3):571-4.
247. Biscetti F, Gaetani E, Flex A, Aprahamian T, Hopkins T, Straface G, et al. Selective activation of peroxisome proliferator-activated receptor (PPAR)alpha and PPAR gamma induces neoangiogenesis through a vascular endothelial growth factor-dependent mechanism. *Diabetes* 2008;57(5):1394-404.
248. Peeters LL, Vigne JL, Tee MK, Zhao D, Waite LL, Taylor RN. PPAR gamma represses VEGF expression in human endometrial cells: implications for uterine angiogenesis. *Angiogenesis* 2005;8(4):373-9.
249. Ito K, Yamamoto T, Ohi M, Kurokawa K, Suzuki K, Yamanaka H. Free/total PSA ratio is a powerful predictor of future prostate cancer morbidity in men with initial PSA levels of 4.1 to 10.0 ng/mL. *Urology* 2003;61(4):760-4.
250. Ramos-Vara JA. Technical aspects of immunohistochemistry. *Vet Pathol* 2005;42(4):405-26.
251. Remmele W, Stegner HE. [Recommendation for uniform definition of an immunoreactive score (IRS) for immunohistochemical estrogen receptor detection (ER-ICA) in breast cancer tissue]. *Pathologe* 1987;8(3):138-40.
252. Auboeuf D, Rieusset J, Fajas L, Vallier P, Frering V, Riou JP, et al. Tissue distribution and quantification of the expression of mRNAs of peroxisome proliferator-activated receptors and liver X receptor-alpha in humans: no alteration in adipose tissue of obese and NIDDM patients. *Diabetes* 1997;46(8):1319-27.
253. QIAGEN. RNeasy Mini Handbook. April 2006.
254. Freeman WM, Walker SJ, Vrana KE. Quantitative RT-PCR: pitfalls and potential. *Biotechniques* 1999;26(1):112-22, 24-5.
255. Schmittgen TD, Zakrajsek BA, Mills AG, Gorn V, Singer MJ, Reed MW. Quantitative reverse transcription-polymerase chain reaction to study mRNA decay: comparison of endpoint and real-time methods. *Anal Biochem* 2000;285(2):194-204.
256. Elbashir SM, Harborth J, Lendeckel W, Yalcin A, Weber K, Tuschl T. Duplexes of 21-nucleotide RNAs mediate RNA interference in cultured mammalian cells. *Nature* 2001;411(6836):494-8.
257. Bernstein E, Caudy AA, Hammond SM, Hannon GJ. Role for a bidentate ribonuclease in the initiation step of RNA interference. *Nature* 2001;409(6818):363-6.
258. Invivogen. psRNA-h7SKGFPzeo Kit instruction manual.
259. promega. Wizard SV Gel and PCR Clean-Up System, Instruction for users. 2005.
260. Hanahan D, Jessee J, Bloom FR. Plasmid transformation of Escherichia coli and other bacteria. *Methods Enzymol* 1991;204:63-113.
261. Hanahan D. Studies on transformation of Escherichia coli with plasmids. *J Mol Biol* 1983;166(4):557-80.
262. Tang X, Nakata Y, Li HO, Zhang M, Gao H, Fujita A, et al. The optimization of preparations of competent cells for transformation of E. coli. *Nucleic Acids Res* 1994;22(14):2857-8.
263. QIAGEN. Plasmid Purification Handbook. 2005.
264. QIAGEN. QIAprep Miniprep Handbook. 2006.
265. Invitrogen. Zeocin™ Selection Reagent, User Guide. 2012.

266. Albini A, Iwamoto Y, Kleinman HK, Martin GR, Aaronson SA, Kozlowski JM, et al. A rapid in vitro assay for quantitating the invasive potential of tumor cells. *Cancer Res* 1987;47(12):3239-45.
267. Biosciences B. BD BioCoat™ Growh Factor Reduced MATRIGEL™ Invasion Chamber, Guidelines for Use. 1996.
268. Frisch SM, Screaton RA. Anoikis mechanisms. *Curr Opin Cell Biol* 2001;13(5):555-62.
269. Anderson SN, Towne DL, Burns DJ, Warrior U. A high-throughput soft agar assay for identification of anticancer compound. *J Biomol Screen* 2007;12(7):938-45.
270. Montesano R, Orci L. Tumor-promoting phorbol esters induce angiogenesis in vitro. *Cell* 1985;42(2):469-77.
271. Ferrara N, Houck KA, Jakeman LB, Winer J, Leung DW. The vascular endothelial growth factor family of polypeptides. *J Cell Biochem* 1991;47(3):211-8.
272. RayBiotech I. Human VEGF ELIZA Kit Protocol. 2012.
273. Kubota Y, Kleinman HK, Martin GR, Lawley TJ. Role of laminin and basement membrane in the morphological differentiation of human endothelial cells into capillary-like structures. *J Cell Biol* 1988;107(4):1589-98.
274. Millipore. In Vitro Angiogenesis Assay Kit instruction.
275. Sherf BA. Dual-Luciferase reporter assay:An advanced co-reporter integrating firefly and *Renilla* luciferase assays. 1996.
276. Promega. pGL3 Luciferase ReporterVector, Technical manual instruction. 12/2008.
277. Mueller MD, Vigne JL, Minchenko A, Lebovic DI, Leitman DC, Taylor RN. Regulation of vascular endothelial growth factor (VEGF) gene transcription by estrogen receptors alpha and beta. *Proc Natl Acad Sci U S A* 2000;97(20):10972-7.
278. Venkatachalam G, Kumar AP, Sakharkar KR, Thangavel S, Clement MV, Sakharkar MK. PPARgamma disease gene network and identification of therapeutic targets for prostate cancer. *J Drug Target* 2011;19(9):781-96.
279. Janik P, Briand P, Hartmann NR. The effect of estrone-progesterone treatment on cell proliferation kinetics of hormone-dependent GR mouse mammary tumors. *Cancer Res* 1975;35(12):3698-704.
280. Malki MI. The tumorigenicity-promoting activity of C-FABP in prostate cancer cells depends on its fatty acid-binding ability (PhD thesis). 2011:129-36.
281. Madsen P, Rasmussen HH, Leffers H, Honore B, Celis JE. Molecular cloning and expression of a novel keratinocyte protein (psoriasis-associated fatty acid-binding protein [PA-FABP]) that is highly up-regulated in psoriatic skin and that shares similarity to fatty acid-binding proteins. *J Invest Dermatol* 1992;99(3):299-305.
282. Masouye I, Saurat JH, Siegenthaler G. Epidermal fatty-acid-binding protein in psoriasis, basal and squamous cell carcinomas: an immunohistological study. *Dermatology* 1996;192(3):208-13.
283. Celis A, Rasmussen HH, Celis P, Basse B, Lauridsen JB, Ratz G, et al. Short-term culturing of low-grade superficial bladder transitional cell carcinomas leads to changes in the expression levels of several proteins involved in key cellular activities. *Electrophoresis* 1999;20(2):355-61.
284. Ostergaard M, Rasmussen HH, Nielsen HV, Vorum H, Orntoft TF, Wolf H, et al. Proteome profiling of bladder squamous cell carcinomas: identification of markers that define their degree of differentiation. *Cancer Res* 1997;57(18):4111-7.
285. Sinha P, Hutter G, Kottgen E, Dietel M, Schadendorf D, Lage H. Increased expression of epidermal fatty acid binding protein, cofilin, and 14-3-3-sigma (stratifin) detected by two-dimensional gel electrophoresis, mass spectrometry and microsequencing of drug-resistant human adenocarcinoma of the pancreas. *Electrophoresis* 1999;20(14):2952-60.

286. Liu RZ, Graham K, Glubrecht DD, Germain DR, Mackey JR, Godbout R. Association of FABP5 expression with poor survival in triple-negative breast cancer: implication for retinoic acid therapy. *Am J Pathol* 2011;178(3):997-1008.
287. Barbus S, Tews B, Karra D, Hahn M, Radlwimmer B, Delhomme N, et al. Differential retinoic acid signaling in tumors of long- and short-term glioblastoma survivors. *J Natl Cancer Inst* 2011;103(7):598-606.
288. Bao ZZ. The relationship between the tumorigenicity-promoting function of C-FABP and its fatty acid-binding ability(PhD thesis). 2010.
289. Malki MI. *The tumorigenicity-promoting activity of C-FABP in prostate cancer cells depends on its fatty acid-binding ability* [PhD thesis], 2011.
290. Lemberger T, Desvergne B, Wahli W. Peroxisome proliferator-activated receptors: a nuclear receptor signaling pathway in lipid physiology. *Annu Rev Cell Dev Biol* 1996;12:335-63.
291. Segawa Y, Yoshimura R, Hase T, Nakatani T, Wada S, Kawahito Y, et al. Expression of peroxisome proliferator-activated receptor (PPAR) in human prostate cancer. *Prostate* 2002;51(2):108-16.
292. Bao ZZ, Malki MI, Forootan SS, Adamson J, Forootan FS, Chen D, et al. A novel cutaneous fatty acid-binding protein-related signaling pathway leading to malignant progression in prostate cancer cells. *Genes and Cancer* 2013;in press.
293. Roobol MJ, Haese A, Bjartell A. Tumour markers in prostate cancer III: biomarkers in urine. *Acta Oncol* 2011;50 Suppl 1:85-9.
294. Theocharis S, Giaginis C, Parasi A, Margeli A, Kakisis J, Agapitos E, et al. Expression of peroxisome proliferator-activated receptor-gamma in colon cancer: correlation with histopathological parameters, cell cycle-related molecules, and patients' survival. *Dig Dis Sci* 2007;52(9):2305-11.
295. Han SW, Greene ME, Pitts J, Wada RK, Sidell N. Novel expression and function of peroxisome proliferator-activated receptor gamma (PPARgamma) in human neuroblastoma cells. *Clin Cancer Res* 2001;7(1):98-104.
296. Zhang GY, Ahmed N, Riley C, Oliva K, Barker G, Quinn MA, et al. Enhanced expression of peroxisome proliferator-activated receptor gamma in epithelial ovarian carcinoma. *Br J Cancer* 2005;92(1):113-9.
297. Lee TW, Chen GG, Xu H, Yip JH, Chak EC, Mok TS, et al. Differential expression of inducible nitric oxide synthase and peroxisome proliferator-activated receptor gamma in non-small cell lung carcinoma. *Eur J Cancer* 2003;39(9):1296-301.
298. Jiang WG, Redfern A, Bryce RP, Mansel RE. Peroxisome proliferator activated receptor-gamma (PPAR-gamma) mediates the action of gamma linolenic acid in breast cancer cells. *Prostaglandins Leukot Essent Fatty Acids* 2000;62(2):119-27.
299. Katagiri Y, Takeda K, Yu ZX, Ferrans VJ, Ozato K, Guroff G. Modulation of retinoid signalling through NGF-induced nuclear export of NGFI-B. *Nat Cell Biol* 2000;2(7):435-40.
300. Jiang M, Shappell SB, Hayward SW. Approaches to understanding the importance and clinical implications of peroxisome proliferator-activated receptor gamma (PPARgamma) signaling in prostate cancer. *J Cell Biochem* 2004;91(3):513-27.
301. Gouni-Berthold I, Berthold HK, Weber AA, Ko Y, Seul C, Vetter H, et al. Troglitazone and rosiglitazone induce apoptosis of vascular smooth muscle cells through an extracellular signal-regulated kinase-independent pathway. *Naunyn Schmiedebergs Arch Pharmacol* 2001;363(2):215-21.
302. Houseknecht KL, Cole BM, Steele PJ. Peroxisome proliferator-activated receptor gamma (PPARgamma) and its ligands: a review. *Domest Anim Endocrinol* 2002;22(1):1-23.
303. Murakami K, Tobe K, Ide T, Mochizuki T, Ohashi M, Akanuma Y, et al. A novel insulin sensitizer acts as a coligand for peroxisome proliferator-activated receptor-alpha (PPAR-alpha) and PPAR-gamma: effect of PPAR-alpha activation on abnormal lipid metabolism in liver of Zucker fatty rats. *Diabetes* 1998;47(12):1841-7.

304. Wang M, Wise SC, Leff T, Su TZ. Troglitazone, an antidiabetic agent, inhibits cholesterol biosynthesis through a mechanism independent of peroxisome proliferator-activated receptor-gamma. *Diabetes* 1999;48(2):254-60.
305. Fire A, Xu S, Montgomery MK, Kostas SA, Driver SE, Mello CC. Potent and specific genetic interference by double-stranded RNA in Caenorhabditis elegans. *Nature* 1998;391(6669):806-11.
306. Paddison PJ, Caudy AA, Hannon GJ. Stable suppression of gene expression by RNAi in mammalian cells. *Proc Natl Acad Sci U S A* 2002;99(3):1443-8.
307. Kamalian L, Forootan SS, Bao ZZ, Zhang Y, Gosney JR, Foster CS, et al. Inhibition of tumourigenicity of small cell lung cancer cells by suppressing Id3 expression. *Int J Oncol* 2010;37(3):595-603.
308. Zhang Y, Forootan SS, Kamalian L, Bao ZZ, Malki MI, Foster CS, et al. Suppressing tumourigenicity of prostate cancer cells by inhibiting osteopontin expression. *Int J Oncol* 2011;38(4):1083-91.
309. Hanahan D, Weinberg RA. The hallmarks of cancer. *Cell* 2000;100(1):57-70.
310. Morgan E, Kannan-Thulasiraman P, Noy N. Involvement of Fatty Acid Binding Protein 5 and PPARbeta/delta in Prostate Cancer Cell Growth. *PPAR Res* 2010;2010.
311. Foster CS, Dodson AR, Ambroisine L, Fisher G, Moller H, Clark J, et al. Hsp-27 expression at diagnosis predicts poor clinical outcome in prostate cancer independent of ETS-gene rearrangement. *Br J Cancer* 2009;101(7):1137-44.
312. Yao S, Bee A, Brewer D, Dodson A, Beesley C, Ke Y, et al. PRKC-zeta Expression Promotes the Aggressive Phenotype of Human Prostate Cancer Cells and Is a Novel Target for Therapeutic Intervention. *Genes Cancer* 2010;1(5):444-64.
313. Bishop-Bailey D. PPARs and angiogenesis. *Biochem Soc Trans* 2011;39(6):1601-5.
314. Kristiansen G, Jacob J, Buckendahl AC, Grutzmann R, Alldinger I, Sipos B, et al. Peroxisome proliferator-activated receptor gamma is highly expressed in pancreatic cancer and is associated with shorter overall survival times. *Clin Cancer Res* 2006;12(21):6444-51.
315. Chung LW, Chang SM, Bell C, Zhau H, Ro JY, von Eschenbach AC. Prostatic carcinogenesis evoked by cellular interaction. *Environ Health Perspect* 1988;77:23-8.
316. Condon MS, Kaplan LA, Crivello JF, Horton L, Bosland MC. Multiple pathways of prostate carcinogenesis analyzed by using cultured cells isolated from rats treated with N-methyl-N-nitrosourea and testosterone. *Mol Carcinog* 1999;25(3):179-86.
317. Ling MT, Chan KW, Choo CK. Androgen induces differentiation of a human papillomavirus 16 E6/E7 immortalized prostate epithelial cell line. *J Endocrinol* 2001;170(1):287-96.
318. Reid AH, Attard G, Barrie E, de Bono JS. CYP17 inhibition as a hormonal strategy for prostate cancer. *Nat Clin Pract Urol* 2008;5(11):610-20.
319. Asangani IA, Dommeti VL, Wang X, Malik R, Cieslik M, Yang R, et al. Therapeutic targeting of BET bromodomain proteins in castration-resistant prostate cancer. *Nature* 2014;510(7504):278-82.
320. Bubendorf L, Kononen J, Koivisto P, Schraml P, Moch H, Gasser TC, et al. Survey of gene amplifications during prostate cancer progression by high-throughout fluorescence in situ hybridization on tissue microarrays. *Cancer Res* 1999;59(4):803-6.
321. Chen CD, Welsbie DS, Tran C, Baek SH, Chen R, Vessella R, et al. Molecular determinants of resistance to antiandrogen therapy. *Nat Med* 2004;10(1):33-9.
322. Visakorpi T, Hyytinen E, Koivisto P, Tanner M, Keinanen R, Palmberg C, et al. In vivo amplification of the androgen receptor gene and progression of human prostate cancer. *Nat Genet* 1995;9(4):401-6.
323. Taylor BS, Schultz N, Hieronymus H, Gopalan A, Xiao Y, Carver BS, et al. Integrative genomic profiling of human prostate cancer. *Cancer Cell* 2010;18(1):11-22.
324. Baylin SB, Jones PA. A decade of exploring the cancer epigenome - biological and translational implications. *Nat Rev Cancer* 2011;11(10):726-34.

325. Bissell MJ, Hines WC. Why don't we get more cancer? A proposed role of the microenvironment in restraining cancer progression. *Nat Med* 2011;17(3):320-9.
326. Yu SQ, Han BM, Shao Y, Wu JT, Zhao FJ, Liu HT, et al. Androgen receptor functioned as a suppressor in the prostate cancer cell line PC3 in vitro and in vivo. *Chin Med J (Engl)* 2009;122(22):2779-83.
327. Jiang Q, Yeh S, Wang X, Xu D, Zhang Q, Wen X, et al. Targeting androgen receptor leads to suppression of prostate cancer via induction of autophagy. *J Urol* 2012;188(4):1361-8.
328. Niu Y, Altuwaijri S, Lai KP, Wu CT, Ricke WA, Messing EM, et al. Androgen receptor is a tumor suppressor and proliferator in prostate cancer. *Proc Natl Acad Sci U S A* 2008;105(34):12182-7.
329. Akiyama H, Tanaka T, Maeno T, Kanai H, Kimura Y, Kishi S, et al. Induction of VEGF gene expression by retinoic acid through Sp1-binding sites in retinoblastoma Y79 cells. *Invest Ophthalmol Vis Sci* 2002;43(5):1367-74.
330. Maeno T, Tanaka T, Sando Y, Suga T, Maeno Y, Nakagawa J, et al. Stimulation of vascular endothelial growth factor gene transcription by all trans retinoic acid through Sp1 and Sp3 sites in human bronchioloalveolar carcinoma cells. *Am J Respir Cell Mol Biol* 2002;26(2):246-53.
331. Shi Q, Le X, Abbruzzese JL, Peng Z, Qian CN, Tang H, et al. Constitutive Sp1 activity is essential for differential constitutive expression of vascular endothelial growth factor in human pancreatic adenocarcinoma. *Cancer Res* 2001;61(10):4143-54.
332. Darrington E, Zhong M, Vo BH, Khan SA. Vascular endothelial growth factor A, secreted in response to transforming growth factor-beta1 under hypoxic conditions, induces autocrine effects on migration of prostate cancer cells. *Asian J Androl* 2012;14(5):745-51.
333. Gonzalez-Moreno O, Lecanda J, Green JE, Segura V, Catena R, Serrano D, et al. VEGF elicits epithelial-mesenchymal transition (EMT) in prostate intraepithelial neoplasia (PIN)-like cells via an autocrine loop. *Exp Cell Res* 2010;316(4):554-67.
334. Nguyen PL, Ma J, Chavarro JE, Freedman ML, Lis R, Fedele G, et al. Fatty acid synthase polymorphisms, tumor expression, body mass index, prostate cancer risk, and survival. *J Clin Oncol* 2010;28(25):3958-64.
335. Hamada S, Horiguchi A, Kuroda K, Ito K, Asano T, Miyai K, et al. Increased fatty acid synthase expression in prostate biopsy cores predicts higher Gleason score in radical prostatectomy specimen. *BMC Clin Pathol* 2014;14(1):3.
336. Migita T, Ruiz S, Fornari A, Fiorentino M, Priolo C, Zadra G, et al. Fatty acid synthase: a metabolic enzyme and candidate oncogene in prostate cancer. *J Natl Cancer Inst* 2009;101(7):519-32.
337. Wang KF, Wu B. [Fatty acid synthase and prostate cancer]. *Zhonghua Nan Ke Xue* 2008;14(8):740-2.

6 APPENDIXES

6.1 APPENDIX A: REAGENTS

Reagents	Supplier

6.1.1 Reagents for cell culture

DMSO	Sigma-Aldrich, Germany
Foetal calf serum	Biosera, East Sussex, UK
L-Glutamine	Lonza, Belgium
Opti-MEM I medium	Gibco, Invitrogen, Paisley, UK
Penicillin/ Streptomycin	Lonza, Belgium
Phosphate buffered saline (tablet)	Gibco, Invitrogen, Paisley, UK
RPMI 1640	PAA, Pasching, Austria
Sodium pyruvate	Sigma, USA
Trypsin	Gibco, Invitrogen, Paisley, UK
Versene	Gibco, Invitrogen, Paisley, UK
X-tremeGENE HP DNA Transfection Reagent	Roche, Germany
X-tremeGENE siRNA Transfection Reagent	Roche, Germany
Zeocin	Invitrogen, CA, USA

6.1.2 Reagents for Western blot

β-mercaptoethanol	Sigma, USA
Ammonium persulfate (APS)	Sigma, USA
Bradford reagent	Sigma, USA
Bromophenol blue	Sigma, USA
CelLytic-M	Sigma, USA
Coomassie brilliant blue	Bio-Rad GmbH, Munchen, Germany
ECL detection kit	GE Healthcare, Buckinghamshire, UK
Glycine	Melford, UK
Kodak Developer	Sigma, USA
Kodak film	GE Healthcare, Buckinghamshire, UK
Kodak Fixer	Sigma, USA
Methanol	Fisher scientific, Loughborough, UK

Reagents	Supplier
Next Gel 12.5%	Amresco, OH, USA
Ponceau S solution	Sigma, USA
PVDF membrane (Immobilon-P)	Millipore, USA
TEMED (NNN'N'-tetramethylethylenediamine)	Sigma, USA
Tris base ultrapure	Melford, UK
Tween-20	Sigma-Aldrich, Germany

6.1.3 Reagents for Immunohistochemistry

Acetone	Sigma, USA
DPX	Bios, Lancashire, UK
EDTA	Sigma, USA
EnVision™ FLEX/DAB+ Chromogen	DakoCytomation, Ely, UK
EnVision™ FLEX/HRP	DakoCytomation, Ely, UK
Ethanol (IMS)	GENTA, Tockwith, UK
Formaldehyde	Sigma, USA
Haematoxylin	Sigma, USA
Hydrogen peroxide 30% (w/w)	BDH, England, UK
Linker (Anti-gout IgG) (AI 5000)	Vector, USA
Scott's tap water	Sigma, USA
Sodium citrate	Sigma, USA
Sodium chloride	Melford, UK
Tris base ultrapure	Melford, UK
Tween-20	Sigma-Aldrich, Germany
Xylene	GENTA, Tockwith, UK

6.1.4 Reagents for RT-PCR

dNTPs	Thermo scientific, UK
DTT	Invitrogen, Paisley, UK
Oligo $(dT)_{20}$	Agilent Technologies, CA, USA
PCR primers	Invitrogen, Paisley, UK
Platinum ®PCR SuperMix High Fidelity	Invitrogen, Paisley, UK

Reagents	Supplier
QIAGEN RNeasy Mini Kit	QIAGEN, CA, USA
SuperScript II Reverse Transcriptase	Agilent Technologies, CA, USA
5× First strand buffer	Agilent Technologies, CA, USA

6.1.5 Reagents for general molecular biology

Ampicillin	Sigma, USA
Absolute ethanol	BDH, England, UK
Agarose	*Genflow*, Fradley, UK
DNA marker III	Roche, England, UK
DNA marker XIV	Roche, England, UK
E. coli GT116 cell	InvivoGen, USA
Glucose	Sigma, USA
Glycerol	Sigma, USA
Isopropanol	BDH, England, UK
LB agar	Sigma, USA
LB broth	Sigma, USA
Magnesium chloride	Sigma, USA
Magnesium sulphate	Sigma, USA
MOPS	Sigma, USA
psiRNA-h7SKGFPzeo plasmid	InvivoGen, USA
QIAGEN Plasmid midi-preparation kit	QIAGEN, CA, USA
QIAGEN Plasmid mini-preparation kit	QIAGEN, CA, USA
Restriction enzymes	New England BioLabs, MA, USA
Restriction enzymes buffers	New England BioLabs, MA, USA
Safe View (Nucleic Acid Stain)	NBS Biological, Cambridgeshire, UK
Tryptone	Sigma, USA
Wizard® DNA Clean-Up System	Promega, WI, USA
Yeast extract	Fisher scientific, Loughborough, UK
Zeocin	Invitrogen, CA, USA

Reagents	Supplier

6.1.6 Reagents for cell proliferation assay

MTT	Sigma, USA

6.1.7 Reagents for cell invasion assay

Crystal violet	Sigma, USA

6.1.8 Reagents for soft agar assay

Low melting point agarose	*Genflow*, Fradley, UK
MTT	Sigma, USA

6.1.9 Reagents for measurement of VEGF

Charcoal stripped FCS	Gibco, Invitrogen, Paisley, UK
Human VEGF ELISA Kit	RayBiotech, GA, USA
Phenol red-free RPMI 1640	Gibco, Invitrogen, Paisley, UK
Recombinant Human VEGF	RayBiotech, GA, USA
TMB	RayBiotech, GA, USA

6.1.10 Reagents for *in vitro* angiogenesis assay

EndoGRO basal medium	Millipore, USA
EndoGRO LS supplement kit	Millipore, USA
In Vitro Angiogenesis Assay Kit	Millipore, USA
MTT	Sigma, USA
Recombinant Human VEGF	RayBiotech, GA, USA

6.1.11 Reagents for dual luciferase reporter assay

Dual Luciferase Reporter Kit	Promega, WI, USA
GW9662	Sigma, USA
Mithramycin A	Sigma, USA
Rosiglitazone	Sigma, USA
X-treme GENE HP DNA Transfection Reagent	Roche, Germany

6.2 APPENDIX B: BUFFERS

6.2.1 Cell Culture

Routine cell culture medium

RPMI medium 1640	500ml
Foetal calf serum	10% (v/v)
Pen-Strep (5000 U/ml)	5ml
L-Glutamine (20mM)	5ml
Sodium pyruvate (100mM)	5ml

Selective medium

Routine medium with Zeocin^{TM} (100µg/ml)

Culture medium for evaluation the expression level of VEGF

Phenol red-free RPMI 1640 medium	500ml
Charcoal stripped FCS	5% (v/v)
Pen-Strep (5000 U/ml)	5ml
L-Glutamine (20mM)	5ml

Culture medium for HUVEC cells (angiogenesis assay)

EndoGRO basal medium	500ml
EndoGRO LS supplement kit	
Charcoal stripped FCS	5% (v/v)

Freezing medium

Routine cell culture medium	92.5% (v/v)
DMSO	7.5% (v/v)

Trypsin/EDTA solution (T/E) (2.5%)

1× Versene	100ml
Trypsin	2.5ml

MTT solution (5mg/ml)

MTT	50mg
PBS	10ml

PBS

PBS	one tablet
dH_2O	500ml
Autoclaved	

6.2.2 Western Blot

1M Tris pH 6.8

Tris base	12.1gr
dH_2O	100ml
pH adjusted with HCl	

10% (w/v) SDS solution

Sodium Dodecyl Sulfate	10gr
dH_2O	100ml

10% (w/v) APS solution

Ammonium persulfate	100mg
dH_2O	1ml

2× SDS-PAGE sample loading buffer (SLB)

1M Tris-HCl (pH 6.8)	2.5ml
Glycerol 40% (v/v)	4ml
Bromophenol blue 0.5% (w/v)	0.8ml
SDS 10%	2ml
β-mercaptoethanol	0.5ml
dH_2O	4.7ml

5× SDS-PAGE sample loading buffer (SLB)

1M Tris-HCl (pH 6.8)	1.25ml
Glycerol 40% (v/v)	15ml
Bromophenol blue 0.5% (w/v)	2.5ml
SDS 10%	5ml
β-mercaptoethanol	1.25ml

Transfer buffer (pH 8.3)

Glycine	14.4g (192mM)
Methanol	20% (v/v)
Tris base	3.03g (25mM)
dH_2O	up to 1Lit
pH adjusted with HCl	

10× TBS buffer (pH 7.6)

Sodium chloride	87.66gr (1500mM)
Tris base	60.58gr (500mM)
dH_2O	up to 1 Lit
pH adjusted with HCl	
Autoclaved	

1×TBS-Tween 1%

10× TBS buffer	100ml
Tween 20	1ml
dH_2O	up to 1 Lit

TBS-T-milk 5% (protoblock)

Dried milk	5gr
1×TBS-T	100ml

6.2.3 Immunohistochemistry

Hydrogen peroxide-Methanol solution

Hydrogen peroxide 30% (w/w)	12ml
Methanol	400ml

Sodium citrate buffer (10mM)

Tris sodium citrate	29.41gr
dH_2O	up to 10 Lit
pH 6; adjusted with HCl	

EDTA buffer (pH 7)

EDTA	37.2gr
Sodium hydroxide	3.2gr
dH_2O	up to 10 Lit

TBS-Tween 5%

Sodium chloride	87.66gr (1500mM)
Tris base	60.58gr (500mM)
Tween 20	5ml
dH_2O	up to 10 Lit
pH adjusted with HCl	

Acid/alcohol 1%

HCl	20ml
IMS	1400ml
dH_2O	60ml

Scott's tap water

$MgSO_4$	20gr
$NaHCO_3$	3.5gr
dH_2O	up to 1 Lit

6.2.4 Molecular Biology

LB medium

LB broth	20gr
dH_2O	1 Lit

Autoclaved

LB agar

LB agar	35gr
dH_2O	1 Lit

Autoclaved

RF 1 buffer (pH 5.8)

KCl	7.456gr (100mM)
$MgCl_2.4H_2O$	9.9gr (50mM)
K-acetate	2.94gr (30mM)
$CaCl_2$	1.5gr (10mM)
Glycerol (v/v)	150ml (15%)
dH_2O	up to 1 Lit

Adjust the pH and sterilized by filtration

RF 2 buffer (pH 6.8)

MOPS	2.1gr (10mM)
KCl	0.745gr (10mM)
$CaCl_2$	11gr (75mM)
Glycerol (v/v)	150ml (15%)
dH_2O	up to 1 Lit

Adjust the pH and sterilized by autoclave

Glucose 20%

Glucose	20gr
dH_2O	10ml

Sterilized by filtration

Magnesium salt solution (2M)

$MgCl_2$	2.033gr (1M)
$MgSO_4$	2.465gr (1M)
dH_2O	10ml

Sterilized by filtration

SOB medium (pH 7)

Tryptone	20gr
Yeast extracts	5gr
NaCl	0.5gr
KCl	0.186gr
dH_2O	up to 1 Lit

Adjust the pH and sterilized by autoclave

SOC medium

SOB medium	4.850ml
Mg^{2+} salt solution (2M)	50µl
Glucose 20%	150µl

Stock medium for bacteria

Glycerol	5ml
LB medium	4ml
Bacteria culture	3ml

10× TBE stock solution

Tris base	108gr (890mM)
Boric acid	55gr (890mM)
EDTA 0.5M, pH 8	40ml (20mM)
dH_2O	up to 1 Lit

Adjust the pH and sterilized by autoclave

50× TBE stock solution

Tris base	242gr
Glacial Acetic Acid	57.1gr
EDTA 0.5M, pH 8	100ml
dH_2O	up to 1 Lit

Adjust the pH and sterilized by autoclave

TE buffer (pH 7.6)

Tris-HCl	1.21gr (10mM)
EDTA	0.3722gr (1mM)
dH_2O	up to 1 Lit

Adjust the pH and sterilized by autoclave

6×DNA loading buffer

Bromophenol blue 0.5%	0.5ml
Xylene cyanol FF	0.5ml
Glycerol in sterile dH_2O (60%)	1ml

6.3 APPENDIX C: EQUIPMENTS

AccuWeigh, WA, USA

Portable Lab Scale

BD Microlance 3, Ireland

Needle

Syringes

BD Biosciences, USA

BD BioCoat™ Growth Factor Reduced (GFR) Matrigel™ Invasion Chamber

BD Plastics, Sunderland, UK

Syringes

Beckman coulter, UK

Microcentrifuge

Becton Dikinson, USA

Falcon 2059 tube

Berthold detection system, Germany

Sirius Luminometer

Bio-Rad, Hemel, UK

Gel electrophoresis rig

Mini-protein 3 cell system

BioTec, Brigend, UK

Spectrophotometer

Borolabs, Basingstoke, UK

CO_2 incubator Model TC2323

Flowgen, Nottingham, UK

Gel drier

Generier bio-one, UK

Tissue culture pipettes (5-50 ml)

Universal tube

Grant Instruments, UK

Water bath

GMI, MJ Research, MN, USA

Thermal cycler (Peltier Thermal Cycler PTC-200)

Heraeus Holding GmbH, Germany

Labofuge 400R (centrifuge)

Labsystem, Finland

Multiskan MS (plate reader)

Labtech International, Ringmer, UK

NanoDrop spectrophotometer

Leica, Germany

Superior Adhesive slide

Leitz Labovert, Luton, UK

Light microscope

Microm, Oxford, UK

Microtome HM355

Millipore, UK

Immobilon, Transfer membrane

Nalgene, UK

Cryobox DNA

Nunc, Denmark

Cell culture filter cap flasks

Cell culture plates

Cryogenic vial

OXFORD OPTRONIX, Oxford, UK

GelCount

QIAGEN, Crawley, UK

Qiagen tip

QIA Shredder spin column

Shandon, UK

Sequenza slide rack

Coverslip (20×40mm)

SLS Ltd., Nottingham, UK

Haemocytometer

Magnificent stirrer

Starlab, Milton Keynes, UK

Microtubes

Pipette tips

Surgipath, UK

Microslide

Tissue cassette

Swann-Morton, Sheffeild, UK

Carbon steel surgical blades

Techne, England, UK

Hot plate (Ori-Block 08-3)

Whatman, England, UK

Whatman filter paper

Weber scientific International, NJ, USA

Haemocytometer slide

6.4 APPENDIX D: LUCIFERASE CONSTRUCTS SEQUENCES

Wild type

5’ GGTACCACTTTGATGTCTGC**AGGCCA**GATGAGGGCTCCAGATGGCACATTGTCAG
AGGGACACACTGTGGCCCCTGTGCCCAGCCCTGGGCTCTCTGTACATGAAGCAACTCCAG
TCCCAAATATGTAGCTGTTTGGGAGGTCAGAAATAGGGGGTCCAGGAGCAAACTCCCCC
CACCCCCTTTCCAAAGCCCATTCCCTCTTTAGCCAGAGCCGGGGTGTGCAGACGGCAGTC
ACTAGGGGGCGCTCGGCCACCACAGGGAAGCTGGGTGAATGGAGCGAGCAGCGTCTTCG
AGAGTGAGGACGTGTGTGTCTGTGTGGGTGAGTGAGTGTGTGCGTGTGGGGTTGAGGGC
GTTGGAGCGGGGAGA**AGGCCA**GGGGTCACTCCAGGATTCCAATAGATCTGTGTGTCCCT
CTCCCCACCCGTCCCTGTCCGGCTCTCCGCCTTCCCCTGCCCCCTTCAATATTCCTAGCAA
AGAGGGAACGGCTCTCAGGCCCTGTCCGCACGTAACCTCACTTTCCTGCTCCCTCCTCGC
CAATGCCCCGCGGGCGCGTGTCTCTGGACAGAGTTTCCGGGGGCGGATGGGTAATTTTCA
GGCTGTGAACCTTGGTGGGGGTCGAGCTTCCCCTTCATTGCGGCGGGCTGCGGGCCAGGC
TTCACTGAGCGTCCGCAGAGCCCGGGCCCGAGCCGCGTGTGGAAGGGCTGAGGCTCGCC
TGTCCCCGCCCCCCGGGGCGGGCCGGGGGCGGGGTCCCGGCGGGGCGGAGCCATGCGCC
CCCCCCTTTTTTTTTTAAAAGTCGGCTGGTAGCGGGGAGGCTCGAG 3’

Mutant1

5’ GGTACCACTTTGATGTCTGC**ATGCAT**GATGAGGGCTCCAGATGGCACATTGTCAGA
GGGACACACTGTGGCCCCTGTGCCCAGCCCTGGGCTCTCTGTACATGAAGCAACTCCAGT
CCCAAATATGTAGCTGTTTGGGAGGTCAGAAATAGGGGGTCCAGGAGCAAACTCCCCCC
ACCCCCTTTCCAAAGCCCATTCCCTCTTTAGCCAGAGCCGGGGTGTGCAGACGGCAGTCA
CTAGGGGGCGCTCGGCCACCACAGGGAAGCTGGGTGAATGGAGCGAGCAGCGTCTTCGA
GAGTGAGGACGTGTGTGTCTGTGTGGGTGAGTGAGTGTGTGCGTGTGGGGTTGAGGGCG
TTGGAGCGGGGAGA**ATGCAT**GGGGTCACTCCAGGATTCCAATAGATCTGTGTGTCCCTC
TCCCCACCCGTCCCTGTCCGGCTCTCCGCCTTCCCCTGCCCCCTTCAATATTCCTAGCAAA
GAGGGAACGGCTCTCAGGCCCTGTCCGCACGTAACCTCACTTTCCTGCTCCCTCCTCGCC
AATGCCCCGCGGGCGCGTGTCTCTGGACAGAGTTTCCGGGGGCGGATGGGTAATTTTCAG
GCTGTGAACCTTGGTGGGGGTCGAGCTTCCCCTTCATTGCGGCGGGCTGCGGGCCAGGCT
TCACTGAGCGTCCGCAGAGCCCGGGCCCGAGCCGCGTGTGGAAGGGCTGAGGCTCGCCT
GTCCCCGCCCCCCGGGGCGGGCCGGGGGCGGGGTCCCGGCGGGGCGGAGCCATGCGCCC
CCCCCTTTTTTTTTTAAAAGTCGGCTGGTAGCGGGGAGGCTCGAG 3’

Mutant2

5’ GGTACCCGTCCCTGTCCGGCTCTCCGCCTTCCCCTGCCCCCTTCAATATTCCTAGCA
AAGAGGGAACGGCTCTCAGGCCCTGTCCGCACGTAACCTCACTTTCCTGCTCCCTCCTCG
CCAATGCCCCGCGGGCGCGTGTCTCTGGACAGAGTTTCCGGGGGCGGATGGGTAATTTTC
AGGCTGTGAACCTTGGTGGGGGTCGAGCTTCCCCTTCATTGCGGCGGGCTGCGGGCCAGG
CTTCACTGAGCGTCCGCAGAGCCCGGGCCCGAGCCGCGTGTGGAAGGGCTGAGGCTCGC
CTGTCCCCGCCCCCCGGGGCGGGCCGGGGGCGGGGTCCCGGCGGGGCGGAGCCATGCGC
CCCCCCCTTTTTTTTTTAAAAGTCGGCTGGTAGCGGGGAGGCTCGAG 3’

Sequence map of three constructs based on human VEGF promoter

Validation of the wild type promoter-VEGF luciferase plasmid alignment

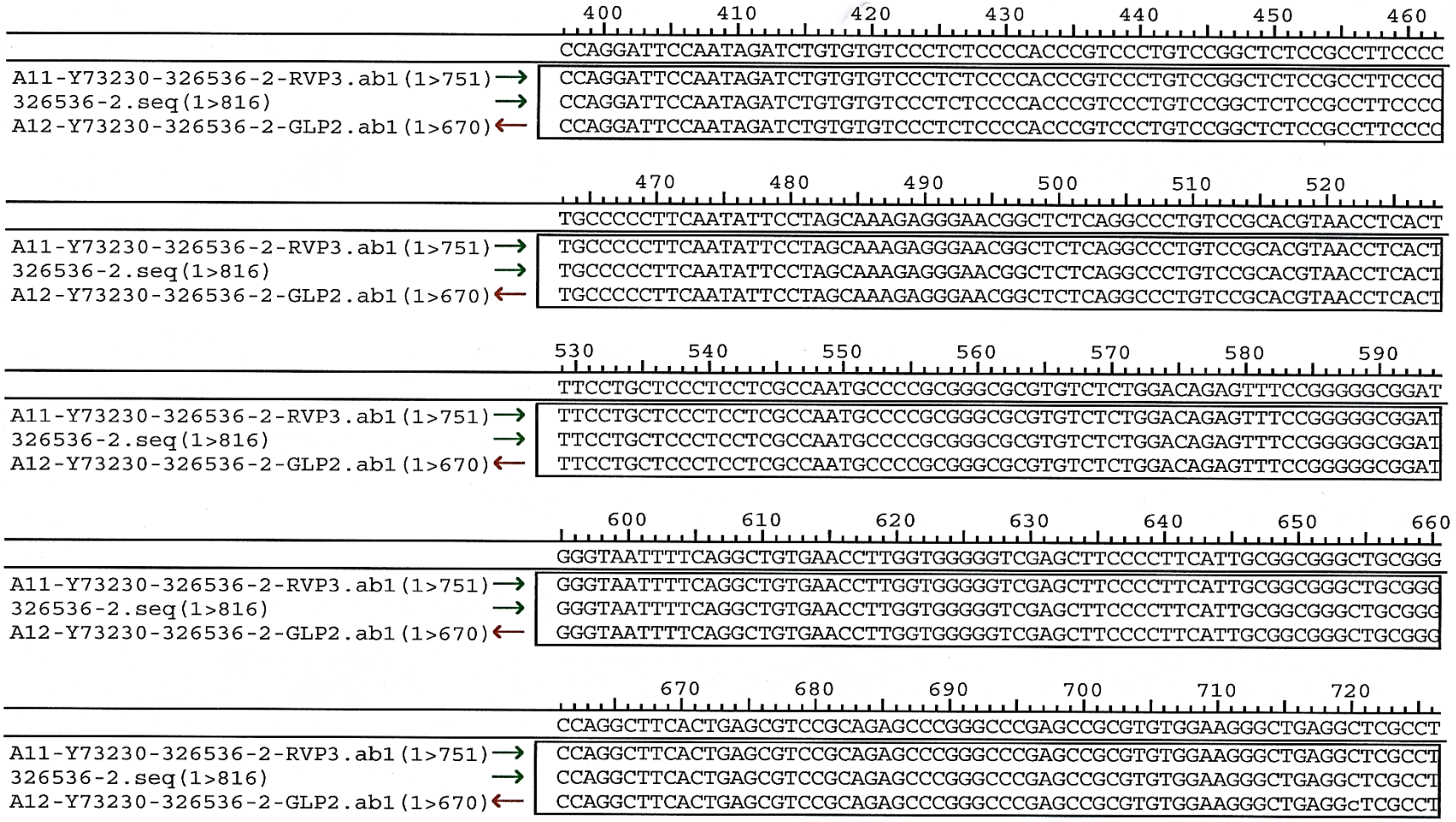

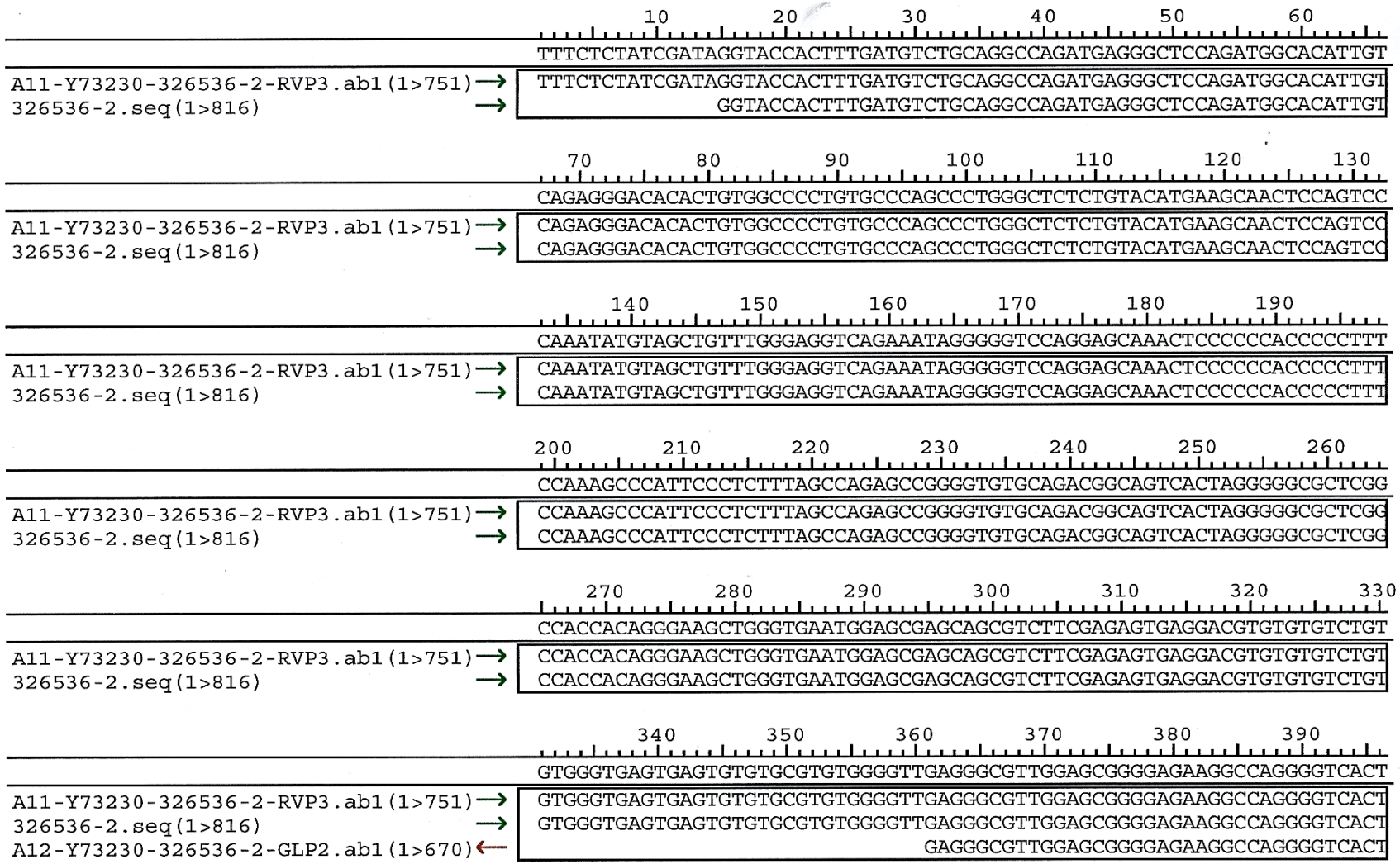
10 20 30 40 50 60
TTTCTCTATCGATAGGTACCACTTTGATGTCTGCAGGCCAGATGAGGGCTCCAGATGGCACATTGT
A11-Y73230-326536-2-RVP3.ab1(1>751)
TTTCTCTATCGATAGGTACCACTTTGATGTCTGCAGGCCAGATGAGGGCTCCAGATGGCACATTGT
326536-2.seq(1>816)
GGTACCACTTTGATGTCTGCAGGCCAGATGAGGGCTCCAGATGGCACATTGT
70 80 90 100 110 120 130
CAGAGGGACACACTGTGGCCCCTGTGCCCAGCCCTGGGCTCTCTGTACATGAAGCAACTCCAGTCC
A11-Y73230-326536-2-RVP3.ab1(1>751)
CAGAGGGACACACTGTGGCCCCTGTGCCCAGCCCTGGGCTCTCTGTACATGAAGCAACTCCAGTCC
326536-2.seq(1>816)
CAGAGGGACACACTGTGGCCCCTGTGCCCAGCCCTGGGCTCTCTGTACATGAAGCAACTCCAGTCC
140 150 160 170 180 190
CAAATATGTAGCTGTTTGGGAGGTCAGAAATAGGGGGTCCAGGAGCAAACTCCCCCCACCCCCTTT
A11-Y73230-326536-2-RVP3.ab1(1>751)
CAAATATGTAGCTGTTTGGGAGGTCAGAAATAGGGGGTCCAGGAGCAAACTCCCCCCACCCCCTTT
326536-2.seq(1>816)
CAAATATGTAGCTGTTTGGGAGGTCAGAAATAGGGGGTCCAGGAGCAAACTCCCCCCACCCCCTTT
200 210 220 230 240 250 260
CCAAAGCCCATTCCCTCTTTAGCCAGAGCCGGGGTGTGCAGACGGCAGTCACTAGGGGGCGCTCGG
A11-Y73230-326536-2-RVP3.ab1(1>751)
CCAAAGCCCATTCCCTCTTTAGCCAGAGCCGGGGTGTGCAGACGGCAGTCACTAGGGGGCGCTCGG
326536-2.seq(1>816)
CCAAAGCCCATTCCCTCTTTAGCCAGAGCCGGGGTGTGCAGACGGCAGTCACTAGGGGGCGCTCGG
270 280 290 300 310 320 330
CCACCACAGGGAAGCTGGGTGAATGGAGCGAGCAGCGTCTTCGAGAGTGAGGACGTGTGTGTCTGT
A11-Y73230-326536-2-RVP3.ab1(1>751)
CCACCACAGGGAAGCTGGGTGAATGGAGCGAGCAGCGTCTTCGAGAGTGAGGACGTGTGTGTCTGT
326536-2.seq(1>816)
CCACCACAGGGAAGCTGGGTGAATGGAGCGAGCAGCGTCTTCGAGAGTGAGGACGTGTGTGTCTGT
340 350 360 370 380 390
GTGGGTGAGTGAGTGTGTGCGTGTGGGGTTGAGGGCGTTGGAGCGGGGAGAAGGCCAGGGGTCACT
A11-Y73230-326536-2-RVP3.ab1(1>751)
GTGGGTGAGTGAGTGTGTGCGTGTGGGGTTGAGGGCGTTGGAGCGGGGAGAAGGCCAGGGGTCACT
326536-2.seq(1>816)
GTGGGTGAGTGAGTGTGTGCGTGTGGGGTTGAGGGCGTTGGAGCGGGGAGAAGGCCAGGGGTCACT
A12-Y73230-326536-2-GLP2.ab1(1>670)
GAGGGCGTTGGAGCGGGGAGAAGGCCAGGGGTCACT

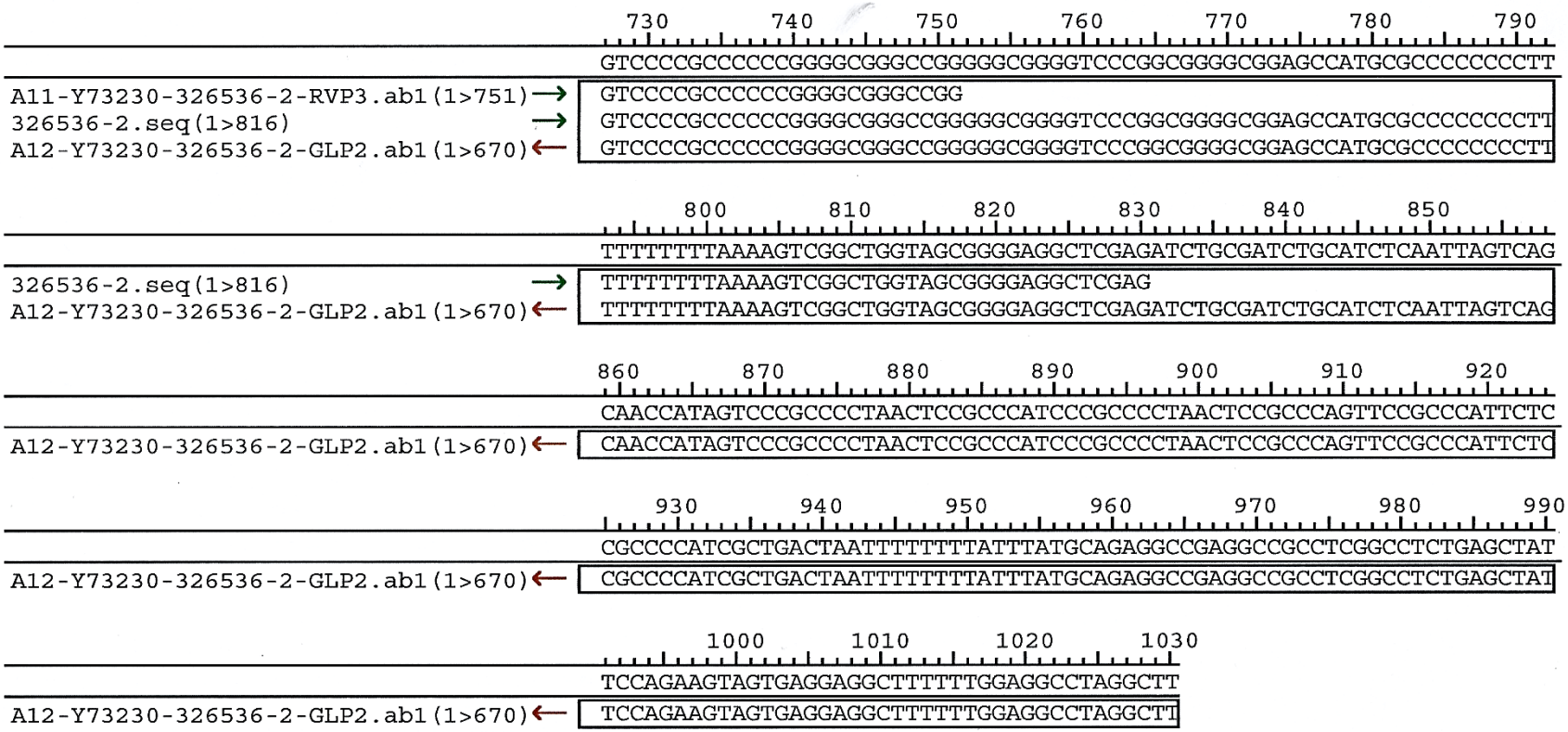
730 740 750 760 770 780 790
GTCCCCGCCCCCCGGGGCGGGCCGGGGGCGGGGTCCCGGCGGGGCGGAGCCATGCGCCCCCCCCTT
A11-Y73230-326536-2-RVP3.ab1(1>751)
GTCCCCGCCCCCCGGGGCGGGCCGG
326536-2.seq(1>816)
GTCCCCGCCCCCCGGGGCGGGCCGGGGGCGGGGTCCCGGCGGGGCGGAGCCATGCGCCCCCCCCTT
A12-Y73230-326536-2-GLP2.ab1(1>670)
GTCCCCGCCCCCCGGGGCGGGCCGGGGGCGGGGTCCCGGCGGGGCGGAGCCATGCGCCCCCCCCTT
800 810 820 830 840 850
TTTTTTTTAAAAGTCGGCTGGTAGCGGGGAGGCTCGAGATCTGCGATCTGCATCTCAATTAGTCAG
326536-2.seq(1>816)
TTTTTTTTAAAAGTCGGCTGGTAGCGGGGAGGCTCGAG
A12-Y73230-326536-2-GLP2.ab1(1>670)
TTTTTTTTAAAAGTCGGCTGGTAGCGGGGAGGCTCGAGATCTGCGATCTGCATCTCAATTAGTCAG
860 870 880 890 900 910 920
CAACCATAGTCCCGCCCCTAACTCCGCCCATCCCGCCCCTAACTCCGCCCAGTTCCGCCCATTCTC
A12-Y73230-326536-2-GLP2.ab1(1>670)
CAACCATAGTCCCGCCCCTAACTCCGCCCATCCCGCCCCTAACTCCGCCCAGTTCCGCCCATTCTC
930 940 950 960 970 980 990
CGCCCCATCGCTGACTAATTTTTTTTATTTATGCAGAGGCCGAGGCCGCCTCGGCCTCTGAGCTAT
A12-Y73230-326536-2-GLP2.ab1(1>670)
CGCCCCATCGCTGACTAATTTTTTTTATTTATGCAGAGGCCGAGGCCGCCTCGGCCTCTGAGCTAT
1000 1010 1020 1030
TCCAGAAGTAGTGAGGAGGCTTTTTTGGAGGCCTAGGCTT
A12-Y73230-326536-2-GLP2.ab1(1>670)
TCCAGAAGTAGTGAGGAGGCTTTTTTGGAGGCCTAGGCTT

Validation of the Mutant1 promoter-VEGF luciferase plasmid alignment

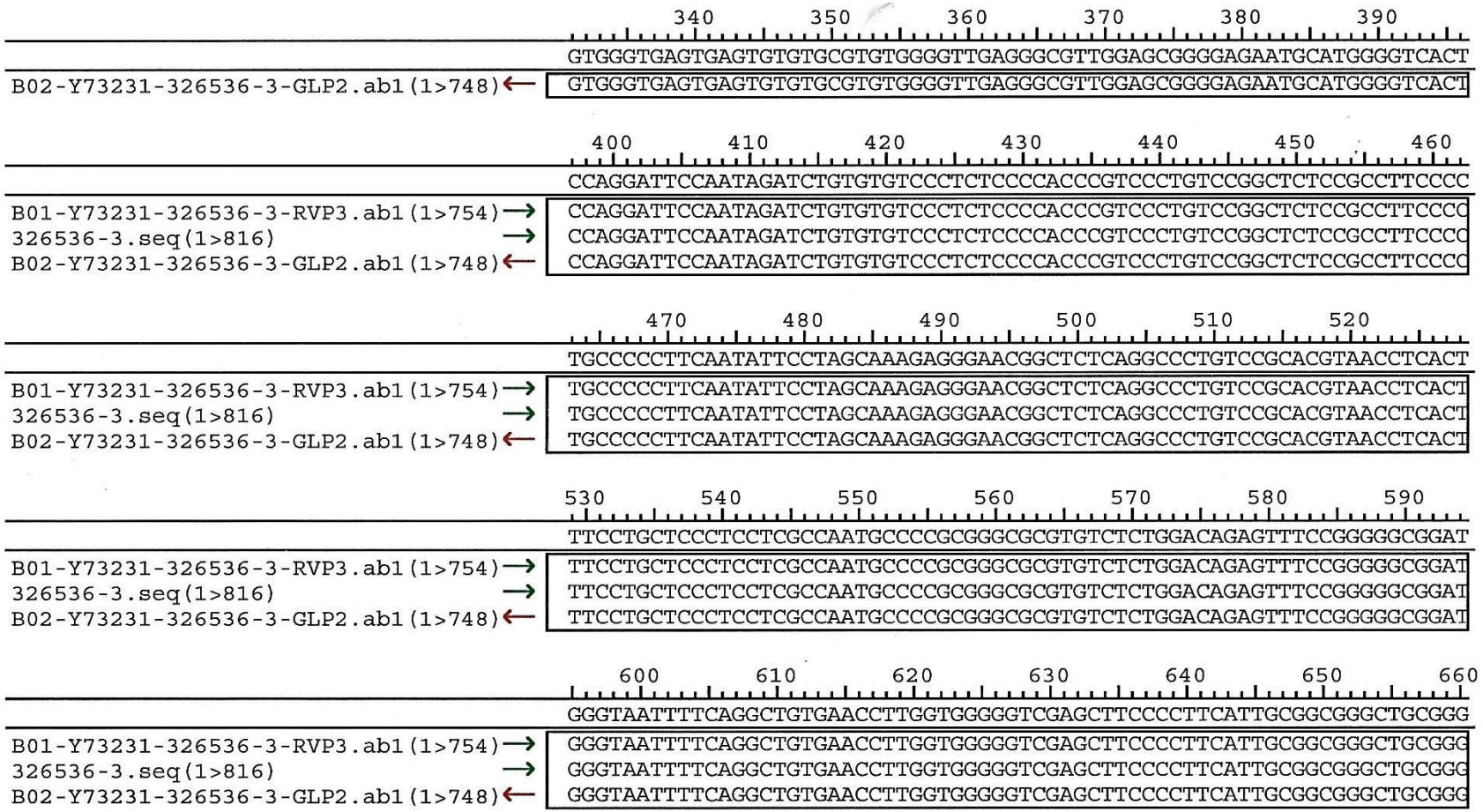

10 20 30 40 50 60
TTTCTCTATCGATAGGTACCACTTTGATGTCTGCATGCATGATGAGGGCTCCAGATGGCACATTGT
B01-Y733231-326536-3-RVP3.ab1 (1>754)
TTTCTCTATCGATAGGTACCACTTTGATGTCTGCATGCATGATGAGGGCTCCAGATGGCACATTGT
326536-3.seq(1>816)
GGTACCACTTTGATGTCTGCATGCATGATGAGGGCTCCAGATGGCACATTGT
70 80 90 100 110 120 130
CAGAGGGACACACTGTGGCCCCTGTGCCCAGCCCTGGGCTCTCTGTACATGAAGCAACTCCAGTCC
B01-Y733231-326536-3-RVP3.ab1 (1>754)
CAGAGGGACACACTGTGGCCCCTGTGCCCAGCCCTGGGCTCTCTGTACATGAAGCAACTCCAGTCC
326536-3.seq(1>816)
CAGAGGGACACACTGTGGCCCCTGTGCCCAGCCCTGGGCTCTCTGTACATGAAGCAACTCCAGTCC
140 150 160 170 180 190
CAAATATGTAGCTGTTTGGGAGGTCAGAAATAGGGGGTCCAGGAGCAAACTCCCCCCCACCCCCTTT
B01-Y733231-326536-3-RVP3.ab1 (1>754)
CAAATATGTAGCTGTTTGGGAGGTCAGAAATAGGGGGTCCAGGAGCAAACTCCCCCCCACCCCCTTT
326536-3.seq(1>816)
CAAATATGTAGCTGTTTGGGAGGTCAGAAATAGGGGGTCCAGGAGCAAACTCCCCCCCACCCCCTTT
200 210 220 230 240 250 260
CCAAAGCCCATTTCCCTCTTTAGCCAGAGCCGGGGTGTGCAGACGGCAGTCACTAGGGGGCGCTCGG
B01-Y733231-326536-3-RVP3.ab1 (1>754)
CCAAAGCCCATTTCCCTCTTTAGCCAGAGCCGGGGTGTGCAGACGGCAGTCACTAGGGGGCGCTCGG
326536-3.seq(1>816)
CCAAAGCCCATTTCCCTCTTTAGCCAGAGCCGGGGTGTGCAGACGGCAGTCACTAGGGGGCGCTCGG
270 280 290 300 310 320 330
CCACCACAGGGAAGCTGGGTGAATGGAGCGAGCAGCGTCTTCGAGAGTGAGGACGTGTGTCTGT
B01-Y733231-326536-3-RVP3.ab1 (1>754)
CCACCACAGGGAAGCTGGGTGAATGGAGCGAGCAGCGTCTTCGAGAGTGAGGACGTGTGTCTGT
326536-3.seq(1>816)
CCACCACAGGGAAGCTGGGTGAATGGAGCGAGCAGCGTCTTCGAGAGTGAGGACGTGTGTCTGT
B02-Y733231-326536-3-GLP2.ab1 (1>748)
GCTGGGTGAATGGAGCGAGCAGCGTCTTCGAGAGTGAGGACGTGTGTCTGT
340 350 360 370 380 390
GTGGGTGAGTGAGTGTGTGCGTGTGGGGTTGAGGCGTTGGAGCGGGGAGAAATGCATGGGGTCACT
B01-Y733231-326536-3-RVP3.ab1 (1>754)
GTGGGTGAGTGAGTGTGTGCGTGTGGGGTTGAGGCGTTGGAGCGGGGAGAAATGCATGGGGTCACT
326536-3.seq(1>816)
GTGGGTGAGTGAGTGTGTGCGTGTGGGGTTGAGGCGTTGGAGCGGGGAGAAATGCATGGGGTCACT

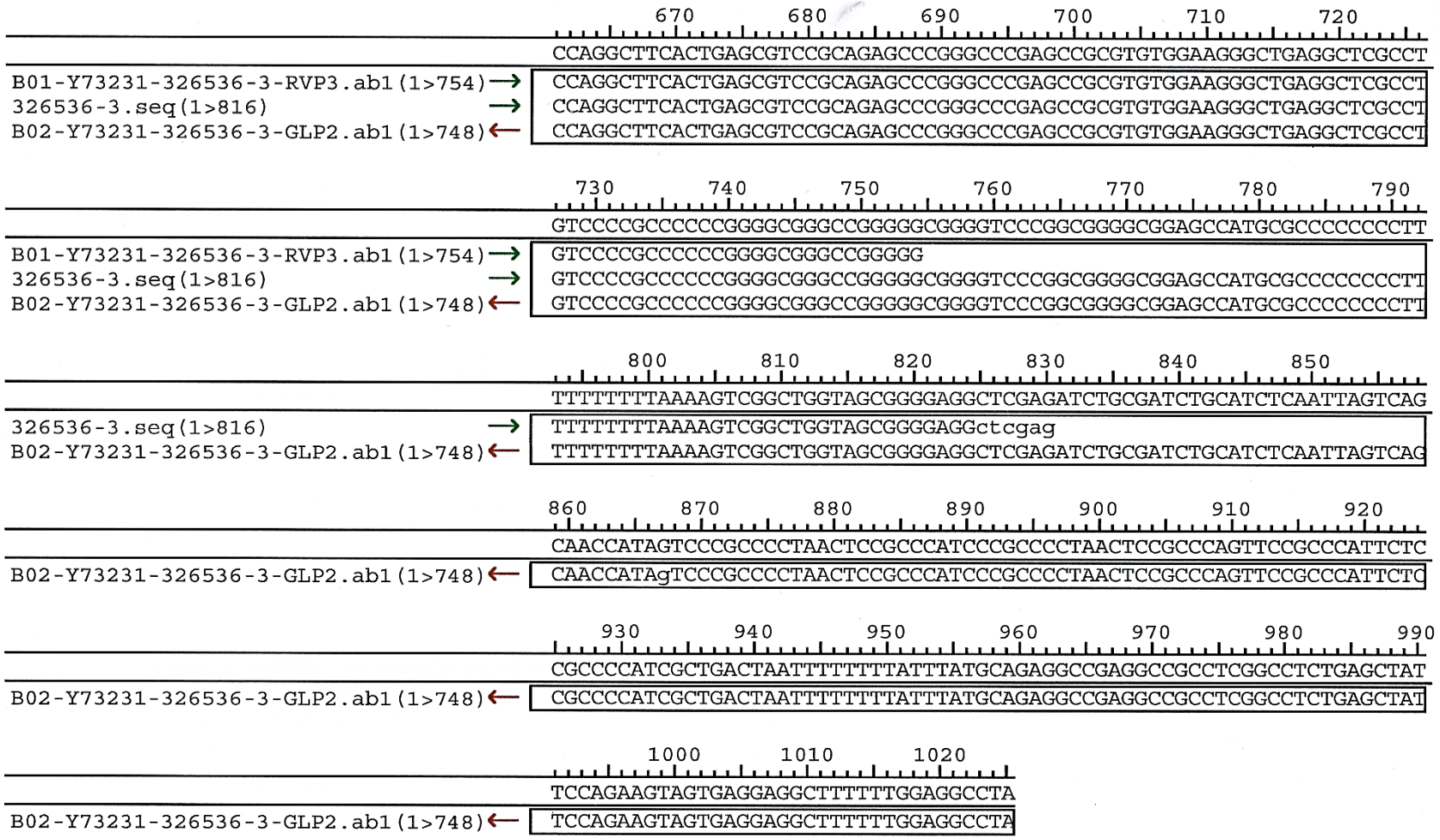
670 680 690 700 710 720
CCAGGCTTCACTGAGCGTCCGCAGAGCCCGGGCCCGAGCCGCGTGTGGAAGGGCTGAGGCTCGCCT
B01-Y73231-326536-3-RVP3.ab1(1>754)
326536-3.seq(1>816)
B02-Y73231-326536-3-GLP2.ab1(1>748)
730 740 750 760 770 780 790
GTCCCCGCCCCCCGGGGCGGGCCGGGGGCGGGGTCCCGGCGGGGCGGAGCCATGCGCCCCCCCCTT
B01-Y73231-326536-3-RVP3.ab1(1>754)
326536-3.seq(1>816)
B02-Y73231-326536-3-GLP2.ab1(1>748)
800 810 820 830 840 850
TTTTTTTTAAAAGTCGGCTGGTAGCGGGGAGGCTCGAGATCTGCGATCTGCATCTCAATTAGTCAG
326536-3.seq(1>816)
B02-Y73231-326536-3-GLP2.ab1(1>748)
860 870 880 890 900 910 920
CAACCATAGTCCCGCCCCTAACTCCGCCCATCCCGCCCCTAACTCCGCCCAGTTCCGCCCATTCTC
B02-Y73231-326536-3-GLP2.ab1(1>748)
930 940 950 960 970 980 990
CGCCCCATCGCTGACTAATTTTTTTTATTTATGCAGAGGCCGAGGCCGCCTCGGCCTCTGAGCTAT
B02-Y73231-326536-3-GLP2.ab1(1>748)
1000 1010 1020
TCCAGAAGTAGTGAGGAGGCTTTTTTGGAGGCCTA
B02-Y73231-326536-3-GLP2.ab1(1>748)

Validation of the Mutant2 promoter-VEGF luciferase plasmid alignment

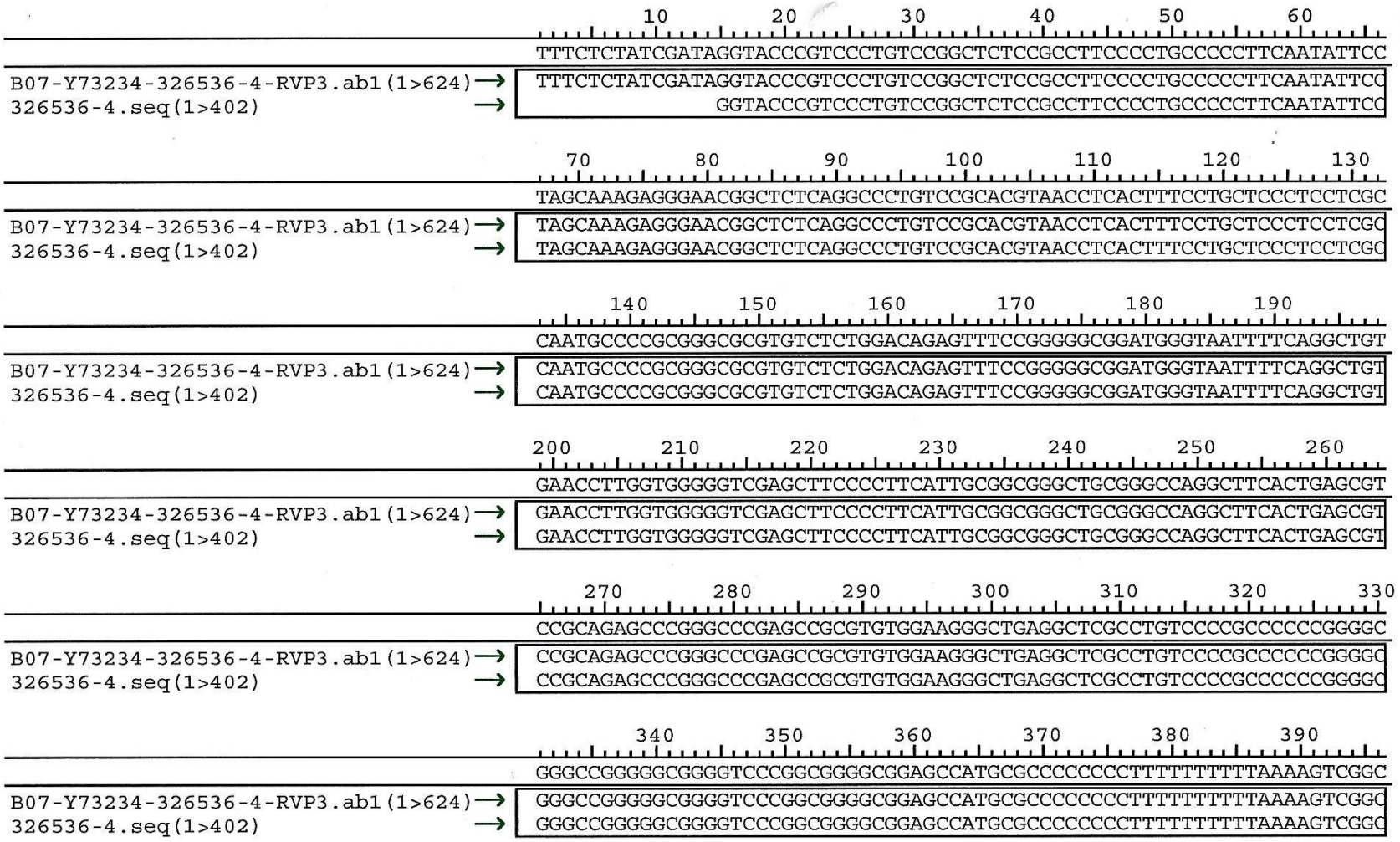

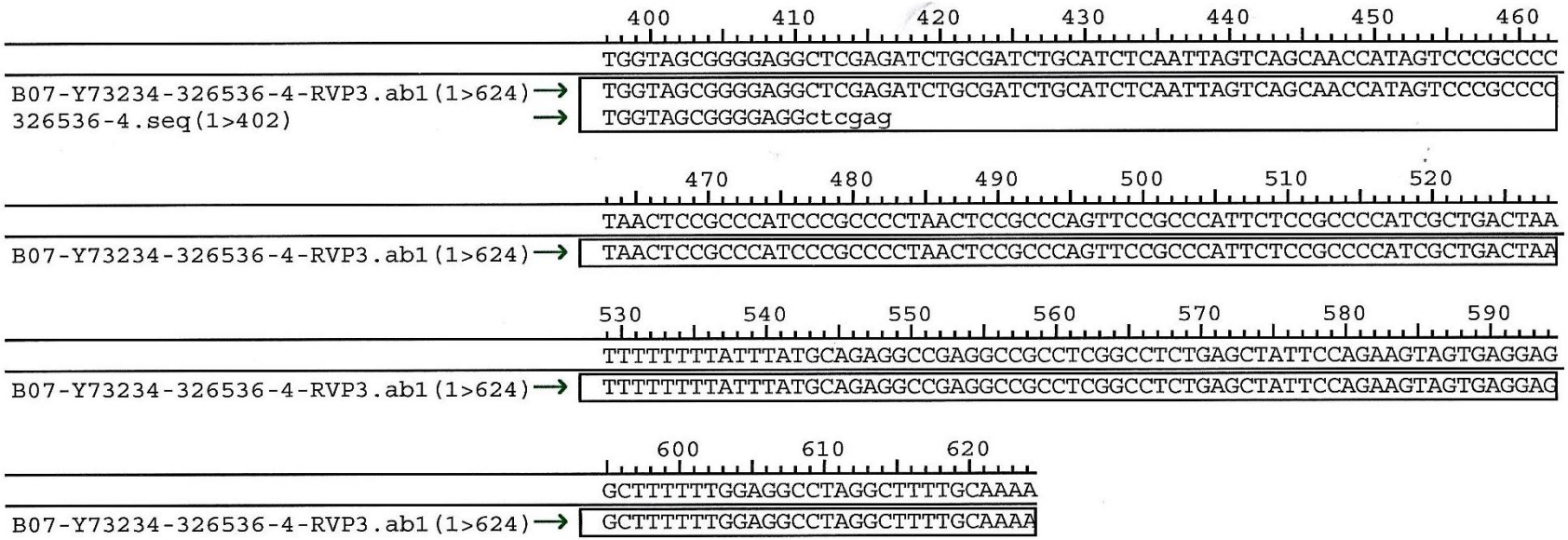
400 410 420 430 440 450 460
TGGTAGCGGGGAGGCTCGAGATCTGCGATCTGCATCTCAATTAGTCAGCAACCATAGTCCCGCCCC
B07-Y73234-326536-4-RVP3.ab1(1>624)
TGGTAGCGGGGAGGCTCGAGATCTGCGATCTGCATCTCAATTAGTCAGCAACCATAGTCCCGCCCC
326536-4.seq(1>402)
TGGTAGCGGGGAGGctcgag
470 480 490 500 510 520
TAACTCCGCCCATCCCGCCCCTAACTCCGCCCAGTTCCGCCCATTCTCCGCCCCATCGCTGACTAA
B07-Y73234-326536-4-RVP3.ab1(1>624)
TAACTCCGCCCATCCCGCCCCTAACTCCGCCCAGTTCCGCCCATTCTCCGCCCCATCGCTGACTAA
530 540 550 560 570 580 590
TTTTTTTTATTTATGCAGAGGCCGAGGCCGCCTCGGCCTCTGAGCTATTCCAGAAGTAGTGAGGAG
B07-Y73234-326536-4-RVP3.ab1(1>624)
TTTTTTTTATTTATGCAGAGGCCGAGGCCGCCTCGGCCTCTGAGCTATTCCAGAAGTAGTGAGGAG
600 610 620
GCTTTTTTGGAGGCCTAGGCTTTTGCAAAA
B07-Y73234-326536-4-RVP3.ab1(1>624)
GCTTTTTTGGAGGCCTAGGCTTTTGCAAAA